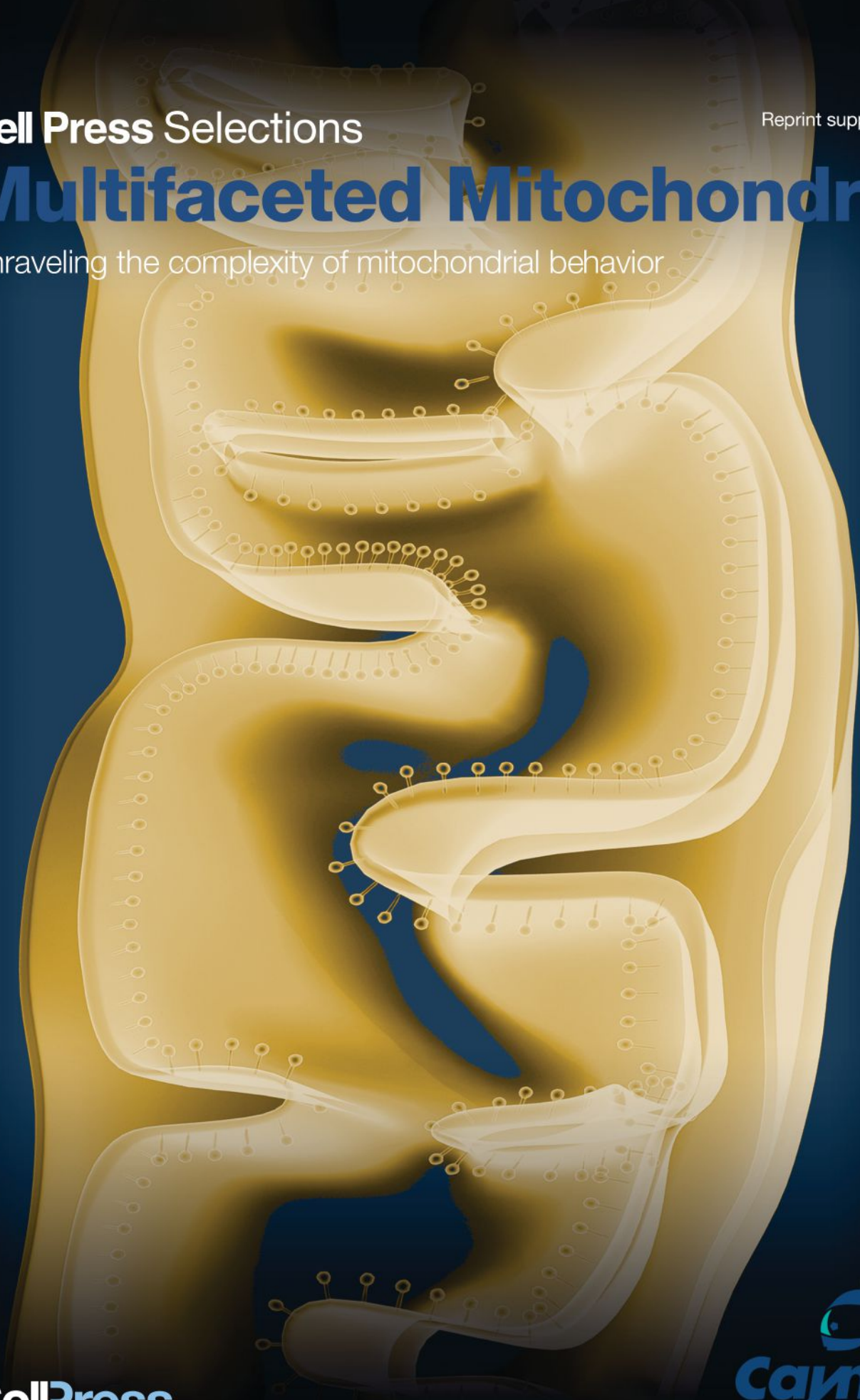


Cell Press Selections

Reprint supplement

Multifaceted Mitochondria

Unraveling the complexity of mitochondrial behavior



BIOENERGETICS ASSAYS

Mitochondrial ETC Activity
Complexes I, II, III, & IV

Mitochondrial Activity
Complex V

Oxygen
Consumption/Glycolysis

Mitochondrial
Membrane Potential

Citrate Synthase
Activity



BIOCHEMICALS • ASSAY KITS • ANTIBODIES
PROTEINS • RESEARCH SERVICES

Visit www.CaymanChem.com/Bioenergetics for
more information on Cayman's Mitochondrial Assays

Call us at 800-364-9897 or Email us at sales@caymanchem.com

Foreword

We are pleased to introduce the latest edition of *Cell Press Selections*. These editorially curated reprint collections highlight a particular area of life science by bringing together articles from the Cell Press journal portfolio. In this selection, we present recent insights into the diverse roles of mitochondria.

Mitochondria perform diverse yet interconnected cellular functions and are dynamically regulated by complex signaling pathways. Interest in this fascinating organelle has recently undergone a renaissance, due to a series of discoveries revealing that mitochondrial function goes beyond the generation of molecular fuel. Mitochondria also play a central role in thermogenesis, differentiation, and cell death and influence an organism's physiology, as well as its pathology. The driving forces behind these discoveries have been in the development of animal models, systems-based approaches, and dynamic imaging techniques and are critical in unraveling the significance and complexity of mitochondrial behavior.

A comprehensive inventory on mitochondrial proteins over the past decade indicates that mammalian mitochondria contain over 1,500 proteins, which vary in a tissue-dependent manner. Not surprisingly, mitochondria are tasked with a myriad of critical roles in anything from regulating inflammatory responses to determining cellular response to chemotherapy. The articles in this selection explore the breadth of this organelle's function (and dysfunction).

We hope that you will enjoy reading this collection of articles and will visit www.cell.com to find other high-quality research and review articles across this rapidly growing field.

Finally, we are grateful for the generosity of Cayman Chemical, who helped to make this reprint collection possible.

For more information about Cell Press Selections:
Gordon Sheffield
Program Director, Cell Press Selections
g.sheffield@cell.com
617-386-2189

MITOCHONDRIAL ACTIVITY ASSAYS ETC

Individually Screen
Complexes I, II, II/III, & IV

Identify the Inhibition
of Specific Complexes

No Antibodies
Required

Adaptable
to HTS



BIOCHEMICALS • ASSAY KITS • ANTIBODIES
PROTEINS • RESEARCH SERVICES

Visit www.CaymanChem.com/Bioenergetics for
more information on Cayman's Mitochondrial Assays

Call us at 800-364-9897 or Email us at sales@caymanchem.com

Multifaceted Mitochondria

Reviews

Mitochondria: In Sickness and in Health

Jodi Nunnari and Anu Suomalainen

Stress-Responsive Regulation of Mitochondria through the ER Unfolded Protein Response

T. Kelly Rainbolt, Jaclyn M. Saunders, and R. Luke Wiseman

Mitochondria: From Cell Death Executioners to Regulators of Cell Differentiation

Atsuko Kasahara and Luca Scorrano

Self and Nonself: How Autophagy Targets Mitochondria and Bacteria

Felix Randow and Richard J. Youle

Articles

Mitochondrial Cristae Shape Determines Respiratory Chain Supercomplexes Assembly and Respiratory Efficiency

Sara Cogliati, Christian Frezza, Maria Eugenia Soriano, Tatiana Varanita, Ruben Quintana-Cabrera, Mauro Corrado, Sara Cipolat, Veronica Costa, Alberto Casarin, Ligia C. Gomes, Ester Perales-Clemente, Leonardo Salviati, Patricio Fernandez-Silva, Jose A. Enriquez, and Luca Scorrano

The Mitochondrial Chaperone TRAP1 Promotes Neoplastic Growth by Inhibiting Succinate Dehydrogenase

Marco Sciacovelli, Giulia Guzzo, Virginia Morello, Christian Frezza, Liang Zheng, Nazarena Nannini, Fiorella Calabrese, Gabriella Laudiero, Franca Esposito, Matteo Landriscina, Paola Defilippi, Paolo Bernardi, and Andrea Rasola

The Intrinsic Apoptosis Pathway Mediates the Pro-Longevity Response to Mitochondrial ROS in *C. elegans*

Callista Yee, Wen Yang, and Siegfried Hekimi

ROS-Triggered Phosphorylation of Complex II by Fgr Kinase Regulates Cellular Adaptation to Fuel Use

Rebeca Acín-Pérez, Isabel Carrascoso, Francesc Baixauli, Marta Roche-Molina, Ana Latorre-Pellicer, Patricio Fernández-Silva, María Mittelbrunn, Francisco Sanchez-Madrid, Acisclo Pérez-Martos, Clifford A. Lowell, Giovanni Manfredi, and José Antonio Enriquez



JOIN THE DEBATE

With Cell Press Reviews

Insight and perspective is a powerful combination. That's why we offer readers a critical examination of the evidence that provokes thought and facilitates discussion within scientific communities.

To propel your research forward, faster, turn to Cell Press Reviews. Our insightful, authoritative reviews—published across the life sciences in our primary research and *Trends* journals—go beyond synthesis and offer a point of view.

Find your way
with Cell Press Reviews

www.cell.com/reviews

CellPress
Your work is our life

Mitochondria: In Sickness and in Health

Jodi Nunnari^{1,*} and Anu Suomalainen^{2,3,*}

¹Department of Molecular and Cellular Biology, University of California, Davis, Davis, CA 95616, USA

²Research Programs Unit, Molecular Neurology, Biomedicum-Helsinki, University of Helsinki, 00290 Helsinki, Finland

³Department of Neurology, Helsinki University Central Hospital, 00290 Helsinki, Finland

*Correspondence: jmnunnari@ucdavis.edu (J.N.), anu.wartiovaara@helsinki.fi (A.S.)

DOI 10.1016/j.cell.2012.02.035

Mitochondria perform diverse yet interconnected functions, producing ATP and many biosynthetic intermediates while also contributing to cellular stress responses such as autophagy and apoptosis. Mitochondria form a dynamic, interconnected network that is intimately integrated with other cellular compartments. In addition, mitochondrial functions extend beyond the boundaries of the cell and influence an organism's physiology by regulating communication between cells and tissues. It is therefore not surprising that mitochondrial dysfunction has emerged as a key factor in a myriad of diseases, including neurodegenerative and metabolic disorders. We provide a current view of how mitochondrial functions impinge on health and disease.

Introduction

Mitochondria arose from an alpha-proteobacterium engulfed by a eukaryotic progenitor (Lane and Martin, 2010). Like their bacterial ancestor, mitochondria are comprised of two separate and functionally distinct outer (OMs) and inner membranes (IMs) that encapsulate the intermembrane space (IMS) and matrix compartments. They also contain a circular genome, mitochondrial DNA (mtDNA), that has been reduced during evolution through gene transfer to the nucleus. mtDNA is organized into discrete nucleoids in the matrix. Interestingly, the closest relatives of many mtDNA-modifying enzymes, such as mtDNA polymerase, are bacteriophage proteins (Lecrenier et al., 1997; Tiranti et al., 1997), suggesting that an infection of the mitochondrial ancestor contributed to the development of mtDNA maintenance machinery. In animals, mtDNA inheritance is almost exclusively maternal, and paternal mtDNA is actively destroyed in many species immediately after fertilization (Al Rawi et al., 2011; Sato and Sato, 2011).

Advances in proteomic, genomic, and bioinformatic approaches have provided a comprehensive inventory of mitochondrial proteins in various eukaryotes (Gaston et al., 2009; Mootha et al., 2003; Pagliarini et al., 2008; Sickmann et al., 2003). This inventory indicates that mammalian mitochondria contain over 1,500 proteins, which vary in a tissue-dependent manner. Because mtDNA encodes only 13 of these proteins, mitochondria depend on the nucleus and other cellular compartments for most of their proteins and lipids. Nuclear-encoded mitochondrial proteins are actively imported and sorted into each mitochondrial compartment (Neupert and Herrmann, 2007; Schmidt et al., 2010), followed by coordinated assembly into macromolecular complexes, comprised of subunits encoded by nuclear and mitochondrial DNA.

Although mammalian mitochondria have retained some bacterial features, it is estimated that only a small percentage of human mitochondria are derived from the original endosymbiont (Gabaldón and Huynen, 2004). However, the bacterial

ancestry of mitochondria and bacteriophage-related mtDNA maintenance systems make the organelle susceptible to antimicrobial drugs: for example, mitochondrial translation is targeted by common antibiotics that block microbial ribosomes (aminoglycosides, tetracyclines) (Hutchin et al., 1993; van den Bogert and Kroon, 1981), and mtDNA maintenance is affected by antiviral nucleoside analogs (Arnaudo et al., 1991). The genetic risk factors underlying drug sensitivity of mitochondrial function are expected to be numerous, but challenging to identify.

The considerable resources a cell must provide to maintain the mitochondrial compartment underscores the varied essential roles it plays. This is further demonstrated by the fact that mitochondrial dysfunction is associated with an increasingly large proportion of human inherited disorders and is implicated in common diseases, such as neurodegenerative disorders, cardiomyopathies, metabolic syndrome, cancer, and obesity. Below we review new developments in mitochondrial biology and discuss their relevance for human disease.

Mitochondrial Defects Cause Diverse and Complex Human Diseases

Human mitochondrial disorders are a genetically heterogeneous group of different diseases, caused by mutations in mitochondrial and/or nuclear DNA, which encompass almost all fields of medicine (Ylikallio and Suomalainen, 2012). Mitochondrial diseases can affect any organ system, manifest at any age, and, depending on where the gene defect lies, be inherited from an autosome, the X chromosome, or maternally. Currently, mitochondrial disorders cannot be cured, and available treatments are directed at relieving symptoms (Suomalainen, 2011).

Mitochondrial diseases display both clinical heterogeneity and have tissue-specific manifestations, as indicated by the fact that mutations in the same mitochondrial protein complex lead to disparate disease phenotypes. For example, defects in respiratory complex I can lead to atrophy of the optic nerve in adults (Wallace et al., 1988) or subacute necrotizing encephalopathy

in infants (Morris et al., 1996). The most common nuclear mutations associated with mitochondrial diseases are found in the gene encoding mitochondrial DNA polymerase γ and can manifest as early-onset hepatocerebral disorder, juvenile catastrophic epilepsy, or adult-onset ataxia-neuropathy syndrome (Euro et al., 2011; Hakonen et al., 2005; Naviaux et al., 1999; Van Goethem et al., 2001). Another example of clinical variability is exhibited by the recently characterized disease group linked to defects in mitochondrial aminoacyl-transfer RNA (tRNA) synthetases (ARS2s), whose known essential function is to join a mitochondrial tRNA with its cognate amino acid to be transferred to the ribosome for protein synthesis. ARS2 defects promote a variety of phenotypes, including cardiomyopathies, cerebral white matter disease, ovarian dysfunction, and hearing loss. (Scheper et al., 2007; Götz et al., 2011; Pierce et al., 2011) The nature of the molecular defect can often explain variations in the severity and age-of-onset of these diseases, but not the variability in tissue-specific manifestations, which may instead be defined by a patient's complement of protective and risk alleles.

Phenotypic variability associated with mtDNA-linked diseases is also due, in part, to the high copy number of mtDNA in mammalian cells, which can consequently contain both mutant and wild-type mtDNAs populations—a situation called heteroplasmy (Holt et al., 1988). While mtDNA mutations in tRNA genes possess high clinical variability not explained by heteroplasmy, in the case of protein-coding gene mutations, the degree of heteroplasmy correlates with the severity of phenotypes. For example, for the T8993C/G mutation of mtDNA, affecting ATPase6, a low mutant load causes pigment retinopathy, ataxia, and neuropathy in adults, whereas a high mutant load causes maternally inherited Leigh syndrome in infants (Holt et al., 1990; Tatuch et al., 1992).

Heteroplasmy can be affected by segregation of mtDNA and by selective mitochondrial degradative pathways. Examples of nonrandom segregation include the nonrandom segregation of neutral mtDNA variants in mice (Battersby et al., 2005; Jokinen et al., 2010), and, in humans, the A3243G tRNA^{Leu(UUR)} mutation, whose load decreases in blood over years (Rahman et al., 2001). In mice, cells with allogenic mtDNA are recognized and targeted by the innate immune system, indicating that mitochondrial DNA-dependent antigen presentation may play a role in mtDNA selection (Ishikawa et al., 2010). Selection of mtDNA may also occur during oogenesis: in mice, mtDNA mutations in protein-coding genes are underrepresented in offspring, suggesting a mechanism that selectively eliminates cells or organelles with the most severe mutations (Fan et al., 2008; Stewart et al., 2008). Surprisingly, the fundamental molecular mechanisms underlying the process of mtDNA distribution in cells and its tissue specificity are poorly understood, given that an understanding of how the nucleoid is regulated is crucial to understanding mitochondrial diseases.

Mitochondria Are Metabolic Signaling Centers

The diverse nature of mitochondrial diseases highlights the many roles mitochondria play in cells and tissues. Mitochondria are best known for producing ATP via oxidative phosphorylation (OXPHOS). In the matrix, tricarboxylic acid cycle (TCA) enzymes generate electron carriers (NADH and FADH₂), which donate

electrons to the IM-localized electron transport chain (ETC). The ETC consists of four protein machines (I–IV), which through sequential redox reactions undergo conformational changes to pump protons from the matrix into the IMS. The first and largest of the respiratory complexes, complex I, is a sophisticated microscale pump consisting of 45 core subunits, whose biogenesis requires an army of assembly factors (Diaz et al., 2011; Efremov and Sazanov, 2011). The proton gradient generated by complexes I, III, and IV is released through the rotary turbine-like ATP synthase machine or complex V, which drives phosphorylation of ADP to ATP (Okuno et al., 2011; Stock et al., 1999). Beyond ATP production, the inner-membrane electrochemical potential generated by OXPHOS is a vital feature of the organelle (Mitchell, 1961). Membrane potential is harnessed for other essential mitochondrial functions, such as mitochondrial protein import (Neupert and Herrmann, 2007), and is used to trigger changes on the molecular level that alter mitochondrial behaviors in response to mitochondrial dysfunction.

Complexes I and III also generate reactive oxygen species (ROS), including oxygen radicals and hydrogen peroxide, which can damage key components of cells, including lipids, nucleic acids, and proteins (Muller et al., 2004; Murphy, 2009). ROS has been suggested to contribute to diseases associated with mitochondrial dysfunction, including neurodegeneration. For example, Leber's hereditary optic neuropathy is associated with mutations that alter the ubiquinone binding pocket of mtDNA-encoded complex I subunits (Pätsi et al., 2008) that likely affect electron delivery from the FeS centers of complex I to ubiquinone, leading to an overreduction of FeS clusters, electron leak, and oxygen radical production.

Multiple lines of evidence indicate that mitochondrial ROS also influence homeostatic signaling pathways to control cell proliferation and differentiation and to contribute to adaptive stress signaling pathways, such as hypoxia (Hamanaka and Chandel, 2010). Observations from premature aging mouse models suggest that hematopoietic progenitors are especially sensitive to ROS and/or redox state changes that promote proliferation and prevent quiescence (Ito et al., 2004; Narasimhaiah et al., 2005). Interestingly, progeroid mtDNA Mutator mice, which accumulate mtDNA mutations, are severely anemic (Chen et al., 2009; Kujoth et al., 2005; Norddahl et al., 2011; Trifunovic et al., 2004) and have an early somatic stem cell dysfunction suppressed by n-acetyl-L-cysteine treatment. These observations imply that ROS/redox signaling affects somatic stem cell function and causes progeroid symptoms (Ahlqvist et al., 2012) and that mitochondrial dysfunction in somatic stem cells may contribute to aging-related degeneration.

In all cell types, mitochondria are the major cellular source of NADH and house parts of the pyrimidine and lipid biosynthetic pathways, including the fatty acid β -oxidation pathway, which converts long chain fatty acids to Acyl-CoA. Mitochondria also regulate cellular levels of metabolites, amino acids, and cofactors for various regulatory enzymes, including chromatin-modifying histone deacetylases. Moreover, mitochondria play a central role in metal metabolism, synthesizing heme and Fe-S clusters (Lill and Mühlhoff, 2008), which are essential components of the major oxygen carrier, hemoglobin, as well as OXPHOS and DNA repair machinery. Mitochondria also

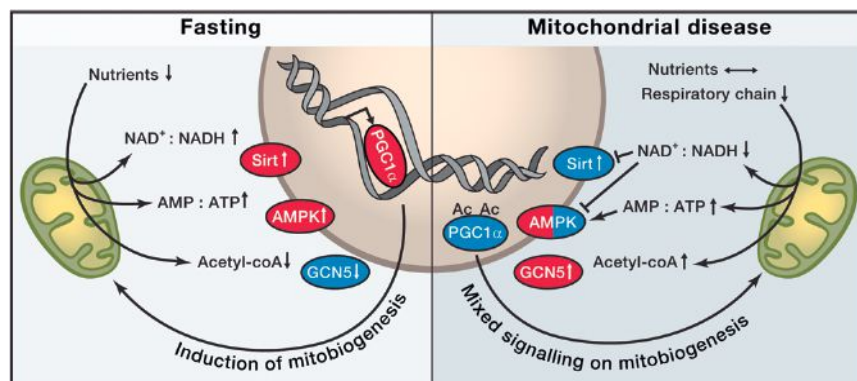


Figure 1. Nutrient Sensors in Fasting and Their Roles in Mitochondrial Disease

Both fasting and mitochondrial disease can modify $\text{NAD}^+:\text{NADH}$ and $\text{AMP}:\text{ATP}$ ratios through decreased nutrient availability or through reduced respiratory chain activity and have the potential to activate (red) nutrient sensors Sirtuin 1 (Sirt, an NAD^+ -dependent histone deacetylase) or AMP-activated kinase (AMPK) and increase mitochondrial biogenesis by activating peroxisome proliferator-activated receptor gamma coactivator 1-alpha (PGC-1alpha). Upon decreased utilization of acetyl-coenzyme A (acetyl-coA), GCN5 (lysine acetyltransferase 2A) is activated and acetylates PGC1alpha, to inactivate it (blue). NAD^+ , nicotinamide adenine dinucleotide, oxidized form; NADH, nicotinamide adenine dinucleotide, reduced form; AMP, adenosine monophosphate; ATP, adenosine triphosphate; Ac, acetyl group.

participate in Ca^{2+} homeostasis, shaping the spatiotemporal distribution of this second messenger by buffering Ca^{2+} flux from the plasma membrane and endoplasmic reticulum (ER) (Baughman et al., 2011; De Stefani et al., 2011).

In neurons, the ability of mitochondria to modulate Ca^{2+} flux is essential for controlling neurotransmitter release, neurogenesis, and neuronal plasticity. In addition, mitochondria supply copious amounts of ATP as well as the TCA intermediates that serve as the building blocks for synthesis of GABA and glutamate neurotransmitters (Sibson et al., 1998; Waagepetersen et al., 2001). Compromised oxidative metabolism may therefore alter neurotransmitter levels and render the brain uniquely sensitive to oxidative energetic deficits, as has been shown for pyruvate carboxylase deficiency (Perry et al., 1985). Mitochondria-mediated lipid synthesis is also critical for neuronal function, as defects in lipoic acid synthase cause severe neonatal-onset epilepsy (Mayr et al., 2011). These additional metabolic functions of mitochondria depend, either directly or indirectly, on OXPHOS, and thus can be secondarily affected by changes in respiration and respiratory complex deficiency.

Mitochondria as Energy Sensors and Beacons

The central roles of mitochondria in metabolism position them as key actors in global energy modulation. An increased need for ATP is met by increasing mitochondrial mass and inducing OXPHOS. For example, an increase of mitochondrial mass and activity is observed after endurance exercise (Hoppeler and Fluck, 2003). The regulation of mitochondrial biogenesis is tightly coordinated with pathways that induce vascularization, enhance oxygen delivery to tissues, and enable oxygen supply to facilitate efficient mitochondrial oxidization of glucose and fat (Arany et al., 2008).

Mitochondrial metabolism is both the basis for and target of nutrient signals that ultimately orchestrate an integrated physiological response. The molecular components that sense energy status include transcription factors, hormones, cofactors, nuclear receptors, and kinases, which detect specific signals of mitochondrial activity, such as the $\text{NAD}^+:\text{NADH}$ ratio, the $\text{AMP}:\text{ATP}$ ratio, or acetyl-CoA levels (Figure 1).

Two key cellular sensors of metabolic status are the AMP-activated protein kinase (AMPK) and Sirt1, an NAD^+ -dependent deacetylase. AMPK is activated by an increase in $\text{AMP}:\text{ATP}$ ratio

and increased ADP concentrations, both of which accompany a decrease in caloric intake or an increase in energy expenditure (Hardie et al., 2011; Mihaylova and Shaw, 2011). Through the phosphorylation of a variety of targets, it upregulates catabolic pathways including gluconeogenesis, OXPHOS, and autophagy, while inhibiting anabolic pathways including cell growth and proliferation (Cantó et al., 2010; Carling et al., 2011). Sirt1 responds to elevated levels of NAD^+ that occur upon starvation and, together with AMPK, coordinately regulates mitochondrial mass, nutrient oxidation, and ATP production to fit a cell's particular needs via the transcription cofactor, peroxisome proliferator-activated receptor gamma coactivator 1 alpha (PGC-1 α) (Cantó et al., 2009, 2010; Jäger et al., 2007; Jenjina et al., 2010; Puigserver et al., 1998; Wu et al., 1999).

Nutrient responses are likely to be highly tissue specific. In the liver, low blood lipid levels induce the nuclear PPAR-alpha receptor, which ultimately induces ketogenesis. In adipose tissue, mitochondria-derived starvation responses trigger lipolysis to provide peripheral tissues with fuels (Kharitonov et al., 2005; Nishimura et al., 2000). In the hypothalamus, AMPK affects neuronal plasticity and transmitter receptor activity to promote food intake and provide neuronal protection in response to hunger (Kuramoto et al., 2007; Yang et al., 2011). During a high nutritional load, multiple cell types exhibit high levels of ATP and NADH levels and the metabolic balance tips toward lipid and glycogen storage, and mitochondrial biogenesis is downregulated, increasing glycolytic ATP synthesis.

How does the interrelationship between nutrient sensing and mitochondrial function contribute to disease? Not surprisingly, alterations in mitochondrial mass and activity are contributory factors in obesity and metabolic syndrome. Comparisons between identical twin pairs discordant for obesity revealed significantly reduced mtDNA levels and decreased mitochondrial mass in the obese twin's adipose tissue, despite identical mtDNA sequences (Pietiläinen et al., 2008). This observation indicates the importance of environmental effects in regulating mitochondrial mass and biogenesis. The discovery of active brown adipose tissue in adult humans has opened up an intriguing avenue in obesity research by clarifying the role of adaptive thermogenesis in counteracting fat storage through UCP1-mediated mitochondrial uncoupling (van Marken Lichtenbelt et al., 2009; Virtanen et al., 2009).

Studies of the Deletor mouse provide a model to interrogate the physiological changes associated with late-onset mitochondrial disease (Tynymäa et al., 2005). Even when these animals receive normal nutrition, their muscle cells misinterpret an OXPHOS defect and decreased ATP synthesis as starvation. Interestingly, a key regulator of anabolic processes, Akt kinase, is also activated under these conditions (Tynymäa et al., 2010). In these mice, induction of mitochondrial biogenesis by high-fat feeding appears to be beneficial by inducing mitochondrial mass and OXPHOS activity (Ahola-Erkkilä et al., 2010). The progressive disease course of mice with cytochrome c oxidase deficiencies can similarly be delayed with treatments that increase mitochondrial biogenesis (Viscomi et al., 2011; Wenz et al., 2008; Yatsuga and Suomalainen, 2012) or that activate AMPK (Viscomi et al., 2011). In these instances, it is likely that AMPK activation leads to an increase in NAD⁺, triggering Sirt1 activation and subsequent PGC-1 α induction of mitochondrial biogenesis (Corton et al., 1995; Golubitzky et al., 2011; Viscomi et al., 2011). Together, these studies suggest that mitochondrial biogenesis is blocked by chronic OXPHOS dysfunction and that increased mitochondrial biogenesis can be beneficial for mitochondrial disease.

Recent work has linked tumor suppressors and oncogenes directly to metabolic sensing and regulation, and has consequently indicated that altered cellular metabolism is a contributory and causative factor in cancer. Cancer cells reprogram the use of two key catabolic molecules, glucose and glutamine via signaling pathways containing known oncogenes, including myc and tumor suppressors, such as the LKB1/AMPK (Vander Heiden et al., 2009). These signaling pathways shunt glucose toward aerobic glycolysis—the so-called Warburg effect (Warburg, 1923)—and glutamine toward glutaminolysis for the purpose of producing amino acids, nucleotides and lipids that are essential for rapid proliferation. In cancer cells, mitochondria play a central role via the TCA cycle in the catabolism of glutamine. The altered metabolism of cancer cells raises the possibility that treatments that shift metabolism toward OXPHOS could be therapeutically effective against cancer. Importantly, mitochondrial metabolic enzymes have been identified as tumor suppressors. Defects in succinate dehydrogenase, fumarate hydratase, and isocitrate dehydrogenase (IDH1) cause inherited paragangliomas, pheochromocytomas, myomas, and gliomas, respectively (Baysal et al., 2000; Tomlinson et al., 2002; Yan et al., 2009). Recent intriguing findings in gliomas indicated that *IDH1* mutations contribute to gliomas via multiple mechanisms, including stabilizing hypoxia-inducible factor 1, as was previously found in other tumorigenic TCA defects, and by altering the methylation of CpG islands and histones, which causes wide-ranging transcriptional consequences that contribute to oncogenesis (Turcan et al., 2012; Lu et al., 2012; Koivunen et al., 2012). The multifaceted roles of *IDH1* mutations in cancer introduce an intriguing role for mitochondrial function in affecting nuclear genomic expression.

Connecting Mitochondrial Form and Function in Homeostasis and Disease

Mitochondrial form and function are intimately linked. The inner membrane is highly structured and differentiated into composi-

tionally and functionally distinct regions (Reichert and Neupert, 2002): the inner boundary region is in close apposition to the OM and facilitates lipid trafficking, mitochondrial protein import, and respiratory complex assembly, the cristae are invaginations that penetrate into the matrix and house assembled respiratory complexes and are thought to increase the local charge density/pH to enhance ATP synthesis via OXPHOS (Strauss et al., 2008; Perkins and Frey, 2000); and crista junctions are tubules that connect the cristae to the boundary and segregate soluble intermembrane space components from the boundary regions. These junctions are restructured during apoptosis to facilitate release of proapoptotic intermembrane space proteins (Frezza et al., 2006). The biogenesis of IM domains is an active process highly dependent on the mitochondrial-specific anionic lipids, phosphatidylethanolamine and cardiolipin, whose transport and levels within mitochondria are tightly controlled by a surprisingly complex set of factors (Osman et al., 2011). Through interactions with lipids and through the formation of inner-membrane supercomplexes, abundant inner-membrane proteins, such as adenine nucleotide translocator, are also important for the structural organization of this membrane (Claypool et al., 2008). In addition, the regulated dimerization/oligomerization of ATP synthase is a major driving force for inner-membrane structure, possibly inducing and/or stabilizing the curvature of crista membranes (Paumard et al., 2002; Strauss et al., 2008). Dedicated structural assemblies have also been implicated in the organization of mitochondrial membranes (Polianskyte et al., 2009), including recent work pointing to a large conserved multiprotein Mitofilin complex (Harner et al., 2011; Hoppins et al., 2011a; von der Malsburg et al., 2011). The importance of OM/IM interactions is underscored by the observation that the Mitofilin complex, termed MitOS, also plays a role in the efficiency of mitochondrial protein import (von der Malsburg et al., 2011), components of which have been implicated in human inherited disorders, including neurological (Jin et al., 1996) and cardiac (Davey et al., 2006) syndromes. Understanding the mechanisms that contribute to the structural organization of the inner membrane will decipher its functions beyond OXPHOS, such as in mtDNA segregation, protein import, and mitochondrial dynamics (Brown et al., 2011).

The lateral organization of the OM is not as well understood, but it serves as a unique signaling platform for pathways such as BCL-2 protein-dependent apoptosis (Chipuk et al., 2010; Bogner et al., 2010) and innate antiviral immunity, which requires the regulated self-assembly of the mitochondrial localized membrane protein, MAVS, into a signaling complex essential for anti-inflammatory interferon response (Wang et al., 2011a). Recent superresolution light microscopy techniques have revealed that the OM import TOM complex is localized in clusters, whose density and distribution are regulated by growth conditions that alter mitochondrial membrane potential (Wurm et al., 2011). This observation highlights that events inside mitochondria regulate the organization and activity of complexes at the mitochondrial surface, which can influence the external structure and behavior of the organelle.

The external structure and the cellular location of mitochondria are critical for their function and depend on highly regulated activities such as mitochondrial division and fusion, motility,

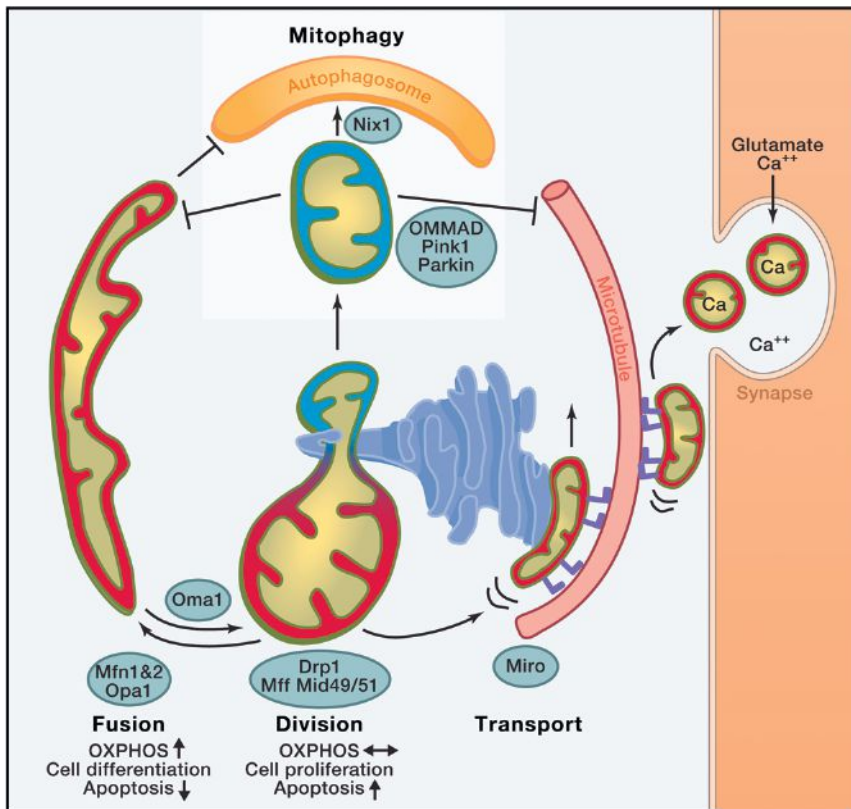


Figure 2. Roles of Mitochondrial Dynamics

Red: mitochondria with high membrane potential, with high oxidative phosphorylation (OXPHOS) activity. Blue: Mitochondria with low membrane potential. Mitofusin 1 or 2 (MFN1, MFN2) mediate mitochondrial outer-membrane fusion in a tissue-specific manner, and OPA1 (optic atrophy gene 1) mediates inner-membrane fusion. The zinc metalloprotease OMA1 proteolytically cleaves OPA1 under low membrane potential conditions, promoting fission. Mitochondrial dynamics factors 49 and 51 or mitochondrial fission factor (Mff) recruit DRP1 onto mitochondria at sites marked by endoplasmic reticulum tubules (ER), and DRP1 mediates mitochondrial division. In cultured cells, upon a decrease in mitochondrial membrane potential, PINK1 kinase recruits Parkin, a ubiquitin E3 ligase, which ubiquitinates several mitochondrial targets, including MFN1 and Miro, to facilitate the degradation of mitochondria via mitophagy. Parkin-mediated ubiquitination triggers OMMAD, outer-mitochondrial membrane-associated degradation—a proteosomal pathway that degrades ubiquitinated OM proteins in a CDC48-dependent manner. OMMAD is probably cell type-dependent and may also function in quality control. In erythrocytes, mitophagy receptor Nix1 is involved in autophagosome recruitment. ER forms close contacts with mitochondria, essential for calcium regulation in cellular microcompartments. Miro (blue feet) is a mitochondrial receptor for kinesin via Milton that facilitates the transport of mitochondria on microtubules in a Ca²⁺-regulated manner. Upon synaptic activity in neurons, influx of glutamate and Ca²⁺ halts mitochondrial transport via Miro to position them at sites of synaptic activity that require Ca²⁺ uptake and ATP.

and tethering. These activities govern the overall shape, connectedness, and location of mitochondria within cells (Figure 2). Although little data are currently available, it is clear that the relative contributions of these activities and the molecular components that mediate them are highly tissue specific—a phenomenon that contributes to the variable manifestations of human mitochondrial diseases.

In metazoans, mitochondrial motility is mediated by Miro, a conserved Ras-like GTPase that links the mitochondrial surface with the microtubule motor protein kinesin Milton (Glater et al., 2006; Hollenbeck and Saxton, 2005; Liu and Hajnóczky, 2009; Wang and Schwarz, 2009). Although the exact mechanism is not understood, Miro serves as a Ca²⁺ sensor that controls mitochondrial motility by virtue of its GTPase domains and its calcium binding EF hand motifs to couple an increase in cytosolic calcium to an inhibition of mitochondrial motility (Macaskill et al., 2009; Saotome et al., 2008; Wang and Schwarz, 2009). This mechanism is particularly important in neurons, where Ca²⁺ influx occurs at presynaptic terminals and postsynaptic dendritic spines due to glutamatergic stimulation. These local increases provide a mechanism to halt mitochondria at the site of neuronal activity, and maintain Ca²⁺ and energetic homeostasis. In this context, Miro may enable neurons to efficiently retain mitochondria at the sites with high Ca²⁺, providing a neuronal protection mechanism. Consistent with this model, the EF hands of Miro mediate glutamatergic regulation of mitochondrial motility and provide a protective mechanism against excitotoxicity (Wang and Schwarz, 2009).

Mitochondrial division and fusion are mediated by the action of large multidomain dynamin-related GTPases that function via self-assembly to remodel diverse membranes in cells (Hoppins et al., 2007). In mammals, mitochondrial division is mediated by a single dynamin-related protein, DRP1, whereas fusion requires two families of dynamin-like proteins, MFN1/MFN2 and OPA1. Evidence suggests that DRP1 divides mitochondria by forming helical structures that wrap around mitochondria (Ingberman et al., 2005; Labrousse et al., 1999; Yoon et al., 2001). Less is known about the mechanism mediating mitochondrial fusion, although it is likely that the self-assembly of the fusion dynamins contributes to membrane tethering and fusion events (DeVay et al., 2009; Griffin and Chan, 2006). The proteins that mediate mitochondrial dynamics are highly regulated and consequently integrated into cellular signaling pathways. For example, DRP1 exists as several splice variants and is modified by a plethora of posttranslational modifications, which integrate its activity with cellular events, such as apoptosis, Ca²⁺ signaling, hypoxic response, and the cell cycle (Strack and Cribbs, 2012).

Loss of either fusion or division activity results in dysfunctional mitochondria. One common explanation for the importance of mitochondrial fusion is the need for exchange of IMS and matrix contents, including mtDNA between mitochondria. In this manner, mitochondrial fusion may buffer partially defects and transient stresses (Chen et al., 2007, 2010; Nunnari et al., 1997). In cultured cells, stressors including UV exposure, cycloheximide treatment, and nutrient deprivation, stimulate

mitochondrial fusion to generate branched and interconnected organelles and improve cell survival (Gomes et al., 2011a, 2011b; Rambold et al., 2011; Tondera et al., 2009). Mitochondrial fusion is balanced by mitochondrial division, which creates organelles of the appropriate size for transport along actin or microtubule networks. Cells that are highly polarized and dependent on mitochondrial function, such as neurons, are especially sensitive to defects in mitochondrial division (Verstreken et al., 2005). A neuronal cell-specific knockout of DRP1 in the mouse results in a decrease in neurites and defective synapse formation, while an increase in mitochondrial division in cultured neurons enhances mitochondrial mass and distribution and stimulates synapse formation (Dickey and Strack, 2011; Ishihara et al., 2009; Li et al., 2004; Wakabayashi et al., 2009).

In cells, inhibition of fusion results in OXPHOS deficiencies, mtDNA loss, and mitochondrial motility defects, and division defects also cause OXPHOS deficiencies and significant increases in ROS production (Chen et al., 2003, 2007; Hermann et al., 1998; Ishihara et al., 2009; Parone et al., 2008; Wakabayashi et al., 2009). In animals, deletions and mutations of the division and fusion machinery cause embryonic lethality, and in humans, recessive defects of DRP1 are associated with early infant mortality and cardiomyopathy (Waterham et al., 2007; Ashrafi et al., 2010). Mutations in MFN2 and OPA1 cause tissue-specific neurodegenerative diseases, Charcot Marie Tooth 2A (CMT2A) and dominant optic atrophy (DOA), respectively (Alexander et al., 2000; Delettre et al., 2000; Züchner et al., 2004). These pathogenic conditions emphasize the important physiological roles and differential requirement of mitochondrial dynamics in different cell types.

Linking Mitochondrial Dynamics with Apoptosis and Autophagy

Mitochondrial division and fusion also impinge on apoptosis by mechanisms that are not yet fully understood (Martinou and Youle, 2011). During apoptosis, mitochondria dramatically fragment as a consequence of an increased recruitment of DRP1 to mitochondria, which is key to the positive regulatory role DRP1 plays in Bax/Bak-mediated mitochondrial outer-membrane permeabilization (MOMP) (Frank et al., 2001; Jagasia et al., 2005; Wasiaik et al., 2007). Although DRP1's positive role in apoptosis is independent of its role in the regulation of mitochondrial structure per se, mitochondrial shape is likely to be an important factor in MOMP (Cassidy-Stone et al., 2008; Montessuit et al., 2010). In contrast, mitochondrial fusion protects cells from apoptotic cell death, and activation of apoptosis coordinately inhibits fusion activity (Lee et al., 2004; Olichon et al., 2003; Sugioka et al., 2004). This protection is in part due to the role of OPA1 in the integrity of crista junctions and its ability to limit the release of proapoptotic IMS components (Cipolat et al., 2006; Frezza et al., 2006). Conversely, BCL-2 proteins play regulatory roles in mitochondrial dynamics in healthy cells, where they stimulate fusion (Cleland et al., 2011; Hoppins et al., 2011b; Karbowski et al., 2006; Rolland et al., 2009). The regulatory network formed by BCL-2 proteins and mitochondrial dynamics proteins may be a contributory factor in the human neurodegenerative diseases associated with mutations in MFN2 and OPA1 (Olichon et al., 2007). Furthermore, the roles of BCL-2 in regulating mito-

chondrial dynamics and in tumors as an antiapoptotic factor link mitochondrial fission and fusion to cancer.

Mitochondrial dynamics are also closely integrated with the mitophagy quality control pathway (Twig et al., 2008; Youle and Narendra, 2011). PINK1, an IMS-localized Ser/Thr kinase, and Parkin, a cytoplasmic E3 ubiquitin ligase, regulate mitophagy in cultured cell models and in fruit-fly muscle. Together these proteins collaborate to sense and trigger the removal of "damaged" mitochondria (Clark et al., 2006; Greene et al., 2003; Narendra et al., 2008; Park et al., 2006). Loss of membrane potential inhibits the degradation of PINK1 and reroutes it to the surface of mitochondria, where it accumulates and recruits Parkin (Kim et al., 2008; Lin and Kang, 2008; Matsuda et al., 2010; Narendra et al., 2010; Vives-Bauza et al., 2010; Ziviani et al., 2010). On the mitochondrial surface Parkin ubiquitinates a specific subset of OM proteins, resulting in their proteasomal degradation by a mechanism that resembles ER-associated degradation pathway (Neutzner et al., 2007; Yoshii et al., 2011; Ziviani et al., 2010; Chan et al., 2011; Heo et al., 2010; Tanaka et al., 2010; Xu et al., 2011). Another mitophagy pathway functions in erythrocyte development, where upon reticulocyte maturation mitochondria are actively eliminated. This mitophagy pathway is dependent on Nix, an OM-associated BH3-only member of BCL-2 family proteins, suggesting that Nix functions as a mitophagy receptor (Sandoval et al., 2008; Schweers et al., 2007). This raises the possibility that other tissue- or condition-specific mitophagy receptors exist. The presence of such receptors and their functions remain to be elucidated. Given the nature of mitophagy, such receptors could, in addition to contributing to quality control, also dramatically impact mtDNA segregation.

Recent studies specifically connect PINK1/Parkin-mediated autophagy with mitochondrial dynamics and motility, providing evidence that Parkin ubiquitinates MFN1, MFN2, and Miro in cultured cells, leading to their degradation and consequently altering mitochondrial behavior (Chan et al., 2011; Gegg et al., 2010; Poole et al., 2010; Tanaka et al., 2010; Wang et al., 2011b; Ziviani et al., 2010). In this context, multiple OM-associated ubiquitin ligases have been identified whose substrates and roles are largely unknown (Anton et al., 2011; Braschi et al., 2009; Durr et al., 2006; Nakamura et al., 2006; Neutzner et al., 2008; Tang et al., 2011). Loss of membrane potential also attenuates mitochondrial fusion via OMA1-mediated cleavage of integral membrane isoforms of OPA1 (Ehse et al., 2009; Head et al., 2009). Consistently, mitophagy is attenuated in cells with decreased mitochondrial division and/or increased fusion activities likely because larger organelles are occluded from autophagosomes. Indeed, nutrient starvation in cultured cells induces the formation of a hyperfused mitochondrial network, which protects mitochondria from elimination via mitophagy (Gomes et al., 2011a; Rambold et al., 2011). In flies, attenuation of mitochondrial fusion or stimulation of mitochondrial division can rescue phenotypes associated with PINK1 or Parkin mutants, and loss of division exacerbates these phenotypes and causes lethality (Deng et al., 2008; Poole et al., 2008). Thus, evidence is consistent with the idea that mitophagy is a pathway that coordinately regulates mitochondrial structure and motility to effectively segregate damaged mitochondria from a healthy network in cells, which facilitates their degradation.

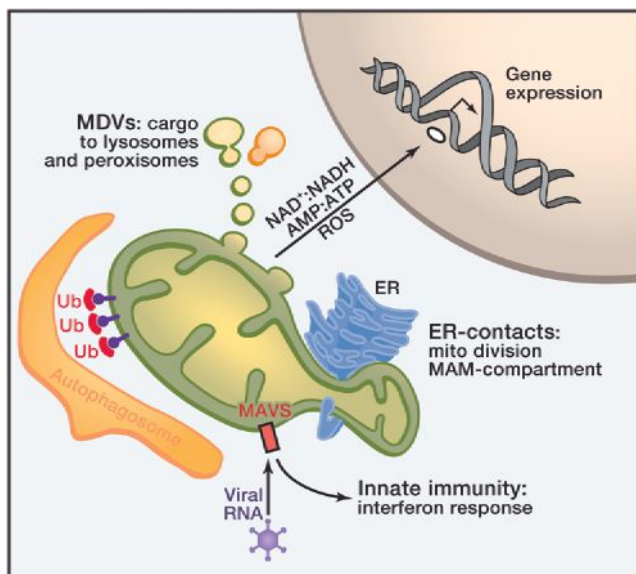


Figure 3. Interorganellar Communication

Ub, ubiquitin; red and blue, proteins in mitochondrial outer membrane are PINK1, a mitochondrial kinase, and the E3 ubiquitin ligase Parkin, recruited onto mitochondria by PINK1; MDV, mitochondria-derived vesicle; NAD, nicotinamide adenine dinucleotide, oxidized form; NADH, nicotinamide adenine dinucleotide, reduced form; AMP, adenosine monophosphate; ATP, adenosine triphosphate; ER, endoplasmic reticulum, tubules of which are marking sites of mitochondrial division; MAVS, mitochondrial antiviral signaling, which is activated by viral RNA; MAM, mitochondrial-associated endoplasmic reticulum membrane.

The relevance of the PINK1/Parkin mitochondrial turnover pathway in animal models has not yet been established; however, defects in this pathway have been suggested to play a role in the development of Parkinson's disease (PD), where a role of PINK1 and Parkin were originally characterized as their mutant forms cause familial early-onset PD (Kitada et al., 1998; Valente et al., 2004). The association of PINK1/Parkin to PD points to their essential role in maintenance of dopaminergic neurons, the cell type in substantia nigra of mesencephalon that most severely degenerates in PD. Data from cell culture models suggest the intriguing possibility that defective mitochondrial quality control contributes more generally to Parkinson-like phenotypes, potentially explaining why mtDNA mutation accumulate in substantia nigra neurons (Bender et al., 2006; Kraytsberg et al., 2006). A recent mouse study, however, questions this simple model. In the PD Mitopark mouse model, progressive depletion of mtDNA in dopaminergic neurons does not lead to the accumulation of mitochondrial Parkin, and loss of Parkin does not affect neurological disease progression (Sterky et al., 2011). This raises the possibility that PINK1/Parkin contribute to PD by mechanisms other than mitophagy. Parkin has been implicated in nonneuronal mediated lipid uptake regulation, raising the possibility that altered lipid metabolism contributes to Parkin-linked PD (Kim et al., 2011). Additionally, mitochondrial dysfunction is linked to PD by early toxicological studies on MPTP, a compound that is metabolized into a complex I inhibitor, MPP⁺. MPP⁺ selectively accumulates in dopaminergic cells and causes symptoms of PD in humans

(Davis et al., 1979; Langston et al., 1983; Vyas et al., 1986). Gene defects that lead to mtDNA mutations, such as dominant mutations of mitochondrial DNA polymerase gamma, also cause PD (Luoma et al., 2004). These observations highlight the complex multifactorial nature of neurodegeneration and point to the need for additional animal studies to elucidate physiological roles of mitophagy and its contribution to PD.

Altered mitochondrial dynamics have also been implicated in neurodegeneration. In cell culture models for neurodegenerative diseases, such as Alzheimer's disease, Parkinson's disease, Huntington's disease, and amyotrophic lateral sclerosis, mitochondria typically fragment in response to the expression of misfolded proteins (Cho et al., 2010; Costa et al., 2010; Lutz et al., 2009; Shirendeb et al., 2012; Song et al., 2011; Wang et al., 2009). Although it is not clear whether mitochondrial fragmentation is a cause or a consequence of the pathogenic process, inhibition of mitochondrial division attenuates disease-associated phenotypes in multiple models of neurodegenerative disease (Cassidy-Stone et al., 2008; Cui et al., 2010; Lackner and Nunnari, 2010). Inhibiting division may also attenuate the ubiquitin dependent turnover of outer-membrane proteins and mitophagy, which would allow essential behaviors like mitochondrial motility to be retained. In this context, it is possible that the mitochondrial motility defects associated with absent or altered MFN1 and MFN2 proteins result from the targeted degradation of Miro (Baloh et al., 2007; Chen et al., 2005).

The role of mitochondrial division and its potential as a therapeutic target for neurodegeneration needs to be further explored in relevant animal models. In addition, as mitochondrial division is essential in mammals, this pathway may have limited therapeutic potential for neurodegeneration. However, more acute ischemic reperfusion injuries and drug toxicities are also associated with increased mitochondrial fragmentation in cultured cells models and in animal models of myocardial infarction and drug induced renal toxicity, inhibition of mitochondrial division has shown therapeutic promise (Brooks et al., 2009; Ong et al., 2010).

The Roles of Interorganellar Contacts in Mitochondrial Biology

Mitochondrial distribution and dynamics are influenced by intimate physical connections between the mitochondrial outer membrane and diverse intracellular membranes, such as the plasma membrane, peroxisomes, ER, autophagosome, and lysosomes, termed mitochondria-associated membranes (MAMs) (Figure 3). MAMs create unique environments or platforms for the localization and activity of components that function in shared interorganellar functions, such as Ca²⁺ homeostasis and lipid biosynthesis (Hayashi et al., 2009; Rizzuto and Pozzan, 2006; Voelker, 2009). Physical tethers are also thought to be important to stably position mitochondria at specific locations within cells, for example, in the axons and dendrites of neurons or in muscle fibers for efficient energy utilization (García-Pérez et al., 2011; Kang et al., 2008).

Communication of mitochondria with intracellular structures also occurs via small vesicles that bud off of mitochondria in a DRP1-independent manner (Neuspiel et al., 2008). Interestingly, treatment of cells with antimycin A, an inhibitor of complex

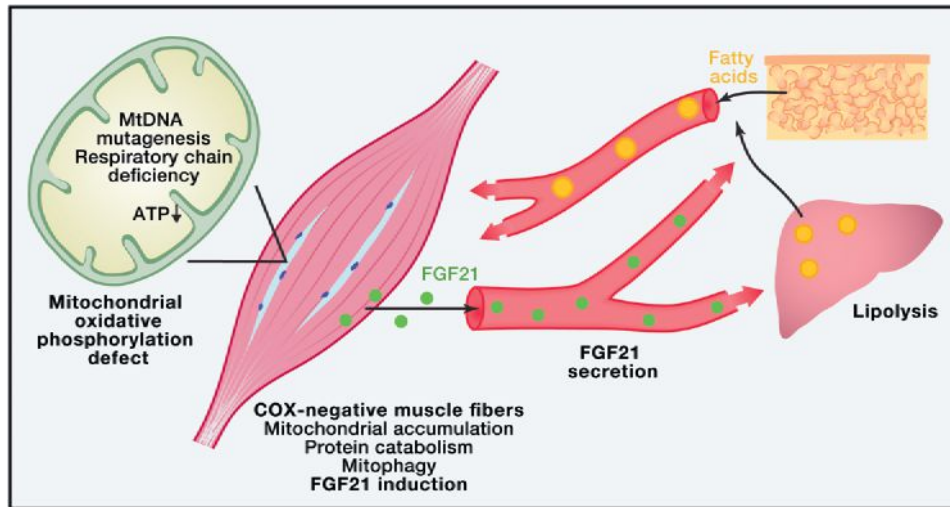


Figure 4. Organismal Effects of Mitochondrial Respiratory Chain Deficiency

Skeletal muscle interprets mitochondrial OXPHOS defect as a starvation response in the presence of normal nutrition. The defective muscle fibers secrete FGF21, a hormone-like cytokine, to blood circulation, mobilizing lipids from storage fat, affecting whole-organism lipid metabolism as a chronic response.

III, stimulates the biogenesis of vesicles that carry mitochondrial cargo that fuse with lysosomes, suggesting that this pathway functions in quality control (Soubannier et al., 2012).

A role for ER mitochondrial contacts has been shown in both mitochondrial division and in apoptosis, which has broader implications for understanding how mitochondrial dysfunction contributes to disease. Ca^{2+} release at ER-mitochondrial contacts may sensitize mitochondria to apoptotic effectors (Breckenridge et al., 2003; Iwasawa et al., 2011; Tabas and Ron, 2011). During mitochondrial division, ER tubules wrap around and likely constrict mitochondria and mark sites of mitochondrial division—a process conserved from yeast to mammals (Friedman et al., 2011). In this context, the observation that Bax colocalizes with DRP1 at sites of mitochondrial constriction during apoptosis (Karbowski et al., 2002; Nechushtan et al., 2001) raises the possibility that Bax-dependent MOMP occurs at and depends on regions of ER-mitochondria contact. ER stress and mitochondrial dysfunction have been implicated in a shared set of diseases associated with altered mitochondrial dynamics. Thus, these observations raise the possibility that alterations in ER-mitochondrial contacts are a contributory factor in human disease (Schon and Przedborski, 2011).

Organismal Roles of Mitochondria

Recent studies demonstrate that a defect in mitochondrial function in one tissue has consequences for the whole organism and have expanded our view of mitochondria beyond their cell autonomous roles. In mouse models of mitochondrial disease and in human patients, OXPHOS-deficient skeletal muscle secretes FGF21, a cytokine that enters the blood and circulates (Suomalainen et al., 2011; Tynnismaa et al., 2010) (Figure 4). FGF21 is a fasting-related hormone, which induces ketogenesis in the liver and mobilizes lipids from adipose tissue for oxidation (Badman et al., 2009; Hotta et al., 2009; Kharitonov et al., 2005). In mitochondrial disease, FGF21 is constitutively secreted from pseudostarving OXPHOS-deficient muscle fibers, resulting in

chronic lipid recruitment from adipose tissue and metabolic derangement (Figure 4). Another muscle-secreted cytokine, irisin, was recently shown to mediate the differentiation of white adipose cells to brown fat in response to exercise and PGC-1 α -induced mitochondrial biogenesis in skeletal muscle (Boström et al., 2012). A non-cell-autonomous mitochondrial regulatory pathway was also reported in *C. elegans*: a tissue-specific RNA interference-mediated knockdown of cytochrome c oxidase subunit in neurons causes a local cellular stress response in neurons that is also communicated to the gut (Durieux et al., 2011). The cellular response is an unfolded protein stress response pathway specific to mitochondria (UPRmt) that also exists in mammals (Haynes and Ron, 2010). UPRmt originates in mitochondria from the accumulation of unassembled respiratory complex subunits and is communicated to the nucleus via an unknown mechanism where it culminates in the regulated expression of mitochondrial protein chaperones, such as HSP-60 (Benedetti et al., 2006; Haynes et al., 2007; Haynes and Ron, 2010; Yoneda et al., 2004; Zhao et al., 2002). The mechanism by which activation of the UPRmt is propagated in a non-cell-autonomous manner is also not known, but has been speculated to occur via a “mitokine” that signals OXPHOS deficiency to the whole organism. In addition to peptides, candidates for long range signaling molecules include metabolites and amino acids, whose levels can be easily sensed by over considerable distances by cells and tissues. The finding that a single dysfunctional tissue or cell can tune or reprogram the whole organism via secreted signaling molecules is a new concept in mitochondrial disease. These relatively unexplored pathways are likely an essential part of pathogenesis and by their secretory nature are attractive targets for therapy.

Several outstanding questions are raised by these observations. Are only some tissues capable of initiating whole-organism energy metabolic reprogramming? In humans, brain-specific mitochondrial disorders show low FGF21 levels (Suomalainen et al., 2011), suggesting that brain tissue is not the source for

FGF21 secretion. Does chronic starvation produce harmful signals that influence disease progression? Is signaling limited to energy deficiency, or can other organelles induce cytokine reprogramming as well? Answers to these questions will provide crucial insight into the tissue specific manifestations of mitochondrial disorders.

Perspective

Mitochondrial function and behavior are central to the physiology of humans and, consequently, “mitochondrial dysfunction” has been implicated in a wide range of diseases that encompass all aspects of medicine. The complexity of mitochondrial functions and thus “mitochondrial dysfunction,” however, are challenges to unravel, but these challenges must be met to determine whether mitochondrial manipulation can be harnessed therapeutically. Continued basic biological approaches are critical so that we can understand on a molecular level known pathways and characterize new pathways that impact mitochondrial behavior and functions. The development of animal models that faithfully mimic human mitochondrial disease mutations is also essential to understand the physiological significance of these pathways, to unravel the highly tissue specific functions and regulation of mitochondria, and to develop therapeutics (Johnson et al., 2007a, 2007b; Tynismaa and Suomalainen, 2009). These systems provide the opportunity to determine how “mitochondrial dysfunction” regulates or alters key pathways, which is another critical piece of the puzzle of mitochondrial-linked diseases. Systems-based approaches, such as mapping the genetic interactions between genes encoding mitochondrial proteins, will be required to elucidate the interactions between mitochondrial functions. The first mitochondrial focused map has now been constructed in yeast and reveals the dense and significant connections between mitochondrial localized pathways distributed in different mitochondrial compartments (Hoppins et al., 2011a). Recent technological developments will allow for systems based biochemical, metabolic and genomic approaches, which will provide invaluable insight into mitochondrial biology. These approaches will enable the construction of a complete mitochondrial network map that will be invaluable for understanding the role of “mitochondrial dysfunction” in human disease. The utilization of next-generation sequencing technology advances that exploit the mitochondrial proteome has and will continue to greatly accelerate these advances (Calvo et al., 2012; Tynismaa et al., 2012). Sequencing advances will continue to lead to the identification of novel mitochondrial proteins and pathways and have already enabled more streamlined diagnosis and the opportunity for genetic counseling for patients with mitochondrial diseases. In combination with intelligent strategies to screen the rich repertoire of existing small molecule libraries, these approaches hold the promise of future cures.

ACKNOWLEDGMENTS

The authors would like to express thanks to members of the Nunnari lab for discussions and manuscript editing. J.N. is supported by National Institutes of Health grants R01GM062942 and R01GM097432. A.S. is supported by

the Sigrid Jusélius Foundation, Jane and Aatos Erkkö Foundation, Academy of Finland, European Research Council, University of Helsinki, and Helsinki University Central Hospital. The authors wish to thank Helena Schmidt for figure art.

REFERENCES

- Ahlgqvist, K.J., Hämäläinen, R.H., Yatsuga, S., Uutela, M., Terzioglu, M., Götz, A., Forsström, S., Salven, P., Angers-Loustau, A., Kopra, O.H., et al. (2012). Somatic progenitor cell vulnerability to mitochondrial DNA mutagenesis underlies progeroid phenotypes in Polg mutator mice. *Cell Metab.* *15*, 100–109.
- Ahola-Erkilä, S., Carroll, C.J., Peltola-Mjösund, K., Tulkki, V., Mattila, I., Seppänen-Laakso, T., Oresic, M., Tynismaa, H., and Suomalainen, A. (2010). Ketogenic diet slows down mitochondrial myopathy progression in mice. *Hum. Mol. Genet.* *19*, 1974–1984.
- Al Rawi, S., Louvet-Vallée, S., Djeddi, A., Sachse, M., Culetto, E., Hajjar, C., Boyd, L., Legouis, R., and Galy, V. (2011). Postfertilization autophagy of sperm organelles prevents paternal mitochondrial DNA transmission. *Science* *334*, 1144–1147.
- Alexander, C., Votruba, M., Pesch, U.E.A., Thiselton, D.L., Mayer, S., Moore, A., Rodriguez, M., Kellner, U., Leo-Kottler, B., Auburger, G., et al. (2000). OPA1, encoding a dynamin-related GTPase, is mutated in autosomal dominant optic atrophy linked to chromosome 3q28. *Nat. Genet.* *26*, 211–215.
- Anton, F., Fres, J.M., Schauss, A., Pinson, B., Praefcke, G.J., Langer, T., and Escobar-Henriques, M. (2011). Ugo1 and Mdm30 act sequentially during Fzo1-mediated mitochondrial outer membrane fusion. *J. Cell Sci.* *124*, 1126–1135.
- Arany, Z., Foo, S.Y., Ma, Y., Ruas, J.L., Bommi-Reddy, A., Girmun, G., Cooper, M., Laznik, D., Chinsomboon, J., Rangwala, S.M., et al. (2008). HIF-independent regulation of VEGF and angiogenesis by the transcriptional coactivator PGC-1 α . *Nature* *451*, 1008–1012.
- Arnaudo, E., Dalakas, M., Shanske, S., Moraes, C.T., DiMauro, S., and Schon, E.A. (1991). Depletion of muscle mitochondrial DNA in AIDS patients with zidovudine-induced myopathy. *Lancet* *337*, 508–510.
- Ashrafian, H., Docherty, L., Leo, V., Towilson, C., Neilan, M., Steeples, V., Lygate, C.A., Hough, T., Townsend, S., Williams, D., et al. (2010). A mutation in the mitochondrial fission gene Dnm11 leads to cardiomyopathy. *PLoS Genet.* *6*, e1001000.
- Badman, M.K., Koester, A., Flier, J.S., Kharitonov, A., and Maratos-Flier, E. (2009). Fibroblast growth factor 21-deficient mice demonstrate impaired adaptation to ketosis. *Endocrinology* *150*, 4931–4940.
- Baloh, R.H., Schmidt, R.E., Pestronk, A., and Milbrandt, J. (2007). Altered axonal mitochondrial transport in the pathogenesis of Charcot-Marie-Tooth disease from mitofusin 2 mutations. *J. Neurosci.* *27*, 422–430.
- Battersby, B.J., Redpath, M.E., and Shoubridge, E.A. (2005). Mitochondrial DNA segregation in hematopoietic lineages does not depend on MHC presentation of mitochondrially encoded peptides. *Hum. Mol. Genet.* *14*, 2587–2594.
- Baughman, J.M., Perocchi, F., Girgis, H.S., Plovanich, M., Belcher-Timme, C.A., Sancak, Y., Bao, X.R., Strittmatter, L., Goldberger, O., Bogorad, R.L., et al. (2011). Integrative genomics identifies MCU as an essential component of the mitochondrial calcium uniporter. *Nature* *476*, 341–345.
- Baysal, B.E., Ferrell, R.E., Willett-Brozick, J.E., Lawrence, E.C., Myssiorek, D., Bosch, A., van der Mey, A., Taschner, P.E., Rubinstein, W.S., Myers, E.N., et al. (2000). Mutations in SDHD, a mitochondrial complex II gene, in hereditary paraganglioma. *Science* *287*, 848–851.
- Bender, A., Krishnan, K.J., Morris, C.M., Taylor, G.A., Reeve, A.K., Perry, R.H., Jaros, E., Hershenson, J.S., Betts, J., Klopstock, T., et al. (2006). High levels of mitochondrial DNA deletions in substantia nigra neurons in aging and Parkinson disease. *Nat. Genet.* *38*, 515–517.
- Benedetti, C., Haynes, C.M., Yang, Y., Harding, H.P., and Ron, D. (2006). Ubiquitin-like protein 5 positively regulates chaperone gene expression in the mitochondrial unfolded protein response. *Genetics* *174*, 229–239.

- Bogner, C., Leber, B., and Andrews, D.W. (2010). Apoptosis: embedded in membranes. *Curr. Opin. Cell Biol.* 22, 845–851.
- Boström, P., Wu, J., Jedrychowski, M.P., Korde, A., Ye, L., Lo, J.C., Rasbach, K.A., Boström, E.A., Choi, J.H., Long, J.Z., et al. (2012). A PGC1- α -dependent myokine that drives brown-fat-like development of white fat and thermogenesis. *Nature* 481, 463–468.
- Braschi, E., Zunino, R., and McBride, H.M. (2009). MAPL is a new mitochondrial SUMO E3 ligase that regulates mitochondrial fission. *EMBO Rep.* 10, 748–754.
- Breckenridge, D.G., Germain, M., Mathai, J.P., Nguyen, M., and Shore, G.C. (2003). Regulation of apoptosis by endoplasmic reticulum pathways. *Oncogene* 22, 8608–8618.
- Brooks, C., Wei, Q., Cho, S.G., and Dong, Z. (2009). Regulation of mitochondrial dynamics in acute kidney injury in cell culture and rodent models. *J. Clin. Invest.* 119, 1275–1285.
- Brown, T.A., Tkachuk, A.N., Shtengel, G., Kopek, B.G., Bogenhagen, D.F., Hess, H.F., and Clayton, D.A. (2011). Superresolution fluorescence imaging of mitochondrial nucleoids reveals their spatial range, limits, and membrane interaction. *Mol. Cell Biol.* 31, 4994–5010.
- Calvo, S.E., Compton, A.G., Hershman, S.G., Lim, S.C., Lieber, D.S., Tucker, E.J., Laskowski, A., Garone, C., Liu, S., Jaffe, D.B., et al. (2012). Molecular diagnosis of infantile mitochondrial disease with targeted next-generation sequencing. *Sci. Transl. Med.* 4, ra10.
- Cantó, C., Gerhart-Hines, Z., Feige, J.N., Lagouge, M., Noriega, L., Milne, J.C., Elliott, P.J., Puigserver, P., and Auwerx, J. (2009). AMPK regulates energy expenditure by modulating NAD⁺ metabolism and SIRT1 activity. *Nature* 458, 1056–1060.
- Cantó, C., Jiang, L.Q., Deshmukh, A.S., Matak, C., Coste, A., Lagouge, M., Zierath, J.R., and Auwerx, J. (2010). Interdependence of AMPK and SIRT1 for metabolic adaptation to fasting and exercise in skeletal muscle. *Cell Metab.* 11, 213–219.
- Carling, D., Mayer, F.V., Sanders, M.J., and Gamblin, S.J. (2011). AMP-activated protein kinase: nature's energy sensor. *Nat. Chem. Biol.* 7, 512–518.
- Cassidy-Stone, A., Chipuk, J.E., Ingberman, E., Song, C., Yoo, C., Kuwana, T., Kurth, M.J., Shaw, J.T., Hinshaw, J.E., Green, D.R., and Nunnari, J. (2008). Chemical inhibition of the mitochondrial division dynamin reveals its role in Bax/Bak-dependent mitochondrial outer membrane permeabilization. *Dev. Cell* 14, 193–204.
- Chan, N.C., Salazar, A.M., Pham, A.H., Sweredoski, M.J., Kolawa, N.J., Graham, R.L., Hess, S., and Chan, D.C. (2011). Broad activation of the ubiquitin-proteasome system by Parkin is critical for mitophagy. *Hum. Mol. Genet.* 20, 1726–1737.
- Chen, H., Detmer, S.A., Ewald, A.J., Griffin, E.E., Fraser, S.E., and Chan, D.C. (2003). Mitofusins Mfn1 and Mfn2 coordinately regulate mitochondrial fusion and are essential for embryonic development. *J. Cell Biol.* 160, 189–200.
- Chen, H., Chomyn, A., and Chan, D.C. (2005). Disruption of fusion results in mitochondrial heterogeneity and dysfunction. *J. Biol. Chem.* 280, 26185–26192.
- Chen, H., McCaffery, J.M., and Chan, D.C. (2007). Mitochondrial fusion protects against neurodegeneration in the cerebellum. *Cell* 130, 548–562.
- Chen, M.L., Logan, T.D., Hochberg, M.L., Shelat, S.G., Yu, X., Wilding, G.E., Tan, W., Kujoth, G.C., Prolla, T.A., Selak, M.A., et al. (2009). Erythroid dysplasia, megaloblastic anemia, and impaired lymphopoiesis arising from mitochondrial dysfunction. *Blood* 114, 4045–4053.
- Chen, H., Vermulst, M., Wang, Y.E., Chomyn, A., Prolla, T.A., McCaffery, J.M., and Chan, D.C. (2010). Mitochondrial fusion is required for mtDNA stability in skeletal muscle and tolerance of mtDNA mutations. *Cell* 141, 280–289.
- Chipuk, J.E., Moldoveanu, T., Llambi, F., Parsons, M.J., and Green, D.R. (2010). The BCL-2 family reunion. *Mol. Cell* 37, 299–310.
- Cho, D.H., Nakamura, T., and Lipton, S.A. (2010). Mitochondrial dynamics in cell death and neurodegeneration. *Cell. Mol. Life Sci.* 67, 3435–3447.
- Cipolat, S., Rudka, T., Hartmann, D., Costa, V., Serneels, L., Craessaerts, K., Metzger, K., Frezza, C., Annaert, W., D'Adamo, L., et al. (2006). Mitochondrial rhomboid PARL regulates cytochrome c release during apoptosis via OPA1-dependent cristae remodeling. *Cell* 126, 163–175.
- Clark, I.E., Dodson, M.W., Jiang, C., Cao, J.H., Huh, J.R., Seol, J.H., Yoo, S.J., Hay, B.A., and Guo, M. (2006). Drosophila pink1 is required for mitochondrial function and interacts genetically with parkin. *Nature* 441, 1162–1166.
- Claypool, S.M., Oktay, Y., Boontheung, P., Loo, J.A., and Koehler, C.M. (2008). Cardiolipin defines the interactome of the major ADP/ATP carrier protein of the mitochondrial inner membrane. *J. Cell Biol.* 182, 937–950.
- Cleland, M.M., Norris, K.L., Karbowski, M., Wang, C., Suen, D.F., Jiao, S., George, N.M., Luo, X., Li, Z., and Youle, R.J. (2011). Bcl-2 family interaction with the mitochondrial morphogenesis machinery. *Cell Death Differ.* 18, 235–247.
- Corton, J.M., Gillespie, J.G., Hawley, S.A., and Hardie, D.G. (1995). 5-aminoimidazole-4-carboxamide ribonucleoside. A specific method for activating AMP-activated protein kinase in intact cells? *Eur. J. Biochem.* 229, 558–565.
- Costa, V., Giacomello, M., Hudec, R., Lopreato, R., Ermak, G., Lim, D., Mallorn, W., Davies, K.J., Carafoli, E., and Scorrano, L. (2010). Mitochondrial fission and cristae disruption increase the response of cell models of Huntington's disease to apoptotic stimuli. *EMBO Mol Med* 2, 490–503.
- Cui, M., Tang, X., Christian, W.V., Yoon, Y., and Tieu, K. (2010). Perturbations in mitochondrial dynamics induced by human mutant PINK1 can be rescued by the mitochondrial division inhibitor mdivi-1. *J. Biol. Chem.* 285, 11740–11752.
- Davey, K.M., Parboosingh, J.S., McLeod, D.R., Chan, A., Casey, R., Ferreira, P., Snyder, F.F., Bridge, P.J., and Bernier, F.P. (2006). Mutation of DNAJC19, a human homologue of yeast inner mitochondrial membrane co-chaperones, causes DCMA syndrome, a novel autosomal recessive Barth syndrome-like condition. *J. Med. Genet.* 43, 385–393.
- Davis, G.C., Williams, A.C., Markey, S.P., Ebert, M.H., Caine, E.D., Reichert, C.M., and Kopin, I.J. (1979). Chronic Parkinsonism secondary to intravenous injection of meperidine analogues. *Psychiatry Res.* 1, 249–254.
- De Stefani, D., Raffaello, A., Teardo, E., Szabò, I., and Rizzuto, R. (2011). A forty-kilodalton protein of the inner membrane is the mitochondrial calcium uniporter. *Nature* 476, 336–340.
- Delettre, C., Lenaers, G., Griffoin, J.-M., Gigarel, N., Lorenzo, C., Belenguer, P., Pelloquin, L., Grosgeorge, J., Turc-Carel, C., Perret, E., et al. (2000). Nuclear gene OPA1, encoding a mitochondrial dynamin-related protein, is mutated in dominant optic atrophy. *Nat. Genet.* 26, 207–210.
- Deng, H., Dodson, M.W., Huang, H., and Guo, M. (2008). The Parkinson's disease genes pink1 and parkin promote mitochondrial fission and/or inhibit fusion in Drosophila. *Proc. Natl. Acad. Sci. USA* 105, 14503–14508.
- DeVay, R.M., Dominguez-Ramirez, L., Lackner, L.L., Hoppins, S., Stahlberg, H., and Nunnari, J. (2009). Coassembly of Mgm1 isoforms requires cardiolipin and mediates mitochondrial inner membrane fusion. *J. Cell Biol.* 186, 793–803.
- Diaz, F., Kotarsky, H., Fellman, V., and Moraes, C.T. (2011). Mitochondrial disorders caused by mutations in respiratory chain assembly factors. *Semin. Fetal Neonatal Med.* 16, 197–204.
- Dickey, A.S., and Strack, S. (2011). PKA/AKAP1 and PP2A/B β 2 regulate neuronal morphogenesis via Drp1 phosphorylation and mitochondrial bioenergetics. *J. Neurosci.* 31, 15716–15726.
- Durieux, J., Wolff, S., and Dillin, A. (2011). The cell-non-autonomous nature of electron transport chain-mediated longevity. *Cell* 144, 79–91.
- Durr, M., Escobar-Henriques, M., Merz, S., Geimer, S., Langer, T., and Westermann, B. (2006). Nonredundant roles of mitochondria-associated F-box proteins Mfb1 and Mdm30 in maintenance of mitochondrial morphology in yeast. *Mol. Biol. Cell* 17, 3745–3755.
- Efremov, R.G., and Sazanov, L.A. (2011). Respiratory complex I: 'steam engine' of the cell? *Curr. Opin. Struct. Biol.* 21, 532–540.
- Ehse, S., Raschke, I., Mancuso, G., Bernacchia, A., Geimer, S., Tondera, D., Martinou, J.C., Westermann, B., Rugarli, E.I., and Langer, T. (2009). Regulation of OPA1 processing and mitochondrial fusion by m-AAA protease isoenzymes and OMA1. *J. Cell Biol.* 187, 1023–1036.

- Euro, L., Farnum, G.A., Palin, E., Suomalainen, A., and Kaguni, L.S. (2011). Clustering of Alpers disease mutations and catalytic defects in biochemical variants reveal new features of molecular mechanism of the human mitochondrial replicase, Pol γ . *Nucleic Acids Res.* *39*, 9072–9084.
- Fan, W., Waymire, K.G., Narula, N., Li, P., Rocher, C., Coskun, P.E., Vannan, M.A., Narula, J., Macgregor, G.R., and Wallace, D.C. (2008). A mouse model of mitochondrial disease reveals germline selection against severe mtDNA mutations. *Science* *319*, 958–962.
- Frank, S., Gaume, B., Bergmann-Leitner, E.S., Leitner, W.W., Robert, E.G., Catez, F., Smith, C.L., and Youle, R.J. (2001). The role of dynamin-related protein 1, a mediator of mitochondrial fission, in apoptosis. *Dev. Cell* *1*, 515–525.
- Frezza, C., Cipolat, S., Martins de Brito, O., Micaroni, M., Beznoussenko, G.V., Rudka, T., Bartoli, D., Polishuck, R.S., Danial, N.N., De Strooper, B., and Scorrano, L. (2006). OPA1 controls apoptotic cristae remodeling independently from mitochondrial fusion. *Cell* *126*, 177–189.
- Friedman, J.R., Lackner, L.L., West, M., DiBenedetto, J.R., Nunnari, J., and Voeltz, G.K. (2011). ER tubules mark sites of mitochondrial division. *Science* *334*, 358–362.
- Gabaldón, T., and Huynen, M.A. (2004). Prediction of protein function and pathways in the genome era. *Cell. Mol. Life Sci.* *61*, 930–944.
- García-Pérez, C., Schneider, T.G., Hajnóczky, G., and Csordás, G. (2011). Alignment of sarcoplasmic reticulum-mitochondrial junctions with mitochondrial contact points. *Am. J. Physiol. Heart Circ. Physiol.* *301*, H1907–H1915.
- Gaston, D., Tsaousis, A.D., and Roger, A.J. (2009). Predicting proteomes of mitochondria and related organelles from genomic and expressed sequence tag data. *Methods Enzymol.* *457*, 21–47.
- Gegg, M.E., Cooper, J.M., Chau, K.Y., Rojo, M., Schapira, A.H., and Taanman, J.W. (2010). Mitofusin 1 and mitofusin 2 are ubiquitinated in a PINK1/parkin-dependent manner upon induction of mitophagy. *Hum. Mol. Genet.* *19*, 4861–4870.
- Glater, E.E., Megeath, L.J., Stowers, R.S., and Schwarz, T.L. (2006). Axonal transport of mitochondria requires miltin to recruit kinesin heavy chain and is light chain independent. *J. Cell Biol.* *173*, 545–557.
- Golubitzky, A., Dan, P., Weissman, S., Link, G., Wikstrom, J.D., and Saada, A. (2011). Screening for active small molecules in mitochondrial complex I deficient patient's fibroblasts, reveals AICAR as the most beneficial compound. *PLoS ONE* *6*, e26883.
- Gomes, L.C., Di Benedetto, G., and Scorrano, L. (2011a). During autophagy mitochondria elongate, are spared from degradation and sustain cell viability. *Nat. Cell Biol.* *13*, 589–598.
- Gomes, L.C., Di Benedetto, G., and Scorrano, L. (2011b). Essential amino acids and glutamine regulate induction of mitochondrial elongation during autophagy. *Cell Cycle* *10*, 2635–2639.
- Götz, A., Tyyntismaa, H., Euro, L., Ellonen, P., Hyötyläinen, T., Ojala, T., Hämäläinen, R.H., Tommiska, J., Raivio, T., Oresic, M., et al. (2011). Exome sequencing identifies mitochondrial alanyl-tRNA synthetase mutations in infantile mitochondrial cardiomyopathy. *Am. J. Hum. Genet.* *88*, 635–642.
- Greene, J.C., Whitworth, A.J., Kuo, I., Andrews, L.A., Feany, M.B., and Palanck, L.J. (2003). Mitochondrial pathology and apoptotic muscle degeneration in *Drosophila parkin* mutants. *Proc. Natl. Acad. Sci. USA* *100*, 4078–4083.
- Griffin, E.E., and Chan, D.C. (2006). Domain interactions within Fzo1 oligomers are essential for mitochondrial fusion. *J. Biol. Chem.* *281*, 16599–16606.
- Hakonen, A.H., Heiskanen, S., Juvonen, V., Lappalainen, I., Luoma, P.T., Rantamaki, M., Goethem, G.V., Lofgren, A., Hackman, P., Paetau, A., et al. (2005). Mitochondrial DNA polymerase W748S mutation: a common cause of autosomal recessive ataxia with ancient European origin. *Am. J. Hum. Genet.* *77*, 430–441.
- Hamanaka, R.B., and Chandel, N.S. (2010). Mitochondrial reactive oxygen species regulate cellular signaling and dictate biological outcomes. *Trends Biochem. Sci.* *35*, 505–513.
- Hardie, D.G., Carling, D., and Gamblin, S.J. (2011). AMP-activated protein kinase: also regulated by ADP? *Trends Biochem. Sci.* *36*, 470–477.
- Harner, M., Körner, C., Walther, D., Mokranjac, D., Kaesmacher, J., Welsch, U., Griffith, J., Mann, M., Reggiori, F., and Neupert, W. (2011). The mitochondrial contact site complex, a determinant of mitochondrial architecture. *EMBO J.* *30*, 4356–4370.
- Hayashi, T., Rizzuto, R., Hajnoczky, G., and Su, T.P. (2009). MAM: more than just a housekeeper. *Trends Cell Biol.* *19*, 81–88.
- Haynes, C.M., and Ron, D. (2010). The mitochondrial UPR - protecting organelle protein homeostasis. *J. Cell Sci.* *123*, 3849–3855.
- Haynes, C.M., Petrova, K., Benedetti, C., Yang, Y., and Ron, D. (2007). ClpP mediates activation of a mitochondrial unfolded protein response in *C. elegans*. *Dev. Cell* *13*, 467–480.
- Head, B., Griparic, L., Amiri, M., Gandre-Babbe, S., and van der Bliek, A.M. (2009). Inducible proteolytic inactivation of OPA1 mediated by the OMA1 protease in mammalian cells. *J. Cell Biol.* *187*, 959–966.
- Heo, J.M., Livnat-Levanon, N., Taylor, E.B., Jones, K.T., Dephoure, N., Ring, J., Xie, J., Brodsky, J.L., Madeo, F., Gygi, S.P., et al. (2010). A stress-responsive system for mitochondrial protein degradation. *Mol. Cell* *40*, 465–480.
- Hermann, G.J., Thatcher, J.W., Mills, J.P., Hales, K.G., Fuller, M.T., Nunnari, J., and Shaw, J.M. (1998). Mitochondrial fusion in yeast requires the transmembrane GTPase Fzo1p. *J. Cell Biol.* *143*, 359–373.
- Hollenbeck, P.J., and Saxton, W.M. (2005). The axonal transport of mitochondria. *J. Cell Sci.* *118*, 5411–5419.
- Holt, I.J., Harding, A.E., and Morgan-Hughes, J.A. (1988). Deletions of muscle mitochondrial DNA in patients with mitochondrial myopathies. *Nature* *331*, 717–719.
- Holt, I.J., Harding, A.E., Petty, R.K., and Morgan-Hughes, J.A. (1990). A new mitochondrial disease associated with mitochondrial DNA heteroplasmy. *Am. J. Hum. Genet.* *46*, 428–433.
- Hoppeler, H., and Fluck, M. (2003). Plasticity of skeletal muscle mitochondria: structure and function. *Med. Sci. Sports Exerc.* *35*, 95–104.
- Hoppins, S., Lackner, L., and Nunnari, J. (2007). The machines that divide and fuse mitochondria. *Annu. Rev. Biochem.* *76*, 751–780.
- Hoppins, S., Collins, S.R., Cassidy-Stone, A., Hummel, E., Devay, R.M., Lackner, L.L., Westermann, B., Schuldiner, M., Weissman, J.S., and Nunnari, J. (2011a). A mitochondrial-focused genetic interaction map reveals a scaffold-like complex required for inner membrane organization in mitochondria. *J. Cell Biol.* *195*, 323–340.
- Hoppins, S., Edlich, F., Cleland, M.M., Banerjee, S., McCaffery, J.M., Youle, R.J., and Nunnari, J. (2011b). The soluble form of Bax regulates mitochondrial fusion via MFN2 homotypic complexes. *Mol. Cell* *41*, 150–160.
- Hotta, Y., Nakamura, H., Konishi, M., Murata, Y., Takagi, H., Matsumura, S., Inoue, K., Fushiki, T., and Itoh, N. (2009). Fibroblast growth factor 21 regulates lipolysis in white adipose tissue but is not required for ketogenesis and triglyceride clearance in liver. *Endocrinology* *150*, 4625–4633.
- Hutchin, T., Haworth, I., Higashi, K., Fischel-Ghodsian, N., Stoneking, M., Saha, N., Arnos, C., and Cortopassi, G. (1993). A molecular basis for human hypersensitivity to aminoglycoside antibiotics. *Nucleic Acids Res.* *21*, 4174–4179.
- Ingerman, E., Perkins, E.M., Marino, M., Mears, J.A., McCaffery, J.M., Hinshaw, J.E., and Nunnari, J. (2005). Dnm1 forms spirals that are structurally tailored to fit mitochondria. *J. Cell Biol.* *170*, 1021–1027.
- Ishihara, N., Nomura, M., Jofuku, A., Kato, H., Suzuki, S.O., Masuda, K., Otera, H., Nakanishi, Y., Nonaka, I., Goto, Y., et al. (2009). Mitochondrial fission factor Drp1 is essential for embryonic development and synapse formation in mice. *Nat. Cell Biol.* *11*, 958–966.
- Ishikawa, K., Toyama-Sorimachi, N., Nakada, K., Morimoto, M., Imanishi, H., Yoshizaki, M., Sasawatari, S., Niikura, M., Takenaga, K., Yonekawa, H., and Hayashi, J. (2010). The innate immune system in host mice targets cells with allogenic mitochondrial DNA. *J. Exp. Med.* *207*, 2297–2305.
- Ito, K., Hirao, A., Arai, F., Matsuoka, S., Takubo, K., Hamaguchi, I., Nomiya, K., Hosokawa, K., Sakurada, K., Nakagata, N., et al. (2004). Regulation of oxidative stress by ATM is required for self-renewal of haematopoietic stem cells. *Nature* *431*, 997–1002.

- Iwasawa, R., Mahul-Mellier, A.-L., Datler, C., Pazarentzos, E., and Grimm, S. (2011). Fis1 and Bap31 bridge the mitochondria-ER interface to establish a platform for apoptosis induction. *EMBO J. 30*, 556–568.
- Jagasia, R., Grote, P., Westermann, B., and Conradt, B. (2005). DRP-1-mediated mitochondrial fragmentation during EGL-1-induced cell death in *C. elegans*. *Nature 433*, 754–760.
- Jäger, S., Handschin, C., St-Pierre, J., and Spiegelman, B.M. (2007). AMP-activated protein kinase (AMPK) action in skeletal muscle via direct phosphorylation of PGC-1 α . *Proc. Natl. Acad. Sci. USA 104*, 12017–12022.
- Jeninga, E.H., Schoonjans, K., and Auwerx, J. (2010). Reversible acetylation of PGC-1: connecting energy sensors and effectors to guarantee metabolic flexibility. *Oncogene 29*, 4617–4624.
- Jin, H., May, M., Tranebjaerg, L., Kendall, E., Fontán, G., Jackson, J., Subramony, S.H., Arena, F., Lubs, H., Smith, S., et al. (1996). A novel X-linked gene, DDP, shows mutations in families with deafness (DFN-1), dystonia, mental deficiency and blindness. *Nat. Genet. 14*, 177–180.
- Johnson, D.T., Harris, R.A., Blair, P.V., and Balaban, R.S. (2007a). Functional consequences of mitochondrial proteome heterogeneity. *Am. J. Physiol. Cell Physiol. 292*, C698–C707.
- Johnson, D.T., Harris, R.A., French, S., Blair, P.V., You, J., Bemis, K.G., Wang, M., and Balaban, R.S. (2007b). Tissue heterogeneity of the mammalian mitochondrial proteome. *Am. J. Physiol. Cell Physiol. 292*, C689–C697.
- Jokinen, R., Marttinen, P., Sandell, H.K., Manninen, T., Teerenhovi, H., Wai, T., Teoli, D., Loredó-Osti, J.C., Shoubridge, E.A., and Battersby, B.J. (2010). Gimap3 regulates tissue-specific mitochondrial DNA segregation. *PLoS Genet. 6*, e1001161.
- Kang, J.S., Tian, J.H., Pan, P.Y., Zald, P., Li, C., Deng, C., and Sheng, Z.H. (2008). Docking of axonal mitochondria by syntaphilin controls their mobility and affects short-term facilitation. *Cell 132*, 137–148.
- Karbowski, M., Lee, Y.J., Gaume, B., Jeong, S.Y., Frank, S., Nechushtan, A., Santel, A., Fuller, M., Smith, C.L., and Youle, R.J. (2002). Spatial and temporal association of Bax with mitochondrial fission sites, Drp1, and Mfn2 during apoptosis. *J. Cell Biol. 159*, 931–938.
- Karbowski, M., Norris, K.L., Cleland, M.M., Jeong, S.Y., and Youle, R.J. (2006). Role of Bax and Bak in mitochondrial morphogenesis. *Nature 443*, 658–662.
- Kharitonov, A., Shiyanova, T.L., Koester, A., Ford, A.M., Micanovic, R., Galbreath, E.J., Sandusky, G.E., Hammond, L.J., Moyers, J.S., Owens, R.A., et al. (2005). FGF-21 as a novel metabolic regulator. *J. Clin. Invest. 115*, 1627–1635.
- Kim, Y., Park, J., Kim, S., Song, S., Kwon, S.K., Lee, S.H., Kitada, T., Kim, J.M., and Chung, J. (2008). PINK1 controls mitochondrial localization of Parkin through direct phosphorylation. *Biochem. Biophys. Res. Commun. 377*, 975–980.
- Kim, K.Y., Stevens, M.V., Akter, M.H., Rusk, S.E., Huang, R.J., Cohen, A., Noguchi, A., Springer, D., Bocharov, A.V., Eggerman, T.L., et al. (2011). Parkin is a lipid-responsive regulator of fat uptake in mice and mutant human cells. *J. Clin. Invest. 121*, 3701–3712.
- Kitada, T., Asakawa, S., Hattori, N., Matsumine, H., Yamamura, Y., Minoshima, S., Yokochi, M., Mizuno, Y., and Shimizu, N. (1998). Mutations in the parkin gene cause autosomal recessive juvenile parkinsonism. *Nature 392*, 605–608.
- Koivunen, P., Lee, S., Duncan, C.G., Lopez, G., Lu, G., Ramkissoon, S., Losman, J.A., Joensuu, P., Bergmann, U., Gross, S., et al. (2012). Transformation by the (R)-enantiomer of 2-hydroxyglutarate linked to EGLN1 activation. *Nature*. Published online February 15, 2012.
- Kraytsberg, Y., Kudryavtseva, E., McKee, A.C., Geula, C., Kowall, N.W., and Khrapko, K. (2006). Mitochondrial DNA deletions are abundant and cause functional impairment in aged human substantia nigra neurons. *Nat. Genet. 38*, 518–520.
- Kujoth, G.C., Hiona, A., Pugh, T.D., Someya, S., Panzer, K., Wohlgenuth, S.E., Hofer, T., Seo, A.Y., Sullivan, R., Jobling, W.A., et al. (2005). Mitochondrial DNA mutations, oxidative stress, and apoptosis in mammalian aging. *Science 309*, 481–484.
- Kuramoto, N., Wilkins, M.E., Fairfax, B.P., Revilla-Sanchez, R., Terunuma, M., Tamaki, K., Iemata, M., Warren, N., Couve, A., Calver, A., et al. (2007). Phospho-dependent functional modulation of GABA(B) receptors by the metabolic sensor AMP-dependent protein kinase. *Neuron 53*, 233–247.
- Labrousse, A.M., Zappaterra, M.D., Rube, D.A., and van der Bliek, A.M. (1999). *C. elegans* dynamin-related protein DRP-1 controls severing of the mitochondrial outer membrane. *Mol. Cell 4*, 815–826.
- Lackner, L.L., and Nunnari, J. (2010). Small molecule inhibitors of mitochondrial division: tools that translate basic biological research into medicine. *Chem. Biol. 17*, 578–583.
- Lane, N., and Martin, W. (2010). The energetics of genome complexity. *Nature 467*, 929–934.
- Langston, J.W., Ballard, P., Tetrad, J.W., and Irwin, I. (1983). Chronic Parkinsonism in humans due to a product of meperidine-analog synthesis. *Science 219*, 979–980.
- Leclercq, N., Van Der Bruggen, P., and Foury, F. (1997). Mitochondrial DNA polymerases from yeast to man: a new family of polymerases. *Gene 185*, 147–152.
- Lee, Y.J., Jeong, S.Y., Karbowski, M., Smith, C.L., and Youle, R.J. (2004). Roles of the mammalian mitochondrial fission and fusion mediators Fis1, Drp1, and Opa1 in apoptosis. *Mol. Biol. Cell 15*, 5001–5011.
- Li, Z., Okamoto, K., Hayashi, Y., and Sheng, M. (2004). The importance of dendritic mitochondria in the morphogenesis and plasticity of spines and synapses. *Cell 119*, 873–887.
- Lill, R., and Mühlenhoff, U. (2008). Maturation of iron-sulfur proteins in eukaryotes: mechanisms, connected processes, and diseases. *Annu. Rev. Biochem. 77*, 669–700.
- Lin, W., and Kang, U.J. (2008). Characterization of PINK1 processing, stability, and subcellular localization. *J. Neurochem. 106*, 464–474.
- Liu, X., and Hajnóczky, G. (2009). Ca²⁺-dependent regulation of mitochondrial dynamics by the Miro-Milton complex. *Int. J. Biochem. Cell Biol. 41*, 1972–1976.
- Lu, C., Ward, P.S., Kapoor, G.S., Rohle, D., Turcan, S., Abdel-Wahab, O., Edwards, C.R., Khanin, R., Figueroa, M.E., Melnick, A., et al. (2012). IDH mutation impairs histone demethylation and results in a block to cell differentiation. *Nature*. Published online February 15, 2012.
- Luoma, P., Melberg, A., Rinne, J.O., Kaukonen, J.A., Nupponen, N.N., Chalmers, R.M., Oldfors, A., Rautakorpi, I., Peltonen, L., Majamaa, K., et al. (2004). Parkinsonism, premature menopause, and mitochondrial DNA polymerase gamma mutations: clinical and molecular genetic study. *Lancet 364*, 875–882.
- Lutz, A.K., Exner, N., Fett, M.E., Schlehe, J.S., Kloos, K., Lämmermann, K., Brunner, B., Kurz-Drexler, A., Vogel, F., Reichert, A.S., et al. (2009). Loss of parkin or PINK1 function increases Drp1-dependent mitochondrial fragmentation. *J. Biol. Chem. 284*, 22938–22951.
- Macaskill, A.F., Rinholm, J.E., Twelvetrees, A.E., Arancibia-Carcamo, I.L., Muir, J., Fransson, A., Aspenstrom, P., Attwell, D., and Kittler, J.T. (2009). Miro1 is a calcium sensor for glutamate receptor-dependent localization of mitochondria at synapses. *Neuron 61*, 541–555.
- Martinou, J.C., and Youle, R.J. (2011). Mitochondria in apoptosis: Bcl-2 family members and mitochondrial dynamics. *Dev. Cell 21*, 92–101.
- Matsuda, N., Sato, S., Shiba, K., Okatsu, K., Saisho, K., Gautier, C.A., Sou, Y.S., Saiki, S., Kawajiri, S., Sato, F., et al. (2010). PINK1 stabilized by mitochondrial depolarization recruits Parkin to damaged mitochondria and activates latent Parkin for mitophagy. *J. Cell Biol. 189*, 211–221.
- Mayr, J.A., Zimmermann, F.A., Fauth, C., Bergheim, C., Meierhofer, D., Radmayr, D., Zschocke, J., Koch, J., and Sperl, W. (2011). Lipoic acid synthetase deficiency causes neonatal-onset epilepsy, defective mitochondrial energy metabolism, and glycine elevation. *Am. J. Hum. Genet. 89*, 792–797.
- Mihaylova, M.M., and Shaw, R.J. (2011). The AMPK signalling pathway coordinates cell growth, autophagy and metabolism. *Nat. Cell Biol. 13*, 1016–1023.
- Mitchell, P. (1961). Coupling of phosphorylation to electron and hydrogen transfer by a chemi-osmotic type of mechanism. *Nature 191*, 144–148.

- Montessuit, S., Somasekharan, S.P., Terrones, O., Lucken-Ardjomande, S., Herzig, S., Schwarzenbacher, R., Manstein, D.J., Bossy-Wetzel, E., Basañez, G., Meda, P., and Martinou, J.C. (2010). Membrane remodeling induced by the dynamin-related protein Drp1 stimulates Bax oligomerization. *Cell* *142*, 889–901.
- Mootha, V.K., Bunkenborg, J., Olsen, J.V., Hjerrild, M., Wisniewski, J.R., Stahl, E., Bolouri, M.S., Ray, H.N., Sihag, S., Kamal, M., et al. (2003). Integrated analysis of protein composition, tissue diversity, and gene regulation in mouse mitochondria. *Cell* *115*, 629–640.
- Morris, A.A., Leonard, J.V., Brown, G.K., Bidouki, S.K., Bindoff, L.A., Woodward, C.E., Harding, A.E., Lake, B.D., Harding, B.N., Farrell, M.A., et al. (1996). Deficiency of respiratory chain complex I is a common cause of Leigh disease. *Ann. Neurol.* *40*, 25–30.
- Muller, F.L., Liu, Y., and Van Remmen, H. (2004). Complex III releases superoxide to both sides of the inner mitochondrial membrane. *J. Biol. Chem.* *279*, 49064–49073.
- Murphy, M.P. (2009). How mitochondria produce reactive oxygen species. *Biochem. J.* *417*, 1–13.
- Nakamura, N., Kimura, Y., Tokuda, M., Honda, S., and Hirose, S. (2006). MARCH-V is a novel mitofusin 2- and Drp1-binding protein able to change mitochondrial morphology. *EMBO Rep.* *7*, 1019–1022.
- Narasimhaiah, R., Tuchman, A., Lin, S.L., and Naegele, J.R. (2005). Oxidative damage and defective DNA repair is linked to apoptosis of migrating neurons and progenitors during cerebral cortex development in Ku70-deficient mice. *Cereb. Cortex* *15*, 696–707.
- Narendra, D., Tanaka, A., Suen, D.F., and Youle, R.J. (2008). Parkin is recruited selectively to impaired mitochondria and promotes their autophagy. *J. Cell Biol.* *183*, 795–803.
- Narendra, D.P., Jin, S.M., Tanaka, A., Suen, D.F., Gautier, C.A., Shen, J., Cookson, M.R., and Youle, R.J. (2010). PINK1 is selectively stabilized on impaired mitochondria to activate Parkin. *PLoS Biol.* *8*, e1000298.
- Naviaux, R.K., Nyhan, W.L., Barshop, B.A., Poulton, J., Markusic, D., Karpinski, N.C., and Haas, R.H. (1999). Mitochondrial DNA polymerase gamma deficiency and mtDNA depletion in a child with Alpers' syndrome. *Ann. Neurol.* *45*, 54–58.
- Nechushtan, A., Smith, C.L., Lamensdorf, I., Yoon, S.H., and Youle, R.J. (2001). Bax and Bak coalesce into novel mitochondria-associated clusters during apoptosis. *J. Cell Biol.* *153*, 1265–1276.
- Neupert, W., and Herrmann, J.M. (2007). Translocation of proteins into mitochondria. *Annu. Rev. Biochem.* *76*, 723–749.
- Neuspiel, M., Schauss, A.C., Braschi, E., Zunino, R., Rippstein, P., Rachubinski, R.A., Andrade-Navarro, M.A., and McBride, H.M. (2008). Cargo-selected transport from the mitochondria to peroxisomes is mediated by vesicular carriers. *Curr. Biol.* *18*, 102–108.
- Neutzner, A., Youle, R.J., and Karbowski, M. (2007). Outer mitochondrial membrane protein degradation by the proteasome. *Novartis Found. Symp.* *287*, 4–14, discussion 14–20.
- Neutzner, A., Benard, G., Youle, R.J., and Karbowski, M. (2008). Role of the ubiquitin conjugation system in the maintenance of mitochondrial homeostasis. *Ann. N Y Acad. Sci.* *1147*, 242–253.
- Nishimura, T., Nakatake, Y., Konishi, M., and Itoh, N. (2000). Identification of a novel FGF, FGF-21, preferentially expressed in the liver. *Biochim. Biophys. Acta* *1492*, 203–206.
- Norddahl, G.L., Pronk, C.J., Wahlestedt, M., Sten, G., Nygren, J.M., Ugale, A., Sigvardsson, M., and Bryder, D. (2011). Accumulating mitochondrial DNA mutations drive premature hematopoietic aging phenotypes distinct from physiological stem cell aging. *Cell Stem Cell* *8*, 499–510.
- Nunnari, J., Marshall, W., Straight, A., Murray, A., Sedat, J.W., and Walter, P. (1997). Mitochondrial transmission during mating in *Saccharomyces cerevisiae* is determined by mitochondrial fusion and fission and the intramitochondrial segregation of mitochondrial DNA. *Mol. Biol. Cell* *8*, 1233–1242.
- Okuno, D., Iino, R., and Noji, H. (2011). Rotation and structure of FoF1-ATP synthase. *J. Biochem.* *149*, 655–664.
- Olichon, A., Baricault, L., Gas, N., Guillou, E., Valette, A., Belenguer, P., and Lenaers, G. (2003). Loss of OPA1 perturbs the mitochondrial inner membrane structure and integrity, leading to cytochrome c release and apoptosis. *J. Biol. Chem.* *278*, 7743–7746.
- Olichon, A., Landes, T., Arnauné-Pelloquin, L., Emorine, L.J., Mils, V., Guichet, A., Delettre, C., Hamel, C., Amati-Bonneau, P., Bonneau, D., et al. (2007). Effects of OPA1 mutations on mitochondrial morphology and apoptosis: relevance to ADOA pathogenesis. *J. Cell. Physiol.* *211*, 423–430.
- Ong, S.B., Subrayan, S., Lim, S.Y., Yellon, D.M., Davidson, S.M., and Hausenloy, D.J. (2010). Inhibiting mitochondrial fission protects the heart against ischemia/reperfusion injury. *Circulation* *121*, 2012–2022.
- Osman, C., Voelker, D.R., and Langer, T. (2011). Making heads or tails of phospholipids in mitochondria. *J. Cell Biol.* *192*, 7–16.
- Pagliarini, D.J., Calvo, S.E., Chang, B., Sheth, S.A., Vafai, S.B., Ong, S.E., Walford, G.A., Sugiana, C., Boneh, A., Chen, W.K., et al. (2008). A mitochondrial protein compendium elucidates complex I disease biology. *Cell* *134*, 112–123.
- Park, J., Lee, S.B., Lee, S., Kim, Y., Song, S., Kim, S., Bae, E., Kim, J., Shong, M., Kim, J.M., and Chung, J. (2006). Mitochondrial dysfunction in *Drosophila* PINK1 mutants is complemented by parkin. *Nature* *441*, 1157–1161.
- Parone, P.A., Da Cruz, S., Tondera, D., Mattenberger, Y., James, D.I., Maechler, P., Barja, F., and Martinou, J.C. (2008). Preventing mitochondrial fission impairs mitochondrial function and leads to loss of mitochondrial DNA. *PLoS ONE* *3*, e3257.
- Pätsi, J., Kervinen, M., Finel, M., and Hassinen, I.E. (2008). Leber hereditary optic neuropathy mutations in the ND6 subunit of mitochondrial complex I affect ubiquinone reduction kinetics in a bacterial model of the enzyme. *Biochem. J.* *409*, 129–137.
- Paumard, P., Vaillier, J., Couly, B., Schaeffer, J., Soubannier, V., Mueller, D.M., Brèthes, D., di Rago, J.P., and Velours, J. (2002). The ATP synthase is involved in generating mitochondrial cristae morphology. *EMBO J.* *21*, 221–230.
- Perkins, G.A., and Frey, T.G. (2000). Recent structural insight into mitochondria gained by microscopy. *Micron* *31*, 97–111.
- Perry, T.L., Haworth, J.C., and Robinson, B.H. (1985). Brain amino acid abnormalities in pyruvate carboxylase deficiency. *J. Inher. Metab. Dis.* *8*, 63–66.
- Pierce, S.B., Chisholm, K.M., Lynch, E.D., Lee, M.K., Walsh, T., Opitz, J.M., Li, W., Klevit, R.E., and King, M.C. (2011). Mutations in mitochondrial histidyl tRNA synthetase HARS2 cause ovarian dysgenesis and sensorineural hearing loss of Perrault syndrome. *Proc. Natl. Acad. Sci. USA* *108*, 6543–6548.
- Pietiläinen, K.H., Naukkarinen, J., Rissanen, A., Saharinen, J., Ellonen, P., Keränen, H., Suomalainen, A., Götz, A., Suortti, T., Yki-Järvinen, H., et al. (2008). Global transcript profiles of fat in monozygotic twins discordant for BMI: pathways behind acquired obesity. *PLoS Med.* *5*, e51.
- Polianskyte, Z., Peitsaro, N., Dapkunas, A., Liobikas, J., Soliymani, R., Lalowski, M., Speer, O., Seitsonen, J., Butcher, S., Cereghetti, G.M., et al. (2009). LACTB is a filament-forming protein localized in mitochondria. *Proc. Natl. Acad. Sci. USA* *106*, 18960–18965.
- Poole, A.C., Thomas, R.E., Andrews, L.A., McBride, H.M., Whitworth, A.J., and Pallanck, L.J. (2008). The PINK1/Parkin pathway regulates mitochondrial morphology. *Proc. Natl. Acad. Sci. USA* *105*, 1638–1643.
- Poole, A.C., Thomas, R.E., Yu, S., Vincow, E.S., and Pallanck, L. (2010). The mitochondrial fusion-promoting factor mitofusin is a substrate of the PINK1/parkin pathway. *PLoS ONE* *5*, e10054.
- Puigserver, P., Wu, Z., Park, C.W., Graves, R., Wright, M., and Spiegelman, B.M. (1998). A cold-inducible coactivator of nuclear receptors linked to adaptive thermogenesis. *Cell* *92*, 829–839.
- Rahman, S., Poulton, J., Marchington, D., and Suomalainen, A. (2001). Decrease of 3243 A→G mtDNA mutation from blood in MELAS syndrome: a longitudinal study. *Am. J. Hum. Genet.* *68*, 238–240.
- Rambold, A.S., Kostecky, B., Elia, N., and Lippincott-Schwartz, J. (2011). Tubular network formation protects mitochondria from autophagosomal

- degradation during nutrient starvation. *Proc. Natl. Acad. Sci. USA* *108*, 10190–10195.
- Reichert, A.S., and Neupert, W. (2002). Contact sites between the outer and inner membrane of mitochondria—role in protein transport. *Biochim. Biophys. Acta* *1592*, 41–49.
- Rizzuto, R., and Pozzan, T. (2006). Microdomains of intracellular Ca²⁺: molecular determinants and functional consequences. *Physiol. Rev.* *86*, 369–408.
- Rolland, S.G., Lu, Y., David, C.N., and Conradt, B. (2009). The BCL-2-like protein CED-9 of *C. elegans* promotes FZO-1/Mfn1,2- and EAT-3/Opa1-dependent mitochondrial fusion. *J. Cell Biol.* *186*, 525–540.
- Sandoval, H., Thiagarajan, P., Dasgupta, S.K., Schumacher, A., Prchal, J.T., Chen, M., and Wang, J. (2008). Essential role for Nix in autophagic maturation of erythroid cells. *Nature* *454*, 232–235.
- Saotome, M., Safulina, D., Szabadkai, G., Das, S., Fransson, A., Aspenstrom, P., Rizzuto, R., and Hajnóczky, G. (2008). Bidirectional Ca²⁺-dependent control of mitochondrial dynamics by the Miro GTPase. *Proc. Natl. Acad. Sci. USA* *105*, 20728–20733.
- Sato, M., and Sato, K. (2011). Degradation of paternal mitochondria by fertilization-triggered autophagy in *C. elegans* embryos. *Science* *334*, 1141–1144.
- Scheper, G.C., van der Kloek, T., van Andel, R.J., van Berkel, C.G., Sissler, M., Smet, J., Muravina, T.I., Serkov, S.V., Uziel, G., Bugiani, M., et al. (2007). Mitochondrial aspartyl-tRNA synthetase deficiency causes leukoencephalopathy with brain stem and spinal cord involvement and lactate elevation. *Nat. Genet.* *39*, 534–539.
- Schmidt, O., Pfanner, N., and Meisinger, C. (2010). Mitochondrial protein import: from proteomics to functional mechanisms. *Nat. Rev. Mol. Cell Biol.* *11*, 655–667.
- Schon, E.A., and Przedborski, S. (2011). Mitochondria: the next (neuro)degeneration. *Neuron* *70*, 1033–1053.
- Schweers, R.L., Zhang, J., Randall, M.S., Loyd, M.R., Li, W., Dorsey, F.C., Kundu, M., Opferman, J.T., Cleveland, J.L., Miller, J.L., and Ney, P.A. (2007). NIX is required for programmed mitochondrial clearance during reticulocyte maturation. *Proc. Natl. Acad. Sci. USA* *104*, 19500–19505.
- Shirendeb, U.P., Calkins, M.J., Manczak, M., Anekonda, V., Dufour, B., McBride, J.L., Mao, P., and Reddy, P.H. (2012). Mutant huntingtin's interaction with mitochondrial protein Drp1 impairs mitochondrial biogenesis and causes defective axonal transport and synaptic degeneration in Huntington's disease. *Hum. Mol. Genet.* *21*, 406–420.
- Sibson, N.R., Dhankhar, A., Mason, G.F., Rothman, D.L., Behar, K.L., and Shulman, R.G. (1998). Stoichiometric coupling of brain glucose metabolism and glutamatergic neuronal activity. *Proc. Natl. Acad. Sci. USA* *95*, 316–321.
- Sickmann, A., Reinders, J., Wagner, Y., Joppich, C., Zahedi, R., Meyer, H.E., Schönfisch, B., Perschil, I., Chacinska, A., Guiard, B., et al. (2003). The proteome of *Saccharomyces cerevisiae* mitochondria. *Proc. Natl. Acad. Sci. USA* *100*, 13207–13212.
- Song, W., Chen, J., Petrilli, A., Liot, G., Klinglmayr, E., Zhou, Y., Poquiz, P., Tjong, J., Pouladi, M.A., Hayden, M.R., et al. (2011). Mutant huntingtin binds the mitochondrial fission GTPase dynamin-related protein-1 and increases its enzymatic activity. *Nat. Med.* *17*, 377–382.
- Soubannier, V., McLelland, G.L., Zunino, R., Braschi, E., Rippstein, P., Fon, E.A., and McBride, H.M. (2012). A vesicular transport pathway shuttles cargo from mitochondria to lysosomes. *Curr. Biol.* *22*, 135–141.
- Sterky, F.H., Lee, S., Wibom, R., Olson, L., and Larsson, N.G. (2011). Impaired mitochondrial transport and Parkin-independent degeneration of respiratory chain-deficient dopamine neurons in vivo. *Proc. Natl. Acad. Sci. USA* *108*, 12937–12942.
- Stewart, J.B., Freyer, C., Elson, J.L., Wredenberg, A., Cansu, Z., Trifunovic, A., and Larsson, N.G. (2008). Strong purifying selection in transmission of mammalian mitochondrial DNA. *PLoS Biol.* *6*, e10.
- Stock, D., Leslie, A.G., and Walker, J.E. (1999). Molecular architecture of the rotary motor in ATP synthase. *Science* *286*, 1700–1705.
- Strack, S., and Cribbs, J.T. (2012). Allosteric modulation of Drp1 assembly and mitochondrial fission by the variable domain. *J. Biol. Chem.*
- Strauss, M., Hofhaus, G., Schröder, R.R., and Kühlbrandt, W. (2008). Dimeric ribbons of ATP synthase shape the inner mitochondrial membrane. *EMBO J.* *27*, 1154–1160.
- Sugioka, R., Shimizu, S., and Tsujimoto, Y. (2004). Fzo1, a protein involved in mitochondrial fusion, inhibits apoptosis. *J. Biol. Chem.* *279*, 52726–52734.
- Suomalainen, A. (2011). Therapy for mitochondrial disorders: little proof, high research activity, some promise. *Semin. Fetal Neonatal Med.* *16*, 236–240.
- Suomalainen, A., Elo, J.M., Pietiläinen, K.H., Hakonen, A.H., Sevastianova, K., Korpela, M., Isohanni, P., Marjavaara, S.K., Tyni, T., Kiuru-Enari, S., et al. (2011). FGF-21 as a biomarker for muscle-manifesting mitochondrial respiratory chain deficiencies: a diagnostic study. *Lancet Neurol.* *10*, 806–818.
- Tabas, I., and Ron, D. (2011). Integrating the mechanisms of apoptosis induced by endoplasmic reticulum stress. *Nat. Cell Biol.* *13*, 184–190.
- Tanaka, A., Cleland, M.M., Xu, S., Narendra, D.P., Suen, D.F., Karbowski, M., and Youle, R.J. (2010). Proteasome and p97 mediate mitophagy and degradation of mitofusins induced by Parkin. *J. Cell Biol.* *191*, 1367–1380.
- Tang, F., Wang, B., Li, N., Wu, Y., Jia, J., Suo, T., Chen, Q., Liu, Y.J., and Tang, J. (2011). RNF185, a novel mitochondrial ubiquitin E3 ligase, regulates autophagy through interaction with BNIP1. *PLoS ONE* *6*, e24367.
- Tatuch, Y., Christodoulou, J., Feigenbaum, A., Clarke, J.T., Wherret, J., Smith, C., Rudd, N., Petrova-Benedict, R., and Robinson, B.H. (1992). Heteroplasmic mtDNA mutation (T→G) at 8993 can cause Leigh disease when the percentage of abnormal mtDNA is high. *Am. J. Hum. Genet.* *50*, 852–858.
- Tiranti, V., Savoia, A., Forti, F., D'Apollito, M.-F., Centra, M., Rocchi, M., and Zeviani, M. (1997). Identification of the gene encoding the human mitochondrial RNA polymerase (h-mtRPOL) by cyberscreening of the Expressed Sequence Tags database. *Hum. Mol. Genet.* *6*, 615–625.
- Tomlinson, I.P., Alam, N.A., Rowan, A.J., Barclay, E., Jaeger, E.E., Kelsell, D., Leigh, I., Gorman, P., Lamlum, H., Rahman, S., et al; Multiple Leiomyoma Consortium. (2002). Germline mutations in FH predispose to dominantly inherited uterine fibroids, skin leiomyomata and papillary renal cell cancer. *Nat. Genet.* *30*, 406–410.
- Tondera, D., Grandemange, S., Jourdain, A., Karbowski, M., Mattenberger, Y., Herzog, S., Da Cruz, S., Clerc, P., Raschke, I., Merkwirth, C., et al. (2009). SLP-2 is required for stress-induced mitochondrial hyperfusion. *EMBO J.* *28*, 1589–1600.
- Trifunovic, A., Wredenberg, A., Falkenberg, M., Spelbrink, J.N., Rovio, A.T., Bruder, C.E., Bohlooly-Y, M., Gidlöf, S., Oldfors, A., Wibom, R., et al. (2004). Premature ageing in mice expressing defective mitochondrial DNA polymerase. *Nature* *429*, 417–423.
- Turcan, S., Rohle, D., Goenka, A., Walsh, L.A., Fang, F., Yilmaz, E., Campos, C., Fabius, A.W.M., Lu, C., Ward, P.S., et al. (2012). IDH1 mutation is sufficient to establish the glioma hypermethylator phenotype. *Nature*. Published online February 15, 2012.
- Twig, G., Elorza, A., Molina, A.J., Mohamed, H., Wikstrom, J.D., Walzer, G., Stiles, L., Haigh, S.E., Katz, S., Las, G., et al. (2008). Fission and selective fusion govern mitochondrial segregation and elimination by autophagy. *EMBO J.* *27*, 433–446.
- Tyynismaa, H., and Suomalainen, A. (2009). Mouse models of mitochondrial DNA defects and their relevance for human disease. *EMBO Rep.* *10*, 137–143.
- Tyynismaa, H., Mjosund, K.P., Wanrooi, S., Lappalainen, I., Ylikallio, E., Jalanko, A., Spelbrink, J.N., Paetau, A., and Suomalainen, A. (2005). Mutant mitochondrial helicase Twinkle causes multiple mtDNA deletions and a late-onset mitochondrial disease in mice. *Proc. Natl. Acad. Sci. USA* *102*, 17687–17692.
- Tyynismaa, H., Carroll, C.J., Raimundo, N., Ahola-Erkkilä, S., Wenz, T., Ruhanen, H., Guse, K., Hemminki, A., Peltola-Mjosund, K.E., Tulkki, V., et al. (2010). Mitochondrial myopathy induces a starvation-like response. *Hum. Mol. Genet.* *19*, 3948–3958.
- Tyynismaa, H., Sun, R., Ahola-Erkkilä, S., Almusa, H., Pöyhönen, R., Korpela, M., Honkaniemi, J., Isohanni, P., Paetau, A., Wang, L., and Suomalainen, A. (2012). Thymidine kinase 2 mutations in autosomal recessive progressive

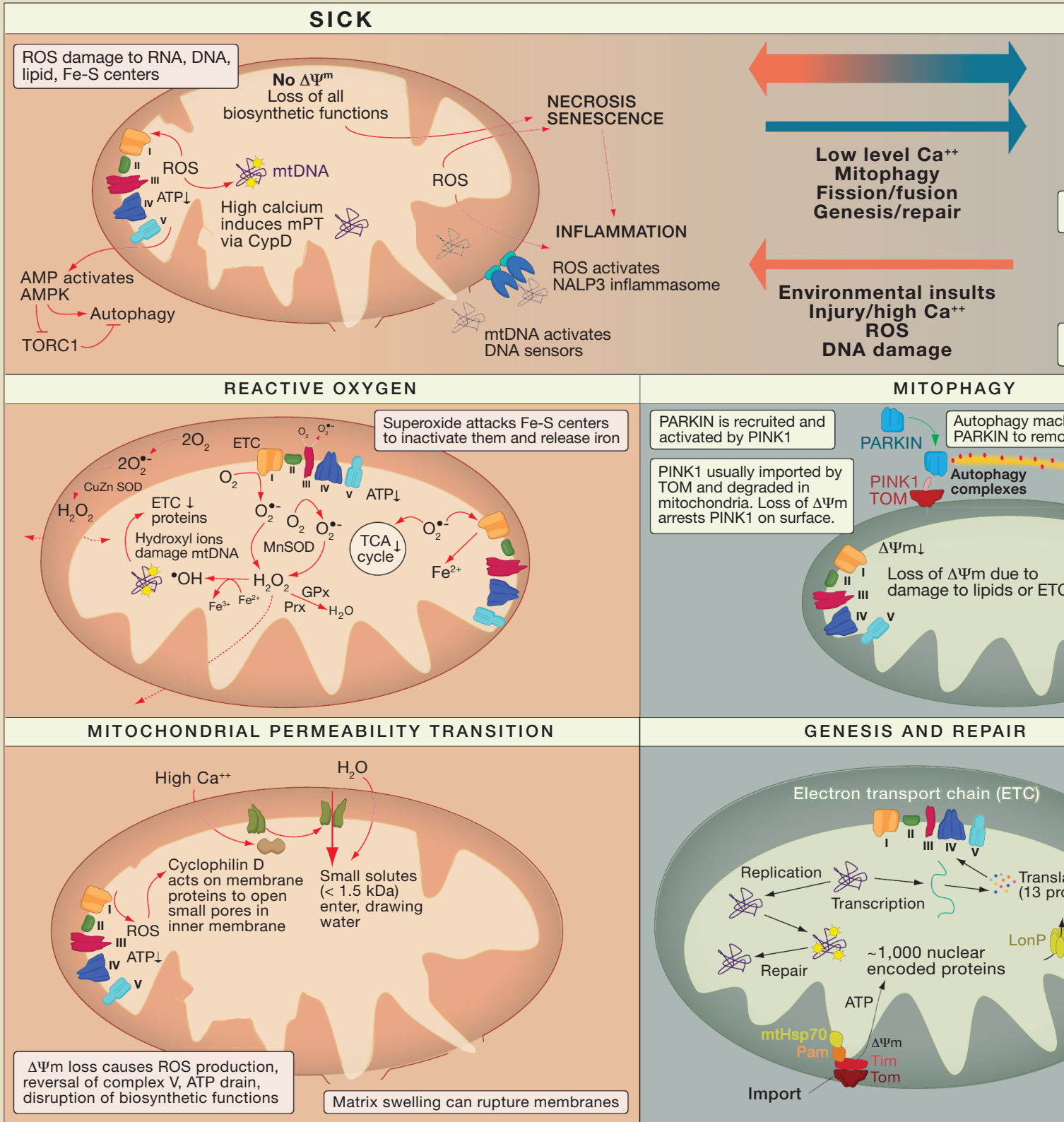
- external ophthalmoplegia with multiple mitochondrial DNA deletions. *Hum. Mol. Genet.* 21, 66–75.
- Valente, E.M., Abou-Sleiman, P.M., Caputo, V., Muqit, M.M., Harvey, K., Gispert, S., Ali, Z., Del Turco, D., Bentivoglio, A.R., Healy, D.G., et al. (2004). Hereditary early-onset Parkinson's disease caused by mutations in PINK1. *Science* 304, 1158–1160.
- van den Bogert, C., and Kroon, A.M. (1981). Tissue distribution and effects on mitochondrial protein synthesis of tetracyclines after prolonged continuous intravenous administration to rats. *Biochem. Pharmacol.* 30, 1706–1709.
- Van Goethem, G., Dermaut, B., Löfgren, A., Martin, J.J., and Van Broeckhoven, C. (2001). Mutation of POLG is associated with progressive external ophthalmoplegia characterized by mtDNA deletions. *Nat. Genet.* 28, 211–212.
- van Marken Lichtenbelt, W.D., Vanhommel, J.W., Smulders, N.M., Dros-saerts, J.M., Kemerink, G.J., Bouvy, N.D., Schrauwen, P., and Teule, G.J. (2009). Cold-activated brown adipose tissue in healthy men. *N. Engl. J. Med.* 360, 1500–1508.
- Vander Heiden, M.G., Cantley, L.C., and Thompson, C.B. (2009). Understanding the Warburg effect: the metabolic requirements of cell proliferation. *Science* 324, 1029–1033.
- Verstreken, P., Ly, C.V., Venken, K.J., Koh, T.W., Zhou, Y., and Bellen, H.J. (2005). Synaptic mitochondria are critical for mobilization of reserve pool vesicles at *Drosophila* neuromuscular junctions. *Neuron* 47, 365–378.
- Virtanen, K.A., Lidell, M.E., Orava, J., Heglind, M., Westergren, R., Niemi, T., Taittonen, M., Laine, J., Savisto, N.J., Enerbäck, S., and Nuutila, P. (2009). Functional brown adipose tissue in healthy adults. *N. Engl. J. Med.* 360, 1518–1525.
- Viscomi, C., Bottani, E., Civiletto, G., Cerutti, R., Moggio, M., Fagioli, G., Schon, E.A., Lamperti, C., and Zeviani, M. (2011). In vivo correction of COX deficiency by activation of the AMPK/PGC-1 α axis. *Cell Metab.* 14, 80–90.
- Vives-Bauza, C., Zhou, C., Huang, Y., Cui, M., de Vries, R.L., Kim, J., May, J., Tocilescu, M.A., Liu, W., Ko, H.S., et al. (2010). PINK1-dependent recruitment of Parkin to mitochondria in mitophagy. *Proc. Natl. Acad. Sci. USA* 107, 378–383.
- Voelker, D.R. (2009). Genetic and biochemical analysis of non-vesicular lipid traffic. *Annu. Rev. Biochem.* 78, 827–856.
- von der Malsburg, K., Müller, J.M., Bohnert, M., Oeljeklaus, S., Kwiatkowska, P., Becker, T., Loniewska-Lwowska, A., Wiese, S., Rao, S., Milenkovic, D., et al. (2011). Dual role of mitofilin in mitochondrial membrane organization and protein biogenesis. *Dev. Cell* 21, 694–707.
- Vyas, I., Heikkilä, R.E., and Nicklas, W.J. (1986). Studies on the neurotoxicity of 1-methyl-4-phenyl-1,2,3,6-tetrahydropyridine: inhibition of NAD-linked substrate oxidation by its metabolite, 1-methyl-4-phenylpyridinium. *J. Neurochem.* 46, 1501–1507.
- Waagepetersen, H.S., Sonnewald, U., Gegelashvili, G., Larsson, O.M., and Schousboe, A. (2001). Metabolic distinction between vesicular and cytosolic GABA in cultured GABAergic neurons using 13C magnetic resonance spectroscopy. *J. Neurosci. Res.* 63, 347–355.
- Wakabayashi, J., Zhang, Z., Wakabayashi, N., Tamura, Y., Fukaya, M., Kensler, T.W., Iijima, M., and Sesaki, H. (2009). The dynamin-related GTPase Drp1 is required for embryonic and brain development in mice. *J. Cell Biol.* 186, 805–816.
- Wallace, D.C., Singh, G., Lott, M.T., Hodge, J.A., Schurr, T.G., Lezza, A.M., Elsas, L.J., 2nd, and Nikoskelainen, E.K. (1988). Mitochondrial DNA mutation associated with Leber's hereditary optic neuropathy. *Science* 242, 1427–1430.
- Wang, X., and Schwarz, T.L. (2009). The mechanism of Ca²⁺-dependent regulation of kinesin-mediated mitochondrial motility. *Cell* 136, 163–174.
- Wang, X., Su, B., Lee, H.G., Li, X., Perry, G., Smith, M.A., and Zhu, X. (2009). Impaired balance of mitochondrial fission and fusion in Alzheimer's disease. *J. Neurosci.* 29, 9090–9103.
- Wang, C., Liu, X., and Wei, B. (2011a). Mitochondrion: an emerging platform critical for host antiviral signaling. *Expert Opin. Ther. Targets* 15, 647–665.
- Wang, X., Winter, D., Ashrafi, G., Schlehe, J., Wong, Y.L., Selkoe, D., Rice, S., Steen, J., LaVoie, M.J., and Schwarz, T.L. (2011b). PINK1 and Parkin target Miro for phosphorylation and degradation to arrest mitochondrial motility. *Cell* 147, 893–906.
- Warburg, O. (1923). The prime cause and prevention of cancer. *Biochem. Z.* 142, 317.
- Wasiak, S., Zunino, R., and McBride, H.M. (2007). Bax/Bak promote sumoylation of DRP1 and its stable association with mitochondria during apoptotic cell death. *J. Cell Biol.* 177, 439–450.
- Waterham, H.R., Koster, J., van Roermund, C.W., Mooyer, P.A., Wanders, R.J., and Leonard, J.V. (2007). A lethal defect of mitochondrial and peroxisomal fission. *N. Engl. J. Med.* 356, 1736–1741.
- Wenz, T., Diaz, F., Spiegelman, B.M., and Moraes, C.T. (2008). Activation of the PPAR/PGC-1 α pathway prevents a bioenergetic deficit and effectively improves a mitochondrial myopathy phenotype. *Cell Metab.* 8, 249–256.
- Wu, Z., Puigserver, P., Andersson, U., Zhang, C., Adelman, G., Mootha, V., Troy, A., Cinti, S., Lowell, B., Scarpulla, R.C., and Spiegelman, B.M. (1999). Mechanisms controlling mitochondrial biogenesis and respiration through the thermogenic coactivator PGC-1. *Cell* 98, 115–124.
- Wurm, C.A., Neumann, D., Lauterbach, M.A., Harke, B., Egner, A., Hell, S.W., and Jakobs, S. (2011). Nanoscale distribution of mitochondrial import receptor Tom20 is adjusted to cellular conditions and exhibits an inner-cellular gradient. *Proc. Natl. Acad. Sci. USA* 108, 13546–13551.
- Xu, S., Peng, G., Wang, Y., Fang, S., and Karbowski, M. (2011). The AAA-ATPase p97 is essential for outer mitochondrial membrane protein turnover. *Mol. Biol. Cell* 22, 291–300.
- Yan, H., Parsons, D.W., Jin, G., McLendon, R., Rasheed, B.A., Yuan, W., Kos, I., Batnig-Haberle, I., Jones, S., Riggins, G.J., et al. (2009). IDH1 and IDH2 mutations in gliomas. *N. Engl. J. Med.* 360, 765–773.
- Yang, Y., Atasoy, D., Su, H.H., and Sternson, S.M. (2011). Hunger states switch a flip-flop memory circuit via a synaptic AMPK-dependent positive feedback loop. *Cell* 146, 992–1003.
- Yatsuga, S., and Suomalainen, A. (2012). Effect of bezafibrate treatment on late-onset mitochondrial myopathy in mice. *Hum. Mol. Genet.* 21, 526–535.
- Ylikallio, E., and Suomalainen, A. (2012). Mechanisms of mitochondrial diseases. *Ann. Med.* 44, 41–59.
- Yoneda, T., Benedetti, C., Urano, F., Clark, S.G., Harding, H.P., and Ron, D. (2004). Compartment-specific perturbation of protein handling activates genes encoding mitochondrial chaperones. *J. Cell Sci.* 117, 4055–4066.
- Yoon, Y., Pitts, K.R., and McNiven, M.A. (2001). Mammalian dynamin-like protein DLP1 tubulates membranes. *Mol. Biol. Cell* 12, 2894–2905.
- Yoshii, S.R., Kishi, C., Ishihara, N., and Mizushima, N. (2011). Parkin mediates proteasome-dependent protein degradation and rupture of the outer mitochondrial membrane. *J. Biol. Chem.* 286, 19630–19640.
- Youle, R.J., and Narendra, D.P. (2011). Mechanisms of mitophagy. *Nat. Rev. Mol. Cell Biol.* 12, 9–14.
- Zhao, Q., Wang, J., Levichkin, I.V., Stasinopoulos, S., Ryan, M.T., and Hoo-genraad, N.J. (2002). A mitochondrial specific stress response in mammalian cells. *EMBO J.* 21, 4411–4419.
- Ziviani, E., Tao, R.N., and Whitworth, A.J. (2010). *Drosophila* parkin requires PINK1 for mitochondrial translocation and ubiquitinates mitofusin. *Proc. Natl. Acad. Sci. USA* 107, 5018–5023.
- Züchner, S., Mersiyanova, I.V., Muglia, M., Bissar-Tadmouri, N., Rochelle, J., Dadali, E.L., Zappia, M., Nelis, E., Patitucci, A., Senderek, J., et al. (2004). Mutations in the mitochondrial GTPase mitofusin 2 cause Charcot-Marie-Tooth neuropathy type 2A. *Nat. Genet.* 36, 449–451.

SnapShot: Mitochondrial Quality Control

Douglas R. Green¹, and Bennett Van Houten²

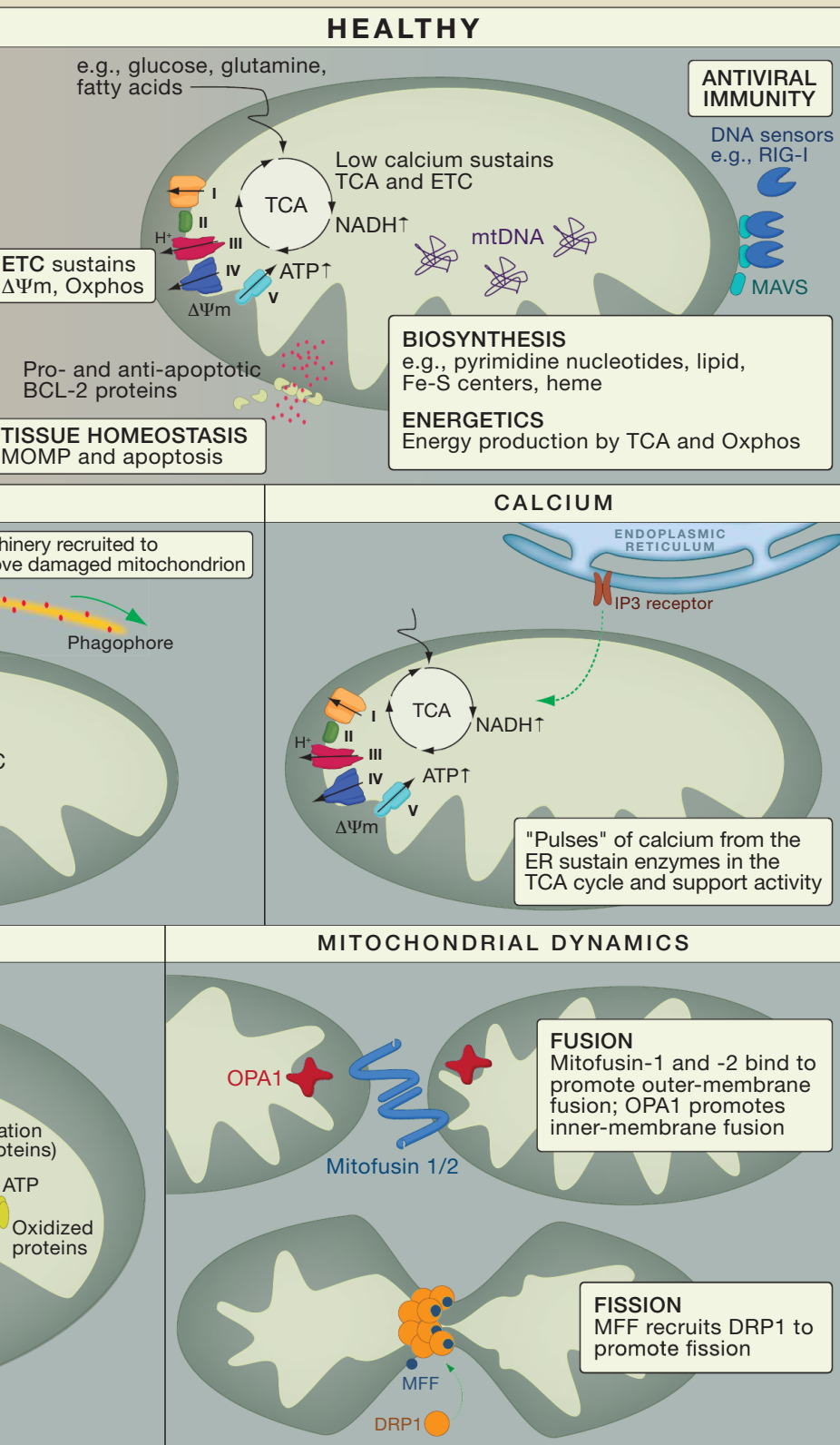
¹Department of Immunology, St. Jude Children's Research Hospital, Memphis, TN 38105-3678, USA

²University of Pittsburgh School of Medicine, University of Pittsburgh, Pittsburgh, PA 15213, USA



Control

Cell



Cayman Chemical is helping make bioenergetics research possible. For more than three decades, Cayman Chemical has been responding to the needs of researchers by producing assay kits, proteins, biochemicals, antibodies, and research services for a diverse range of research areas. With an established catalog of more than 8,000 products and a variety of custom services, our community of scientists applies their deep knowledge of life sciences to assemble focused product lines for the analysis of vital biological systems. Our bioenergetics reagents and contract services deliver accurate, reproducible, and reliable data on cellular metabolism, allowing researchers to create a full mitochondrial function and toxicity profile. All of our products are backed by in-house scientists—the same scientists develop the products, answer your questions, and analyze your samples through Cayman's contract research services.

We continue to create novel assays as the field of bioenergetics evolves. Discover our line of bioenergetics research tools and services at caymanchem.com/bioenergetics.



(800) 364-9897 www.caymanchem.com

Stress-responsive regulation of mitochondria through the ER unfolded protein response

T. Kelly Rainbolt, Jaclyn M. Saunders, and R. Luke Wiseman

Department of Molecular and Experimental Medicine, Department of Chemical Physiology, The Scripps Research Institute, La Jolla, CA 92037, USA

The endoplasmic reticulum (ER) and mitochondria form physical interactions involved in the regulation of biologic functions including mitochondrial bioenergetics and apoptotic signaling. To coordinate these functions during stress, cells must coregulate ER and mitochondria through stress-responsive signaling pathways such as the ER unfolded protein response (UPR). Although the UPR is traditionally viewed as a signaling pathway responsible for regulating ER proteostasis, it is becoming increasingly clear that the protein kinase RNA (PKR)-like endoplasmic reticulum kinase (PERK) signaling pathway within the UPR can also regulate mitochondria proteostasis and function in response to pathologic insults that induce ER stress. Here, we discuss the contributions of PERK in coordinating ER–mitochondrial activities and describe the mechanisms by which PERK adapts mitochondrial proteostasis and function in response to ER stress.

ER stress impacts mitochondrial function through interorganellar signaling

The traditional view of ER and mitochondria as discreet intracellular organelles has been profoundly altered in recent years. Unlike the well-defined organelles described in cell biology textbooks, the ER and mitochondria are highly dynamic and undergo continuous structural and spatial reorganization in response to specific cellular signals. An interesting aspect of these organelles is that they form physical ER–mitochondrial contacts (reviewed in [1–3]). These contacts facilitate the transfer of metabolites, including lipids and Ca^{2+} , between the ER and mitochondria that are involved in the regulation of biologic functions including lipid homeostasis, mitochondrial metabolism, and the regulation of apoptotic signaling (Box 1). Thus, ER–mitochondrial contacts serve as a platform for interorganellar communication, essential for the coordination of cellular function.

A consequence of the physical and functional interaction between ER and mitochondria is that mitochondria

function is sensitive to pathologic insults that induce ER stress (defined by the increased accumulation of misfolded proteins within the ER lumen). ER stress can be transmitted to mitochondria by alterations in the transfer of metabolites such as Ca^{2+} or by stress-responsive signaling pathways, directly influencing mitochondrial functions. Depending on the extent of cellular stress, the stress signaling from the ER to mitochondria can result in pro-survival or proapoptotic adaptations in mitochondrial function.

During the early adaptive phase of ER stress, ER–mitochondrial contacts increase, promoting Ca^{2+} transfer between these organelles [4]. This increase in Ca^{2+} flux into mitochondria stimulates mitochondrial metabolism through the activity of Ca^{2+} -regulated dehydrogenases involved in the tricarboxylic acid (TCA) cycle. The increased activity of these dehydrogenases promotes mitochondrial respiratory chain activity, resulting in a transient increase in mitochondrial ATP synthesis during the initial phase of ER stress. This surge in bioenergetic capacity increases the available energetic resources to mount an adaptive response and alleviate ER stress. Alternatively, chronic exposure to ER stress negatively impacts cellular metabolism by reducing mitochondrial respiration and decreasing cellular ATP levels [4,5]. This has been shown to lead to depletion of Ca^{2+} stores in the ER and increased Ca^{2+} within mitochondria ([6,7] and discussed below). Ultimately, this signaling results in mitochondrial fragmentation and the opening of the mitochondrial permeability transition pore (MPTP), which initiates intrinsic apoptotic signaling and programmed cell death. Varying levels of ER stress in multiple cell types have also been reported to impact other mitochondrial functions including mitochondrial DNA (mtDNA) biogenesis [8], the transcription of respiratory chain subunits [5], and increases in mitochondrial-derived reactive oxygen species (ROS) [5,9,10], further reflecting the capacity for ER stress to influence mitochondrial function.

Many metabolic diseases including nonalcoholic fatty liver disease, type 2 diabetes (T2D), and obesity are associated with unresolved ER stress, suggesting that mitochondrial dysfunction in these diseases may be dysregulated through mechanisms involving ER stress-dependent alterations in ER–mitochondria communication [11,12]. For example, stress-dependent alterations

Corresponding author: Wiseman, R.L. (wiseman@scripps.edu).

Keywords: mitochondrial proteostasis; mitochondrial quality control; unfolded protein response (UPR); PERK; eIF2 α phosphorylation.

1043-2760/

© 2014 Elsevier Ltd. All rights reserved. <http://dx.doi.org/10.1016/j.tem.2014.06.007>

Box 1. Metabolite transfer through ER-mitochondrial contacts

ER and mitochondria form tight physical junctions stabilized by tethering complexes anchored in the ER and mitochondrial outer membrane (reviewed in [1–3]). In higher eukaryotes, these tethers are mediated by interactions between ER-localized MFN2 with MFN2 and MFN1 in the mitochondrial outer membrane. These tight interactions facilitate the transfer of metabolites between the two organelles (Figure 1).

Transfer of Ca^{2+} between the ER and mitochondria is a major function for ER-mitochondrial contacts and is carried out through the IP_3R and VDAC transporters localized to the ER and mitochondria outer membranes, respectively (see [1–3]). These channels form a tight interaction stabilized by the cytosolic isoform of the mitochondrial HSP70 chaperone HSPA9/GRP75/mortalin. Ca^{2+} is imported into the mitochondrial matrix through the high-capacity, low-affinity mitochondrial Ca^{2+} uniporter (MCU). The close physical proximity between these various Ca^{2+} transporters at ER-mitochondrial contacts increases local Ca^{2+} concentration to levels sufficient to drive import through MCU into the mitochondrial matrix.

Flux of Ca^{2+} through the ER-mitochondrial contacts is highly regulated by accessory proteins both at the ER and mitochondria membranes [1–3,6]. ER-localized phosphofurin acidic cluster sorting protein 2 (PACS2) recruits the chaperone calnexin to the ER luminal face of MAMs to mediate their formation and stability. The ER Sigma-1 receptor stabilizes IP_3R and promotes protective ER to mitochondria Ca^{2+} exchange in response to ER Ca^{2+} depletion. Alternatively, MCU regulators including MICU1 and MCUR1 have also been identified to influence ER-mitochondria Ca^{2+} transfer and Ca^{2+} -regulated mitochondrial activities [1–3,6]. ER-mitochondrial Ca^{2+} transfer is also influenced by a truncated isoform of SERCA (S1T) localized to MAMs that can promote ER Ca^{2+} leakage and mitochondria Ca^{2+} overload associated with cellular death [1–3]. These regulators provide a significant level of control over ER-mitochondrial Ca^{2+} transfer, reflecting the importance of this process in cellular physiology.

Apart from Ca^{2+} , other metabolites including lipids are also transferred between the ER and mitochondria through ER-mitochondrial contacts [1–3]. Lipid biosynthesis enzymes involved in the synthesis of phospholipids, cholesterol metabolites, and sphingolipids localize to the ER and mitochondrial membranes. Lipid transfer between the ER and mitochondria is required for the biosynthesis of these critical metabolites, including cardiolipin (CL). CL has been shown to have a variety of essential functions in the mitochondria including maintaining membrane curvature at cristae tips and providing structural integrity to both electron transport chain and mitochondrial

import complex components [93–96]. The synthesis of CL involves the transfer of ER-derived phosphatidic acid to the mitochondrial inner membrane followed by the action of a cascade of mitochondrial enzymes including cardiolipin synthase (CLS). Thus, maintaining ER-mitochondrial contacts is critical for the proper synthesis of essential lipids, such as CL, and for maintaining normal mitochondrial function and cellular physiology.

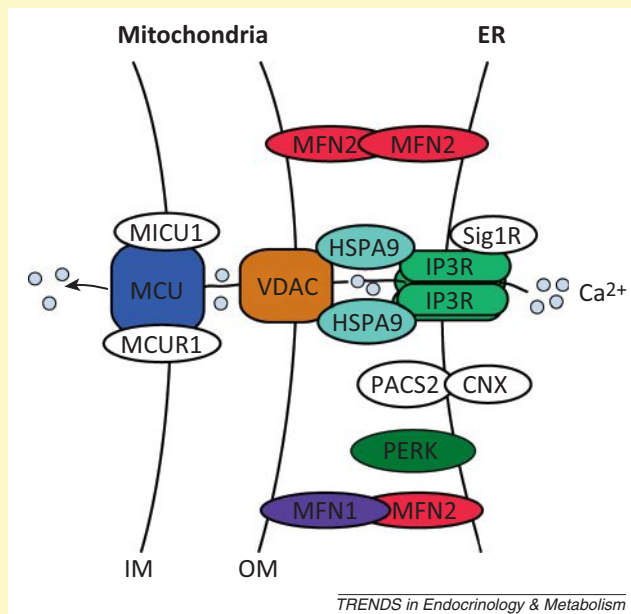


Figure 1. Illustration of the components and interactions of proteins localized to ER-mitochondrial contacts. The colored proteins represent core components of ER-mitochondrial contacts required for organelle tethering (MFN2 and MFN1) or Ca^{2+} transfer between these organelles (IP_3R , VDAC, MCU, and HSPA9). The white proteins are regulatory factors that influence the Ca^{2+} signaling through ER-mitochondrial contacts. Abbreviations: ER, endoplasmic reticulum; MFN, Mitofusin; IP_3R , inositol trisphosphate receptor; VDAC, voltage-dependent anion-selective channel; MCU, mitochondrial Ca^{2+} uniporter.

in ER-mitochondrial Ca^{2+} transfer has been proposed to contribute to the pathophysiology of T2D where increased cytosolic calcium leads to aberrant insulin signaling in the pancreas and disrupted routine metabolic functions (e.g., gluconeogenesis) in the liver [13]. Increased activation of TOR signaling has also been linked to the development of metabolic disease [14]. Interestingly, in addition to promoting a diabetic phenotype, ablation of tuberous sclerosis complex (TSC), a suppressor of TOR activity, also induces chronic ER stress. Alleviation of this ER stress reestablishes insulin sensitivity even in the background of sustained TOR activation suggesting that chronic UPR activation has detrimental metabolic consequences [15].

ER stress and mitochondrial dysfunction are also intricately linked in the pathology of other diseases including $\alpha 1$ -antitrypsin deficiency [16,17], cardiovascular disorders [18,19], and neurodegenerative diseases such as Alzheimer's disease [20,21], Parkinson's disease [22,23], and amyotrophic lateral sclerosis [24,25]. Despite the pathologic relationship between ER stress and mitochondrial dysfunction in these diseases, the specific contributions of altered ER-mitochondrial communication in disease pathogenesis are only beginning to come to light. For example,

familial Alzheimer's disease is associated with mutations in presenilins 1 and 2 (PS1 and PS2), which are involved in the generation of the toxic Amyloid β ($\text{A}\beta$) peptide [20,21]. PS1 and PS2 are enriched in a subcompartment of the ER physically associated with mitochondria called mitochondrial-associated ER membranes (MAMs) and appears to be involved in coordinating ER-mitochondrial Ca^{2+} and lipid transfer, suggesting that these mutations could directly contribute to disease pathogenesis through alterations in ER-mitochondrial signaling [20,21,26–29]. These data suggest that dysregulation of ER-mitochondrial signaling could broadly contribute to the pathogenesis of human diseases with diverse etiologies. Therefore, the possibility of intervening in the transfer of chronic ER stress to mitochondria could be a promising avenue for therapeutic development for many of the debilitating diseases mentioned above.

The PERK signaling pathway of the UPR regulates mitochondrial function during ER stress

The predominant stress-responsive signaling pathway that regulates cellular physiology during ER stress is the UPR (reviewed in [30–32]). The UPR consists of three

integrated signaling pathways activated downstream of the transmembrane ER stress sensor proteins inositol requiring enzyme 1 (IRE1), activating transcription factor 6 (ATF6), and PERK. ER stress-dependent activation of these pathways protect essential ER activities and relieve ER stress through transient translational attenuation and the transcriptional upregulation of stress-responsive genes primarily involved in the regulation of ER protein homeostasis (or proteostasis). Although ATF6 and IRE1 primarily function to regulate ER proteostasis and function [30–32], it is becoming increasingly apparent that, in addition to its role in regulating ER proteostasis, the PERK arm of the UPR also has an important role in regulating mitochondrial proteostasis and function during conditions of ER stress.

PERK activation influences cellular physiology during ER stress through translational attenuation and transcriptional signaling

PERK signaling is initiated in response to ER stress by the dissociation of the ER heat shock protein 70 (HSP70) chaperone binding immunoglobulin protein (BiP) from the PERK sensing domain localized to the ER lumen (Figure 1) [30–32]. Dissociation of BiP leads to the activation of PERK through a mechanism involving PERK dimerization and autophosphorylation of the cytosolic PERK kinase domain. The active, phosphorylated PERK kinase selectively phosphorylates the serine 51 residue of the α subunit of eukaryotic initiation factor 2 (eIF2 α) [33]. This phosphorylation inhibits the activity of the eIF2B GTP exchange factor involved in ribosomal translation initiation [34,35]. Thus, the initial impact of PERK on cellular physiology is a global attenuation of new protein synthesis that reduces the folding load of newly synthesized proteins entering the ER lumen, freeing ER proteostasis factors to alleviate the toxic accumulation of misfolded proteins within the ER lumen.

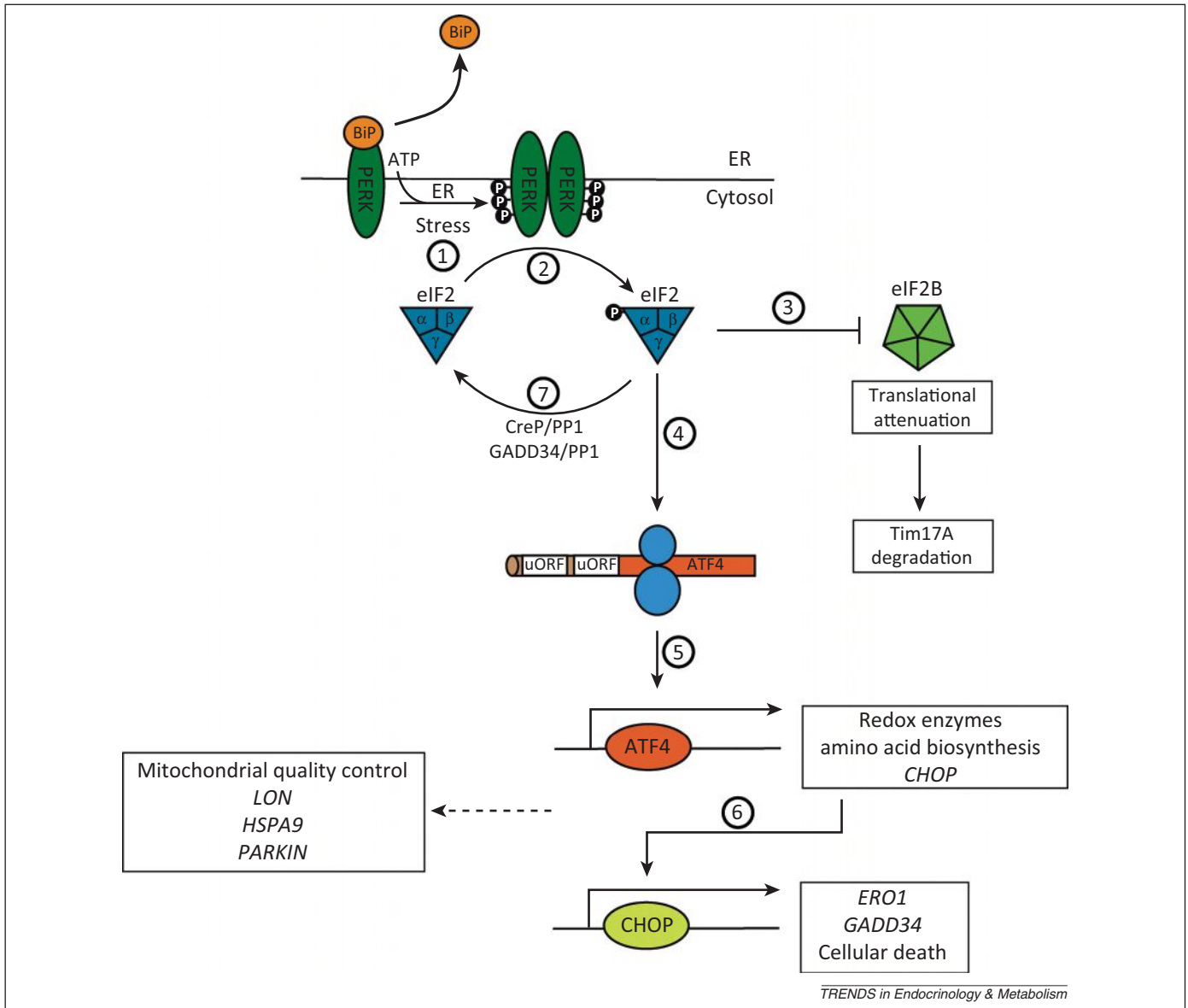
Interestingly, eIF2 α phosphorylation also results in the activation of stress-responsive proteins. Transcripts of these proteins are selectively translated during conditions of eIF2 α phosphorylation through a mechanism dependent on upstream open reading frames (uORFs) in their mRNA [34,35]. One of the predominant genes translated downstream of PERK-dependent eIF2 α phosphorylation is the stress-responsive transcription factor ATF4 [9,36]. ATF4 induces the expression of a variety of stress-responsive genes involved in critical biologic processes including cellular redox maintenance, amino acid biosynthesis, and other stress-responsive transcription factors including the C/EBP homologous protein (CHOP/GADD153) [9,36]. CHOP in turn is involved in the induction of additional stress-responsive genes including ER oxidase 1 (ERO1) and the protein phosphatase 1 (PP1) regulatory subunit GADD34/PPP1R15A [37–39], which dephosphorylates eIF2 α and restores translational integrity in a well-established negative feedback loop of PERK signaling [40,41]. Additionally, in response to chronic ER stress and subsequent PERK activation, high levels of CHOP can also promote activation of intrinsic apoptotic signaling pathways (discussed below). Thus, through this dual prosurvival/proapoptotic signaling mechanism, PERK

serves as a critical regulator of cellular fate during conditions of ER stress. Importantly, whereas ER stress induces eIF2 α phosphorylation through PERK, other eIF2 α kinases such as PKR (interferon-induced, double-stranded RNA-activated protein kinase), GCN2 (general control nonderepressible 2), and HRI (heme-regulated inhibitor) induce eIF2 α phosphorylation in response to other cellular insults including viral infection, nutrient deprivation, heme deficiency, and oxidative stress [35,42].

PERK coordinates ER–mitochondrial activities in the presence and absence of ER stress

PERK is intimately involved in defining ER–mitochondrial interorganellar signaling. PERK is enriched in MAMs (the subcompartment of the ER that interacts with mitochondria), localizing this ER stress sensor to ER–mitochondrial contact sites [43,44] (Box 1). PERK has been proposed to interact with the mitochondrial tethering protein Mitofusin-2 (MFN2), indicating that PERK may stabilize ER–mitochondrial contacts [45]. Consistent with this prediction, genetic depletion of PERK disturbs ER morphology and reduces the number of ER–mitochondrial contacts [43]. Furthermore, PERK depletion in MFN2^{−/−} mouse embryonic fibroblasts (MEFs) reduces ROS, normalizes mitochondrial respiration, and improves mitochondrial morphology [45]. These results suggest a functional interaction between MFN2 and PERK involved in dictating ER–mitochondrial contacts, although the underlying physical relationship between these proteins requires further characterization. The stabilizing effects of PERK on ER–mitochondrial interactions appear to be dependent on the PERK cytosolic kinase domain as overexpression of PERK lacking this domain does not rescue defects in ER–mitochondrial contacts [43]. By contrast, overexpression of a kinase dead PERK restored ER–mitochondrial contacts to levels similar to those observed in wild type cells [43]. This indicates that stabilization of ER–mitochondrial contacts afforded by PERK is likely to be structural in nature and not dependent on canonical PERK signaling through eIF2 α .

Apart from the structural role for PERK in stabilizing ER–mitochondrial contacts, cells deficient in PERK signaling have defects in mitochondrial functions. PERK-deficient cells show defects in regulating electron transport chain activity reflected by increased basal and maximal respiration [45]. They also show perturbed responses to ER stress including an abnormal increase in ROS and defects in mtDNA biogenesis [8–10]. The regulation of intrinsic apoptosis is also impaired in PERK-deficient cells. PERK^{−/−} cells are hypersensitized to apoptosis induced by the sarco/endoplasmic reticulum Ca²⁺ ATPase (SERCA) inhibitor thapsigargin or the inhibitor of N-linked glycosylation tunicamycin [39,43,46], while these same cells are more resistant to apoptosis induced by ER-derived ROS [43]. Disrupting downstream PERK signaling also sensitizes mitochondria to stress *in vivo*. For example, conditional knockin of the nonphosphorylatable serine 51 to alanine (S51A) eIF2 α mutant (eIF2 α ^{S51A}, a mutant resistant to ER stress-induced, PERK-dependent eIF2 α phosphorylation [33]; Figure 1) into the pancreas leads to mitochondrial damage in pancreatic β cells – a cell type highly dependent on UPR signaling due to maintain high



TRENDS in Endocrinology & Metabolism

Figure 1. PERK-dependent signaling through eIF2 α phosphorylation. In response to ER stress, the ER Hsp70 chaperone BiP dissociates from PERK, inducing PERK autophosphorylation and dimerization (step 1). Active PERK selectively phosphorylates the α subunit of eIF2 (eIF2 α) (step 2). Phosphorylated eIF2 α inhibits the eIF2B GTP exchange factor, resulting in global translation attenuation (step 3). This results in the downstream degradation of the core TIM23 subunit Tim17A and reduced mitochondrial protein import. Alternatively, certain stress-responsive genes such as the transcription factor ATF4 are selectively translated during conditions of eIF2 α phosphorylation through upstream open reading frames (uORFs) localized to the 5' UTR, allowing synthesis of these proteins during stress (step 4). Active ATF4 induces expression of cellular proteostasis genes involved in cellular redox and amino acid biosynthesis, as well as additional stress-responsive transcription factors such as CHOP (step 5). CHOP in turn is involved in the induction of additional stress-responsive genes including ER oxidase 1 (ERO1), the protein phosphatase 1 (PP1) regulatory subunit GADD34 and cell death factors (step 6). This pathway is repressed through dephosphorylation of eIF2 α through the activity of PP1 mediated by the constitutively expressed regulatory subunit CreP/PPP1R15B or the stress-induced regulatory subunit GADD34/PPP1R15A (step 7). Mitochondrial quality control factors including *LON*, *HSPA9*, and *PARKIN* are also transcriptionally induced during ER stress through PERK-dependent ATF4 activation, although the specific downstream transcription factors required for their transcription are currently undefined. Adapted from [30]. Abbreviations: PERK, protein kinase RNA (PKR)-like endoplasmic reticulum kinase; ER, endoplasmic reticulum; Hsp70, heat shock protein 70; BiP, binding immunoglobulin protein; eIF2 α , α subunit of eukaryotic initiation factor 2; TIM23, translocase of the inner membrane 23; ATF4, activating transcription factor 4; CHOP, C/EBP homologous protein.

levels of insulin secretion [32]. Furthermore, PERK mutations in humans have been suggested to induce hepatic mitochondrial dysfunctions associated with the rare disease Wolcott–Rallison syndrome, although this genetic relationship requires further study [47,48].

Altered PERK activity contributes to the pathogenesis of metabolic diseases

ER and mitochondria in specialized tissues such as the pancreatic islets and liver are critical for maintaining

glucose and lipid homeostasis in organisms. Metabolic disease states such as T2D and obesity have been clearly linked to both ER and mitochondria dysfunction. Although cellular studies have suggested a protective role for the PERK arm of UPR in the acute phase of ER stress, sustained activation of PERK is detrimental, promoting apoptosis and tissue inflammation [49]. In chronic metabolic disease such as diabetes associated with obesity, sustained activation of PERK may overwhelm the ability of cells to restore homeostasis and favor pathogenesis. For

example in diabetic *ob/ob* mice, ER stress appears to promote diabetic pathology including insulin insensitivity and glucose intolerance. Chemical chaperones such as 4-phenylbutyric acid (4-PBA) or tauroursodeoxycholic acid (TUDCA) alleviate ER stress by facilitating the folding of proteins in the ER. Administration of these molecules attenuates UPR signaling and restores metabolic homeostasis [50]. Further supporting a role for dysfunction in ER–mitochondrial communication in the pathology of metabolic disease, ablation of MFN2 in liver or skeletal muscle likewise leads to diabetic phenotypes. These are associated with sustained PERK activation and mishandling of glucose in these tissues [51]. Cell based studies suggest that suppression of PERK signaling either by knockdown of PERK or alleviating ER stress improve the metabolic disruptions in MFN2^{-/-} cells [45]. These data suggest that although typical transient UPR signaling may be beneficial in resolving ER stress and preserving mitochondrial function, sustained activation of the UPR can promote pathophysiologic changes in metabolism and disease.

The above results suggest that PERK has a protective role in regulating mitochondrial function in the presence or absence of ER stress. Despite this evidence, it is difficult to determine whether the mitochondrial defects in PERK-deficient cells reflect a decreased capacity for PERK to directly regulate mitochondrial function or an indirect consequence of aberrant PERK signaling that impair mitochondrial function. Regardless, new results are emerging that highlight a protective role for PERK in regulating mitochondrial proteostasis and function in response to acute ER stress, which are discussed below.

The regulation of mitochondrial quality control through PERK signaling

Mitochondrial quality control pathways regulate mitochondrial proteostasis during stress to prevent the accumulation of misfolded proteins that can lead to mitochondrial

dysfunction and cellular pathology. Mitochondria maintain their proteome on three distinct organizational levels: molecular, organellar, and cellular fate via apoptosis [52,53]. The capacity to differentially influence mitochondrial proteostasis through these pathways provides a mechanism to sensitively regulate mitochondrial integrity in response to the diverse extents and types of cellular insults encountered in human physiology. As discussed below, PERK directly influences mitochondrial quality control at each organizational level, suggesting that PERK signaling is a primary mechanism for regulating mitochondrial proteostasis and function during ER stress (Figure 2).

PERK-dependent regulation of molecular quality control pathways

In response to moderate levels of stress, mitochondrial proteostasis is maintained by a network of quality control factors involved in mitochondrial protein import, folding, and proteolytic pathways (Box 2). PERK affects the composition and activity of these pathways through both transcriptional and post-translational mechanisms, directly increasing cellular capacity to protect the mitochondrial proteome from damage that can occur in response to ER stress (e.g., increased ROS).

PERK activation induces the downstream expression of mitochondrial quality control factors such as the matrix-localized AAA⁺ quality control protease LON during ER stress [9,37,54] (Figure 1). Although the specific transcription factors required for the increased expression of LON remain to be identified, this process requires the activity of the PERK-regulated transcription factor ATF4 [54]. LON is a critical regulator of mitochondrial proteostasis that functions in many aspects of mitochondrial biology including the degradation of oxidatively damaged mitochondrial proteins [55–57], the assembly of electron transport chain complex IV [54,58], and the regulation of mtDNA transcription and replication through the degradation of the

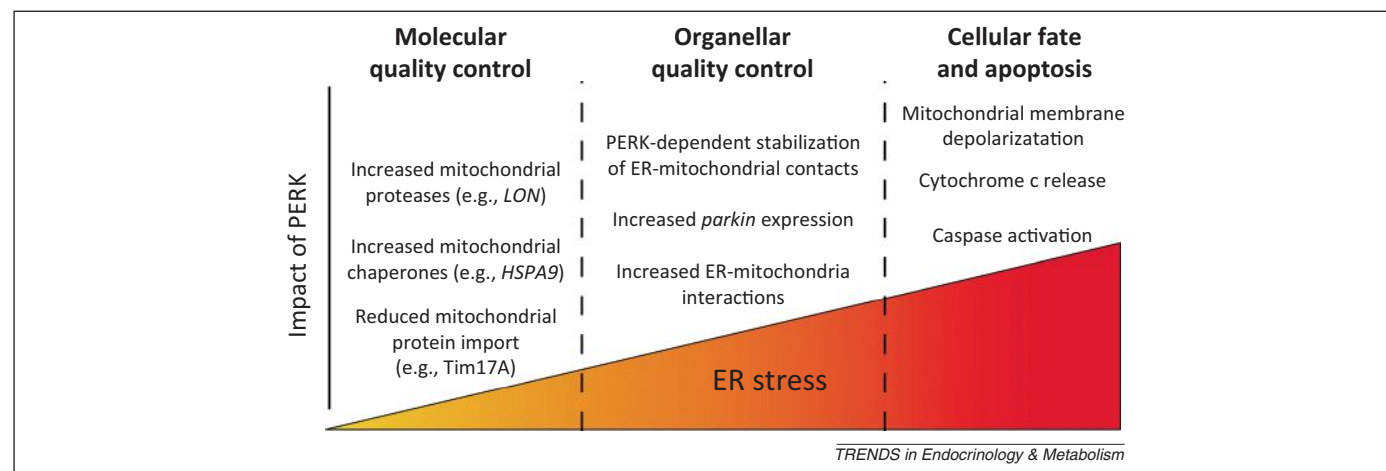


Figure 2. PERK activity regulates mitochondrial quality control on the molecular, organellar, and cellular level. In response to increasing levels of stress, cells regulate mitochondria on three levels mediated by molecular, organellar, and cellular quality control pathways. PERK activity directly influences each of these levels of quality control regulation. In response to mild levels of ER stress, PERK adapts molecular quality control pathways through the transcriptional induction of mitochondrial proteases (e.g., LON) and chaperones (e.g., HSPA9) downstream of the PERK-regulated transcription factor ATF4. PERK activation also adapts mitochondrial protein import activity through the degradation of the core TIM23 subunit Tim17A. In response to more moderate levels of ER stress, PERK influences mitochondrial quality control on the organellar level. PERK directly stabilizes ER–mitochondrial contacts and promotes formation of ER–mitochondrial interactions through the transcriptional upregulation of Parkin. In response to severe stresses, PERK is directly involved in the activation of mitochondrial-derived intrinsic apoptotic signaling through both transcriptional and post-translational mechanisms that induce mitochondrial membrane depolarization, cytochrome c release, and caspase activation. Abbreviations: PERK, protein kinase RNA (PKR)-like endoplasmic reticulum kinase; ER, endoplasmic reticulum; TIM23, translocase of the inner membrane 23; ATF4, activating transcription factor 4.

Box 2. Molecular mitochondrial quality control pathways

The vast majority of the mitochondrial proteome is encoded by the nuclear genome. These proteins are synthesized on cytosolic ribosomes and are directed to mitochondria by mitochondrial-targeting sequences (MTS) localized to the N terminus or internally within the polypeptide sequence (reviewed in [60,71]). These targeting sequences direct nuclear-encoded mitochondrial proteins to the translocase of the outer mitochondrial membrane (TOM) complex, which facilitates translocation across the outer mitochondrial membrane into the intermembrane space (IMS) (Figure 1). In the IMS, polypeptides are sorted to specific multisubunit translocases and pathways that facilitate targeting to different intramitochondrial environments. For example, the 2/3 of the mitochondrial proteome targeted to the mitochondrial matrix as soluble proteins or single-pass inner membrane proteins are directed to the translocase of the inner membrane 23 (TIM23) by N-terminal targeting sequences. TIM23 facilitates translocation across the inner membrane into the mitochondrial matrix in a process dependent on the ATP-dependent activity of the mitochondrial HSP70 HSPA9/mortalin/Grp75 in the presequence associated motor (PAM) complex and the electrochemical gradient across the inner mitochondrial membrane. Once localized, the N-terminal targeting sequence is removed by mitochondrial processing peptidase (MPP), releasing the mature polypeptide to engage colocalized mitochondrial chaperoning pathways including the mitochondrial HSP70 chaperoning pathway [HSPA9 (mortalin)/DNAJA3 (Tid1)/GRPEL1], the HSP60 chaperonin (HSP60/HSP10), and the mitochondrial HSP90-like chaperone TRAP1 of the mitochondrial matrix [97]. The interactions with these chaperones and folding factors facilitate the proper folding of mitochondrial proteins into their functional conformation. Alternatively, proteins unable to fold into functional conformations or those that are damaged or misfolded during stress are degraded by ATP-dependent mitochondrial quality control proteases localized throughout mitochondria including the soluble matrix proteins LON and CLPP/CLPX and the inner membrane proteases AFG3L2 and paraplegin (with active sites directed towards the mitochondrial matrix) and YME1L (with active sites directed towards the IMS) [52].

The importance of these quality control pathways is evident, as mutations in genes encoding many of these quality control factors including HSP60, SPG7, and AFG3L2 predispose individuals to numerous diseases including many neurodegenerative disorders [53]. Furthermore, the expression of these proteins is highly regulated during stress through stress-responsive signaling pathways such as the mitochondrial unfolded protein response (UPR^{mt}) – a stress-responsive signaling pathway that induces mitochondrial proteostasis genes following mitochondrial matrix stress [73]. Thus, through the activity of these mitochondrial proteostasis pathways and through their regulation by stress-responsive signaling pathways such as the UPR^{mt} and the PERK arm of the UPR mitochondrial proteostasis is maintained in response to a wide range of pathologic insults, preventing the aberrant accumulation of misfolded proteins within mitochondria that can disrupt mitochondrial function.

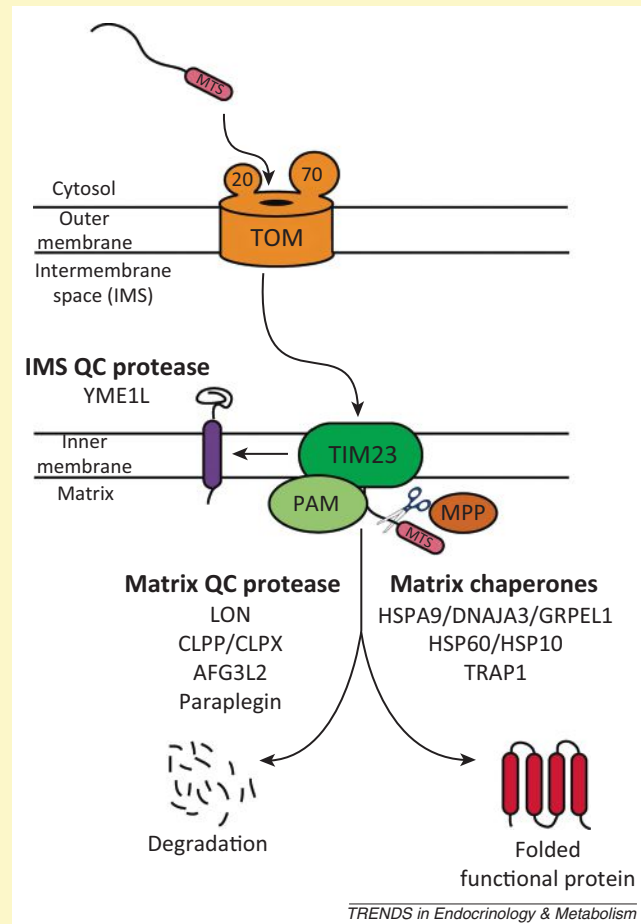


Figure 1. Illustration showing the molecular pathways responsible for the import, folding, and proteolysis of nuclear-encoded mitochondrial proteins targeted to the mitochondrial matrix. Mitochondrial matrix-targeted proteins and single-pass inner membrane proteins are directed to the TOM–TIM23 import pathway for translocation across the outer and inner mitochondrial membranes in a mechanism dependent on the ATPase activity of HSPA9 in the PAM complex and the electrochemical gradient across the outer and inner mitochondrial membranes. Following translocation, the N-terminal targeting sequence is removed by MPP, releasing the mature polypeptide to interact with mitochondrial chaperones that facilitate folding into a functional conformation. Proteins unable to fold or those unable to maintain their folded conformation are degraded by the activity of mitochondrial quality control proteases. Abbreviations: TOM, translocase of the outer membrane; TIM23, translocase of the inner membrane 23; MPP, mitochondrial processing peptidase; PAM, presequence associated motor.

mitochondrial transcription factor TFAM [59]. Overexpression of LON and LON variants has been shown to prevent mitochondrial dysfunction in response to Brefeldin A-induced ER stress [54], suggesting that PERK-dependent increases in LON protect the mitochondrial proteome during ER stress.

Other mitochondrial quality control factors such as the HSP70 ATP-dependent chaperone HSPA9/GRP75/mortalin are also induced downstream of PERK during ER stress through a mechanism dependent on ATF4 [9,54] (Figure 1). HSPA9 is involved in several protective mitochondrial proteostasis functions including the import of newly synthesized proteins into mitochondria [60,61], the refolding of misfolded or aggregated proteins within the mitochondrial matrix [62], and the cytosolic linking of ER–mito-

chondrial contacts through interactions with inositol trisphosphate receptor (IP₃R), a membrane glycoprotein Ca²⁺ channel activated by inositol trisphosphate, and voltage-dependent anion-selective channel protein 1 (VDAC1), a major component of the outer mitochondrial membrane [63]. Again, overexpression of HSPA9 attenuates ROS and increases cellular viability during ER stress induced by glucose deprivation, suggesting that PERK-dependent increases in HSPA9 protect mitochondrial function during ER stress [64]. Similarly, HSPA9 overexpression attenuates cell toxicity induced by proteotoxic Aβ involved in Alzheimer's disease [65,66], whereas HSPA9 knockdown sensitizes cells to Aβ toxicity [65,67]. The importance for HSPA9 regulation is also evident *in vivo*, where alterations in HSPA9 post-translational modifications and/or protein

levels have been found in patients with neurodegenerative disorders such as Parkinson's disease and Alzheimer's disease [68].

PERK also influences mitochondrial proteostasis through translational attenuation. The core Tim17A subunit of the translocase of the inner membrane 23 (TIM23) import complex is selectively degraded following translational attenuation induced by eIF2 α phosphorylation [69]. TIM23 is responsible for importing mitochondrial proteins across the inner mitochondria membrane (Box 2). Adapting TIM23-dependent import, such as through Tim17A degradation, has been proposed to promote mitochondrial proteostasis through multiple mechanisms [69]. Reduced TIM23 import will decrease mitochondrial accumulation of newly synthesized, unfolded proteins that challenge mitochondrial proteostasis pathways, reducing the folding load on mitochondrial chaperones and proteases and freeing these factors to protect the integrity of the established mitochondrial proteome – a protective mechanism similar to that afforded to the ER environment by PERK-dependent translational attenuation. Adapting TIM23 subunit composition could also alter the selectivity of mitochondrial protein import, providing a mechanism to directly adapt mitochondrial proteome composition and function during ER stress, a mechanism similar to that mediated by post-translational phosphorylation of the translocase of the outer membrane (TOM) [70,71]. Finally, attenuation of TIM23-dependent import provides a mechanism for the activation of stress-responsive transcription factors such as the mammalian homolog of *Caenorhabditis elegans* ATFS-1 (activating transcription factor associated with stress-1) – a transcription factor involved in the upregulation of mitochondrial proteostasis genes whose activation requires stress-dependent reductions in mitochondrial protein import [72,73].

The capacity for PERK to regulate mitochondrial proteostasis pathways during ER stress displays distinct parallels to the role for the UPR in regulating ER proteostasis pathways involved in ER protein folding, trafficking, and degradation. These results demonstrate an emerging role for UPR signaling in coordinating the regulation of ER and mitochondrial environments during ER stress through PERK signaling. Similarly, other eIF2 α kinases have also been shown to influence mitochondrial quality control in response to stresses including inflammation, mitochondrial dysfunction, and lipotoxicity [74–76]. This indicates that eIF2 α phosphorylation is a general mechanism to protect mitochondria during conditions of stress. As new transcriptional and proteomic approaches are being applied to study the impact of stress on cellular physiology, additional mitochondrial proteostasis factors will likely be identified to be transcriptionally or post-translationally regulated through PERK or other eIF2 α kinases, further defining the intricate role for this pathway in regulating mitochondria proteostasis environments in response to pathologic insults.

PERK-dependent regulation of organellar quality control

Global mitochondrial dysfunction induced by stress can be further corrected through organellar quality control pathways involved in mitochondrial fusion and fission processes (reviewed in [77,78]). Mitochondrial fusion can rescue

global defects in specific mitochondrial pathways (e.g., electron transport chain) through content mixing, allowing restoration of pathway integrity in the absence of new protein synthesis. Mitochondrial fusion proteins can also promote protective interactions with other organelles such as the ER, facilitating the exchange of metabolites that can stimulate mitochondria function. Alternatively, mitochondrial fission allows cells to segregate dysfunctional mitochondria (often identified by depolarization of the mitochondrial membrane). Once segregated, these mitochondria can be targeted to organellar degradation by the lysosome in a process referred to as mitophagy.

Above, we discuss the structural role for PERK in stabilizing ER–mitochondrial contacts, reflecting a protective role for PERK in mitochondrial organellar quality control. During ER stress, PERK signaling can also regulate organellar mitochondrial quality control through the transcriptional upregulation of the E3 ligase Parkin through the downstream activation of the PERK-regulated transcription factor ATF4 [79,80]. Parkin overexpression increases ER–mitochondrial interactions favoring interorganellar Ca²⁺ exchange and mitochondrial bioenergetics [81]. Conversely, depletion of Parkin decreases ER–mitochondrial contacts, indicating a defect in ER–mitochondrial tethering [81]. Parkin overexpression also attenuates ER stress-induced cell death, suggesting a protective role for PERK-dependent Parkin induction [79–82]. Parkin has many functions that could be protective during ER stress including the ubiquitination of specific substrates to target them to proteasomal degradation, removal of damaged mitochondria through mitophagy, and nondegradative functions that promote cellular physiology during stress [83]. Although the specific contributions of PERK-dependent increases in Parkin expression on ER–mitochondrial or mitochondrial organellar quality control remain to be further established, the capacity for cells to increase Parkin during conditions of ER stress provides an additional level of mitochondrial quality control to promote mitochondria proteostasis and function.

PERK-dependent regulation of cellular fate

In response to cellular insults too severe to be corrected by adaptive responses such as those described above, cellular quality control pathways initiate apoptotic signaling and programmed cell death (reviewed in [7,84]). Severe ER stress has been connected to multiple cell death cascades including calpain activation, caspase-12 activation, and most prominently mitochondrial initiation of intrinsic apoptosis. In this latter process, ER stress leads to MPTP opening, membrane depolarization, and release of cytochrome *c* through a mechanism involving oligomerization of BAX and BAK, the central proapoptotic BCL-2 (B cell lymphoma 2) family proteins, on the mitochondrial outer membrane [7,85]. Free cytochrome *c* in the cytosol induces formation of the apoptosome, activation of initiator caspase-9, and subsequent activation of the executioners caspase-3/caspase-7 that mediate the cell death program.

The PERK arm of the UPR extensively connects ER stress to intrinsic apoptosis. Chronic activation of PERK by sustained ER stress induces high expression of the transcription factor CHOP downstream of ATF4. CHOP^{-/-}

cells show a significant attenuation in ER stress-induced apoptosis, implicating this transcription factor in ER stress-induced cellular death [86,87]. CHOP appears to play multiple roles in apoptosis related to the regulation of mitochondrial-derived apoptotic signaling. It can drive the transcription of proapoptotic BCL-2 protein family members such as BiM (BCL-2 interacting mediator of cell death) and PUMA (p53 upregulated modulator of apoptosis) and repress production of the prosurvival BCL-2 protein thus favoring the oligomerization of BAX/BAK at the mitochondrial outer membrane [88,89]; however, this is not observed in all cells suggesting cell type-specific signaling [37]. In addition, translational attenuation induced by PERK suppresses the activity of prosurvival MCL-1 due to its short half-life compounding the promotion of proapoptotic signaling induced by CHOP [90]. Similarly, PERK-dependent translational attenuation and ATF4 activation decreases levels of prosurvival X-linked inhibitors of apoptosis (XIAP), which directly inhibits caspase activity [91]. CHOP-dependent expression of other target genes including GADD34 and ERO1 have also been proposed to induce apoptosis through increased ROS [92]. CHOP has also been suggested to promote the expression of ATF5, which can enhance apoptotic signaling through the increased expression of NOXA, a proapoptotic BCL-2 family protein that promotes BAX/BAK-dependent apoptosis [39]. Finally, the coactivation of ATF4 and CHOP downstream of PERK is suggested to influence cell survival by increasing protein synthesis, leading to increases in ROS and depleting ATP to trigger apoptotic signaling [37].

Despite the heavy focus on CHOP, overexpression of CHOP alone is insufficient to induce apoptosis, indicating that other mechanisms must similarly contribute to PERK-dependent apoptotic signaling [37]. This could be, in part, attributed to contributions of other UPR signaling pathways, such as the IRE1-dependent recruitment of tumor necrosis factor receptor-associated factor 2 (TRAF2) and induction of c-Jun N-terminal kinase (JNK) signaling (reviewed in [7,84]). The inherent complexity of UPR-mediated apoptotic signaling likely reflects the requirement for multiple checks and balances when defining cellular fate following pathologic insults that induce ER stress; such a level of redundancy results from the dual nature of the UPR in dictating prosurvival and proapoptotic signaling in response to ER stress. Additionally, different cells likely depend on distinct pathways to influence ER stress-induced cellular death through direct modulation of mitochondrial effectors (e.g., BAX/BAK oligomerization) or through post-translational regulation of proapoptotic signals such as Ca²⁺ mobilization and ROS. Ultimately, this level of complexity underscores the importance of ER-mitochondrial coordination and PERK signaling in dictating cell fate decisions in response to pathologic insults that induce ER stress.

Concluding remarks and future perspectives

The study of ER-mitochondrial contacts and the regulatory pathways that coordinate their interorganellar functions is in its infancy. Despite significant progress in the past 5 years, we are only beginning to understand the critical regulatory role of signaling pathways in coordinating ER-mitochondrial function in the context

Box 3. Outstanding questions

- What are the contributions of ER stress-dependent alterations in ER-mitochondrial signaling for the pathophysiology of human diseases?
- What are the molecular factors that interact with PERK at sites of ER-mitochondrial contact sites and how do they influence PERK-dependent regulation of mitochondrial function?
- How does PERK-dependent adaptation of mitochondrial quality control pathways influence mitochondrial proteostasis and function during conditions of ER stress?
- What are the specific molecular factors that underlie the complexity of mitochondrial-derived apoptotic signaling induced downstream of PERK?

of cellular stress. Here, we describe our current understanding of the contributions of PERK and PERK-regulated signaling on ER-mitochondrial communication and the regulation of mitochondrial proteostasis. These results demonstrate the capacity for PERK to coordinate ER and mitochondrial function in response to ER stress as part of the global UPR. In addition to the questions brought up in the context of this review (Box 3), new exciting questions are emerging as ongoing research efforts define the molecular mechanisms by which stress-responsive signaling pathways such as those regulated by PERK influence mitochondrial proteostasis and function. For example, does PERK signaling intersect with other stress-responsive signaling pathways involved in regulating mitochondrial proteostasis and function during stress (e.g., other arms of the ER UPR or the mitochondrial UPR)? Do other stress-responsive eIF2 α kinases similarly influence mitochondrial proteostasis and function in response to non-ER stress based cellular insults (e.g., nutrient deprivation, oxidative stress, viral infection)? Is there a therapeutic opportunity to attenuate mitochondrial dysfunction in human disease by targeting adaptive PERK signaling pathways that promote mitochondrial proteostasis and function or in suppressing chronic signaling that may promote pathology? These are just a few examples of the exciting questions that make the study of UPR-dependent regulation of mitochondrial function an exciting area for future research.

Acknowledgments

We apologize to all of the researchers whose work we were unable to reference owing to space limitations. We thank Cole Haynes (Memorial Sloan Kettering Cancer Center, MSKCC) and Jonathan Lin (The University of California, San Diego, UCSD) for comments on this manuscript. This work was funded by the Ellison Medical Foundation and Arnold and Arlene Goldstein.

References

- 1 de Brito, O.M. and Scorrano, L. (2010) An intimate liaison: spatial organization of the endoplasmic reticulum-mitochondria relationship. *EMBO J.* 29, 2715–2723
- 2 Kornmann, B. (2013) The molecular hug between the ER and the mitochondria. *Curr. Opin. Cell Biol.* 25, 443–448
- 3 van Vliet, A. *et al.* (2014) New functions of mitochondria associated membranes in cellular signaling. *Biochim. Biophys. Acta* <http://dx.doi.org/10.1016/j.bbamcr.2014.03.009>
- 4 Bravo, R. *et al.* (2011) Increased ER-mitochondrial coupling promotes mitochondrial respiration and bioenergetics during early phases of ER stress. *J. Cell Sci.* 124, 2143–2152

- 5 Koo, H.J. *et al.* (2012) Endoplasmic reticulum stress impairs insulin signaling through mitochondrial damage in SH-SY5Y cells. *Neurosignals* 20, 265–280
- 6 Rizzuto, R. *et al.* (2012) Mitochondria as sensors and regulators of calcium signalling. *Nat. Rev. Mol. Cell Biol.* 13, 566–578
- 7 Urra, H. *et al.* (2013) When ER stress reaches a dead end. *Biochim. Biophys. Acta* 1833, 3507–3517
- 8 Zheng, M. *et al.* (2012) Sensing endoplasmic reticulum stress by protein kinase RNA-like endoplasmic reticulum kinase promotes adaptive mitochondrial DNA biogenesis and cell survival via heme oxygenase-1/carbon monoxide activity. *FASEB J.* 26, 2558–2568
- 9 Harding, H.P. *et al.* (2003) An integrated stress response regulates amino acid metabolism and resistance to oxidative stress. *Mol. Cell* 11, 619–633
- 10 Cullinan, S.B. and Diehl, J.A. (2004) PERK-dependent activation of Nrf2 contributes to redox homeostasis and cell survival following endoplasmic reticulum stress. *J. Biol. Chem.* 279, 20108–20117
- 11 Gentile, C.L. *et al.* (2011) Fatty acids and the endoplasmic reticulum in nonalcoholic fatty liver disease. *Biofactors* 37, 8–16
- 12 Lee, J. and Ozcan, U. (2014) Unfolded protein response signaling and metabolic diseases. *J. Biol. Chem.* 289, 1203–1211
- 13 Lim, J.H. *et al.* (2009) Coupling mitochondrial dysfunction to endoplasmic reticulum stress response: a molecular mechanism leading to hepatic insulin resistance. *Cell. Signal.* 21, 169–177
- 14 Laplante, M. and Sabatini, D.M. (2012) mTOR signaling in growth control and disease. *Cell* 149, 274–293
- 15 Ozcan, U. *et al.* (2008) Loss of the tuberous sclerosis complex tumor suppressors triggers the unfolded protein response to regulate insulin signaling and apoptosis. *Mol. Cell* 29, 541–551
- 16 Perlmutter, D.H. (2011) Alpha-1-antitrypsin deficiency: importance of proteasomal and autophagic degradative pathways in disposal of liver disease-associated protein aggregates. *Annu. Rev. Med.* 62, 333–345
- 17 Teckman, J.H. (2013) Liver disease in α -1 antitrypsin deficiency: current understanding and future therapy. *COPD* 10 (Suppl. 1), 35–43
- 18 Doroudgar, S. and Glembotski, C.C. (2013) New concepts of endoplasmic reticulum function in the heart: programmed to conserve. *J. Mol. Cell. Cardiol.* 55, 85–91
- 19 Verdejo, H.E. *et al.* (2012) Mitochondria, myocardial remodeling, and cardiovascular disease. *Curr. Hypertens. Rep.* 14, 532–539
- 20 De Strooper, B. and Scorrano, L. (2012) Close encounter: mitochondria, endoplasmic reticulum and Alzheimer's disease. *EMBO J.* 31, 4095–4097
- 21 Schon, E.A. and Area-Gomez, E. (2013) Mitochondria-associated ER membranes in Alzheimer disease. *Mol. Cell. Neurosci.* 55, 26–36
- 22 Cali, T. *et al.* (2011) Mitochondria, calcium, and endoplasmic reticulum stress in Parkinson's disease. *Biofactors* 37, 228–240
- 23 Mercado, G. *et al.* (2013) An ER centric view of Parkinson's disease. *Trends Mol. Med.* 19, 165–175
- 24 Prell, T. *et al.* (2013) Calcium-dependent protein folding in amyotrophic lateral sclerosis. *Cell Calcium* 54, 132–143
- 25 Boillee, S. *et al.* (2006) ALS: a disease of motor neurons and their nonneuronal neighbors. *Neuron* 52, 39–59
- 26 Area-Gomez, E. *et al.* (2009) Presenilins are enriched in endoplasmic reticulum membranes associated with mitochondria. *Am. J. Pathol.* 175, 1810–1816
- 27 Area-Gomez, E. *et al.* (2012) Upregulated function of mitochondria-associated ER membranes in Alzheimer disease. *EMBO J.* 31, 4106–4123
- 28 Kipanyula, M.J. *et al.* (2012) Ca²⁺ dysregulation in neurons from transgenic mice expressing mutant presenilin 2. *Aging Cell* 11, 885–893
- 29 Zampese, E. *et al.* (2011) Presenilin 2 modulates endoplasmic reticulum (ER)–mitochondria interactions and Ca²⁺ cross-talk. *Proc. Natl. Acad. Sci. U.S.A.* 108, 2777–2782
- 30 Wiseman, R.L. *et al.* (2010) SnapShot: the unfolded protein response. *Cell* 140, 590.e2
- 31 Walter, P. and Ron, D. (2011) The unfolded protein response: from stress pathway to homeostatic regulation. *Science* 334, 1081–1086
- 32 Wang, S. and Kaufman, R.J. (2012) The impact of the unfolded protein response on human disease. *J. Cell. Biol.* 197, 857–867
- 33 Scheuner, D. *et al.* (2001) Translational control is required for the unfolded protein response and in vivo glucose homeostasis. *Mol. Cell* 7, 1165–1176
- 34 Hinnebusch, A.G. (2014) The scanning mechanism of eukaryotic translation initiation. *Annu. Rev. Biochem.* 83, 779–812
- 35 Sonenberg, N. and Hinnebusch, A.G. (2009) Regulation of translation initiation in eukaryotes: mechanisms and biological targets. *Cell* 136, 731–745
- 36 Harding, H.P. *et al.* (2000) Regulated translation initiation controls stress-induced gene expression in mammalian cells. *Mol. Cell* 6, 1099–1108
- 37 Han, J. *et al.* (2013) ER-stress-induced transcriptional regulation increases protein synthesis leading to cell death. *Nat. Cell Biol.* 15, 481–490
- 38 Marciniak, S.J. *et al.* (2004) CHOP induces death by promoting protein synthesis and oxidation in the stressed endoplasmic reticulum. *Genes Dev.* 18, 3066–3077
- 39 Teske, B.F. *et al.* (2013) CHOP induces activating transcription factor 5 (ATF5) to trigger apoptosis in response to perturbations in protein homeostasis. *Mol. Biol. Cell* 24, 2477–2490
- 40 Novoa, I. *et al.* (2001) Feedback inhibition of the unfolded protein response by GADD34-mediated dephosphorylation of eIF2 α . *J. Cell. Biol.* 153, 1011–1022
- 41 Ma, Y. and Hendershot, L.M. (2003) Delineation of a negative feedback regulatory loop that controls protein translation during endoplasmic reticulum stress. *J. Biol. Chem.* 278, 34864–34873
- 42 Wek, R.C. *et al.* (2006) Coping with stress: eIF2 kinases and translational control. *Biochem. Soc. Trans.* 34, 7–11
- 43 Verfaillie, T. *et al.* (2012) PERK is required at the ER–mitochondrial contact sites to convey apoptosis after ROS-based ER stress. *Cell Death Differ.* 19, 1880–1891
- 44 Liu, Z.W. *et al.* (2013) Protein kinase RNA-like endoplasmic reticulum kinase (PERK) signaling pathway plays a major role in reactive oxygen species (ROS)-mediated endoplasmic reticulum stress-induced apoptosis in diabetic cardiomyopathy. *Cardiovasc. Diabetol.* 12, 158
- 45 Munoz, J.P. (2013) Mfn2 modulates the UPR and mitochondrial function via repression of PERK. *EMBO J.* 32, 2348–2361
- 46 Gupta, S. *et al.* (2012) NOXA contributes to the sensitivity of PERK-deficient cells to ER stress. *FEBS Lett.* 586, 4023–4030
- 47 Engelman, G. *et al.* (2008) Recurrent acute liver failure and mitochondriopathy in a case of Wolcott–Rallison syndrome. *J. Inherit. Metab. Dis.* 31, 540–546
- 48 Sovik, O. *et al.* (2008) Wolcott–Rallison syndrome with 3-hydroxydicarboxylic aciduria and lethal outcome. *J. Inherit. Metab. Dis.* 31 (Suppl. 2), S293–S297
- 49 Hotamisligil, G.S. (2010) Endoplasmic reticulum stress and the inflammatory basis of metabolic disease. *Cell* 140, 900–917
- 50 Ozcan, U. *et al.* (2006) Chemical chaperones reduce ER stress and restore glucose homeostasis in a mouse model of type 2 diabetes. *Science* 313, 1137–1140
- 51 Sebastian, D. *et al.* (2012) Mitofusin 2 (Mfn2) links mitochondrial and endoplasmic reticulum function with insulin signaling and is essential for normal glucose homeostasis. *Proc. Natl. Acad. Sci. U.S.A.* 109, 5523–5528
- 52 Baker, M.J. *et al.* (2011) Quality control of mitochondrial proteostasis. *Cold Spring Harb. Perspect. Biol.* 3, a007559
- 53 Rugarli, E.I. and Langer, T. (2012) Mitochondrial quality control: a matter of life and death for neurons. *EMBO J.* 31, 1336–1349
- 54 Hori, O. *et al.* (2002) Transmission of cell stress from endoplasmic reticulum to mitochondria: enhanced expression of Lon protease. *J. Cell Biol.* 157, 1151–1160
- 55 Bender, T. *et al.* (2010) The role of protein quality control in mitochondrial protein homeostasis under oxidative stress. *Proteomics* 10, 1426–1443
- 56 Ngo, J.K. and Davies, K.J. (2009) Mitochondrial Lon protease is a human stress protein. *Free Radic. Biol. Med.* 46, 1042–1048
- 57 Bota, D.A. and Davies, K.J. (2002) Lon protease preferentially degrades oxidized mitochondrial aconitase by an ATP-stimulated mechanism. *Nat. Cell Biol.* 4, 674–680
- 58 Fukuda, R. *et al.* (2007) HIF-1 regulates cytochrome oxidase subunits to optimize efficiency of respiration in hypoxic cells. *Cell* 129, 111–122
- 59 Matsushima, Y. *et al.* (2010) Mitochondrial Lon protease regulates mitochondrial DNA copy number and transcription by selective degradation of mitochondrial transcription factor A (TFAM). *Proc. Natl. Acad. Sci. U.S.A.* 107, 18410–18415

- 60 Schmidt, O. *et al.* (2010) Mitochondrial protein import: from proteomics to functional mechanisms. *Nat. Rev. Mol. Cell Biol.* 11, 655–667
- 61 Chacinska, A. *et al.* (2009) Importing mitochondrial proteins: machineries and mechanisms. *Cell* 138, 628–644
- 62 Iosefson, O. *et al.* (2012) Reactivation of protein aggregates by mortalin and Tid1 – the human mitochondrial Hsp70 chaperone system. *Cell Stress Chaperones* 17, 57–66
- 63 Szabadkai, G. *et al.* (2006) Chaperone-mediated coupling of endoplasmic reticulum and mitochondrial Ca²⁺ channels. *J. Cell Biol.* 175, 901–911
- 64 Liu, Y. *et al.* (2005) Effect of GRP75/mthsp70/PBP74/mortalin overexpression on intracellular ATP level, mitochondrial membrane potential and ROS accumulation following glucose deprivation in PC12 cells. *Mol. Cell Biochem.* 268, 45–51
- 65 Qu, M. *et al.* (2011) Mortalin overexpression attenuates β -amyloid-induced neurotoxicity in SH-SY5Y cells. *Brain Res.* 1368, 336–345
- 66 Qu, M. *et al.* (2012) Inhibition of mitochondrial permeability transition pore opening is involved in the protective effects of mortalin overexpression against β -amyloid-induced apoptosis in SH-SY5Y cells. *Neurosci. Res.* 72, 94–102
- 67 Park, S.J. *et al.* (2014) Down-regulation of mortalin exacerbates A β -mediated mitochondrial fragmentation and dysfunction. *J. Biol. Chem.* 289, 2195–2204
- 68 Kaul, S.C. *et al.* (2007) Three faces of mortalin: a housekeeper, guardian and killer. *Exp. Gerontol.* 42, 263–274
- 69 Rainbolt, T.K. *et al.* (2013) Stress-regulated translational attenuation adapts mitochondrial protein import through Tim17A degradation. *Cell Metab.* 18, 908–919
- 70 Schmidt, O. *et al.* (2011) Regulation of mitochondrial protein import by cytosolic kinases. *Cell* 144, 227–239
- 71 Harbauer, A.B. *et al.* (2014) The protein import machinery of mitochondria – a regulatory hub in metabolism, stress, and disease. *Cell Metab.* 19, 357–372
- 72 Nargund, A.M. *et al.* (2012) Mitochondrial import efficiency of ATFS-1 regulates mitochondrial UPR activation. *Science* 337, 587–590
- 73 Haynes, C.M. *et al.* (2013) Evaluating and responding to mitochondrial dysfunction: the mitochondrial unfolded-protein response and beyond. *Trends Cell Biol.* 23, 311–318
- 74 Baker, B.M. *et al.* (2012) Protective coupling of mitochondrial function and protein synthesis via the eIF2 α kinase GCN-2. *PLoS Genet.* 8, e1002760
- 75 Viader, A. *et al.* (2013) Aberrant Schwann cell lipid metabolism linked to mitochondrial deficits leads to axon degeneration and neuropathy. *Neuron* 77, 886–898
- 76 Rath, E. *et al.* (2012) Induction of dsRNA-activated protein kinase links mitochondrial unfolded protein response to the pathogenesis of intestinal inflammation. *Gut* 61, 1269–1278
- 77 Youle, R.J. and van der Bliek, A.M. (2012) Mitochondrial fission, fusion, and stress. *Science* 337, 1062–1065
- 78 Chan, D.C. (2012) Fusion and fission: interlinked processes critical for mitochondrial health. *Annu. Rev. Genet.* 46, 265–287
- 79 Sun, X. *et al.* (2013) ATF4 protects against neuronal death in cellular Parkinson's disease models by maintaining levels of parkin. *J. Neurosci.* 33, 2398–2407
- 80 Bouman, L. *et al.* (2011) Parkin is transcriptionally regulated by ATF4: evidence for an interconnection between mitochondrial stress and ER stress. *Cell Death Differ.* 18, 769–782
- 81 Cali, T. *et al.* (2013) Enhanced parkin levels favor ER–mitochondria crosstalk and guarantee Ca²⁺ transfer to sustain cell bioenergetics. *Biochim. Biophys. Acta* 1832, 495–508
- 82 Imai, Y. *et al.* (2000) Parkin suppresses unfolded protein stress-induced cell death through its E3 ubiquitin-protein ligase activity. *J. Biol. Chem.* 275, 35661–35664
- 83 Winklhofer, K.F. (2014) Parkin and mitochondrial quality control: toward assembling the puzzle. *Trends Cell Biol.* 24, 332–341
- 84 Tabas, I. and Ron, D. (2011) Integrating the mechanisms of apoptosis induced by endoplasmic reticulum stress. *Nat. Cell Biol.* 13, 184–190
- 85 Brunelle, J.K. and Letai, A. (2009) Control of mitochondrial apoptosis by the Bcl-2 family. *J. Cell Sci.* 122, 437–441
- 86 Zinszner, H. *et al.* (1998) CHOP is implicated in programmed cell death in response to impaired function of the endoplasmic reticulum. *Genes Dev.* 12, 982–995
- 87 Oyadomari, S. *et al.* (2002) Targeted disruption of the Chop gene delays endoplasmic reticulum stress-mediated diabetes. *J. Clin. Invest.* 109, 525–532
- 88 Puthalakath, H. *et al.* (2007) ER stress triggers apoptosis by activating BH3-only protein Bim. *Cell* 129, 1337–1349
- 89 Reimertz, C. *et al.* (2003) Gene expression during ER stress-induced apoptosis in neurons: induction of the BH3-only protein Bbc3/PUMA and activation of the mitochondrial apoptosis pathway. *J. Cell Biol.* 162, 587–597
- 90 Fritsch, R.M. *et al.* (2007) Translational repression of MCL-1 couples stress-induced eIF2 α phosphorylation to mitochondrial apoptosis initiation. *J. Biol. Chem.* 282, 22551–22562
- 91 Hiramatsu, N. *et al.* (2014) Translational and posttranslational regulation of XIAP by eIF2 α and ATF4 promotes ER stress-induced cell death during the unfolded protein response. *Mol. Biol. Cell.* 25, 1411–1420
- 92 Song, B. *et al.* (2008) Chop deletion reduces oxidative stress, improves beta cell function, and promotes cell survival in multiple mouse models of diabetes. *J. Clin. Invest.* 118, 3378–3389
- 93 Osman, C. *et al.* (2011) Making heads or tails of phospholipids in mitochondria. *J. Cell Biol.* 192, 7–16
- 94 Shinzawa-Itoh, K. *et al.* (2007) Structures and physiological roles of 13 integral lipids of bovine heart cytochrome c oxidase. *EMBO J.* 26, 1713–1725
- 95 Gebert, N. *et al.* (2009) Mitochondrial cardiolipin involved in outer-membrane protein biogenesis: implications for Barth syndrome. *Curr. Biol.* 19, 2133–2139
- 96 Tatsuta, T. *et al.* (2014) Mitochondrial lipid trafficking. *Trends Cell Biol.* 24, 44–52
- 97 Voos, W. (2013) Chaperone-protease networks in mitochondrial protein homeostasis. *Biochim. Biophys. Acta* 1833, 388–399

Cell Press content is widely accessible

At Cell Press we place a high priority on ensuring that all of our journal content is widely accessible and on working with the community to develop the best ways to achieve that goal.

Here are just some of those initiatives...

Open archives

We provide free access to Cell Press research journals 12 months following publication

Access for developing nations

We provide free & low-cost access through programs like Research4Life

Open access journal

We launched Cell Reports - a new Open Access journal spanning the life sciences

Funding body agreements

We work cooperatively and successfully with major funding bodies

Public access

Full-text online via ScienceDirect is also available to the public via walk in user access from any participating library

Submission to PubMed Central

Cell Press deposits accepted manuscripts on our authors' behalf for a variety of funding bodies, including NIH and HHMI, to PubMed Central (PMC)

www.cell.com/cellpress/access



Mitochondria: from cell death executioners to regulators of cell differentiation

Atsuko Kasahara¹ and Luca Scorrano^{2,3}

¹ Department of Pathology and Immunology, University of Geneva, 1211 Geneva, Switzerland

² Department of Biology, University of Padua, 35121 Padua, Italy

³ Dulbecco–Telethon Institute, Venetian Institute of Molecular Medicine, 35129 Padua, Italy

Most, if not all mitochondrial functions, including adenosine-5'-triphosphate (ATP) production and regulation of apoptosis and Ca²⁺ homeostasis, are inextricably linked to mitochondrial morphology and dynamics, a process controlled by a family of GTP-dependent dynamin related 'mitochondria-shaping' proteins. Mitochondrial fusion and fission directly influence mitochondrial metabolism, apoptotic and necrotic cell death, autophagy, muscular atrophy and cell migration. In this review, we discuss the recent evidence indicating that mitochondrial dynamics influence complex signaling pathways, affect gene expression and define cell differentiation. These findings extend the importance of mitochondria to developmental biology, far beyond their mere bioenergetic role.

Mitochondrial morphology and cell biology

From a purely mitochondria-centric point of view, mitochondria can be regarded as the crucial organelles in determining cell fate. Indeed, whether a cell lives or dies depends on mitochondria. Not only do they participate in numerous essential biosynthetic and metabolic pathways, as well as in calcium and redox homeostasis, but they are also key regulators of apoptosis [1–3].

Mitochondria continually fuse and divide, and their quality, distribution, size, and motility are finely tuned [4,5]. The equilibrium between fusion and fission shapes the complex mitochondrial network in healthy cells. Depending on the physiological condition, this equilibrium can be perturbed and mitochondria can appear fragmented, such as during apoptosis [6], or elongated, such as during starvation [7]. The dynamics of mitochondria influences how the cell responds to environmental cues playing a critical role in cell fate. In this review, we discuss the current understanding of mitochondrial fusion and fission in mammals, and discuss evidence that supports roles for mitochondrial morphological changes in determining not only the response to cell stress, but also the emerging

Corresponding author: Scorrano, L. (luca.scorrano@unipd.it).

Keywords: mitochondrial dynamics; differentiation; cardiomyocyte; heart; hair follicle; DRP1; MFN; OPA1; Notch signaling; Ca²⁺.

0962-8924/

© 2014 Elsevier Ltd. All rights reserved. <http://dx.doi.org/10.1016/j.tcb.2014.08.005>

Glossary

Calcineurin: Ca²⁺ dependent serine-threonine protein phosphatase. Calcineurin is well known to dephosphorylate nuclear factor of activated T cells (NFAT) to induce its nuclear import. Calcineurin activity is inhibited by immunosuppressant cyclosporine A and FK506.

Dynamin related protein 1: in mammals mitochondrial fission depends on the action of dynamin-related protein 1 (DRP1), a large cytoplasmic GTPase that translocates to mitochondria at sites of fission, oligomerizes, and drives organelle fragmentation.

Mitochondrial respiration: mitochondrial oxidative phosphorylation is conducted by electron transport chain complexes that are accommodated in the cristae inner mitochondrial membrane. All complexes, except complex II, are composed of subunits encoded by nuclear genes. All four complexes are constituted of nuclear and mitochondrial DNA-encoded subunits. Using oxygen, mitochondrial respiration produces significant quantities of ATP, while it generates deleterious compounds, such as reactive oxygen species, as byproducts.

Mitofusins: in mammals, mitochondrial fusion depends on two outer membrane highly homologous proteins of the dynamin superfamily called mitofusin (MFN) 1 and 2. They participate in membrane tethering and use the energy of the hydrolysis of GTP to bend and fuse membranes by a still unclear mechanism. In addition, MFN2 tethers ER and mitochondria and is mutated in a genetic peripheral neuropathy called Charcot-Marie-Tooth IIa.

Notch signaling: a highly conserved pathway required for cell–cell communication in tissue differentiation, development, and renewal [79]. Both its receptors and ligands are transmembrane proteins. In canonical Notch signaling, the Notch receptor is cleaved to produce Notch intercellular domain (NICD), the active form of Notch, upon ligand binding. This NICD migrates to the nucleus where it associates with DNA-binding protein CSL (or CBF1/RBP- κ) to activate Notch target genes [79]. In the case of non-canonical signaling, regulation is independent of ligand and/or CSL. For example, membrane-bound Notch associates with active β -catenin, a core factor in Wnt signaling, and degrades active β -catenin [102].

NF- κ B signaling: nuclear factor kappa-light-chain-enhancer of activated B cells (NF- κ B), is a dimeric transcription factor composed of five family members: RelA (p65), p105/p50 (NF- κ B1), p100/p52 (NF- κ B2), c-Rel, and RelB, and is a crucial regulator of the immune system, stress responses, apoptosis, and differentiation [91]. The canonical pathway is stimulated by reactive oxygen species, lipopolysaccharides, and signals from cytokine receptors (tumor necrosis factor (TNF) receptor, interleukin 1 receptor, and Toll-like receptors). The non-canonical pathway is activated by specific members of the TNF family (Lymphotoxin- β , B cell activating factor, and CD40 ligand) to induce translocation of NF- κ B/RelB:p52 complex into the nucleus.

Optic Atrophy 1: in mammals Optic Atrophy 1 (OPA1) mediates inner membrane fusion. It belongs to the same superfamily of MFNs, but it is anchored to the inner membrane. In addition to controlling fusion, it regulates cristae biogenesis and remodeling.

Wnt signaling: in the canonical pathway, Wnt-protein binds to members of the Frizzled family receptor with a transcriptional coactivator β -catenin to regulate gene transcription during embryonic development. In non-canonical pathways, planar cell polarity pathway controls cell morphology by modulating cytoskeleton, while the Wnt/calcium pathway regulates calcium mobilization [98]. Wnt signaling directs cell proliferation, cell polarity, and cell fate determination during embryonic development and adult tissue homeostasis. Therefore, mutations in the components of Wnt pathway are involved in several disorders, such as cancer and metabolic diseases [98].

evidence that point to a crucial role for mitochondrial dynamics in cell differentiation.

Regulators of mitochondrial shape

The double membrane-bound architecture of mitochondria is regulated and maintained by a family of 'mitochondria-shaping' proteins. Mitochondrial fusion is mediated by the dynamin-related GTPases Mitofusin (MFN) 1 and 2, and by Optic Atrophy 1 (OPA1) (Figure 1A) (see Glossary).

MFN1 and MFN2 fuse the outer mitochondrial membrane (OMM). They form homo- and hetero-dimers that undergo conformational changes upon GTP hydrolysis in order to effect OMM fusion [8,9]. In addition to serving as key molecules in mitochondrial fusion, MFNs participate in specific forms of autophagy. MFNs are ubiquitinated by the cytosolic E3 ubiquitin ligase Parkin and degraded by the proteasome during mitochondrial autophagy (mitophagy) [10,11]. Upon cellular stress, MFN2 can be phosphorylated

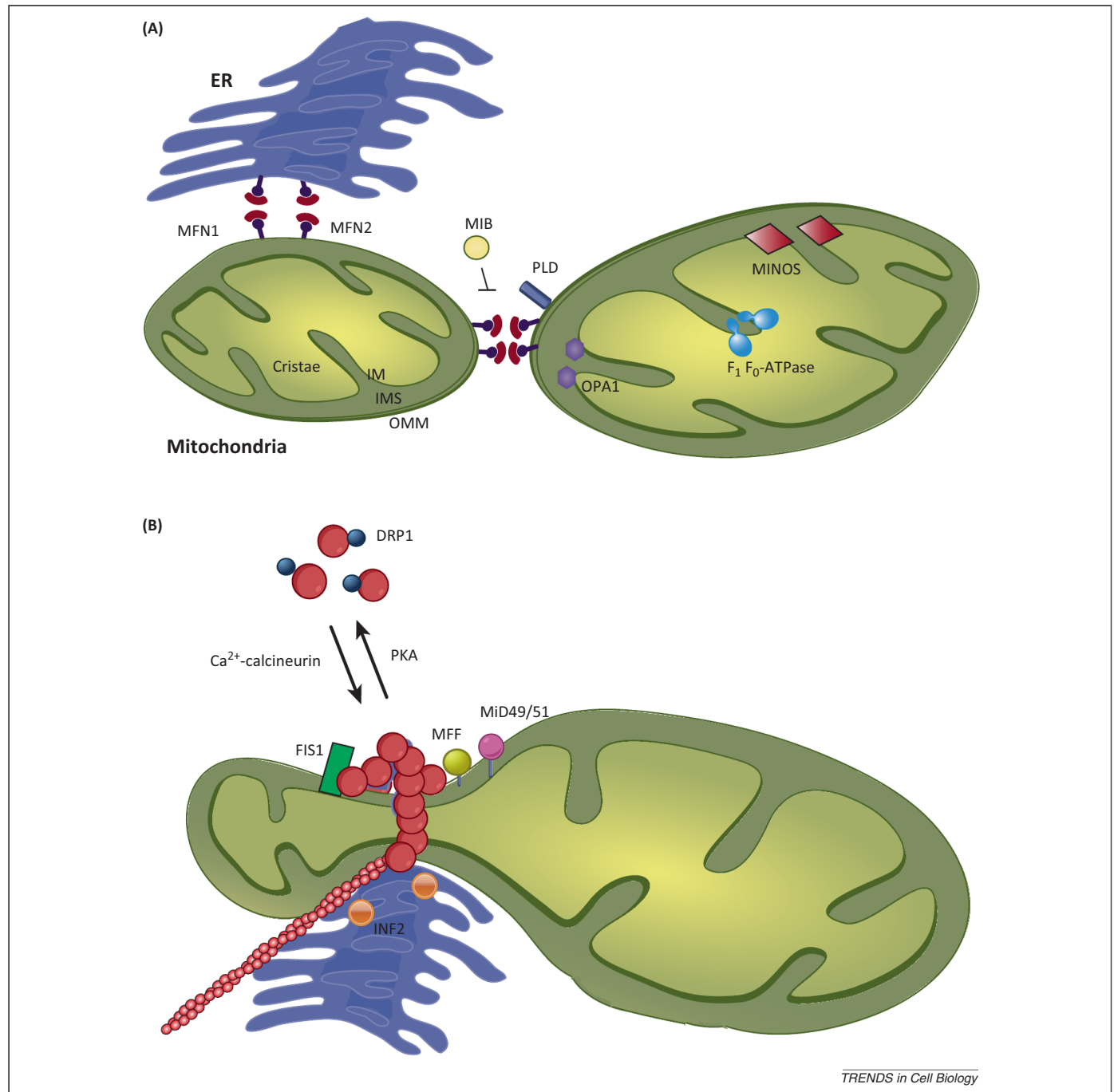


Figure 1. Regulation of mitochondrial dynamics. **(A)** A cartoon depicting the main proteins involved in mitochondrial fusion. In the small mitochondrion, the additional role of mitofusins (MFNs) in endoplasmic reticulum (ER)–mitochondria tethering is shown. They participate in the core reaction of outer mitochondrial membrane (OMM) fusion. MIB inhibits MFNs fusion activity, while phospholipase D (PLD), by providing lipid remodeling, facilitates it. Inner membrane (IM) fusion depends on Optic Atrophy 1 (OPA1), which additionally regulates cristae biogenesis and remodeling, together with the prohibitin–MINOS complex that controls cristae junction formation and dimers of the F₁F₀ ATPase that contribute to curve the cristae. Abbreviation: IMS, intermembrane space. **(B)** The mechanism of mitochondrial fission. Dynamamin-related protein-1 (DRP1) is normally phosphorylated and sequestered in the cytoplasm. At the endoplasmic reticulum (ER)–mitochondria contact site where ER tubules cross over and wrap around mitochondria in presence of F-actin and its ER receptor INF2, dephosphorylated dynamamin-related protein 1 (DRP1) is recruited to the OMM where it oligomerizes and interacts with its receptors MFF, MiD49/51, and FIS1, and mediates mitochondrial constriction.

Box 1. The ER–mitochondria juxtaposition in cell signaling and death

Interorganellar communication between ER and mitochondria is critical for mitochondrial energy and phospholipid metabolism, Ca²⁺ signaling, and cell death [103]. At the contact sites between these two organelles, their membranes do not fuse but tether, suggesting the existence of molecular bridges that set the distance between them. These tethers are of protein nature and their constituents have recently been elucidated. In yeast, the ER–mitochondria encounter structure (ERMES) consists of the OMM proteins mitochondrial distribution and morphology protein (Mdm) 10 and 34, the ER membrane protein GTPase EF-hand protein of mitochondria 1 (Gem1), mitochondrial morphology protein 1 (Mmm1), and the cytoplasmic protein known as Mdm12 [104]. In mammals, the mitochondrial profusion protein MFN2 directly tethers the two structures [105]. A fraction of MFN2 also localizes in the ER membrane, where it tethers the ER to mitochondria by a homotypic interaction with MFN2, or by a heterotypic interaction with MFN1 on the OMM. These interactions regulate mitochondrial Ca²⁺ uptake from the ER (Figure 1A), as well as the transfer of lipids from ER to mitochondria [78,106,107], highlighting how physical tethering participates in inter-organellar communication. Several other proteins involved in the generation, regulation, and maintenance of the

tethering have been identified, including FIS1 [43], B cell receptor associated protein 31 (BAP31) [55], and the multifunctional sorting protein PACS-2 [108]. MFN2-dependent tethers can be modulated, as exemplified by the changes in tethering mediated by MITOL, a mitochondrial ubiquitin ligase that ubiquitinates MFN2 [109], and by levels of the putative tumor suppressor trichoplein/mitostatin that counteract the tethering [110].

In addition to the metabolic and signaling function, ER–mitochondria contact sites also determine the position of mitochondrial division. Mitochondrial fission occurs where ER tubules cross over and wrap around mitochondria to mediate mitochondrial constriction before DRP1 recruitment [111] (Figure 1B). Notwithstanding that the nature of this fission tether is unclear, actin filaments concentrate at this interface and pharmacological disruption of F-actin attenuates fission and recruitment of DRP1 to the OMM [112]. Indeed, ER-localization of inverted formin 2 (INF2) is required for DRP1-mediated mitochondrial fission [113] and actin filaments accumulate at the INF2-enriched ER–mitochondria contact sites (Figure 1B). Which factors determine these contact sites, and whether they are structurally and functionally different from the metabolic ones described above, remains unclear.

by c-Jun N terminal kinase (JNK), leading to its ubiquitin-mediated proteasomal degradation, mitochondrial fragmentation, and apoptotic cell death [12]. Alternatively, *in vivo*, the mitophagy component serine/threonine *PTEN*-induced putative kinase1 (PINK1) can phosphorylate MFN2, thereby converting it into a mitochondrial receptor to recruit parkin and facilitate its ubiquitination for mitophagy [13]. In addition to its role in mitochondrial fusion, MFN2 is a key component of the machinery that tethers mitochondria to the ER generating a platform that regulates mitochondrial and cellular signaling (Box 1).

OPA1 is located in the inner mitochondrial membrane (IMM), facing the inner membrane space (IMS), where, together with MFN1, it controls IMM fusion [14]. OPA1 pro-fusion activity is regulated by a complex set of proteolytic modifications by mitochondrial matrix ATPase (m-AAA) proteases, paraplegin [15], and OMA1 [16,17], and by the inner membrane-AAA (i-AAA) protease Yme1 [18,19]. The processed short forms of OPA1 are substrates for the rhomboid protease presenilin associated rhomboid like (PARL) that produces a quantitatively small, intermembrane space soluble fraction of OPA1 that does not participate in fusion, but regulates cristae morphology and apoptosis (Box 2) [20].

Additionally, the IMM protein Leucine zipper-EF-hand containing transmembrane protein 1 (LETM1), whose downregulation induces mitochondrial fragmentation [21], and Phospholipase D (PLD), which promotes fusion by hydrolyzing cardiolipin to generate phosphatidic acid downstream of MFNs membrane tethering [22], have been identified as components of the mitochondrial fusion machinery. Prohibitins (PHB) are IMM proteins that play a role in mitochondrial fusion by regulating OPA1 processing. For instance, deletion of PHB2 leads to loss of the fusion-competent OPA1 long isoforms [23]. Future studies should aim at identifying additional profusion proteins, and detailing the molecular mechanism of IMM fusion and cristae reorganization concerted with OMM fusion. The combination of structural data and reconstituted *in vitro*

systems could advance our understanding of the mechanisms driving the coordinate fusion of the two membranes.

In contrast to mitochondrial fusion, mitochondrial fission is mediated by the cytosolic soluble dynamin-related protein 1 (DRP1) [24] (Figure 1B). Calcineurin mediates DRP1 Ser 637 dephosphorylation [25], triggering DRP1 translocation from the cytoplasm to mitochondria, where it interacts with its OMM docking adaptors (FIS1, MFF, and MiD49/51, also known as MIEF2/1) [26,27]. DRP1 oligomerizes and forms spiral filaments that drive mitochondrial constriction and fragmentation [28]. DRP1 activity is regulated by post-translational modifications, such as phosphorylation, dephosphorylation, ubiquitination, small ubiquitin-like modifier (SUMO)-ylation, deSUMOylation, and S-nitrosylation [26]. For example, phosphorylation at Ser 637 by cyclic AMP-dependent protein kinase A (PKA) inhibits DRP1 GTPase activity [29], consequently driving mitochondrial elongation during starvation [7]. In addition, cyclin B dependent kinase phosphorylates Ser 616 of DRP1, leading to mitotic mitochondrial fragmentation, thereby facilitating equal mitochondria distribution to daughter cells [30]. Furthermore, Parkin ubiquitinates DRP1 for proteasomal degradation [31] while the E3 ubiquitin ligases MARCH5 ubiquitinates DRP1 to alter mitochondrial morphology [32–34]. Finally, S-nitrosylation of DRP1 is observed in the brains of Alzheimer's disease patients and triggers mitochondrial fragmentation *in vitro* [35]. Irrespective of the signal driving its mitochondrial translocation, DRP1 physically interacts with MFF on the OMM to promote mitochondrial fission [36,37]. MiD49/51 are also involved in DRP1 recruitment to the OMM, and induce unopposed fusion [38,39] or inhibit DRP1 activity, favoring mitochondrial elongation [40]. Similar to its yeast homologue, mammalian FIS1 was also initially thought to be the primary adaptor of DRP1 at the OMM [41,42]; however, the role of FIS1 in mitochondrial fission appears controversial. While *Fis1* knockout does not affect mitochondrial morphology or DRP1 translocation to mitochondria [36], FIS1 interacts with MiD49/51 and reverses MiD49/51-induced mitochondrial fusion. Additionally,

Box 2. Cristae biogenesis and remodeling

The IMM can be subdivided into two different compartments: the inner boundary membrane, which is in proximity to the OMM; and the membrane invaginations called cristae. Cristae accommodate the respiratory chain complexes, thereby optimizing oxidative phosphorylation because their convoluted surface increases the bioenergetic membrane surface. Since cytochrome *c* is the only water soluble component of the respiratory chain, it comes as little surprise that most of it is confined in the cristae and that the junctions between the cristae and the IMM constitute a barrier to limit its diffusion in the IMS. Cristae junctions are kept tight by oligomers of OPA1 (Figure 1A). During apoptosis, OPA1 oligomers are disrupted, cristae junctions widen and cytochrome *c* is redistributed in the IMS from where it can be released in the cytosol [58]. In addition to OPA1, other factors involved in cristae shape include the F_1F_0 -ATP synthase, whose dimers or oligomeric assemblies affect the formation of cristae tips [114–117] and the protein mitofilin, homologous of yeast Fcj1p [118]. In yeast, the molecular components of the IMM shaping machinery have been more extensively characterized: a large mitochondrial inner-membrane organizing system (MICOS) is required for maintaining IMM architecture (Figure 1A). Indeed, mutations in one of the MICOS components lead to cristae disorganization characterized by the detachment of cristae from the inner boundary membrane, or the loss of cristae junctions [118–122]. MICOS is composed of Fcj1, Mio10, Aim13, and Aim37/Mio27, whose mammalian homologues are Mitofilin, MINOS1, CHCHD3, and MOMA-1 [118,123]. Consequently, the characteristic structure of the IMM appears to be formed and regulated by the combined action of OPA1, F_1F_0 -ATP synthase, and the megadalton protein complex MICOS. Interestingly, MICOS physically interacts with the OMM protein complex, such as the translocase of the outer membrane (TOM), and the sorting and assembly machinery (SAM). Both TOM and SAM complexes are major machineries of mitochondrial protein transport [119–122,124–126].

FIS1-null cells like MFF-null cells, show elongated mitochondria and impaired DRP1 recruitment to mitochondria [39]. One possibility, recently substantiated by experimental data, is that FIS1 binds to MFF, localizes at the endoplasmic reticulum (ER)–mitochondria interface and regulates mitophagy, thereby explaining its roles in mitochondrial morphology [43]. The availability of mouse models of *Fis1* ablation could clarify the role of this protein in mitochondrial fission.

In addition to the core components described above, other factors have been described to be involved in mitochondrial fission, such as Endophilin B1 [44], MTP18 [45], MIB [46], and GDAP1 [47]. Recent evidence added an unexpected player to the fragmentation of mitochondria, showing a pivotal role for the ER and the ER–mitochondria interface, as detailed in Box 1.

Mitochondrial morphology and cell stress

In order for an apoptotic signal to induce cell death, several changes must occur in mitochondria including mitochondrial fragmentation, cristae remodeling and mitochondrial outer membrane permeabilization (MOMP). These changes culminate in the release of cytochrome *c* and other pro-apoptotic factors, such as serine protease OMI/HtrA2, Smac/Diablo, endonuclease G, and apoptosis inducing factor (AIF), ultimately triggering caspase activation and cell death [6]. Therefore, it is not surprising that mitochondrial morphology and integrity play critical roles in apoptosis.

During apoptosis, DRP1 translocates from the cytosol to mitochondria, and promotes the oligomerization of the proapoptotic regulator Bcl-2-associated X protein (BAX), which facilitates MOMP to promote cell death [48,49]. Indeed, inhibition of DRP1 protects cells from apoptosis [50], suggesting mitochondrial fragmentation during apoptosis could be the consequence of enhanced fission. Indeed, recent studies suggest apoptosis depends on the post-translational modifications of DRP1, as has been shown for mitochondrial fission [26]. A pseudophosphorylation mutant of DRP1 induces mitochondrial elongation and renders cells resistant to apoptotic stimuli, while a mutant mimicking its dephosphorylation favors mitochondrial fragmentation and increases cell vulnerability [29]. Furthermore, DRP1 SUMOylation increases during apoptosis, correlating with the stable association of DRP1 to the OMM in a Bax/Bak dependent manner [51]. In addition to its role in apoptotic cell death, DRP1 is also required for the regulation of programmed necrotic cell death, through its dephosphorylation by mitochondrial protein phosphatase PGAM5 [52]. Other components of the fission machinery may also be involved in apoptosis, because downregulation of FIS1 inhibits cells death [53]. However, a mutation in the intermembrane region of FIS1 sustains fission activity but fails to induce apoptosis, suggesting that FIS1 regulates mitochondrial fragmentation and apoptosis separately [54]. Moreover, during apoptosis the activation of the apical caspase-8 can be modulated by FIS1 in concert with a resident ER protein called B cell associated protein 31 (BAP31) through a mechanism that is still poorly understood, but that might involve ER–mitochondria Ca^{2+} transfer [55].

In addition to enhanced fission, apoptosis can also be amplified by the inhibition of the fusion machinery. In fact, MFN1 or MFN2 silencing induces mitochondrial fragmentation and promotes apoptosis, while overexpression of these proteins leads to mitochondrial elongation and delays apoptotic cell death by inhibiting Bax/Bak oligomerization and cytochrome *c* release [56]. Similarly, downregulation of OPA1 induces apoptosis characterized by mitochondrial fragmentation, cristae disorganization, cytochrome *c* release, and caspase-dependent apoptotic nuclear events [57]. Conversely OPA1 overexpression protects cells from apoptosis by counteracting cristae remodeling and by stabilizing mitochondrial function [20,58,59]. Taken together, mitochondrial ultrastructure and morphology appear to be key players in the regulation of apoptotic as well as necrotic cell death.

In addition to its role in irreversible cell damage, mitochondrial dynamics is involved in autophagy. Mitochondrial fusion could be regarded as a compensation mechanism to ensure the mixing and unifying of mitochondrial components, such as mitochondrial proteins and metabolites, while mitochondrial fission could be considered an elimination process to segregate morphologically and functionally deleterious organelles from healthy ones. Terminally damaged or dysfunctional mitochondria undergo fission and are engulfed by the autophagic membrane, which leads to the formation of an autophagosome that targets damaged mitochondria to the lysosome [60] in a process called mitophagy. Mitophagy is distinct from

macroautophagy, which represents a non-selective cellular self-degradation process involved in the degradation of bulk cytoplasmic components, proteins, or entire organelles in nutrient depleted conditions [60]. In addition to its role in quality control, mitophagy not only removes damaged mitochondria, but also eliminates undamaged mitochondria during reticulocyte maturation into mature red blood cells [61–63], in a process mediated by the Bcl-2 family member, NIX (also known as Bnip3L) [64]. In mammalian cells, PINK1 and parkin, which are mutated in autosomal recessive Parkinson's disease, are emerging as key regulators of mitophagy [60]. Low membrane potential, a symptom of dysfunctional mitochondria, triggers the selective recruitment of Parkin to defective mitochondria in a PINK1-dependent manner [65,66]. In contrast, during macroautophagy induced by starvation, the rising cellular pool of cAMP activates PKA which inhibits DRP1. Consequently, mitochondria elongate, and are spared from autophagic degradation; therefore, preserving a major energy supply required by the cell under starving conditions [7]. Thus, opposite morphological features characterize the mitochondrial response to mitophagy and macroautophagy, underlining the importance of mitochondrial shape for the ability of the cell to respond to different cues.

Mitochondrial morphology in development and differentiation

Given the importance of mitochondria in intermediate metabolism, they have been regarded as key suppliers of the ATP required for development and differentiation. Not surprisingly, defects in embryogenesis and in tissue differentiation and development caused by gene disruption experiments of mitochondria shaping proteins in the mouse have been interpreted as the consequence of impaired bioenergetics or apoptosis [8,67,68]. Loss of *Mfn2*, but not *Mfn1* causes severe defects in the placental trophoblast giant cell layer during embryonic development [8]. Similarly, ablation of *Mfn2*, but not *Mfn1*, in the cerebellum leads to a failure in dendritic outgrowth, spine formation, and Purkinje cell survival [69]. Therefore, MFN2 seems more critical than MFN1 for embryogenesis and neuron development. Furthermore, the loss of MFNs in skeletal muscles causes muscle atrophy characterized by mitochondrial dysfunction, mtDNA depletion and mutations, and compensatory mitochondrial proliferation [70]. Conditional ablation of MFNs in adult hearts induces lethal dilated cardiomyopathy with fragmented mitochondria [71]. OPA1 mutations are associated with developmental defects such as dominant optic atrophy, while heterozygote *Opa1* mutant mice displays specific phenotypes in retinal ganglion cells, such as disorganized dendritic morphology and optic nerve degeneration [72,73]. Interestingly, not only does OPA1 downregulation affect retinal ganglion cells, but these mice also exhibit decreased motor skills [74], impaired mitochondrial permeability transition pore (PTP) opening in cardiac cells [75], and late onset cardiomyopathy [76]. All the tissues that are affected by MFNs and OPA1 ablation are susceptible to mitochondrial dysfunction given their high energy demand, further substantiating a model in which ablation

of mitochondrial fusion affects energy production, and hence, development or adult tissue homeostasis.

In contrast, recent studies suggest a different paradigm in which mitochondria are not simply bystanders in the differentiation and developmental process, but rather their activity, shape and localization directly influences nuclear programs and ultimately cell fate. One clue that these organelles might be more than ATP suppliers during development comes from the significant role of mitochondria in Ca^{2+} signaling [2], a pathway that impacts numerous, crucial cellular events like transcription, apoptosis, excitability, exocytosis, and motility [77]. Moreover, changes in OPA1 levels accompany the differentiation of placental trophoblast cells to favor steroidogenesis [78]. Beyond Ca^{2+} signaling, recent findings suggest that mitochondria unexpectedly control Notch, NF- κ B, and Wnt signaling pathways (Table 1).

Notch signaling and mitochondria

Notch signaling is essential for proliferation, survival, migration, stem cell maintenance, and embryonic and adult differentiation and development [79]. Canonical Notch signaling is activated through the cleavage of the transmembrane domain of the Notch receptor by the γ -secretase complex upon binding to its ligand, which leads to the production of Notch intercellular domain (NICD). NICD migrates to the nucleus where it associates with the DNA-binding protein CSL (or CBF1/RBP-jk), to activate Notch target genes [79]. In contrast to nuclear localization of NICD in canonical Notch signaling, NICD localizes in the cytosol when the non-canonical Notch pathway is activated. Cytosolic NICD inhibits mitochondrial fragmentation and protects from apoptosis by inhibiting Bax oligomerization, which is coordinated by Akt and MFNs [80] (Figure 2A). Although this is the first observation of a link between mitochondrial dynamics and Notch signaling, the detailed molecular mechanism by which NICD–Akt axis acts with MFNs to prevent apoptotic cell death remains unclear.

Another link between mitochondria and Notch signaling comes from the analysis of *Drosophila* follicle cells. Genetic ablation of DRP1 inhibits follicle cell differentiation, but maintains proliferation via Notch inactivation, while Notch signaling is enhanced normally during post-mitotic differentiation [81] (Figure 2B). However, it is unknown how highly fused mitochondria (or DRP1 downregulation) inactivate Notch in follicle cells. Recent data suggest a possible mechanism by which mitochondrial shape impinges on canonical Notch signaling, at least during cardiomyocyte differentiation (Figure 2C), where Notch is a known differentiation inhibitor [82]. Although ablation of both MFNs in the embryonic mouse heart is lethal, the precise mechanisms leading to heart malformation were unclear. According to the classic paradigm, inhibition of mitochondrial fusion could result in bioenergetic crisis and excess apoptosis. Surprisingly, however, the heart of fusion-deficient mice is characterized by a reduction in the number of cardiomyocytes and by a defect in cellular proliferation, indicating that fusion impinges on cellular functions other than apoptosis. Indeed an unbiased RNA sequencing approach identified that myocyte enhancer

Table 1. Mitochondria in signaling pathways

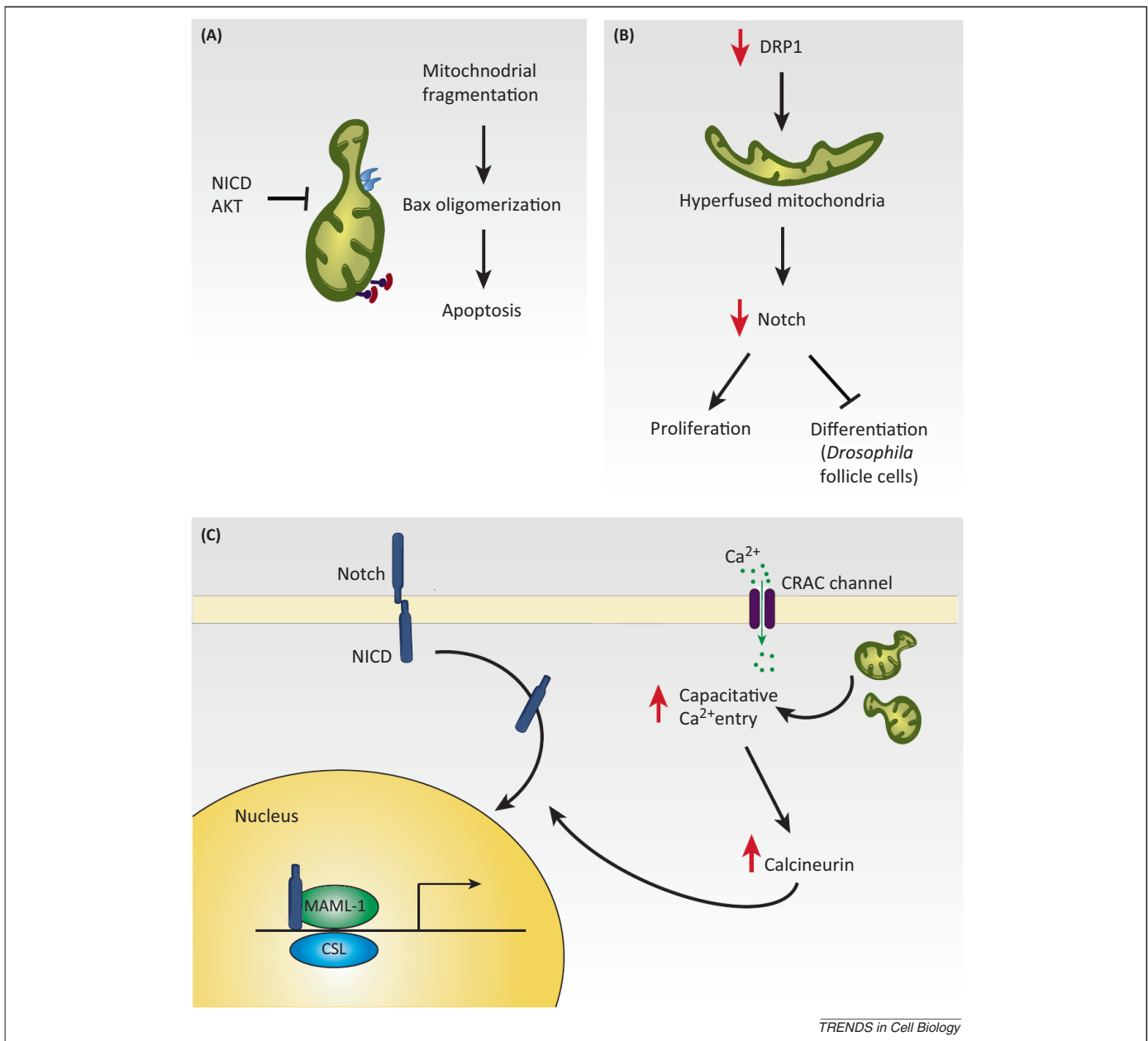
Mitochondria	Effect	Refs
Notch signaling		
Mitofusins	• Inhibits mitochondrial fragmentation during apoptosis	[80]
DRP downregulation	• Inactivates Notch and inhibits follicle cell differentiation in <i>Drosophila</i>	[81]
MFN/OPA downregulation	• Notch activation via calcineurin • Increase in active NICD in nucleus	[83]
Mitochondrial ROS	• Suppresses Notch signaling in epidermal differentiation	[84]
Metabolic switch	• Activated Notch leads to glycolysis via PI3K/AKT • Downregulation of Notch induces glycolysis via p53	[85]
Mitochondrial respiration	• Influences respiratory chain complex assembly • Reduces ATP production directly interacting with PINK1 • <i>Drosophila</i> lethal point mutation in Notch reduces enzyme activities of NADH oxidase, NADH dehydrogenase, succinate dehydrogenase, and alpha-glycerophosphate dehydrogenase • Notch activation downregulates complex I and II subunits • Notch 3 mutation reduces complex I activity	[86–90]
NF-κB signaling		
Metabolic switch	• Downregulation of NF-κB decreases SCO2, a p53 target gene that is a subunit of cytochrome c oxidase	[92]
OPA1	• Enhances linear ubiquitination of NF-κB essential modulator (NEMO) • Upregulates OPA1 for mitochondrial integrity	[93]
MAVS	• Downregulation reduces NF-κB activation upon virus infection • Overexpression increases NF-κB activation and boosts antiviral response	[95]
Wnt signaling		
Mitochondrial biogenesis	• Recombinant Wnt3a increases mtDNA content, oxygen consumption, respiratory capacity, and ROS production	[99]
Mitochondrial apoptosis	• Activation of Wnt/β-catenin signaling in hematopoietic progenitor cells induces mitochondrial dependent apoptosis	[97]
Mitochondrial dynamics	• Wnt5a induces mitochondrial fragmentation in hippocampal neurons followed by re-elongation in a time-dependent manner	[100]

factor-2c (MEF2c) mRNA levels are downregulated in the MFNs knockout embryonic heart, pointing to a differentiation defect. Mapping the differentiation of mitochondrial fusion-deficient mouse embryonic stem cells (ESCs) during cardiomyocyte development revealed that the altered subcellular mitochondrial distribution in those ESCs results in increased cytoplasmic Ca²⁺ load and calcineurin activity. Furthermore, these changes caused a sustained increase in Notch1 nuclear translocation and activation, consistent with the observed reduction in the levels of the NICD binding competitor MEF2c [83]. A pharmacological rise in intracellular Ca²⁺ levels fully recapitulates the calcineurin dependent Notch1 activation, while calcineurin inhibition normalizes Notch1 activity and rescues cardiomyocyte differentiation in fusion-deficient ESCs. Therefore, mitochondrial shape and localization impact nuclear programs of differentiation through the interconnection between Ca²⁺, calcineurin, and Notch signaling [83]. Whether Notch signaling is downstream of mitochondria in tissues other than the heart remains to be seen, but these findings open novel possibilities to explore whether mitochondrial shape participates in the plethora of cellular and developmental processes controlled by Notch.

In a different model of differentiation, reactive oxygen species (ROS), and not Ca²⁺, emerged as the signal emanating from mitochondria to affect Notch signaling. Conditional knockout of mitochondrial transcription factor A (TFAM) in keratinocytes increased the proliferation of epidermal cells, but inhibited epidermal differentiation via the suppression of mitochondrial ROS and Notch signaling, which is required for epidermal differentiation [84]. This finding suggests that several different signals are

used by mitochondria to influence the nuclear differentiation program. It is conceivable that organelles can influence complex pathways of development and differentiation in a similar manner.

It is important to note that the crosstalk between mitochondria and nuclear signaling is bidirectional. The same Notch cascade that is controlled by mitochondria during differentiation can regulate mitochondrial metabolism. The metabolic switch from oxidative to glycolytic frequently occurs in cancer cells, and is related to tumor growth and invasion suggesting that the nuclear programs coordinating the acquisition of the malignant phenotype impinge on mitochondria. In breast cancer cells, for example, activated Notch shifts metabolism toward glycolysis via activation of the phosphatidylinositol 3-kinase/AKT serine/threonine kinase pathway, while downregulation of Notch induces glycolysis in a p53-dependent manner, suggesting that mitochondrial respiration is inhibited in these cells [85]. The Akt pathway is also recruited by Notch to protect mitochondria from apoptotic permeabilization, by activating MFNs and inducing mitochondrial elongation [80]. A non-canonical Notch signaling pathway was indeed found to regulate mitochondrial respiratory function directly, through potential interactions with the mitophagy component PINK1, and select respiratory chain subunits [86], similar to early observations in *Drosophila* where Notch signaling affects mitochondrial respiration [87,88]. Recently, using a comparative proteomics approach, canonical Notch activation was found to downregulate the levels of respiratory chain subunits, such as components of complex I NADH-ubiquinone oxidoreductase NDUF51, and NDUFV2 subunits, and complex II Succinate dehydrogenase SDHA



TRENDS in Cell Biology

Figure 2. Mitochondrial dynamics and Notch signaling. **(A)** In the non-canonical Notch pathway, the cytosolic Notch intercellular domain (NICD) inhibits mitochondrial fragmentation during apoptosis induced by the Bcl-2 family Bax and staurosporine, and protects the cell from apoptotic cell death via Akt and mitofusins (MFNs). **(B)** Dynamin-related protein-1 (DRP1) downregulation induces hyperfused mitochondria, and inhibits follicle cell differentiation, but maintains proliferation via Notch inactivation. **(C)** Upon Notch ligand binding to the Notch receptor, an ADAM metalloprotease and a γ -secretase complex cleaves the Notch receptor and releases the NICD, which migrates into the nucleus. NICD interacts with the DNA binding protein CSL (also called CBF1/RBP-jk) and recruits a coactivator complex composed of Mastermind (MAML-1), and other transcription factors to activate Notch target genes. Notch signaling, which inhibits cardiac cell differentiation, is activated in fusion-deficient embryonic stem cells (ESCs) where mitochondria are fragmented and accumulate in the cell periphery. Because of fragmented mitochondria in the cell periphery, a negative feedback to the CRAC channel is attenuated, and capacitative Ca^{2+} entry and activity of the Ca^{2+} dependent phosphatase calcineurin are increased. Activated calcineurin does not affect the production of NICD from full length Notch receptor, but does affect its migration to the nucleus, or stability or binding ability to the transcription complex of NICD.

subunit [89]. In addition, a patient study showed that Notch3 mutation induces the reduction of complex I activity [90], suggesting strong link exists between Notch signaling and mitochondrial respiratory chain complex I; however, the detailed molecular mechanism by which Notch signaling modulates mitochondrial respiration has yet to be uncovered.

NF- κ B signaling and mitochondria

A similar metabolic switch can be operated by nuclear factor kappa-light-chain-enhancer of activated B cells

(NF- κ B), a transcription factor composed of five family members: RelA (p65), p105/p50 (NF- κ B1), p100/p52 (NF- κ B2), c-Rel, and RelB. NF- κ B is a key regulator of the immune and inflammatory responses and plays a crucial role in cell survival, proliferation, adhesion and angiogenesis [91]. Downregulation of RelA causes a shift from oxidative metabolism to glycolysis via p53, by reducing the p53 target SCO2, a subunit of the mitochondrial cytochrome c oxidase, with the predicted reduction of mitochondrial respiration [92]. Surprisingly, OPA1 has been identified as an NF- κ B target gene in a pathway linking

the mitophagy ubiquitin ligase Parkin to the protection of cells from apoptosis. Indeed, Parkin induces the linear ubiquitination of the NF- κ B essential modulator (NEMO) ultimately increasing OPA1 levels, thereby protecting cells from apoptosis [93]. These results indicate that mitochondrial morphology and nuclear signaling are interconnected by unexpected pathways beyond established models, such as mitophagy. Indeed, mitochondrial antiviral signaling protein (MASV, also known as VISA) which localizes in the OMM, interacts with MFN2 [94], and mediates NF- κ B signaling activation in response to viral infection [95,96].

Wnt signaling and mitochondria

Wnt is another nuclear signaling pathway impinging on mitochondria. In the canonical pathway, Wnt binds to members of the Frizzled family, thereby regulating the LEF/TCF transcription factor family along with the transcriptional coactivator β -catenin to control genes regulating cell fate and morphogenesis. For example, canonical Wnt3a increases mitochondrial biogenesis, mtDNA contents, oxygen consumption, respiration capacity, and ROS levels. Furthermore, the activation of β -catenin in hematopoietic progenitor cells activates the mitochondrial apoptotic pathway, with loss of mitochondrial membrane potential and caspase 3 and 9 cleavage [97]. Additionally, Wnt activates a non-canonical pathway that regulates planar cell polarity by stimulating cytoskeletal reorganization and calcium mobilization [98]. Specifically the non-canonical Wnt5a antagonizes the Wnt3a effect on mitochondria [99]. Moreover, non-canonical Wnt5a, but not canonical Wnt3a, modulates mitochondrial morphology in hippocampal neurons by inducing mitochondrial fragmentation followed by re-elongation in a circuit that needs to be further elucidated [100]. Whether mitochondrial morphology reciprocally affects Wnt signaling during cell development and differentiation remains to be explored.

These examples indicate that mitochondria work as hubs to coordinate signaling cascades in response to intra-extracellular cues, ultimately controlling not only cell survival, but also fate, differentiation, and development. In addition, by studying the contribution of mitochondrial dynamics and physiology to cell fate, previously unknown crossroads between signaling cascades that contribute to development and differentiation will be unveiled.

Concluding remarks

The core components of the mammalian mitochondrial fusion–fission machinery have been identified, and growing evidence suggests that mitochondrial morphology regulates apoptosis, ER-communication, autophagy, neurodegenerative disorders, and cancer [101]. The recent discoveries that mitochondria are not only targets of nuclear signaling cascades, but also influencers of these pathways to define the differentiation program of stem cells *in vitro* and *in vivo*, adds a novel layer of complexity to the role of these ancient endosymbionts. They are not only innocent bystanders that simply amplify cellular cues, but are also active players that signal to the nucleus to define perhaps the most crucial property of multicellular organisms: differentiation and development. What a remarkable revenge

for a parasite domesticated to serve as a metabolic and signaling platform!

Acknowledgments

L.S. is a Senior Scientist of the Dulbecco Telethon Institute. Research in his laboratory is supported by Telethon Italy GGP12162, GPP10005, AIRC Italy, ERC ERMITO, FP7 CIG CristOpa, and MIUR FIRB Automed.

References

- Ernster, L. and Schatz, G. (1981) Mitochondria: a historical review. *J. Cell Biol.* 91, 227s–255s
- Rizzuto, R. *et al.* (2000) Mitochondria as all-round players of the calcium game. *J. Physiol.* 529 (Pt 1), 37–47
- Scorrano, L. (2009) Opening the doors to cytochrome c: changes in mitochondrial shape and apoptosis. *Int. J. Biochem. Cell Biol.* 41, 1875–1883
- Frederick, R.L. and Shaw, J.M. (2007) Moving mitochondria: establishing distribution of an essential organelle. *Traffic* 8, 1668–1675
- Fischer, F. *et al.* (2012) Mitochondrial quality control: an integrated network of pathways. *Trends Biochem. Sci.* 37, 284–292
- Suen, D.F. *et al.* (2008) Mitochondrial dynamics and apoptosis. *Genes Dev.* 22, 1577–1590
- Gomes, L.C. *et al.* (2011) During autophagy mitochondria elongate, are spared from degradation and sustain cell viability. *Nat. Cell Biol.* 13, 589–598
- Chen, H. *et al.* (2003) Mitofusins Mfn1 and Mfn2 coordinately regulate mitochondrial fusion and are essential for embryonic development. *J. Cell Biol.* 160, 189–200
- Koshiba, T. *et al.* (2004) Structural basis of mitochondrial tethering by mitofusin complexes. *Science* 305, 858–862
- Tanaka, A. *et al.* (2010) Proteasome and p97 mediate mitophagy and degradation of mitofusins induced by Parkin. *J. Cell Biol.* 191, 1367–1380
- Gegg, M.E. *et al.* (2010) Mitofusin 1 and mitofusin 2 are ubiquitinated in a PINK1/parkin-dependent manner upon induction of mitophagy. *Hum. Mol. Genet.* 19, 4861–4870
- Leboucher, G.P. *et al.* (2012) Stress-induced phosphorylation and proteasomal degradation of mitofusin 2 facilitates mitochondrial fragmentation and apoptosis. *Mol. Cell* 47, 547–557
- Chen, Y. and Dorn, G.W., 2nd (2013) PINK1-phosphorylated mitofusin 2 is a Parkin receptor for culling damaged mitochondria. *Science* 340, 471–475
- Cipolat, S. *et al.* (2004) OPA1 requires mitofusin 1 to promote mitochondrial fusion. *Proc. Natl. Acad. Sci. U.S.A.* 101, 15927–15932
- Ishihara, N. *et al.* (2006) Regulation of mitochondrial morphology through proteolytic cleavage of OPA1. *EMBO J.* 25, 2966–2977
- Ehse, S. *et al.* (2009) Regulation of OPA1 processing and mitochondrial fusion by m-AAA protease isoenzymes and OMA1. *J. Cell Biol.* 187, 1023–1036
- Head, B. *et al.* (2009) Inducible proteolytic inactivation of OPA1 mediated by the OMA1 protease in mammalian cells. *J. Cell Biol.* 187, 959–966
- Griparic, L. *et al.* (2007) Regulation of the mitochondrial dynamin-like protein Opa1 by proteolytic cleavage. *J. Cell Biol.* 178, 757–764
- Song, Z. *et al.* (2007) OPA1 processing controls mitochondrial fusion and is regulated by mRNA splicing, membrane potential, and Yme1L. *J. Cell Biol.* 178, 749–755
- Cipolat, S. *et al.* (2006) Mitochondrial rhomboid PARL regulates cytochrome c release during apoptosis via OPA1-dependent cristae remodeling. *Cell* 126, 163–175
- Dimmer, K.S. *et al.* (2008) LETM1, deleted in Wolf-Hirschhorn syndrome is required for normal mitochondrial morphology and cellular viability. *Hum. Mol. Genet.* 17, 201–214
- Choi, S.Y. *et al.* (2006) A common lipid links Mfn-mediated mitochondrial fusion and SNARE-regulated exocytosis. *Nat. Cell Biol.* 8, 1255–1262
- Merkwirth, C. *et al.* (2008) Prohibitins control cell proliferation and apoptosis by regulating OPA1-dependent cristae morphogenesis in mitochondria. *Genes Dev.* 22, 476–488

- 24 Smirnova, E. *et al.* (2001) Dynamin-related protein Drp1 is required for mitochondrial division in mammalian cells. *Mol. Biol. Cell* 12, 2245–2256
- 25 Cereghetti, G.M. *et al.* (2008) Dephosphorylation by calcineurin regulates translocation of Drp1 to mitochondria. *Proc. Natl. Acad. Sci. U.S.A.* 105, 15803–15808
- 26 Elgass, K. *et al.* (2013) Recent advances into the understanding of mitochondrial fission. *Biochim. Biophys. Acta* 1833, 150–161
- 27 Liu, T. *et al.* (2013) The mitochondrial elongation factors MIEF1 and MIEF2 exert partially distinct functions in mitochondrial dynamics. *Exp. Cell Res.* 319, 2893–2904
- 28 Mears, J.A. *et al.* (2011) Conformational changes in Dnm1 support a contractile mechanism for mitochondrial fission. *Nat. Struct. Mol. Biol.* 18, 20–26
- 29 Cribbs, J.T. and Strack, S. (2007) Reversible phosphorylation of Drp1 by cyclic AMP-dependent protein kinase and calcineurin regulates mitochondrial fission and cell death. *EMBO Rep.* 8, 939–944
- 30 Taguchi, N. *et al.* (2007) Mitotic phosphorylation of dynamin-related GTPase Drp1 participates in mitochondrial fission. *J. Biol. Chem.* 282, 11521–11529
- 31 Wang, H. *et al.* (2011) Parkin ubiquitinates Drp1 for proteasome-dependent degradation: implication of dysregulated mitochondrial dynamics in Parkinson disease. *J. Biol. Chem.* 286, 11649–11658
- 32 Yonashiro, R. *et al.* (2006) A novel mitochondrial ubiquitin ligase plays a critical role in mitochondrial dynamics. *EMBO J.* 25, 3618–3626
- 33 Karbowski, M. *et al.* (2007) The mitochondrial E3 ubiquitin ligase MARCH5 is required for Drp1 dependent mitochondrial division. *J. Cell Biol.* 178, 71–84
- 34 Nakamura, N. *et al.* (2006) MARCH-V is a novel mitofusin 2- and Drp1-binding protein able to change mitochondrial morphology. *EMBO Rep.* 7, 1019–1022
- 35 Cho, D.H. *et al.* (2009) S-nitrosylation of Drp1 mediates beta-amyloid-related mitochondrial fission and neuronal injury. *Science* 324, 102–105
- 36 Otera, H. *et al.* (2010) Mff is an essential factor for mitochondrial recruitment of Drp1 during mitochondrial fission in mammalian cells. *J. Cell Biol.* 191, 1141–1158
- 37 Gandre-Babbe, S. and van der Bliek, A.M. (2008) The novel tail-anchored membrane protein Mff controls mitochondrial and peroxisomal fission in mammalian cells. *Mol. Biol. Cell* 19, 2402–2412
- 38 Palmer, C.S. *et al.* (2011) MiD49 and MiD51, new components of the mitochondrial fission machinery. *EMBO Rep.* 12, 565–573
- 39 Loson, O.C. *et al.* (2013) Fis1, Mff, MiD49, and MiD51 mediate Drp1 recruitment in mitochondrial fission. *Mol. Biol. Cell* 24, 659–667
- 40 Zhao, J. *et al.* (2011) Human MIEF1 recruits Drp1 to mitochondrial outer membranes and promotes mitochondrial fusion rather than fission. *EMBO J.* 30, 2762–2778
- 41 Yoon, Y. *et al.* (2003) The mitochondrial protein hFis1 regulates mitochondrial fission in mammalian cells through an interaction with the dynamin-like protein DLP1. *Mol. Cell. Biol.* 23, 5409–5420
- 42 Stojanovski, D. *et al.* (2004) Levels of human Fis1 at the mitochondrial outer membrane regulate mitochondrial morphology. *J. Cell Sci.* 117, 1201–1210
- 43 Shen, Q. *et al.* (2014) Mutations in Fis1 disrupt orderly disposal of defective mitochondria. *Mol. Biol. Cell* 25, 145–159
- 44 Karbowski, M. *et al.* (2004) Endophilin B1 is required for the maintenance of mitochondrial morphology. *J. Cell Biol.* 166, 1027–1039
- 45 Tondera, D. *et al.* (2005) The mitochondrial protein MTP18 contributes to mitochondrial fission in mammalian cells. *J. Cell Sci.* 118, 3049–3059
- 46 Eura, Y. *et al.* (2006) Identification of a novel protein that regulates mitochondrial fusion by modulating mitofusin (Mfn) protein function. *J. Cell Sci.* 119, 4913–4925
- 47 Pedrola, L. *et al.* (2005) GDAP1, the protein causing Charcot-Marie-Tooth disease type 4A, is expressed in neurons and is associated with mitochondria. *Hum. Mol. Genet.* 14, 1087–1094
- 48 Cassidy-Stone, A. *et al.* (2008) Chemical inhibition of the mitochondrial division dynamin reveals its role in Bax/Bak-dependent mitochondrial outer membrane permeabilization. *Dev. Cell* 14, 193–204
- 49 Montessuit, S. *et al.* (2010) Membrane remodeling induced by the dynamin-related protein Drp1 stimulates Bax oligomerization. *Cell* 142, 889–901
- 50 Frank, S. *et al.* (2001) The role of dynamin-related protein 1, a mediator of mitochondrial fission, in apoptosis. *Dev. Cell* 1, 515–525
- 51 Wasiak, S. *et al.* (2007) Bax/Bak promote sumoylation of DRP1 and its stable association with mitochondria during apoptotic cell death. *J. Cell Biol.* 177, 439–450
- 52 Wang, Z. *et al.* (2012) The mitochondrial phosphatase PGAM5 functions at the convergence point of multiple necrotic death pathways. *Cell* 148, 228–243
- 53 Lee, Y.J. *et al.* (2004) Roles of the mammalian mitochondrial fission and fusion mediators Fis1, Drp1, and Opa1 in apoptosis. *Mol. Biol. Cell* 15, 5001–5011
- 54 Alroi, E. *et al.* (2006) The mitochondrial fission protein hFis1 requires the endoplasmic reticulum gateway to induce apoptosis. *Mol. Biol. Cell* 17, 4593–4605
- 55 Iwasawa, R. *et al.* (2011) Fis1 and Bap31 bridge the mitochondria-ER interface to establish a platform for apoptosis induction. *EMBO J.* 30, 556–568
- 56 Sugioka, R. *et al.* (2004) Fzo1, a protein involved in mitochondrial fusion, inhibits apoptosis. *J. Biol. Chem.* 279, 52726–52734
- 57 Olichon, A. *et al.* (2003) Loss of OPA1 perturbs the mitochondrial inner membrane structure and integrity, leading to cytochrome c release and apoptosis. *J. Biol. Chem.* 278, 7743–7746
- 58 Frezza, C. *et al.* (2006) OPA1 controls apoptotic cristae remodeling independently from mitochondrial fusion. *Cell* 126, 177–189
- 59 Cogliati, S. *et al.* (2013) Mitochondrial cristae shape determines respiratory chain supercomplexes assembly and respiratory efficiency. *Cell* 155, 160–171
- 60 Youle, R.J. and Narendra, D.P. (2011) Mechanisms of mitophagy. *Nat. Rev. Mol. Cell Biol.* 12, 9–14
- 61 Kundu, M. *et al.* (2008) Ulk1 plays a critical role in the autophagic clearance of mitochondria and ribosomes during reticulocyte maturation. *Blood* 112, 1493–1502
- 62 Zhang, J. *et al.* (2009) Mitochondrial clearance is regulated by Atg7-dependent and -independent mechanisms during reticulocyte maturation. *Blood* 114, 157–164
- 63 Mortensen, M. *et al.* (2010) Loss of autophagy in erythroid cells leads to defective removal of mitochondria and severe anemia in vivo. *Proc. Natl. Acad. Sci. U.S.A.* 107, 832–837
- 64 Sandoval, H. *et al.* (2008) Essential role for Nix in autophagic maturation of erythroid cells. *Nature* 454, 232–235
- 65 Narendra, D. *et al.* (2008) Parkin is recruited selectively to impaired mitochondria and promotes their autophagy. *J. Cell Biol.* 183, 795–803
- 66 Narendra, D.P. *et al.* (2010) PINK1 is selectively stabilized on impaired mitochondria to activate Parkin. *PLoS Biol.* 8, e1000298
- 67 Alavi, M.V. *et al.* (2007) A splice site mutation in the murine Opa1 gene features pathology of autosomal dominant optic atrophy. *Brain* 130, 1029–1042
- 68 Davies, V.J. *et al.* (2007) Opa1 deficiency in a mouse model of autosomal dominant optic atrophy impairs mitochondrial morphology, optic nerve structure and visual function. *Hum. Mol. Genet.* 16, 1307–1318
- 69 Chen, H. *et al.* (2007) Mitochondrial fusion protects against neurodegeneration in the cerebellum. *Cell* 130, 548–562
- 70 Chen, H. *et al.* (2010) Mitochondrial fusion is required for mtDNA stability in skeletal muscle and tolerance of mtDNA mutations. *Cell* 141, 280–289
- 71 Chen, Y. *et al.* (2011) Mitochondrial fusion is essential for organelle function and cardiac homeostasis. *Circ. Res.* 109, 1327–1331
- 72 Williams, P.A. *et al.* (2010) Opa1 deficiency in a mouse model of dominant optic atrophy leads to retinal ganglion cell dendroathy. *Brain* 133, 2942–2951
- 73 White, K.E. *et al.* (2009) OPA1 deficiency associated with increased autophagy in retinal ganglion cells in a murine model of dominant optic atrophy. *Invest. Ophthalmol. Vis. Sci.* 50, 2567–2571
- 74 Alavi, M.V. *et al.* (2009) Subtle neurological and metabolic abnormalities in an Opa1 mouse model of autosomal dominant optic atrophy. *Exp. Neurol.* 220, 404–409
- 75 Piquereau, J. *et al.* (2012) Down-regulation of OPA1 alters mouse mitochondrial morphology, PTP function, and cardiac adaptation to pressure overload. *Cardiovasc. Res.* 94, 408–417

- 76 Chen, L. *et al.* (2012) OPA1 Mutation and late onset cardiomyopathy: mitochondrial dysfunction and mtDNA instability. *J. Am. Heart Assoc.* 1, e003012
- 77 Clapham, D.E. (2007) Calcium signaling. *Cell* 131, 1047–1058
- 78 Wasilewski, M. *et al.* (2012) Optic atrophy 1-dependent mitochondrial remodeling controls steroidogenesis in trophoblasts. *Curr. Biol.* 22, 1228–1234
- 79 Kopan, R. and Ilagan, M.X. (2009) The canonical Notch signaling pathway: unfolding the activation mechanism. *Cell* 137, 216–233
- 80 Perumalsamy, L.R. *et al.* (2010) Notch-activated signaling cascade interacts with mitochondrial remodeling proteins to regulate cell survival. *Proc. Natl. Acad. Sci. U.S.A.* 107, 6882–6887
- 81 Mitra, K. *et al.* (2012) DRP1-dependent mitochondrial fission initiates follicle cell differentiation during *Drosophila* oogenesis. *J. Cell Biol.* 197, 487–497
- 82 Nemir, M. *et al.* (2006) Induction of cardiogenesis in embryonic stem cells via downregulation of Notch1 signaling. *Circ. Res.* 98, 1471–1478
- 83 Kasahara, A. *et al.* (2013) Mitochondrial fusion directs cardiomyocyte differentiation via calcineurin and Notch signaling. *Science* 342, 734–737
- 84 Hamanaka, R.B. *et al.* (2013) Mitochondrial reactive oxygen species promote epidermal differentiation and hair follicle development. *Sci. Signal.* 6, ra8
- 85 Landor, S.K. *et al.* (2011) Hypo- and hyperactivated Notch signaling induce a glycolytic switch through distinct mechanisms. *Proc. Natl. Acad. Sci. U.S.A.* 108, 18814–18819
- 86 Lee, K.S. *et al.* (2013) Roles of PINK1, mTORC2, and mitochondria in preserving brain tumor-forming stem cells in a noncanonical Notch signaling pathway. *Genes Dev.* 27, 2642–2647
- 87 Thorig, G.E. *et al.* (1981) The action of the notch locus in *Drosophila melanogaster*. I. Effects of the notch8 deficiency on mitochondrial enzymes. *Mol. Gen. Genet.* 182, 31–38
- 88 Thorig, G.E. *et al.* (1981) The action of the notch locus in *Drosophila melanogaster*. II. Biochemical effects of recessive lethals on mitochondrial enzymes. *Genetics* 99, 65–74
- 89 Basak, N.P. *et al.* (2014) Alteration of mitochondrial proteome due to activation of Notch1 signaling pathway. *J. Biol. Chem.* 289, 7320–7334
- 90 de la Pena, P. *et al.* (2001) Mitochondrial dysfunction associated with a mutation in the Notch3 gene in a CADASIL family. *Neurology* 57, 1235–1238
- 91 Johnson, R.F. and Perkins, N.D. (2012) Nuclear factor-kappaB, p53, and mitochondria: regulation of cellular metabolism and the Warburg effect. *Trends Biochem. Sci.* 37, 317–324
- 92 Mauro, C. *et al.* (2011) NF-kappaB controls energy homeostasis and metabolic adaptation by upregulating mitochondrial respiration. *Nat. Cell Biol.* 13, 1272–1279
- 93 Muller-Rischart, A.K. *et al.* (2013) The E3 ligase parkin maintains mitochondrial integrity by increasing linear ubiquitination of NEMO. *Mol. Cell* 49, 908–921
- 94 Yasukawa, K. *et al.* (2009) Mitofusin 2 inhibits mitochondrial antiviral signaling. *Sci. Signal.* 2, ra47
- 95 Seth, R.B. *et al.* (2005) Identification and characterization of MAVS, a mitochondrial antiviral signaling protein that activates NF-kappaB and IRF 3. *Cell* 122, 669–682
- 96 McBride, H.M. *et al.* (2006) Mitochondria: more than just a powerhouse. *Curr. Biol.* 16, R551–R560
- 97 Ming, M. *et al.* (2012) Activation of Wnt/beta-catenin protein signaling induces mitochondria-mediated apoptosis in hematopoietic progenitor cells. *J. Biol. Chem.* 287, 22683–22690
- 98 Clevers, H. and Nusse, R. (2012) Wnt/beta-catenin signaling and disease. *Cell* 149, 1192–1205
- 99 Yoon, J.C. *et al.* (2010) Wnt signaling regulates mitochondrial physiology and insulin sensitivity. *Genes Dev.* 24, 1507–1518
- 100 Silva-Alvarez, C. *et al.* (2013) Canonical Wnt signaling protects hippocampal neurons from Abeta oligomers: role of non-canonical Wnt-5a/Ca(2+) in mitochondrial dynamics. *Front. Cell. Neurosci.* 7, 97
- 101 Corrado, M. *et al.* (2012) Mitochondrial dynamics in cancer and neurodegenerative and neuroinflammatory diseases. *Int. J. Cell Biol.* 2012, 729290
- 102 Kwon, C. *et al.* (2011) Notch post-translationally regulates beta-catenin protein in stem and progenitor cells. *Nat. Cell Biol.* 13, 1244–1251
- 103 de Brito, O.M. and Scorrano, L. (2010) An intimate liaison: spatial organization of the endoplasmic reticulum-mitochondria relationship. *EMBO J.* 29, 2715–2723
- 104 Kornmann, B. *et al.* (2009) An ER-mitochondria tethering complex revealed by a synthetic biology screen. *Science* 325, 477–481
- 105 de Brito, O.M. and Scorrano, L. (2008) Mitofusin 2 tethers endoplasmic reticulum to mitochondria. *Nature* 456, 605–610
- 106 Hailey, D.W. *et al.* (2010) Mitochondria supply membranes for autophagosome biogenesis during starvation. *Cell* 141, 656–667
- 107 Area-Gomez, E. *et al.* (2012) Upregulated function of mitochondria-associated ER membranes in Alzheimer disease. *EMBO J.* 31, 4106–4123
- 108 Simmen, T. *et al.* (2005) PACS-2 controls endoplasmic reticulum-mitochondria communication and Bid-mediated apoptosis. *EMBO J.* 24, 717–729
- 109 Sugiura, A. *et al.* (2013) MITOL regulates endoplasmic reticulum-mitochondria contacts via Mitofusin2. *Mol. Cell* 51, 20–34
- 110 Cerqua, C. *et al.* (2010) Trichoplein/mitostatin regulates endoplasmic reticulum-mitochondria juxtaposition. *EMBO Rep.* 11, 854–860
- 111 Friedman, J.R. *et al.* (2011) ER tubules mark sites of mitochondrial division. *Science* 334, 358–362
- 112 De Vos, K.J. *et al.* (2005) Mitochondrial function and actin regulate dynamin-related protein 1-dependent mitochondrial fission. *Curr. Biol.* 15, 678–683
- 113 Korobova, F. *et al.* (2013) An actin-dependent step in mitochondrial fission mediated by the ER-associated formin INF2. *Science* 339, 464–467
- 114 Buzhynskyy, N. *et al.* (2007) Rows of ATP synthase dimers in native mitochondrial inner membranes. *Biophys. J.* 93, 2870–2876
- 115 Strauss, M. *et al.* (2008) Dimer ribbons of ATP synthase shape the inner mitochondrial membrane. *EMBO J.* 27, 1154–1160
- 116 Rabl, R. *et al.* (2009) Formation of cristae and crista junctions in mitochondria depends on antagonism between Fcj1 and Su e/g. *J. Cell Biol.* 185, 1047–1063
- 117 Davies, K.M. *et al.* (2011) Macromolecular organization of ATP synthase and complex I in whole mitochondria. *Proc. Natl. Acad. Sci. U.S.A.* 108, 14121–14126
- 118 John, G.B. *et al.* (2005) The mitochondrial inner membrane protein mitofilin controls cristae morphology. *Mol. Biol. Cell* 16, 1543–1554
- 119 von der Malsburg, K. *et al.* (2011) Dual role of mitofilin in mitochondrial membrane organization and protein biogenesis. *Dev. Cell* 21, 694–707
- 120 Harner, M. *et al.* (2011) The mitochondrial contact site complex, a determinant of mitochondrial architecture. *EMBO J.* 30, 4356–4370
- 121 Hoppins, S. *et al.* (2011) A mitochondrial-focused genetic interaction map reveals a scaffold-like complex required for inner membrane organization in mitochondria. *J. Cell Biol.* 195, 323–340
- 122 Alkhaja, A.K. *et al.* (2012) MINOS1 is a conserved component of mitofilin complexes and required for mitochondrial function and cristae organization. *Mol. Biol. Cell* 23, 247–257
- 123 van der Laan, M. *et al.* (2012) Role of MINOS in mitochondrial membrane architecture and biogenesis. *Trends Cell Biol.* 22, 185–192
- 124 Xie, J. *et al.* (2007) The mitochondrial inner membrane protein mitofilin exists as a complex with SAM50, metaxins 1 and 2, coiled-coil-helix coiled-coil-helix domain-containing protein 3 and 6 and DnaJC11. *FEBS Lett.* 581, 3545–3549
- 125 Darshi, M. *et al.* (2011) ChChd3, an inner mitochondrial membrane protein, is essential for maintaining crista integrity and mitochondrial function. *J. Biol. Chem.* 286, 2918–2932
- 126 Ott, C. *et al.* (2012) Sam50 functions in mitochondrial intermembrane space bridging and biogenesis of respiratory complexes. *Mol. Cell Biol.* 32, 1173–1188

Self and Nonself: How Autophagy Targets Mitochondria and Bacteria

Felix Randow^{1,2,*} and Richard J. Youle^{3,*}

¹MRC Laboratory of Molecular Biology, Division of Protein and Nucleic Acid Chemistry, Francis Crick Avenue, Cambridge CB2 0QH, UK

²University of Cambridge, Department of Medicine, Addenbrooke's Hospital, Cambridge CB2 0QQ, UK

³Surgical Neurology Branch, National Institute of Neurological Disorders and Stroke, National Institutes of Health Bethesda, MD 20892, USA

*Correspondence: randow@mrc-lmb.cam.ac.uk (F.R.), youler@ninds.nih.gov (R.J.Y.)

<http://dx.doi.org/10.1016/j.chom.2014.03.012>

Autophagy is an evolutionarily conserved pathway that transports cytoplasmic components for degradation into lysosomes. Selective autophagy can capture physically large objects, including cell-invading pathogens and damaged or superfluous organelles. Selectivity is achieved by cargo receptors that detect substrate-associated “eat-me” signals. In this Review, we discuss basic principles of selective autophagy and compare the “eat-me” signals and cargo receptors that mediate autophagy of bacteria and bacteria-derived endosymbionts—i.e., mitochondria.

The maintenance of cellular homeostasis requires the controlled elimination of cellular components. Autophagy is of particular importance in this respect, since, in contrast to the proteasome and other cytosolic degradation machinery, autophagy can achieve the degradation of physically large and chemically diverse substrates including protein aggregates, cellular organelles, and even cytosol-invading pathogens (Deretic et al., 2013; Levine et al., 2011; Mizushima and Komatsu, 2011; Randow and Münz, 2012). Evolutionarily, autophagy is thought to have originated as a starvation-induced pathway that nonselectively degrades cytosolic compounds into building blocks and thereby provides energy and maintains essential anabolic processes even when external resources are limiting. How autophagy engulfs specific cargo is a particularly interesting problem for which much progress has been achieved recently. In this Review, we will discuss and compare how autophagy eliminates cytosol-invading bacteria and damaged or excess mitochondria, a conundrum conceptually related to the immune system's task of distinguishing self from non-self and further complicated by the evolutionary relatedness of mitochondria and bacteria. We therefore will focus on how “eat-me” signals and cargo receptors provide specificity for these cellular processes.

Overview of Autophagy

Macroautophagy (hereafter autophagy) is an evolutionarily conserved cellular activity that delivers cytosolic material into double-membrane vesicles, called autophagosomes, that eventually fuse with late endosomes or lysosomes (Mizushima and Komatsu, 2011). Autophagosome biogenesis proceeds along a stereotypical path (Weidberg et al., 2011). Initially a crescent-shaped double membrane forms, which is known as an isolation membrane or phagophore. The phagophore subsequently grows and sequesters cytosolic material, which, upon fusion of the phagophore edge, becomes fully enclosed inside the autophagosome. Autophagosomes finally mature into organelles competent to fuse with lysosomes, whereupon lysosomal enzymes degrade the autophagosome contents including the inner autophagosomal membrane.

Autophagosome biogenesis requires the coordinated action of about 15 “core” autophagy-related or ATG genes, several of which associate into protein complexes (Mizushima et al., 2011). ATG9, the only polytopic transmembrane protein essential for autophagy, and the ULK complex are independently recruited to nascent phagophores upon amino acid starvation. Then ULK kinase activity recruits the VPS34 lipid kinase complex that produces membrane patches rich in phosphatidylinositol 3-phosphate (PI(3)P) (Russell et al., 2013). Phagophores are generated de novo from these PI(3)P-enriched domains at ER-mitochondria contact sites under the control of PI(3)P-binding proteins such as WIPI1/2 (Hamasaki et al., 2013). Phagophore biogenesis requires extensive membrane remodeling, including the formation of ER-derived, PI(3)P-enriched omegasomes marked by DFCP1, another PI(3)P-binding protein (Axe et al., 2008).

The elongation and ultimate closure of phagophores relies on the conjugation of two ubiquitin-like proteins, ATG12 and ATG8, to ATG5 and the lipid phosphatidyl ethanolamine (PE), respectively (Mizushima et al., 2011). To catalyze the lipidation of ATG8 the ATG12~ATG5 conjugate associates with ATG16 into an E3-like enzyme complex, whose localization, together with more upstream components, specifies the site of autophagosome biogenesis. While yeasts encode only a single ATG8 gene, humans harbor six orthologs that cluster into the LC3 and GABARAP subfamilies (Weidberg et al., 2011). Membrane-associated LC3/GABARAP provide docking sites for receptors that deliver specific cargo to phagophores during selective autophagy (Boyle and Randow, 2013; Johansen and Lamark, 2011).

Selective Autophagy

Starvation-induced autophagy is a nonselective process that degrades randomly engulfed cytosolic components in order to fuel the cell in lean times and to provide building blocks for anabolic activities. In contrast, the task of selective autophagy is the elimination of specific cytosolic objects in the maintenance of cellular homeostasis, such as bacteria, damaged organelles, or protein aggregates (Weidberg et al., 2011). Selectivity is achieved by receptors that enforce physical proximity between cargo and

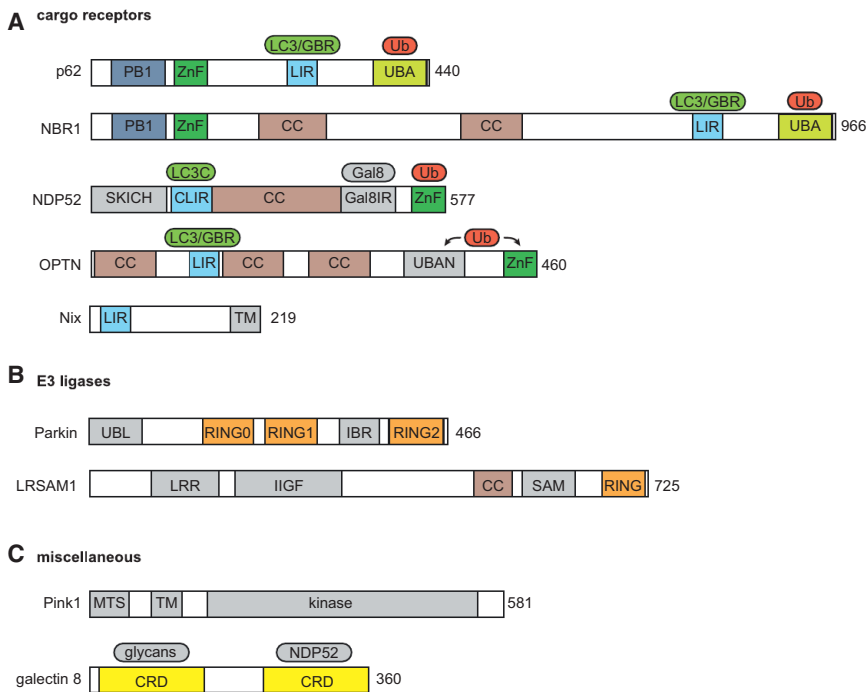


Figure 1. Domain Structure and Ligands of Cargo Receptors, E3 Ligases, and Miscellaneous Proteins Mediating Mitophagy and Antibacterial Autophagy

Shared domains and ligands are color coded; unique domains and ligands in gray. (A) is modified from Boyle and Randow (2013).

autophagy machinery due to simultaneous binding of “eat-me” signals on the prospective cargo and LC3/GABARAP on phagophores (Boyle and Randow, 2013; Johansen and Lamark, 2011). Cargo receptors have emerged by convergent evolution and subsequent gene duplication events; currently known are at least five members (p62 and its paralog NBR1, NDP52 and its paralog T6BP, and optineurin) (Figure 1). The interaction of cargo receptors with LC3/GABARAP relies on the formation of an intermolecular β sheet to which the cargo receptor contributes a single strand, the so-called LC3-interacting region (LIR). Negatively charged residues adjacent to the LIR motif contribute to the interaction, sometimes in a phosphorylation-dependent and therefore regulable manner (Wild et al., 2011). Cargo receptors displaying consensus variants of the LIR motif W/FxxI/L/V interact promiscuously with most if not all LC3/GABARAP family members. However, specificity for individual LC3/GABARAP proteins can be provided by more extreme variants of the LIR motif, such as the ILVV peptide occurring in NDP52, which binds selectively to LC3C (von Muhlinen et al., 2012). This selectivity of NDP52 for LC3C entrusts an essential role to LC3C in NDP52-dependent selective autophagy. Why NDP52 in contrast to other cargo receptors relies selectively on LC3C remains unknown but preferential binding could enable NDP52 to control a specific step of autophagosome biogenesis—a suggestion that supports the general concept of specific functions for the LC3 and GABARAP subfamilies in phagophore elongation and maturation, respectively, although species specific differences exist (Weidberg et al., 2010)

Mitophagy

Mitochondria are eliminated by autophagy when the demand for metabolic capacity declines, for example in yeast when they change from log-phase growth to the stationary phase (Abelio-

vich, 2011) and in cone visual cells during hibernation (Remé and Young, 1977). Mitochondria are completely cleared by autophagy during the differentiation of specialized tissues, such as eye lens fiber cells (Costello et al., 2013) and red blood cells (Heynen et al., 1985). Another mode of mitophagy occurs in many metazoan cell types to selectively cull damaged mitochondria from the intracellular pool, apparently to help maintain quality control (Youle and van der Bliek, 2012).

The molecular mechanisms of mitophagy during the clearance of mitochondria upon reticulocyte differentiation in mammalian cells are becoming understood. The mitochondrial outer-membrane protein, NIX/BNIP3L, was found to be dramatically upregulated during reticulocyte differentiation into mature red blood cells (Aerbajinai et al., 2003). Subsequent work revealed that circulating red blood cells in NIX knockout mice atypically retain mitochondria that are normally removed by mitophagy, establishing an important function in mitochondrial clearance for this mitochondrial membrane protein (Sandoval et al., 2008; Schweers et al., 2007). Although Nix was found to have a consensus LC3 interaction region (LIR) motif that binds to both LC3 and GABARAP (Novak et al., 2010), suggesting it functions to recruit mitochondria into isolation membranes/phagophores, *in vivo* experiments indicate additional unknown functions for Nix during mitophagy more important than LIR-mediated docking to LC3 (Zhang et al., 2012).

The molecular mechanisms mediating quality-control mitophagy in mammalian cells have become understood in recent years (Twig and Shirihai, 2011; Youle and van der Bliek, 2012). The mitochondrial kinase, PINK1, detects damaged mitochondria and subsequently recruits and activates the RBR E3 ubiquitin ligase, Parkin (Matsuda et al., 2010; Narendra et al., 2010). Parkin, in turn, ubiquitinates proteins on the outer mitochondrial membrane surface that likely initiate autophagosome isolation membrane encapsulation of the damaged mitochondria (Figure 2). This selective autophagy of damaged mitochondria is thought to mediate quality control (Narendra et al., 2008). Interestingly, autosomal recessive mutations in either PINK1 or Parkin cause early onset Parkinson’s disease, suggesting that insufficient mitochondrial quality control may be to blame. PINK1 is able to “sense” mitochondrial “quality” based on its turnover mechanism; PINK1 undergoes rapid and constitutive degradation in healthy mitochondria by the inner mitochondrial membrane protease PARL following import through the TOM and TIM membrane translocation complexes. When the

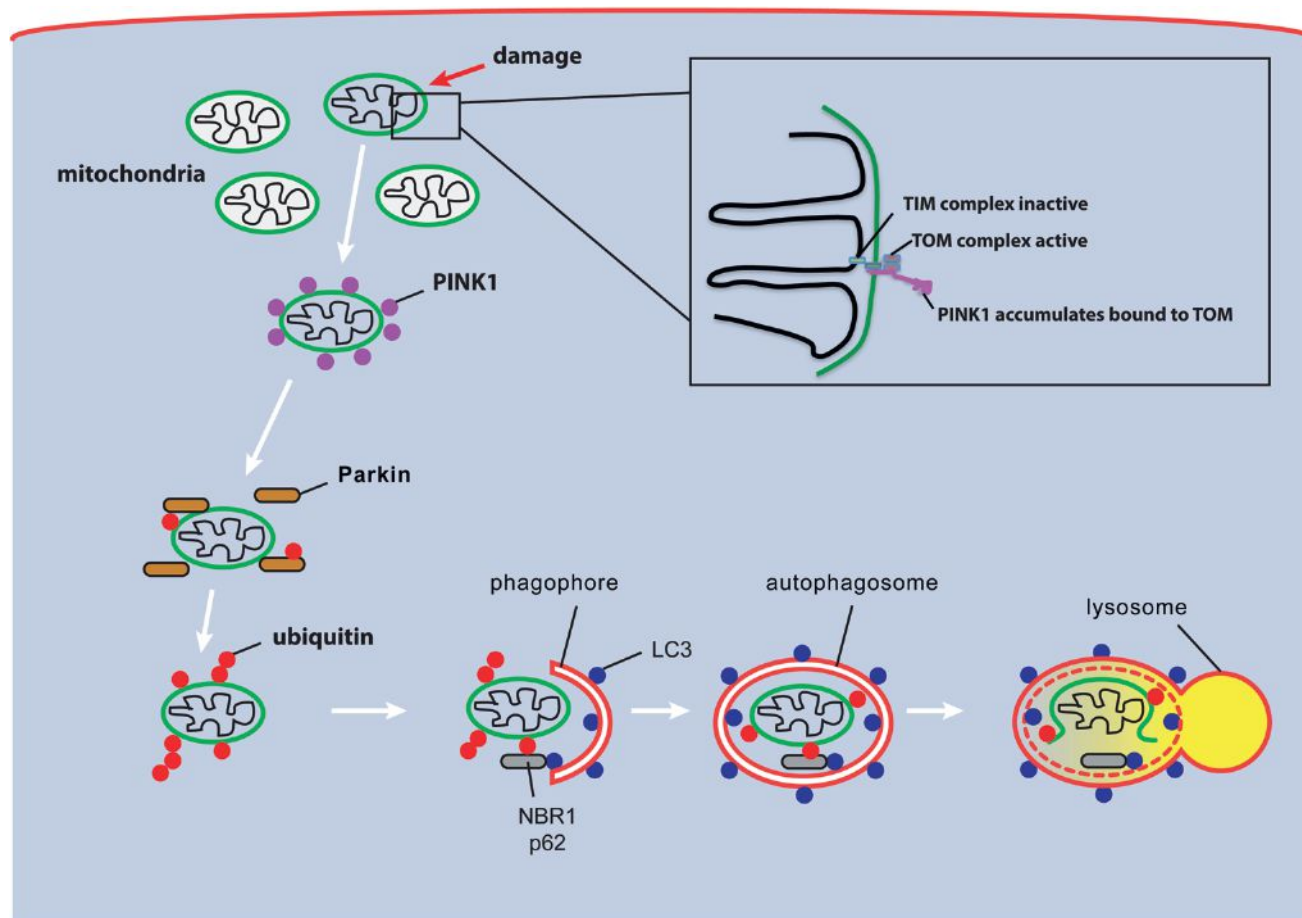


Figure 2. PINK1 and Parkin Mediate Mitochondrial Quality Control by Inducing Mitophagy

(Upper-right inset) PINK1 is constitutively degraded in healthy mitochondria through import via TIM and TOM translocation complexes and cleavage by PARL in the inner membrane followed by proteasomal degradation. Mitochondrial damage prevents PINK1 import and cleavage, allowing the kinase to accumulate on the outer mitochondrial membrane. (Top left to bottom right) When a mitochondrion loses membrane potential or accumulates misfolded proteins, PINK1 accumulates on the outer mitochondrial membrane. The PINK1 kinase recruits Parkin to mitochondria from the cytosol and activates the E3 ligase to ubiquitinate outer mitochondrial membranes. These ubiquitinated proteins act as “eat-me” signals for cargo adaptors that signal autophagosome engulfment of the mitochondrion.

membrane potential across the inner mitochondrial membrane that is normally generated by oxidative phosphorylation deteriorates, PINK1 import into the inner mitochondrial membrane and cleavage by PARL are blocked. PINK1 instead starts to accumulate on the outer mitochondrial membrane with its kinase domain facing the cytosol where Parkin resides (Figure 2). On the outer mitochondrial membrane PINK1 associates in a 2:1 molecular complex with the TOM import machinery (Lazarou et al., 2012; Okatsu et al., 2013). PINK1 also accumulates on the outer mitochondrial membrane when misfolded proteins aggregate in the matrix compartment (Jin and Youle, 2013), suggesting that mitochondrial import or PINK1 proteolysis are shut down in response to mitochondrial stress. PINK1 therefore selectively accumulates only on those mitochondria within a cell population that are dysfunctional and thus flags them for elimination (Narendra et al., 2010).

The accumulation of active PINK1 on mitochondria recruits Parkin and activates its latent HECT/RING hybrid mechanism of ubiquitin transfer. The crystal structure of Parkin shows how the enzyme is held in the cytosol in an autoinhibited form (Riley

et al., 2013; Trempe et al., 2013; Wauer and Komander, 2013). Although the structure of active Parkin remains unknown, it appears to form a dimer or multimer upon activation. PINK1 kinase activity is required for Parkin activation, but it is not clear what the essential PINK1 substrate is. PINK1 ectopically placed on peroxisomes recruits Parkin to peroxisomes ruling out mitochondria-specific PINK1 substrates as essential intermediates of Parkin activation (Lazarou et al., 2012). Other models indicate that PINK1 autophosphorylation (Okatsu et al., 2012) or Parkin phosphorylation (Kondapalli et al., 2012) are involved or that an unknown cytosolic protein is the essential PINK1 substrate mediating Parkin translocation.

Once activated, Parkin ubiquitinates scores of substrates on the mitochondria and in the cytosol (Sarraf et al., 2013). Which, if any, of these individual substrates is essential for autophagy remains unknown. Ubiquitin chain linkage or ubiquitin chain density above a certain threshold may be as or more important than the identity of the ubiquitinated substrate—as discussed below in relation to the role of ubiquitin in xenophagy. Parkin appears to attach several ubiquitin chain linkages types, including K48-

K63-, and K27-linked chains, to proteins located on the outer mitochondrial surface (Chan et al., 2011; Geisler et al., 2010; van Wijk et al., 2012). The K63-linked ubiquitin chains are likely to be important for recruitment of the cargo receptor p62 (Geisler et al., 2010) and other adaptor proteins that can engage phagophore-bound LC3 and GABARAP via LIR motifs. The K48-linked ubiquitin chains are likely involved in the recruitment of the AAA+ ATPase p97 (Tanaka et al., 2010) and the proteasome (Chan et al., 2011) to mitochondria, which respectively mediate the extraction and proteasomal degradation of ubiquitinated outer mitochondrial membrane proteins. The robust proteasomal elimination of outer mitochondrial membrane proteins appears capable of rupturing the outer membrane and may yield a membrane damage signal that triggers mitophagy and recruitment of autophagosome machinery downstream of Parkin (Yoshii et al., 2011).

Parkin-mediated mitophagy also involves noncanonical adaptor proteins that guide autophagic targeting of mitochondria. Notably, two RabGAPs, TBC1D15 and TBC1D17, which are bound to the outer mitochondrial membrane protein, Fis1, interact with LC3/GABARAP and participate in isolation membrane formation during Parkin-mediated mitophagy (Yamano et al., 2014). Despite identical core LIR motifs, TBC1D15 and TBC1D17 bind differentially to LC3 and GABARAP members of the ATG8 family. Interestingly, both require their RabGAP activity in the conserved TBC domain to restrict excessive LC3 protein accumulation during mitophagy. This stems from excessive Rab7 activity in the absence of RabGAP activity that appears normally to be involved in LC3 membrane recruitment and trafficking to mitochondria during mitophagy but not during starvation-induced autophagy.

Additionally, recent evidence suggests that autophagic machinery can be recruited to targeted mitochondria independent of LC3. Ulk1, Atg14, DFCP1, WIPI-1, and Atg16L1 (Itakura et al., 2012) are recruited to autophagosomes associated with Parkin-bound and ubiquitin-labeled mitochondria even in the absence of membrane bound LC3. Ulk1 and Atg9A recruitment to damaged mitochondria are downstream of Parkin activity but independent of one another. What signals the independent recruitment of autophagy machinery proteins to mitochondria-associated isolation membranes is unknown but may stem from different linkage types of ubiquitin chains.

Mitochondrial fission is associated with mitophagy either to reduce the size of elongated mitochondria to facilitate engulfment by autophagosomes or to prevent damaged mitochondria from fusing with healthy mitochondria and impairing them by the exchange of damaged proteins and lipids (Twig et al., 2008). Interestingly, Parkin ubiquitinates the mitochondrial fission proteins Mfn1 and Mfn2 possibly to actively prevent mitochondrial refusion in both *Drosophila* and mammalian cells (Gegg et al., 2010; Poole et al., 2010; Tanaka et al., 2010; Ziviani et al., 2010). This conclusion is corroborated by genetic studies in *Drosophila* where promotion of mitochondrial fission compensates for loss of PINK1 and Parkin and inhibition of fission exacerbates the phenotype of PINK1 and Parkin loss (Deng et al., 2008; Park et al., 2009; Poole et al., 2008; Yu et al., 2011). Mitochondrial trafficking is inhibited by Parkin-mediated ubiquitination and proteasomal degradation of the adaptor protein Miro that links mitochondria to kinesin motors, which may

facilitate autophagic engulfment by stalling organelle mobility (Wang et al., 2011; Weihofen et al., 2009). Although recent results in *Drosophila* support the model that PINK1 and Parkin mediate mitophagy in vivo (Burman et al., 2012; Pimenta de Castro et al., 2012; Vincow et al., 2013), whether defects in mitophagy cause Parkinson's disease remains unclear.

Antibacterial Autophagy (Xenophagy)

Autophagy and autophagy genes have been implicated through unbiased genome-wide association studies in antibacterial defense and in inflammatory conditions such as Crohn's disease (Deretic et al., 2013). Susceptibility genes for Crohn's disease include NOD2, which mediates the cytosolic response to peptidoglycan fragments, IRGM, the sole human member of a large family of antimicrobial GTPases, and ATG16L1, a core autophagy gene. Exon sequencing of patients with Crohn's disease recently identified a missense mutation in the cargo receptor NDP52, present at low frequency in the general population, as a potential risk factor (Ellinghaus et al., 2013). Functional activities associated with these risk factors, for example the NOD2-mediated recruitment of ATG16L1 to the site of bacterial entry, suggest that autophagy may provide functionally important defense against cell-invading bacteria in Crohn's disease (Travassos et al., 2010). However, the role of ATG16 in antibacterial defense might be more complex as the disease-associated allele is of high prevalence and a hypomorphic ATG16 allele enhances resistance of mice to *Citrobacter rodentium*, an intestinal pathogen, and to uropathogenic *Escherichia coli* (Marchiando et al., 2013; Wang et al., 2012). Exposure to multiple pathogens and/or nonautophagy related functions of ATG16L1, for example the secretion of antimicrobial peptides from Paneth cells, may be additional confounding factors (Cadwell et al., 2008). Despite this apparent complexity, deletion of ATG5 from intestinal epithelial cells has recently provided direct experimental evidence for a protective in vivo role of autophagy against invasion of the intestinal epithelium by both opportunistic invasive commensals (*Enterococcus faecalis*) and intestinal pathogens (*Salmonella enterica* serovar Typhimurium [S. Typhimurium]) (Benjamin et al., 2013).

These and other intracellular bacteria and parasites inhabit specific compartments. Most dwell inside vacuoles, which they manipulate and in many cases prevent from fusing with lysosomes, the cell's major degradative organelle and a source of potent antimicrobial effectors. In contrast, the cytosol with its vast abundance of nutrients is inhabited by a comparably small number of bacterial species. This apparent paradox is largely caused by cell-autonomous antibacterial effector mechanisms, in particular by autophagy (Randow et al., 2013), although it should be noted that compartmentalization is not absolute and that temporary breaches of phagosomal membranes may be part of the life cycle of several bacterial pathogens (Huang and Brumell, 2014). Autophagy represents a fundamental host cell response to invasion by a variety of bacteria including *Shigella flexneri* (Ogawa et al., 2005), *Listeria monocytogenes* (Py et al., 2007), *S. Typhimurium* (Birmingham et al., 2006), and *Mycobacterium tuberculosis* (Gutierrez et al., 2004). The impressive degree to which autophagy antagonizes bacterial invasion of the cytosol is, at least in part, due to the existence of multiple

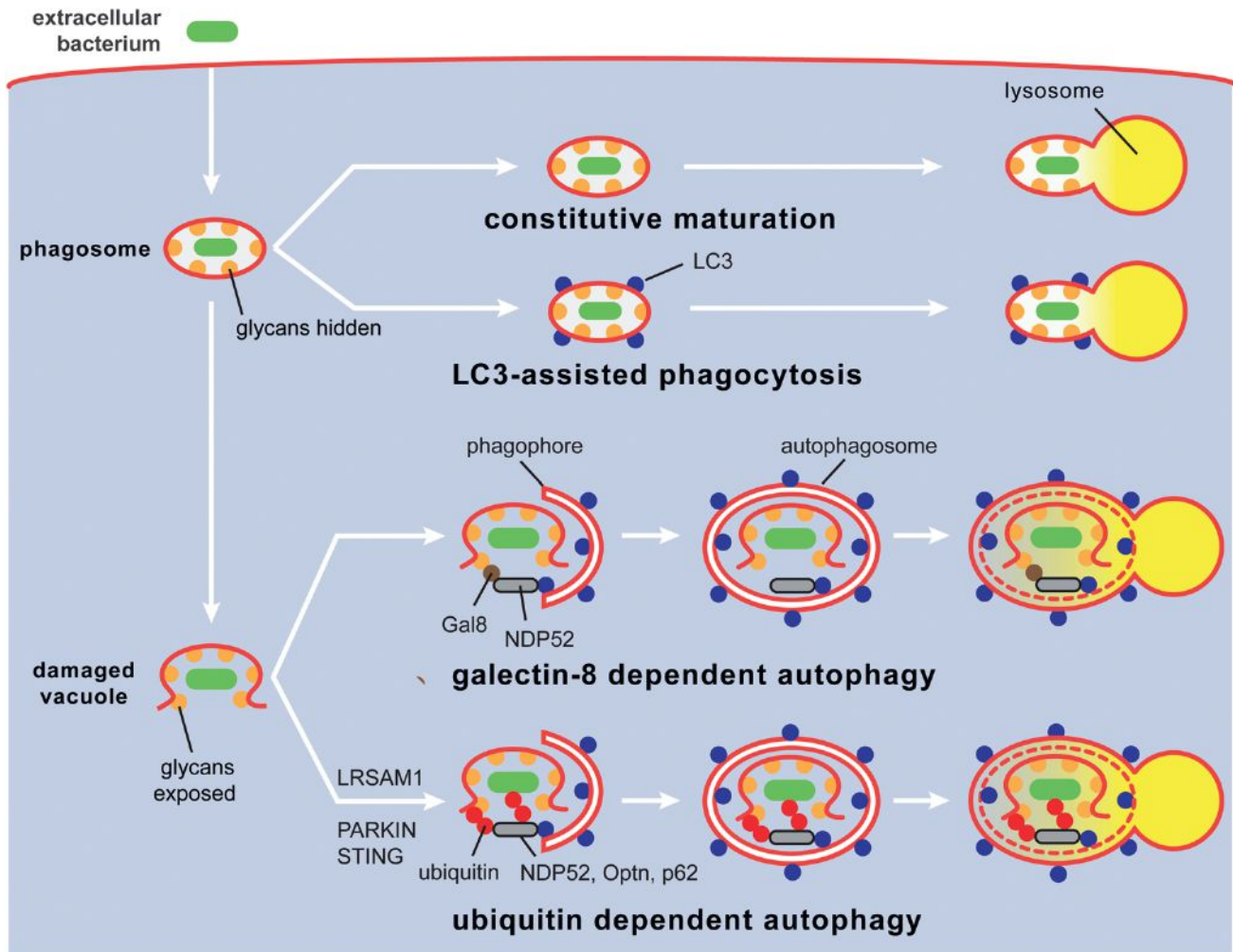


Figure 3. Targeting of Intracellular Bacteria for Lysosomal Destruction by Xenophagy

(Top) Phagosomes mature constitutively and ultimately deliver their bacterial cargo to lysosomes. During LC3-assisted phagocytosis (LAP), conjugation of LC3/GABARAP to the limiting phagosomal membrane promotes phagosome maturation. (Bottom) On damaged vacuoles, exposure of otherwise hidden glycans recruits the danger receptor galectin-8, whose accumulation provides an “eat-me” signal for the cargo receptor NDP52, thereby inducing autophagy. The ubiquitin coat deposited by LRSAM1 and Parkin around cytosol-exposed bacteria (which may still be in association with vacuolar membrane remnants) serves as an alternative “eat-me” signal for multiple cargo receptors (NDP52, Optn, p62), thereby inducing autophagy.

autophagy-related pathways that together establish a multilayered and synergistic defense network (Figure 3) (Boyle and Randow, 2013; Deretic et al., 2013; Levine et al., 2011). Evolutionary evidence for the importance of autophagy is provided by the variety of bacterial adaptations that inhibit or even usurp autophagy (Huang and Brummel, 2014).

During host cell invasion, bacteria are initially taken up into a membrane-surrounded compartment. Upon detection of microorganisms inside the (undamaged) vacuole by Toll-like receptors (TLRs), LC3/GABARAP can become directly conjugated to the limiting membrane of the bacterium-containing vacuole in a process termed LC3-assisted phagocytosis (LAP). LAP requires only a subset of ATGs, for example the ATG5/12/16 complex, but not the most upstream ATGs, such as FIP200 in the ULK complex, since conjugation of LC3 to the vacuolar membrane does not involve *de novo* phagophore formation (Martinez et al., 2011). Conjugation of LC3/GABARAP to pathogen-containing

vacuoles promotes content killing by enhancing lysosomal fusion.

Transition of bacteria from their vacuole into the cytosol, which is an essential step in the life cycle of all cytosol-dwelling bacteria, causes massive damage to the limiting vacuolar membrane and exposes glycans and other molecules normally hidden inside the vacuole to the cytosol. Cells detect breaches to the integrity of the endolysosomal compartment with the help of galectins, a family of cytosolic lectins specific for $\beta(1-4)$ -linked galactosides that are present abundantly in post-golgi compartments but are lacking in the cytosol (Dupont et al., 2009; Thurston et al., 2012). Cytosolic detection of host-derived glycans via galectins is a remarkably versatile principle of pathogen detection as it enables cells to sense the entry of evolutionarily distant pathogens including Gram-negative and Gram-positive bacteria as well as nonenveloped viruses (Denard et al., 2012; Dupont et al., 2009; Thurston et al., 2012). Although mammals

encode about a dozen galectins, so far only galectins 1, 3, 8, and 9 have been found to sense damaged bacteria-containing vacuoles (Thurston et al., 2012). Accumulation of galectin-8 on damaged vesicles provides an “eat-me” signal for the cargo receptor NDP52, thereby triggering autophagy and restricting the ability of *S. Typhimurium* to enter the host cytosol (Li et al., 2013; Thurston et al., 2012).

A second “eat-me” signal is produced when cells coat bacteria with polyubiquitin (Perrin et al., 2004). The substrates of antibacterial ubiquitylation have not been identified so far. However, it seems likely that bacteria are directly ubiquitylated and that host proteins associated with bacteria, including proteins of the vacuolar remnants, are also substrate for ubiquitylation (Fujita et al., 2013). Whether ubiquitylation of any particular substrate is essential for antibacterial autophagy is unknown, although it seems likely that a larger number of bacteria-associated proteins become ubiquitylated and that therefore the ubiquitin coat per se is of greater importance than the identity of the ubiquitylated substrate. It is clear, however, that ubiquitin chains of different linkage types, including K48-, K63-, and M1-linked chains, constitute the bacterial ubiquitin coat (Collins et al., 2009; Manzanillo et al., 2013; van Wijk et al., 2012). The linkage type analysis is still preliminary as it relied on the availability of either linkage-specific antibodies or ubiquitin-binding proteins of appropriate specificity. Further chain types may therefore contribute to the bacterial coat and be detected in the future either by mass spectrometry or once additional probes are utilized. The bacterial ubiquitin coat is sensed by at least four cargo receptors, namely NDP52, p62, NBR1, and optineurin, of which all except NBR1 are essential to restrict bacterial proliferation and therefore execute unique functions (Mostowy et al., 2011; Thurston et al., 2009; Wild et al., 2011; Zheng et al., 2009). While the essential contribution of NDP52 might be explained by its unique abilities to sense the galectin-8 eat-me signal on damaged vacuoles (Thurston et al., 2012) and to selectively bind LC3C (von Muhlinen et al., 2012), the nonredundant roles of p62 and optineurin in antibacterial autophagy indicate that their function is also not limited to binding LC3/GABARAP and the ubiquitin “eat-me” signal (Wild et al., 2011; Zheng et al., 2009). The possibility that p62 and optineurin are essential solely because they sense different ubiquitin-linkage types appears unlikely since the cargo receptor NBR1, although accumulating on ubiquitin-coated bacteria, is not essential to restrict bacterial proliferation (Mostowy et al., 2011; Zheng et al., 2009).

Insights into the identity of the antibacterial E3 ubiquitin ligases and the nature of the ubiquitylation process have been obtained recently. LRSAM1, a RING-domain E3 ligase, has been found to generate the ubiquitin “eat-me” signal around *S. Typhimurium* in a manner dependent on its leucine-rich repeat (LRR) domain, a fold that mediates pathogen recognition in TLRs and other pattern-recognition receptors (PRR). If LRSAM1 is indeed a PRR, its ligand must be widely distributed as LRSAM1 colocalizes with both Gram-negative and Gram-positive bacteria, although its activity does not extend to *Mycobacterium tuberculosis* (*M. tuberculosis*) (Huett et al., 2012; Manzanillo et al., 2013). For the latter species, the RBR E3 ligase Parkin (PARK2), discussed above for its role in mitophagy, is required to generate the ubiquitin “eat-me” signal (Manzanillo et al., 2013). Parkin alleles that predispose to the development of

Parkinson’s disease (PARK2 T240R, P437L) are impaired in coating *M. tuberculosis* with ubiquitin, while polymorphisms in noncoding regions of PARK2 are associated with increased susceptibility to *Mycobacterium leprae* and *S. Typhi* (Ali et al., 2006; Manzanillo et al., 2013; Mira et al., 2004). In contrast to LRSAM1, Parkin acts on bacteria still contained in vacuoles as revealed by their inaccessibility to antibody staining (Huett et al., 2012; Manzanillo et al., 2013), although limited permeabilization of the vacuolar membrane seems likely to occur given the dependence of Parkin recruitment and ubiquitin deposition on ESX-1, the bacterial type VII secretion system. Ubiquitin coating of *M. tuberculosis* also requires STING (Watson et al., 2012), a receptor for cytosolic cyclic dinucleotides, i.e., cyclic di-GMP, cyclic di-AMP and cyclic GAMP (Danilchanka and Mekalanos, 2013). All three cyclic dinucleotides are bacterial second messengers, while cyclic GAMP is also generated by host-encoded cGAS, the recently identified cytosolic DNA receptor (Danilchanka and Mekalanos, 2013). Although the epistatic relationship of STING and Parkin has not been experimentally addressed yet, the requirement of either gene for the development of the ubiquitin coat around *M. tuberculosis* (Manzanillo et al., 2013; Watson et al., 2012) suggests that they act in the same pathway. Considering the established functions of the two proteins, Parkin acts most likely downstream of STING and is, based on the available literature (Manzanillo et al., 2013; Watson et al., 2012), predicted to be activated by *M. tuberculosis* DNA. However, how such DNA gains access to the host cytosol remains to be clarified.

Outlook

It is interesting to compare the mechanisms involved in the autophagy of endosymbiont mitochondria with those of pathogenic bacteria: self versus nonself. Mitophagy relies on dedicated sentinels such as Nix and PINK1 in mammals and ATG32 in yeast (Kanki et al., 2009; Okamoto et al., 2009), which are all membrane spanning proteins located on the outer mitochondrial membrane. In contrast, bacteria are recognized by cytosolic sensors such as STING and galectin-8 (Thurston et al., 2012; Watson et al., 2012), components of innate immunity pathways, that are recruited to the pathogens or their surrounding phagosome. Following these distinct initiation steps, mitophagy and xenophagy share some common themes. Notably, ubiquitination of mitochondria and bacteria (or their surrounding phagosome membranes) is a shared means to recruit autophagosomal machinery. The E3 ligase Parkin ubiquitinates mitochondria subsequent to its recruitment and activation by the mitochondrial kinase PINK1. Interestingly, Parkin also ubiquitin coats *M. tuberculosis* (or the surrounding phagosome) (Manzanillo et al., 2013). What recruits the normally cytosolic Parkin to the *Mycobacterium*-containing vacuole and derepresses the autoinhibited E3 ligase activity of Parkin during xenophagy remains to be identified. A kinase localized to the pathogen that functions as PINK1 does in mitophagy is a likely candidate. However, another E3 ubiquitin ligase, LRSAM1, is involved in ubiquitin coating of *S. Typhimurium* and there are likely more E3 ligases to be identified in xenophagy (Huett et al., 2012). Adaptor proteins such as p62 and NBR1 are recruited to mitochondria during Parkin-mediated mitophagy and to bacteria during xenophagy that in turn bind to LC3 on preautophagosomal membranes. While

p62, NBR1 and likely NDP52 recognize K63 linked ubiquitin chains on mitochondria, NDP52 also recognizes galectin-8 bound to bacterial permeabilized phagosomes independent of ubiquitin binding.

Likewise, p62 is recruited independently of ubiquitin binding to nascent phagophores (Itakura and Mizushima, 2011) during starvation-induced autophagy, further suggesting we have much more to learn about adaptor function in selective autophagy.

As outlined in this review, much progress has been made recently on the identity and generation of cargo-associated “eat-me” signals and on the cargo receptors that mediate selective autophagy. From these studies a simple model has emerged, in which selectivity is achieved by receptors that bridge cargo and phagophores. However, this model implies that cargo and pre-existing phagophores occur in each other’s proximity. Such condition may occur frequently enough for selective autophagy of certain cargos, for example protein aggregates, or for cargos that could be safely transported to a location where phagophores are generated. However, in order to preempt the threat of bacterial proliferation, anti-bacterial autophagy needs to be initiated with high efficiency in exactly the location where the bacterium has been detected. Since even the most upstream autophagy components, for example ATG9 and the ULK kinase complex, colocalize transiently with invading *S. Typhimurium* and also depolarized mitochondria, it is tempting to speculate that the prospective cargo is indeed able to instruct the autophagy machinery to generate phagophores in its proximity (Itakura et al., 2012; Kageyama et al., 2011). While the membrane source for phagophore formation has been an important problem for the autophagy field in general, in selective autophagy the question becomes how phagophores are generated in situ.

ACKNOWLEDGMENTS

We apologize to all colleagues whose work could not be cited due to space limitations. Work in the authors’ laboratories was supported by the MRC (U105170648, FR) and the National Institute of Neurological Disorders and Stroke intramural program (to R.Y.). We thank members of our laboratories for invaluable discussions.

REFERENCES

Abeliovich, H. (2011). Stationary-phase mitophagy in respiring *Saccharomyces cerevisiae*. *Antioxid. Redox Signal.* *14*, 2003–2011.

Aerbajinai, W., Giattina, M., Lee, Y.T., Raffeld, M., and Miller, J.L. (2003). The proapoptotic factor Nix is coexpressed with Bcl-xL during terminal erythroid differentiation. *Blood* *102*, 712–717.

Ali, S., Vollaard, A.M., Widjaja, S., Surjadi, C., van de Vosse, E., and van Dissel, J.T. (2006). PARK2/PACRG polymorphisms and susceptibility to typhoid and paratyphoid fever. *Clin. Exp. Immunol.* *144*, 425–431.

Axe, E.L., Walker, S.A., Manifava, M., Chandra, P., Roderick, H.L., Habermann, A., Griffiths, G., and Ktistakis, N.T. (2008). Autophagosome formation from membrane compartments enriched in phosphatidylinositol 3-phosphate and dynamically connected to the endoplasmic reticulum. *J. Cell Biol.* *182*, 685–701.

Benjamin, J.L., Sumpter, R., Jr., Levine, B., and Hooper, L.V. (2013). Intestinal epithelial autophagy is essential for host defense against invasive bacteria. *Cell Host Microbe* *13*, 723–734.

Birmingham, C.L., Smith, A.C., Bakowski, M.A., Yoshimori, T., and Brumell, J.H. (2006). Autophagy controls Salmonella infection in response to damage to the Salmonella-containing vacuole. *J. Biol. Chem.* *281*, 11374–11383.

Boyle, K.B., and Randow, F. (2013). The role of ‘eat-me’ signals and autophagy cargo receptors in innate immunity. *Curr. Opin. Microbiol.* *16*, 339–348.

Burman, J.L., Yu, S., Poole, A.C., Decal, R.B., and Pallanck, L. (2012). Analysis of neural subtypes reveals selective mitochondrial dysfunction in dopaminergic neurons from parkin mutants. *Proc. Natl. Acad. Sci. USA* *109*, 10438–10443.

Cadwell, K., Liu, J.Y., Brown, S.L., Miyoshi, H., Loh, J., Lennerz, J.K., Kishi, C., Kc, W., Carrero, J.A., Hunt, S., et al. (2008). A key role for autophagy and the autophagy gene Atg16l1 in mouse and human intestinal Paneth cells. *Nature* *456*, 259–263.

Chan, N.C., Salazar, A.M., Pham, A.H., Sweredoski, M.J., Kolawa, N.J., Graham, R.L.J., Hess, S., and Chan, D.C. (2011). Broad activation of the ubiquitin-proteasome system by Parkin is critical for mitophagy. *Hum. Mol. Genet.* *20*, 1726–1737.

Collins, C.A., De Mazière, A., van Dijk, S., Carlsson, F., Klumperman, J., and Brown, E.J. (2009). Atg5-independent sequestration of ubiquitinated mycobacteria. *PLoS Pathog.* *5*, e1000430.

Costello, M.J., Brennan, L.A., Basu, S., Chauss, D., Mohamed, A., Gilliland, K.O., Johnsen, S., Menko, A.S., and Kantorow, M. (2013). Autophagy and mitophagy participate in ocular lens organelle degradation. *Exp. Eye Res.* *116*, 141–150.

Daniilchanka, O., and Mekalanos, J.J. (2013). Cyclic dinucleotides and the innate immune response. *Cell* *154*, 962–970.

Denard, J., Beley, C., Kotin, R., Lai-Kuen, R., Blot, S., Leh, H., Asokan, A., Samulski, R.J., Moullier, P., Voit, T., et al. (2012). Human galectin 3 binding protein interacts with recombinant adeno-associated virus type 6. *J. Virol.* *86*, 6620–6631.

Deng, H., Dodson, M.W., Huang, H., and Guo, M. (2008). The Parkinson’s disease genes pink1 and parkin promote mitochondrial fission and/or inhibit fusion in *Drosophila*. *Proc. Natl. Acad. Sci. USA* *105*, 14503–14508.

Deretic, V., Saitoh, T., and Akira, S. (2013). Autophagy in infection, inflammation and immunity. *Nat. Rev. Immunol.* *13*, 722–737.

Dupont, N., Lacas-Gervais, S., Bertout, J., Paz, I., Freche, B., Van Nhieu, G.T., van der Goot, F.G., Sansonetti, P.J., and Lafont, F. (2009). Shigella phagocytic vacuolar membrane remnants participate in the cellular response to pathogen invasion and are regulated by autophagy. *Cell Host Microbe* *6*, 137–149.

Ellinghaus, D., Zhang, H., Zeissig, S., Lipinski, S., Till, A., Jiang, T., Stade, B., Bromberg, Y., Ellinghaus, E., Keller, A., et al. (2013). Association between variants of PRDM1 and NDP52 and Crohn’s disease, based on exome sequencing and functional studies. *Gastroenterology* *145*, 339–347.

Fujita, N., Morita, E., Itoh, T., Tanaka, A., Nakaoka, M., Osada, Y., Umemoto, T., Saitoh, T., Nakatogawa, H., Kobayashi, S., et al. (2013). Recruitment of the autophagic machinery to endosomes during infection is mediated by ubiquitin. *J. Cell Biol.* *203*, 115–128.

Gegg, M.E., Cooper, J.M., Chau, K.-Y., Rojo, M., Schapira, A.H.V., and Taanman, J.-W. (2010). Mitofusin 1 and mitofusin 2 are ubiquitinated in a PINK1/parkin-dependent manner upon induction of mitophagy. *Hum. Mol. Genet.* *19*, 4861–4870.

Geisler, S., Holmström, K.M., Skujat, D., Fiesel, F.C., Rothfuss, O.C., Kahle, P.J., and Springer, W. (2010). PINK1/Parkin-mediated mitophagy is dependent on VDAC1 and p62/SQSTM1. *Nat. Cell Biol.* *12*, 119–131.

Gutierrez, M.G., Master, S.S., Singh, S.B., Taylor, G.A., Colombo, M.I., and Deretic, V. (2004). Autophagy is a defense mechanism inhibiting BCG and *Mycobacterium tuberculosis* survival in infected macrophages. *Cell* *119*, 753–766.

Hamasaki, M., Furuta, N., Matsuda, A., Nezu, A., Yamamoto, A., Fujita, N., Oomori, H., Noda, T., Haraguchi, T., Hiraoka, Y., et al. (2013). Autophagosomes form at ER-mitochondria contact sites. *Nature* *495*, 389–393.

Heynen, M.J., Tricot, G., and Verwilghen, R.L. (1985). Autophagy of mitochondria in rat bone marrow erythroid cells. Relation to nuclear extrusion. *Cell Tissue Res.* *239*, 235–239.

- Huang, J., and Brumell, J.H. (2014). Bacteria-autophagy interplay: a battle for survival. *Nat. Rev. Microbiol.* 12, 101–114.
- Huett, A., Heath, R.J., Begun, J., Sassi, S.O., Baxt, L.A., Vyas, J.M., Goldberg, M.B., and Xavier, R.J. (2012). The LRR and RING domain protein LRSAM1 is an E3 ligase crucial for ubiquitin-dependent autophagy of intracellular *Salmonella* Typhimurium. *Cell Host Microbe* 12, 778–790.
- Itakura, E., Kishi-Itakura, C., Koyama-Honda, I., and Mizushima, N. (2012). Structures containing Atg9A and the ULK1 complex independently target depolarized mitochondria at initial stages of Parkin-mediated mitophagy. *J. Cell Sci.* 125, 1488–1499.
- Itakura, E., and Mizushima, N. (2011). p62 Targeting to the autophagosome formation site requires self-oligomerization but not LC3 binding. *J. Cell Biol.* 192, 17–27.
- Jin, S.M., and Youle, R.J. (2013). The accumulation of misfolded proteins in the mitochondrial matrix is sensed by PINK1 to induce PARK2/Parkin-mediated mitophagy of polarized mitochondria. *Autophagy* 9, 1750–1757.
- Johansen, T., and Lamark, T. (2011). Selective autophagy mediated by autophagic adapter proteins. *Autophagy* 7, 279–296.
- Kageyama, S., Omori, H., Saitoh, T., Sone, T., Guan, J.-L., Akira, S., Imamoto, F., Noda, T., and Yoshimori, T. (2011). The LC3 recruitment mechanism is separate from Atg9L1-dependent membrane formation in the autophagic response against *Salmonella*. *Mol. Biol. Cell* 22, 2290–2300.
- Kanki, T., Wang, K., Cao, Y., Baba, M., and Klionsky, D.J. (2009). Atg32 is a mitochondrial protein that confers selectivity during mitophagy. *Dev. Cell* 17, 98–109.
- Kondapalli, C., Kazlauskaitė, A., Zhang, N., Woodroof, H.I., Campbell, D.G., Gourlay, R., Burchell, L., Walden, H., Macartney, T.J., Deak, M., et al. (2012). PINK1 is activated by mitochondrial membrane potential depolarization and stimulates Parkin E3 ligase activity by phosphorylating Serine 65. *Open Biol.* 2, 120080.
- Lazarou, M., Jin, S.M., Kane, L.A., and Youle, R.J. (2012). Role of PINK1 binding to the TOM complex and alternate intracellular membranes in recruitment and activation of the E3 ligase Parkin. *Dev. Cell* 22, 320–333.
- Levine, B., Mizushima, N., and Virgin, H.W. (2011). Autophagy in immunity and inflammation. *Nature* 469, 323–335.
- Li, S., Wandel, M.P., Li, F., Liu, Z., He, C., Wu, J., Shi, Y., and Randow, F. (2013). Sterical hindrance promotes selectivity of the autophagy cargo receptor NDP52 for the danger receptor galectin-8 in antibacterial autophagy. *Sci. Signal.* 6, ra9.
- Manzanillo, P.S., Ayres, J.S., Watson, R.O., Collins, A.C., Souza, G., Rae, C.S., Schneider, D.S., Nakamura, K., Shiloh, M.U., and Cox, J.S. (2013). The ubiquitin ligase parkin mediates resistance to intracellular pathogens. *Nature* 501, 512–516.
- Marchiando, A.M., Ramanan, D., Ding, Y., Gomez, L.E., Hubbard-Lucey, V.M., Maurer, K., Wang, C., Ziel, J.W., van Rooijen, N., Nuñez, G., et al. (2013). A deficiency in the autophagy gene Atg16L1 enhances resistance to enteric bacterial infection. *Cell Host Microbe* 14, 216–224.
- Martinez, J., Almendinger, J., Oberst, A., Ness, R., Dillon, C.P., Fitzgerald, P., Hengartner, M.O., and Green, D.R. (2011). Microtubule-associated protein 1 light chain 3 alpha (LC3)-associated phagocytosis is required for the efficient clearance of dead cells. *Proc. Natl. Acad. Sci. USA* 108, 17396–17401.
- Matsuda, N., Sato, S., Shiba, K., Okatsu, K., Saisho, K., Gautier, C.A., Sou, Y.-S., Saiki, S., Kawajiri, S., Sato, F., et al. (2010). PINK1 stabilized by mitochondrial depolarization recruits Parkin to damaged mitochondria and activates latent Parkin for mitophagy. *J. Cell Biol.* 189, 211–221.
- Mira, M.T., Alcais, A., Nguyen, V.T., Moraes, M.O., Di Flumeri, C., Vu, H.T., Mai, C.P., Nguyen, T.H., Nguyen, N.B., Pham, X.K., et al. (2004). Susceptibility to leprosy is associated with PARK2 and PACRG. *Nature* 427, 636–640.
- Mizushima, N., and Komatsu, M. (2011). Autophagy: renovation of cells and tissues. *Cell* 147, 728–741.
- Mizushima, N., Yoshimori, T., and Ohsumi, Y. (2011). The role of Atg proteins in autophagosome formation. *Annu. Rev. Cell Dev. Biol.* 27, 107–132.
- Mostowy, S., Sancho-Shimizu, V., Hamon, M.A., Simeone, R., Brosch, R., Johansen, T., and Cossart, P. (2011). p62 and NDP52 proteins target intracytosolic *Shigella* and *Listeria* to different autophagy pathways. *J. Biol. Chem.* 286, 26987–26995.
- Narendra, D.P., Jin, S.M., Tanaka, A., Suen, D.-F., Gautier, C.A., Shen, J., Cookson, M.R., and Youle, R.J. (2010). PINK1 is selectively stabilized on impaired mitochondria to activate Parkin. *PLoS Biol.* 8, e1000298.
- Narendra, D., Tanaka, A., Suen, D.-F., and Youle, R.J. (2008). Parkin is recruited selectively to impaired mitochondria and promotes their autophagy. *J. Cell Biol.* 183, 795–803.
- Novak, I., Kirkin, V., McEwan, D.G., Zhang, J., Wild, P., Rozenknop, A., Rogov, V., Löhr, F., Popovic, D., Occhipinti, A., et al. (2010). Nix is a selective autophagy receptor for mitochondrial clearance. *EMBO Rep.* 11, 45–51.
- Ogawa, M., Yoshimori, T., Suzuki, T., Sagara, H., Mizushima, N., and Sasakawa, C. (2005). Escape of intracellular *Shigella* from autophagy. *Science* 307, 727–731.
- Okamoto, K., Kondo-Okamoto, N., and Ohsumi, Y. (2009). Mitochondria-anchored receptor Atg32 mediates degradation of mitochondria via selective autophagy. *Dev. Cell* 17, 87–97.
- Okatsu, K., Oka, T., Iguchi, M., Imamura, K., Kosako, H., Tani, N., Kimura, M., Go, E., Koyano, F., Funayama, M., et al. (2012). PINK1 autophosphorylation upon membrane potential dissipation is essential for Parkin recruitment to damaged mitochondria. *Nat. Commun.* 3, 1016.
- Okatsu, K., Uno, M., Koyano, F., Go, E., Kimura, M., Oka, T., Tanaka, K., and Matsuda, N. (2013). A dimeric PINK1-containing complex on depolarized mitochondria stimulates Parkin recruitment. *J. Biol. Chem.* 288, 36372–36384.
- Park, J., Lee, G., and Chung, J. (2009). The PINK1-Parkin pathway is involved in the regulation of mitochondrial remodeling process. *Biochem. Biophys. Res. Commun.* 378, 518–523.
- Perrin, A.J., Jiang, X., Birmingham, C.L., So, N.S., and Brumell, J.H. (2004). Recognition of bacteria in the cytosol of mammalian cells by the ubiquitin system. *Curr. Biol.* 14, 806–811.
- Pimenta de Castro, I., Costa, A.C., Lam, D., Tufi, R., Fedele, V., Moiso, N., Dinsdale, D., Deas, E., Loh, S.H.Y., and Martins, L.M. (2012). Genetic analysis of mitochondrial protein misfolding in *Drosophila melanogaster*. *Cell Death Differ.* 19, 1308–1316.
- Poole, A.C., Thomas, R.E., Andrews, L.A., McBride, H.M., Whitworth, A.J., and Pallanck, L.J. (2008). The PINK1/Parkin pathway regulates mitochondrial morphology. *Proc. Natl. Acad. Sci. USA* 105, 1638–1643.
- Poole, A.C., Thomas, R.E., Yu, S., Vincow, E.S., and Pallanck, L. (2010). The mitochondrial fusion-promoting factor mitofusin is a substrate of the PINK1/parkin pathway. *PLoS ONE* 5, e10054.
- Py, B.F., Lipinski, M.M., and Yuan, J. (2007). Autophagy limits *Listeria monocytogenes* intracellular growth in the early phase of primary infection. *Autophagy* 3, 117–125.
- Randow, F., and Münz, C. (2012). Autophagy in the regulation of pathogen replication and adaptive immunity. *Trends Immunol.* 33, 475–487.
- Randow, F., MacMicking, J.D., and James, L.C. (2013). Cellular self-defense: how cell-autonomous immunity protects against pathogens. *Science* 340, 701–706.
- Remé, C.E., and Young, R.W. (1977). The effects of hibernation on cone visual cells in the ground squirrel. *Invest. Ophthalmol. Vis. Sci.* 16, 815–840.
- Riley, B.E., Lougheed, J.C., Callaway, K., Velasquez, M., Brecht, E., Nguyen, L., Shaler, T., Walker, D., Yang, Y., Regnstrom, K., et al. (2013). Structure and function of Parkin E3 ubiquitin ligase reveals aspects of RING and HECT ligases. *Nat. Commun.* 4, 1982.
- Russell, R.C., Tian, Y., Yuan, H., Park, H.W., Chang, Y.-Y., Kim, J., Kim, H., Neufeld, T.P., Dillin, A., and Guan, K.-L. (2013). ULK1 induces autophagy by phosphorylating Beclin-1 and activating VPS34 lipid kinase. *Nat. Cell Biol.* 15, 174–1750.
- Sandoval, H., Thiagarajan, P., Dasgupta, S.K., Schumacher, A., Prchal, J.T., Chen, M., and Wang, J. (2008). Essential role for Nix in autophagic maturation of erythroid cells. *Nature* 454, 232–235.

- Sarraf, S.A., Raman, M., Guarani-Pereira, V., Sowa, M.E., Huttlin, E.L., Gygi, S.P., and Harper, J.W. (2013). Landscape of the PARKIN-dependent ubiquitylome in response to mitochondrial depolarization. *Nature* *496*, 372–376.
- Schweers, R.L., Zhang, J., Randall, M.S., Loyd, M.R., Li, W., Dorsey, F.C., Kundu, M., Opferman, J.T., Cleveland, J.L., Miller, J.L., and Ney, P.A. (2007). NIX is required for programmed mitochondrial clearance during reticulocyte maturation. *Proc. Natl. Acad. Sci. USA* *104*, 19500–19505.
- Tanaka, A., Cleland, M.M., Xu, S., Narendra, D.P., Suen, D.-F., Karbowski, M., and Youle, R.J. (2010). Proteasome and p97 mediate mitophagy and degradation of mitofusins induced by Parkin. *J. Cell Biol.* *191*, 1367–1380.
- Thurston, T.L.M., Ryzhakov, G., Bloor, S., von Muhlinen, N., and Randow, F. (2009). The TBK1 adaptor and autophagy receptor NDP52 restricts the proliferation of ubiquitin-coated bacteria. *Nat. Immunol.* *10*, 1215–1221.
- Thurston, T.L.M., Wandel, M.P., von Muhlinen, N., Foeglein, A., and Randow, F. (2012). Galectin 8 targets damaged vesicles for autophagy to defend cells against bacterial invasion. *Nature* *482*, 414–418.
- Travassos, L.H., Carneiro, L.A.M., Ramjeet, M., Hussey, S., Kim, Y.-G., Magalhães, J.G., Yuan, L., Soares, F., Chea, E., Le Bourhis, L., et al. (2010). Nod1 and Nod2 direct autophagy by recruiting ATG16L1 to the plasma membrane at the site of bacterial entry. *Nat. Immunol.* *11*, 55–62.
- Trempe, J.-F., Sauvé, V., Grenier, K., Seirafi, M., Tang, M.Y., Ménade, M., Al-Abdul-Wahid, S., Krett, J., Wong, K., Kozlov, G., et al. (2013). Structure of parkin reveals mechanisms for ubiquitin ligase activation. *Science* *340*, 1451–1455.
- Twig, G., and Shirihai, O.S. (2011). The interplay between mitochondrial dynamics and mitophagy. *Antioxid. Redox Signal.* *14*, 1939–1951.
- Twig, G., Elorza, A., Molina, A.J.A., Mohamed, H., Wikstrom, J.D., Walzer, G., Stiles, L., Haigh, S.E., Katz, S., Las, G., et al. (2008). Fission and selective fusion govern mitochondrial segregation and elimination by autophagy. *EMBO J.* *27*, 433–446.
- van Wijk, S.J.L., Fiskin, E., Putyrski, M., Pampaloni, F., Hou, J., Wild, P., Kensch, T., Grecco, H.E., Bastiaens, P., and Dikic, I. (2012). Fluorescence-Based Sensors to Monitor Localization and Functions of Linear and K63-Linked Ubiquitin Chains in Cells. *Molecular Cell* *47*, 797–809.
- Vincow, E.S., Merrihew, G., Thomas, R.E., Shulman, N.J., Beyer, R.P., MacCoss, M.J., and Pallanck, L.J. (2013). The PINK1-Parkin pathway promotes both mitophagy and selective respiratory chain turnover in vivo. *Proc. Natl. Acad. Sci. USA* *110*, 6400–6405.
- von Muhlinen, N., Akutsu, M., Ravenhill, B.J., Foeglein, A., Bloor, S., Rutherford, T.J., Freund, S.M.V., Komander, D., and Randow, F. (2012). LC3C, Bound Selectively by a Noncanonical LIR Motif in NDP52, Is Required for Antibacterial Autophagy. *Mol. Cell* *48*, 329–342.
- Wang, C., Mendonsa, G.R., Symington, J.W., Zhang, Q., Cadwell, K., Virgin, H.W., and Mysorekar, I.U. (2012). Atg16L1 deficiency confers protection from uropathogenic *Escherichia coli* infection in vivo. *Proc. Natl. Acad. Sci. USA* *109*, 11008–11013.
- Wang, X., Winter, D., Ashrafi, G., Schlehe, J., Wong, Y.L., Selkoe, D., Rice, S., Steen, J., LaVoie, M.J., and Schwarz, T.L. (2011). PINK1 and Parkin target Miro for phosphorylation and degradation to arrest mitochondrial motility. *Cell* *147*, 893–906.
- Watson, R.O., Manzanillo, P.S., and Cox, J.S. (2012). Extracellular *M. tuberculosis* DNA targets bacteria for autophagy by activating the host DNA-sensing pathway. *Cell* *150*, 803–815.
- Wauer, T., and Komander, D. (2013). Structure of the human Parkin ligase domain in an autoinhibited state. *EMBO J.* *32*, 2099–2112.
- Weidberg, H., Shvets, E., and Elazar, Z. (2011). Biogenesis and cargo selectivity of autophagosomes. *Annu. Rev. Biochem.* *80*, 125–156.
- Weidberg, H., Shvets, E., Shpilka, T., Shimron, F., Shinder, V., and Elazar, Z. (2010). LC3 and GATE-16/GABARAP subfamilies are both essential yet act differently in autophagosome biogenesis. *EMBO J.* *29*, 1792–1802.
- Weihofen, A., Thomas, K.J., Ostaszewski, B.L., Cookson, M.R., and Selkoe, D.J. (2009). Pink1 forms a multiprotein complex with Miro and Milton, linking Pink1 function to mitochondrial trafficking. *Biochemistry* *48*, 2045–2052.
- Wild, P., Farhan, H., McEwan, D.G., Wagner, S., Rogov, V.V., Brady, N.R., Richter, B., Korac, J., Waidmann, O., Choudhary, C., et al. (2011). Phosphorylation of the autophagy receptor optineurin restricts *Salmonella* growth. *Science* *333*, 228–233.
- Yamano, K., Fogel, A.I., Wang, C., van der Bliek, A.M., Youle, R.J., Wang, C., Trichet, M., van der Bliek, A.M., Boulogne, C., Youle, R.J., et al. (2014). Mitochondrial Rab GAPs govern autophagosome biogenesis during mitophagy. *Elife* *3*, e01612.
- Yoshii, S.R., Kishi, C., Ishihara, N., and Mizushima, N. (2011). Parkin mediates proteasome-dependent protein degradation and rupture of the outer mitochondrial membrane. *J. Biol. Chem.* *286*, 19630–19640.
- Youle, R.J., and van der Bliek, A.M. (2012). Mitochondrial fission, fusion, and stress. *Science* *337*, 1062–1065.
- Yu, W., Sun, Y., Guo, S., and Lu, B. (2011). The PINK1/Parkin pathway regulates mitochondrial dynamics and function in mammalian hippocampal and dopaminergic neurons. *Hum. Mol. Genet.* *20*, 3227–3240.
- Zhang, J., Loyd, M.R., Randall, M.S., Waddell, M.B., Kriwacki, R.W., and Ney, P.A. (2012). A short linear motif in BNIP3L (NIX) mediates mitochondrial clearance in reticulocytes. *Autophagy* *8*, 1325–1332.
- Zheng, Y.T., Shahnazari, S., Brech, A., Lamark, T., Johansen, T., and Brumell, J.H. (2009). The adaptor protein p62/SQSTM1 targets invading bacteria to the autophagy pathway. *J. Immunol.* *183*, 5909–5916.
- Ziviani, E., Tao, R.N., and Whitworth, A.J. (2010). *Drosophila* parkin requires PINK1 for mitochondrial translocation and ubiquitinates mitofusins. *Proc. Natl. Acad. Sci. USA* *107*, 5018–5023.

Mitochondrial Cristae Shape Determines Respiratory Chain Supercomplexes Assembly and Respiratory Efficiency

Sara Cogliati,^{1,2} Christian Frezza,¹ Maria Eugenia Soriano,^{1,2} Tatiana Varanita,^{1,2} Ruben Quintana-Cabrera,^{1,2} Mauro Corrado,^{1,3} Sara Cipolat,¹ Veronica Costa,¹ Alberto Casarin,⁴ Ligia C. Gomes,¹ Ester Perales-Clemente,⁵ Leonardo Salvati,⁴ Patricio Fernandez-Silva,⁶ Jose A. Enriquez,^{5,*} and Luca Scorrano^{1,2,3,*}

¹Dulbecco-Telethon Institute, Venetian Institute of Molecular Medicine, Via Orus 2, 35129 Padova, Italy

²Department of Biology, University of Padova, Via U. Bassi 58B, 35121 Padova, Italy

³IRCCS Fondazione Santa Lucia, Via Ardeatina 306, 00143 Rome, Italy

⁴Clinical Genetics Unit, Department of Woman and Child Health, University of Padova, Via Giustiniani 3, 35128 Padova, Italy

⁵Centro Nacional de Investigaciones Cardiovasculares Carlos III, Melchor Fernández Almagro 3, 28029 Madrid, Spain

⁶Departamento de Bioquímica y Biología Molecular y Celular, Facultad de Ciencias, Universidad de Zaragoza, Pedro Cerbuna 12, 50009 Zaragoza, Spain

*Correspondence: jaenriquez@cnic.es (J.A.E.), luca.scorrano@unipd.it (L.S.)

<http://dx.doi.org/10.1016/j.cell.2013.08.032>

This is an open-access article distributed under the terms of the Creative Commons Attribution-NonCommercial-No Derivative Works License, which permits non-commercial use, distribution, and reproduction in any medium, provided the original author and source are credited.

SUMMARY

Respiratory chain complexes assemble into functional quaternary structures called supercomplexes (RCS) within the folds of the inner mitochondrial membrane, or cristae. Here, we investigate the relationship between respiratory function and mitochondrial ultrastructure and provide evidence that cristae shape determines the assembly and stability of RCS and hence mitochondrial respiratory efficiency. Genetic and apoptotic manipulations of cristae structure affect assembly and activity of RCS in vitro and in vivo, independently of changes to mitochondrial protein synthesis or apoptotic outer mitochondrial membrane permeabilization. We demonstrate that, accordingly, the efficiency of mitochondria-dependent cell growth depends on cristae shape. Thus, RCS assembly emerges as a link between membrane morphology and function.

INTRODUCTION

Mitochondria are key organelles in intermediate cellular metabolism, energy conversion, and calcium homeostasis (Dimmer and Scorrano, 2006). They also integrate and amplify apoptosis induced by intrinsic stimuli, releasing cytochrome *c* and other proapoptotic factors required for the activation of caspases (Green and Kroemer, 2004). Cytochrome *c* release is regulated by proteins of the BCL-2 family that control the permeabilization of the outer membrane (OMM) (Danial and Korsmeyer, 2004).

Energy conversion occurs at the inner mitochondrial membrane (IMM) that can be further divided into two subcompart-

ments: the so-called “boundary membrane” and the cristae, separated from the former by narrow tubular junctions (Frey and Mannella, 2000). The cristae shape is dynamic: upon activation of mitochondrial respiration, “orthodox” mitochondria become “condensed,” with an expanded cristae space (Hackenbrock, 1966). During apoptosis, the curvature of the cristae membrane is inverted in a remodeling process required for the complete release of cytochrome *c*, normally confined in the cristae (Scorrano et al., 2002; Frezza et al., 2006; Yamaguchi et al., 2008). Cristae remodeling occurs in response to proapoptotic BH3-only BCL-2 family members, such as BID, BIM-S, and BNIP3, and independently of the outer membrane multidomain BCL-2 family members BAX and BAK (Scorrano et al., 2002; Cipolat et al., 2006; Yamaguchi et al., 2008). Whether changes in morphology of the cristae, where respiratory chain complexes (RCCs) mainly localize (Vogel et al., 2006), affect oxidative phosphorylation efficiency, as originally predicted (Hackenbrock, 1966), is unclear. This issue is further complicated by the assembly of RCC in supercomplexes (RCS) (Schägger, 1995; Acín-Pérez et al., 2008), quaternary supramolecular structures that, by channeling electrons among individual RCCs, allow the selective use of RCC subsets for nicotinic adenine dinucleotide (NADH)- or flavin adenine dinucleotide-derived electrons (Lapuente-Brun et al., 2013). Such a supramolecular organization is common in cristae: also, the mitochondrial ATP synthase is assembled into dimers with greater adenosine triphosphatase (ATPase) activity (Campanella et al., 2008; Gomes et al., 2011). Interestingly, cristae shape and ATPase dimers are linked: in yeast mutants where the ATPase cannot dimerize, cristae are disorganized (Paumard et al., 2002; Minauro-Sanmiguel et al., 2005; Strauss et al., 2008), whereas in mammalian cells, increased cristae density favors ATPase dimerization during autophagy (Gomes et al., 2011). On the contrary, despite their importance in mitochondrial bioenergetics,

the relationship between RCS and cristae shape remains unclear.

Mitochondrial morphology and ultrastructure depends on “mitochondria-shaping” proteins that regulate organellar fusion and fission (Gripatic and van der Bliek, 2001). Mitofusins (MFN) 1 and 2, highly homologous dynamin-related proteins of the OMM, orchestrate fusion (Santel and Fuller, 2001; Legros et al., 2002; Chen et al., 2003; Santel et al., 2003). MFN1 primarily participates in fusion, cooperating with the IMM dynamin-related protein optic atrophy 1 (OPA1) (Cipolat et al., 2004), whereas MFN2 also tethers mitochondria to the endoplasmic reticulum (de Brito and Scorrano, 2008). Mitochondrial fission is regulated by the cytoplasmic dynamin-related protein 1 that, upon calcineurin-dependent dephosphorylation, translocates to mitochondria (Yoon et al., 2001; Smirnova et al., 2001; Cereghetti et al., 2008). Genetic depletion of OPA1 leads to disorganization of the cristae (Frezza et al., 2006), and oligomers that contain a soluble and a membrane-bound form of OPA1 keep the cristae junctions tight, independently from OPA1 role in fusion (Frezza et al., 2006; Cipolat et al., 2006). During apoptosis, these oligomers are early targets of BID, BIM-S, and BNIP3, as well as of intrinsic death stimuli (Frezza et al., 2006; Yamaguchi et al., 2008; Landes et al., 2010; Costa et al., 2010). Whereas our knowledge of the molecular determinants of cristae shape and their role in apoptosis is increasing, the relationship between cristae morphology and mitochondrial function remains unexplored. We therefore set out to genetically dissect whether and how cristae shape regulates mitochondrial respiration. We show that cristae morphology determines assembly and stability of RCS and hence optimal mitochondrial respiratory function during life and death of the cell.

RESULTS

Genetic Dissection of Outer Membrane Permeabilization from Cristae Remodeling

Whether apoptotic cristae remodeling that maximizes cytochrome *c* release from mitochondria affects mitochondrial function is unclear, mainly because it occurs around the same time as outer membrane permeabilization (Scorrano et al., 2002). In order to genetically dissociate the two processes, we inspected the primary structure of the prototypical cristae remodeling inducer BCL-2 family member BID for homology with peptides known to perturb the mitochondrial inner membrane, like mastoparan, a 14 amino acid wasp venom component (Pfeiffer et al., 1995). Interestingly, BID membrane inserting $\alpha 6$ helix as well as the transmembrane domains of Bnip3 and BimS that also remodel cristae (Yamaguchi et al., 2008; Landes et al., 2010) displayed homology to mastoparan (Figures S1A and S1B available online). To exploit the role of this homologous sequence in cristae remodeling, we mutagenized the two highly conserved 157 and 158 Lys *H. sapiens* BID residues to Ala (BID^{KKAA}) (Figure S1C). Because this mutation did not impair caspase-8 cleaved recombinant BID (cBID) integration in purified mouse liver mitochondria (MLM) (Wei et al., 2000; Figure S1D), we could measure its biological activity using an established quantitative, specific cytochrome *c* release ELISA (Scorrano et al., 2002). cBID efficiently released cytochrome *c* from purified mitochondria,

whereas a BH3 domain G94E mutant was, as expected, inactive (Wei et al., 2000) and the cBID^{KKAA} mutant released ~25%–30% more cytochrome *c* than the baseline (Figure 1A), a figure close to the amount of free intermembrane space cytochrome *c* (Scorrano et al., 2002). BAK oligomerization was superimposable in cBID or cBID^{KKAA}-treated mitochondria (Figure 1B); conversely, two established assays of intramitochondrial cytochrome *c* redistribution, the cytochrome *b₅*-dependent extramitochondrial NADH oxidation and the ratio of ascorbate-driven over tetramethyl-p-phenylenediamine (TMPD)-driven respiration (Scorrano et al., 2002), indicated that cBID^{KKAA} mobilized the cristae cytochrome *c* pool less efficiently than cBID (Figures 1C and 1D). Indeed, cBID^{KKAA} was unable to remodel mitochondrial cristae, as indicated by morphometric analysis of electron micrographs of mitochondria treated with the BID mutants (Figures 1E and 1F) (Scorrano et al., 2002). Cristae remodeling is associated with the disruption of high molecular weight (HMW) OPA1 oligomers (Frezza et al., 2006). Western blots of blue native gel electrophoresis (BNGE) of mitochondrial proteins revealed four major OPA1-containing complexes. Upon treatment with cBID, OPA1 rapidly disappeared from ~720 kDa HMW complexes (Figures 1G, S1E, and S1F). These HMW forms of OPA1 were similarly targeted by cBID^{G94E} but significantly less by cBID^{KKAA}, as determined by BNGE (Figure 1H, quantification in [I]). Chemical crosslinking experiments (Frezza et al., 2006) further confirmed that the OPA1-containing oligomer is disrupted by the mutants of cBID able to induce cristae remodeling (Figures S1G and S1H). Finally, we measured the killing efficiency of these truncated BID (tBID) mutants expressed in mouse embryonic fibroblasts (MEFs). Only tBID efficiently killed MEFs: tBID^{KKAA} and tBID^{G94E} elicited comparable low levels of cell death, whereas the double tBID^{KKAA,G94E} mutant appeared completely ineffective (Figure 1J), suggesting that both outer membrane permeabilization and mitochondrial cristae remodeling are required for BID-induced apoptosis. In conclusion, BID^{KKAA} is deficient in cristae remodeling, cytochrome *c* release, and induction of apoptosis.

RCS Disassemble during Cristae Remodeling

The BID^{KKAA} mutant dissociates outer membrane permeabilization from cristae remodeling and can be used to investigate the relationship between the latter and mitochondrial function. We therefore measured the effect of the BID mutants on the respiratory control ratio (RCR), an index of respiratory efficiency, of mitochondria incubated with excess exogenous cytochrome *c* and NADH (to compensate for the potential effects of inner membrane or outer membrane [OM] permeabilization). cBID reduced RCR only when mitochondria were energized with substrates for complex I (glutamate/malate) but not when they were fed with substrates entering the electron transport chain at complex II (succinate) or complex IV (ascorbate + TMPD) (Figure 2A; data not shown). Interestingly, these changes were recapitulated by the BH3 domain mutant cBID^{G94E} that does not permeabilize the OM but not by the cristae remodeling-deficient mutants cBID^{KKAA} and cBID^{KKAA,G94E} (Figure 2B). Maximal (uncoupled) respiration was similarly affected by the cBID mutants tested, ruling out that BID alters RCR, because it affects ATPase or activity or ATP/ADP exchange (Figure S2A). These experiments

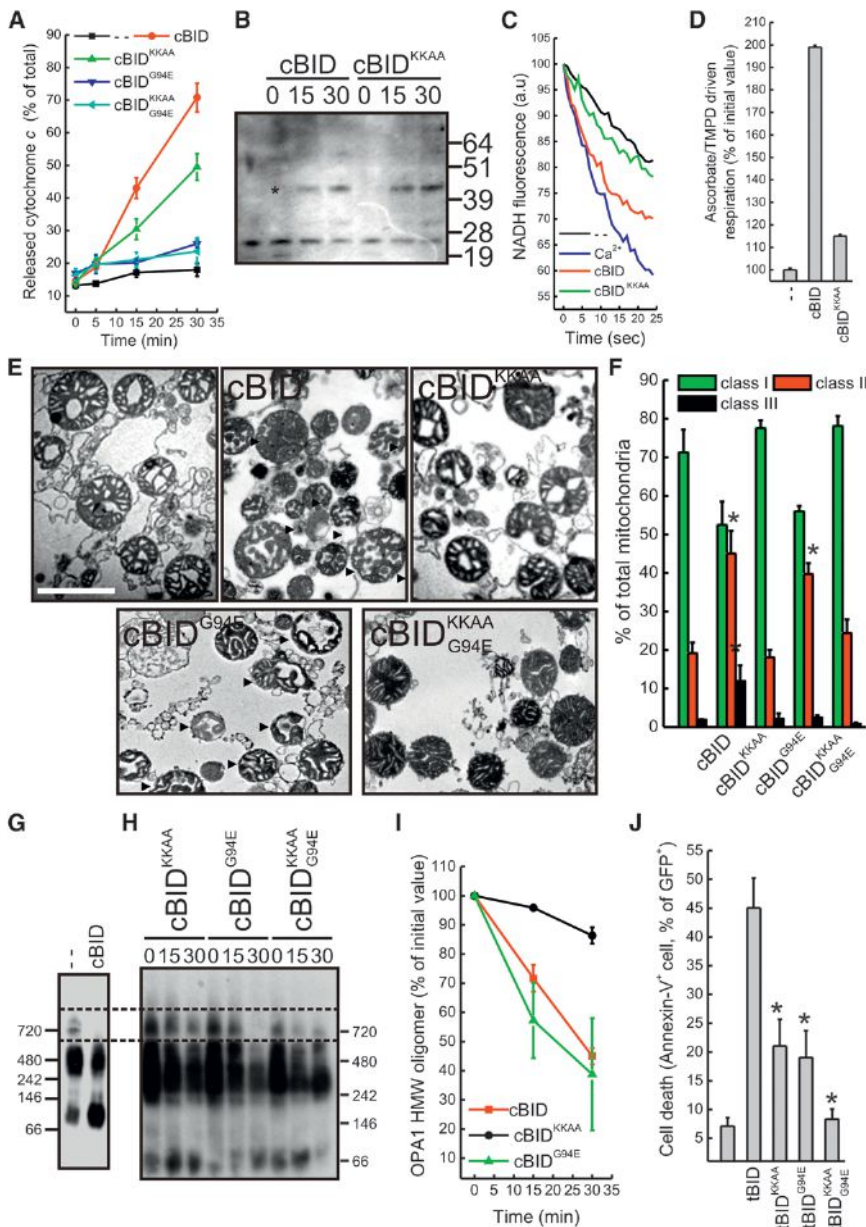


Figure 1. Two Conserved Lys in BID α 6 Helix Are Required for Cristae Remodeling

(A) Mitochondria were treated for the indicated times with the indicated mutants of cBID, and cytochrome c release was measured by ELISA. Data represent average \pm SEM of five independent experiments.

(B) Mitochondria treated with the indicated mutants of cBID for the indicated min were cross-linked with 1 mM BMH for 30 min, spun, and the pellets were separated by SDS-PAGE and immunoblotted using anti-BAK antibody. The asterisks denote BAK oligomers.

(C) Mitochondria were treated as indicated (Ca^{2+} , 200 μ M), and cytochrome b_5 -dependent NADH fluorescence changes were recorded. a.u., arbitrary units.

(D) Mitochondria were treated for 15 min with the indicated BID mutants, transferred into the chamber of a Clark's type O_2 electrode, and the ascorbate/TMPD-driven respiration ratio was determined. Data represent average \pm SEM of four independent experiments.

(E) Representative electron microscopy fields of mitochondria treated for 15 min with the indicated cBID mutants (as in [E]). Mitochondria were assigned to morphological classes I–III as in Scorrano et al. (2002). Data represent average \pm SEM of three independent experiments. The asterisk denotes $p < 0.05$ in a paired sample Student's t test versus untreated.

(G and H) BNAGE analysis of OPA1 oligomers in MLM treated for 30 min (G) or for the indicated minutes (H), as indicated. The boxed area indicates the HMW complexes of OPA1.

(I) Densitometric analysis of OPA1 HMW complexes. Experiments were as in (H). Data represent average \pm SEM of four independent experiments.

(J) MEFs were transfected with the pMIG plasmid containing the indicated insert and after 48 hr cell death was determined cytofluorimetrically as the percentage of Annexin-V $^+$, GFP $^+$ cells. Data represent average \pm SEM of four independent experiments. The asterisk denotes $p < 0.05$ in a paired sample Student's t test versus tBID. See also Figure S1.

suggest that cristae remodeling causes complex I-dependent changes in mitochondrial bioenergetics.

Complex I is further assembled in quaternary functional RCS with complexes III and IV (I + III and I + III + IV), whereas most complex II is not found in RCS (Acín-Pérez et al., 2008). Thus, the reduction in complex I-supported respiration could be a consequence of specific inhibition of complex I or of issues in RCS function. Even after 30 min of acute BID treatment, the specific complex I NADH-ubiquinone reductase activity of purified mitochondria was unaltered (data not shown), prompting us to investigate RCS assembly and stability in situ. We therefore took advantage of *Bax* $^{-/-}$, *Bak* $^{-/-}$ (DKO) MEFs, resistant to mitochondrial permeabilization, cytochrome c release, and apoptosis triggered by expression of tBID (Wei et al., 2001).

Upon transduction of metabolically labeled DKO MEFs with tBID but not with tBID KKAA that does not cause cristae remodeling (Figure S2B), the RCS radioactivity signal as well as the RCS/complex V radioactivity ratio were reduced (Figures 2C and 2D), and we observed a reduction in the autoradiographic signal of cytochrome *b* retrieved in RCS compared to that in free complex III (Figures 2E and 2F). Whereas this result could suggest that complex III was incorporated less efficiently into RCS, immunoblotting for the complex I subunit NDUFA9 revealed that RCSs were also destabilized in DKO cells (Figure 2G). Functionally, only cBID and cBID G94E that cause cristae remodeling but not cBID KKAA reduced glutamate-supported RCR in DKO mitochondria (Figure 2H). Thus, BID destabilizes RCS and selectively reduces glutamate-dependent RCR.

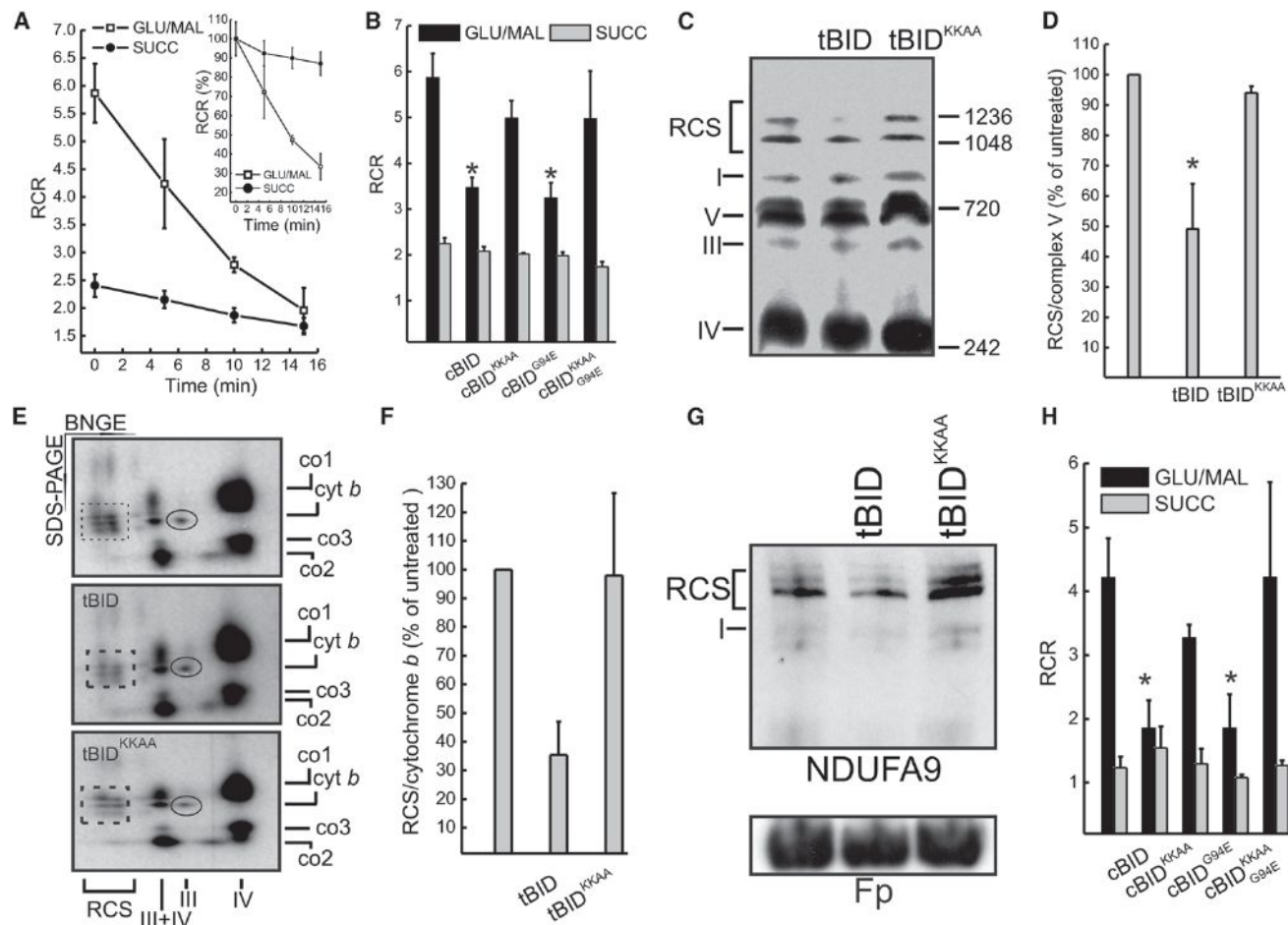


Figure 2. Respiratory Chain Supercomplexes Are Disassembled during Cristae Remodeling

(A) RCR of mitochondria energized with 5 mM/2.5 mM glutamate/malate (GLU/MAL) or 10 mM succinate (SUCC) treated for the indicated times with cBID. Data represent average \pm SEM of five independent experiments. Inset, RCR values normalized to $t = 0$.

(B) Experiments were as in (A), except that mitochondria were incubated with the indicated mutants of cBID for 15 min. Data represent average \pm SEM of four independent experiments. The asterisk denotes $p < 0.05$ in a paired sample Student's t test versus untreated.

(C) BNGE of mitochondrial OXPHOS protein from DKO MEFs transduced as indicated and, after 2 days, metabolically labeled for 2 hr and lysed after 24 hr. Equal amounts of protein (100 μ g) were separated by BNGE, and radioactivity was detected in the fixed and dried gels for 1 week. RCC and RCS of the respiratory chain are indicated.

(D) Densitometric analysis of the autoradiographic RCS/complex V signal ratio. Data represent average \pm SEM of three independent experiments performed as in (E). The asterisk denotes $p < 0.05$ in a paired sample Student's t test versus untreated.

(E) 2D BN/SDS PAGE analysis of mitochondrial OXPHOS proteins from DKO MEFs transduced as indicated, metabolically labeled for 2 hr, and lysed after 24 hr. Equal amount (50 μ g) of proteins were separated in native condition, and then the lanes were excised and proteins separated by a second dimension SDS-PAGE. The gels were dried and the signal was detected following 1 week of exposure. RCC and RCS of the respiratory chain as well as the single-labeled proteins are indicated. Boxes and circles indicate RCS and cytochrome b , respectively.

(F) Densitometric analysis of the ratio of autoradiographic signal between supercomplex (boxed) and complex assembled cytochrome b (circled). Data represent average \pm SEM of three independent experiments. The asterisk denotes $p < 0.05$ in a paired sample Student's t test versus untreated.

(G) BNGE analysis of OXPHOS proteins in mitochondria from DKO MEFs transduced as indicated. Equal amounts (100 μ g) of proteins were separated in native conditions, transferred onto PVDF membranes, and probed with the indicated antibodies. RCC and RCS are indicated.

(H) RCR of DKO mitochondria energized with 5 mM/2.5 mM GLU/MAL or 10 mM SUCC treated for 15 min with the indicated cBID mutants. Data represent average \pm SEM of four independent experiments. The asterisk denotes $p < 0.05$ in a paired sample Student's t test versus untreated.

See also Figure S2.

Conditional Ablation of *Opa1* Alters Cristae Shape and RCS Assembly

To verify whether RCS disorganization was a general consequence of altered cristae shape, we turned to cells lacking *Opa1*, a key regulator of cristae morphology (Frezza et al.,

2006). However, chronic *Opa1* depletion impaired mitochondrial DNA (mtDNA) levels and translation (Figures S3A and S3B), complicating the analysis of the relationship between *Opa1* and RCS and calling for a model of conditional *Opa1* ablation. We produced, by homologous recombination, C57BL6/J

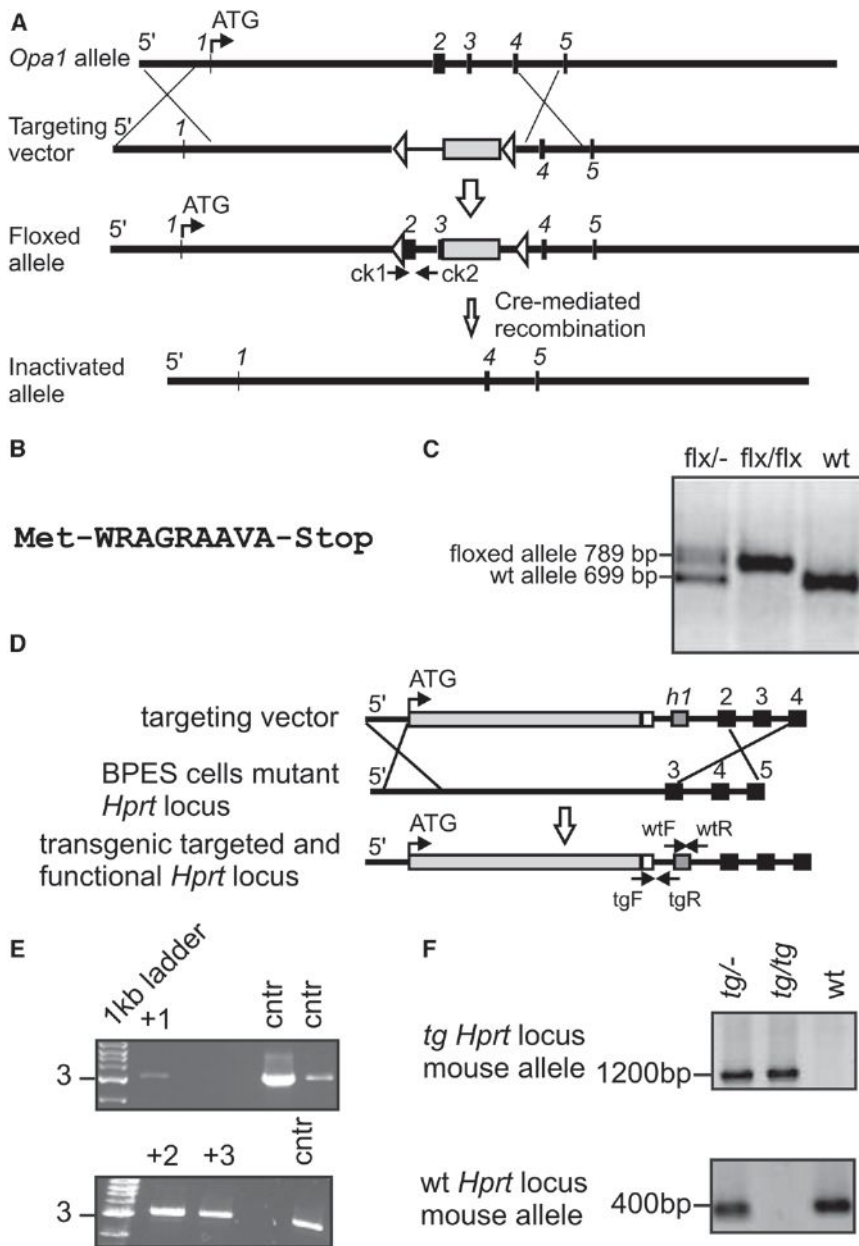


Figure 3. Generation of *Opa1*^{flx/flx} and *Opa1*^{tg} Mice

(A) Maps of the wild-type *Opa1* allele, the targeting vector, the conditional floxed allele, and the inactivated *Opa1* allele. The 5' UTR, exons (black boxes), LoxP sites (white arrows), FRT recombination sites, and PGK-neomycin cassette (white box) are indicated. The locations of PCR primers (*ck1* = primer check1 forward, *ck2* = primer check2 reverse) are indicated. Dimensions are not in scale. (B) Prediction of the maximal possible aberrant OPA1 protein.

(C) RT-PCR analysis of transcripts in heterozygous (flx/-), homozygous (flx/flx), and WT mice. (D) Maps of the targeting vector, the mutant *Hprt* locus of BPES cells, and the transgenic targeted and functional *Hprt* locus. The 5' UTR, the human β -ACTIN promoter and *Opa1* gene (light gray box), poly A (white box), human exon 1 of *Hprt* locus (*h1*, dark gray box), and *Hprt* locus exons (black boxes) are indicated. The locations of PCR primers (WTF, WT forward; WTR, WT reverse; tgF, transgenic forward; tgR, transgenic reverse) are indicated. Dimensions are not in scale.

(E) RT-PCR screening of ESC clones. The positive clones are indicated.

(F) RT-PCR analysis of transcripts in heterozygous (tg/-), homozygous (tg/tg), and WT mice.

See also Figure S3.

embryonic stem cells with loxP sites inserted in the *Opa1* gene (*Opa1*^{flx/flx}), which were then microinjected in C57BL6/J blastocysts to generate *Opa1*^{flx/flx} mice. Following Cre-mediated recombination, the deletion of exons 2 and 3 resulted in an aberrant exon1–exon4 transcript with a stop codon immediately after exon 1, producing a predicted 10 amino acid (aa) residual protein (Figures 3A and 3B). Chimerism and germ-line transmission of the offspring was tested by PCR, and germ-line transmittants were bred to homozygosity (Figure 3C). Fibroblasts isolated from the diaphragm of homozygous *Opa1*^{flx/flx} 7-week-old male mice (MAFs) were immortalized and used for subsequent analysis. OPA1 was completely ablated 24 hr after adenoviral delivery of Cre recombinase (Figure 4A) and, as expected, mito-

chondria were fragmented (Figures 4B and 4C) with defects in cristae shape (Figures 4D and 4E). Four days after Cre-mediated *Opa1* ablation, mtDNA copy number (Figure 4F) and translation (Figures 4G and 4H) were unaffected, allowing us to specifically address the role of OPA1 and cristae shape in RCS assembly using an assay based on the incorporation of radiolabeled mtDNA-encoded proteins into RCC and RCS (Acín-Pérez et al., 2008). Upon acute *Opa1* ablation, the assembly of mtDNA-encoded subunits into RCC was not affected (data not shown). We therefore followed the RCS assembly rate (measured as the ratio between RCS and complex V radioactivity throughout the chase period) that resulted ~8-fold slower when *Opa1* was ablated from *Opa1*^{flx/flx} MAFs (Figures 4I and 4J). A similar reduction in the RCS assembly rate was observed in *Opa1*^{-/-} MEFs (Figure S3C), suggesting that, in absence of *Opa1*, RCC are less superassembled, irrespective of their initial levels. To test if acute *Opa1* ablation altered RCS in vivo, we tail vein-injected Cre-expressing adenoviruses in *Opa1*^{flx/flx} animals. After 72 hr, OPA1 levels in liver mitochondria were reduced by ~50% (Figure S4A), cristae morphology was abnormal (Figure S4B), RCS were reduced (Figure S4C), and glutamate/malate RCR was impaired (Figure 4K). These experiments of conditional ablation of *Opa1* identify a role for cristae shape in RCS assembly in vitro and in vivo.

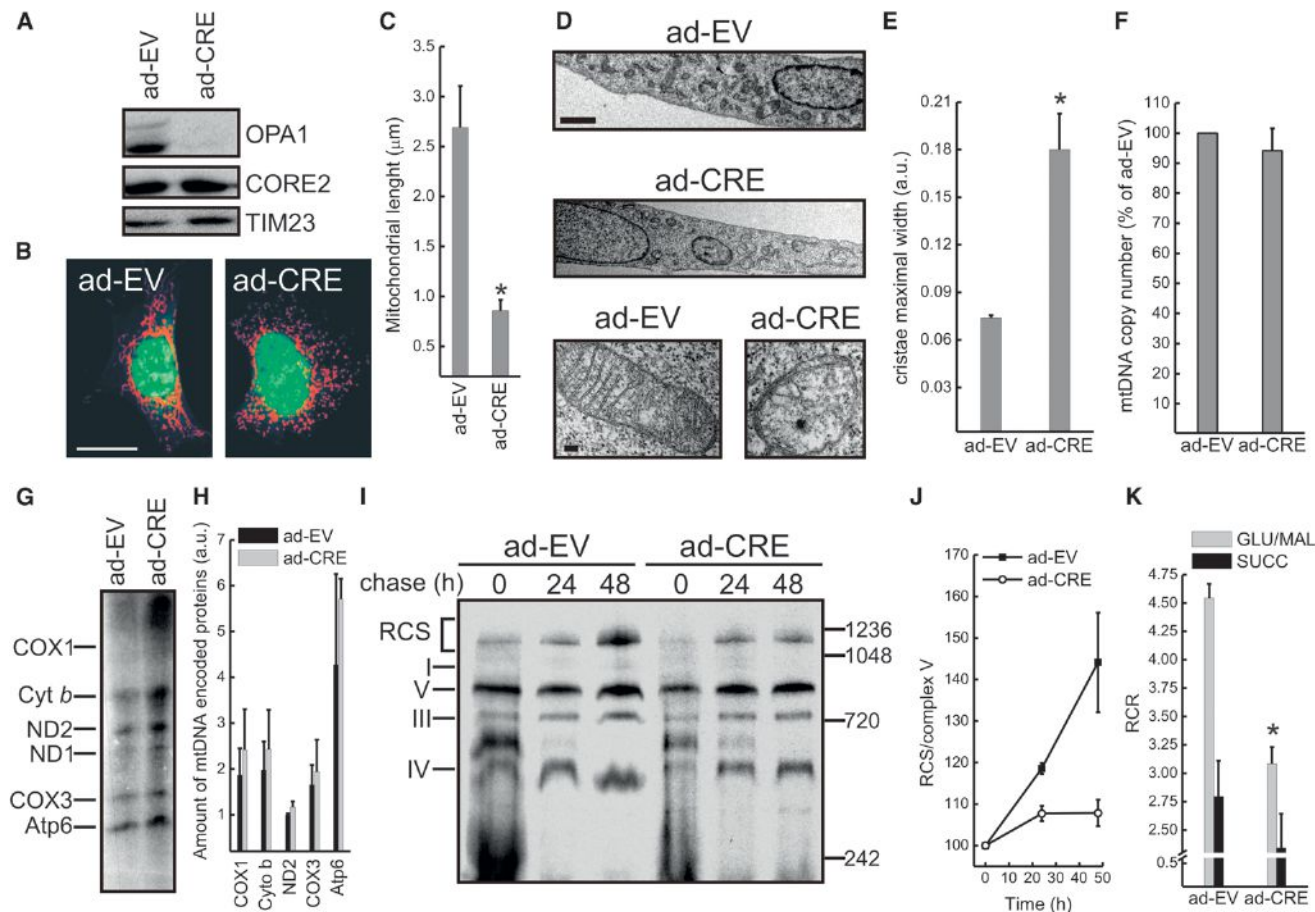


Figure 4. Acute Ablation of *Opa1* Alters Mitochondrial Morphology, Cristae Shape, and RCS Assembly

(A) *Opa1*^{flx/flx} MAFs were infected with bicistronic adenoviruses carrying the indicated insert (EV, empty vector; CRE, Cre recombinase) upstream of GFP and, after 24 hr, equal amounts of proteins (20 μg) were separated by SDS-PAGE and immunoblotted with the indicated antibodies.

(B) *Opa1*^{flx/flx} MAFs were infected with the indicated adenoviruses and, after 24 hr, fixed, immunostained using an anti-TOM20 antibody, and representative confocal images acquired. The green cytoplasmic staining identifies the coexpression of GFP. The scale bar represents 20 μm.

(C) Average mitochondrial major axis length. Experiments were as in (B). Data represent average ± SEM of four independent experiments (five mitochondria per cell, at least 50 cells/experiment). The asterisk denotes $p < 0.05$ in a paired sample Student's *t* test versus ad-EV.

(D) *Opa1*^{flx/flx} MAFs were infected with the indicated adenoviruses and, after 24 hr, fixed and processed for electron microscopy. The scale bars represent 2 μm (top) and 200 nm (bottom).

(E) Morphometric analysis of cristae width in 40 randomly selected mitochondria of *Opa1*^{flx/flx} MAFs infected with the indicated adenoviruses. Data represent average ± SEM of three independent experiments. The asterisk denotes $p < 0.05$ in a paired sample Student's *t* test versus ad-EV.

(F) Mitochondrial DNA copy number quantification. mtDNA was amplified by RT-PCR from total DNA of *Opa1*^{flx/flx} MAFs infected with the indicated adenoviruses. Data are normalized to MAFs infected with control adenovirus and represent average ± SEM of four independent experiments.

(G) mtDNA translation assay. *Opa1*^{flx/flx} MAFs infected as indicated were metabolically labeled in presence of emetine and lysed after 30 min. Protein samples (40 μg) were separated by SDS-PAGE, and the radioactivity was detected in the fixed and dried gels for 3 days. The mtDNA encoded proteins are indicated.

(H) Densitometric analysis of the mtDNA-encoded proteins. Experiments are as in (G). Data represent average ± SEM of four independent experiments.

(I) RCS assembly assay. *Opa1*^{flx/flx} MAFs were infected as indicated and, after 24 hr, metabolically labeled for 2 hr and then chased for the indicated times. Equal amounts of protein (100 μg) were separated by BN PAGE, and radioactivity was detected in the fixed and dried gels for 1 week. RCC and RCS of the respiratory chain are indicated.

(J) Densitometric analysis of the incorporation rate of radioactivity into supercomplexes. Values are normalized for the autoradiographic signal of complex V. Data represent average ± SEM from three independent experiments performed as in (H).

(K) RCR of mitochondria isolated from livers of *Opa1*^{flx/flx} mice 3 days after tail-vein injection of the indicated adenoviruses, energized with 5 mM/2.5 mM GLU/MAL or 10 mM SUCC. Data represent average ± SEM of four independent experiments. The asterisk denotes $p < 0.05$ in a paired sample Student's *t* test versus ad-EV.

See also Figure S4.

Overexpression of *Opa1* Increases RCS Assembly

The model linking cristae shape to RCS predicts that higher OPA1 levels should favor RCS assembly. To verify this hypo-

thesis, we wanted to generate a mouse model of *Opa1* overexpression. Very high OPA1 levels are, however, toxic, causing paradoxical mitochondrial fragmentation (Cipolat

et al., 2004): we therefore targeted, by homologous recombination in the murine X chromosome *Hprt* region, a transgene-carrying mouse variant 1 *Opa1* under the human β -actin promoter (*Opa1^{tg}*) (Figure 3D). The integration into microinjected BPES embryonic stem cells was verified by PCR (Figure 3E), and the cells were microinjected into C57BL6/J blastocysts. Six generated agouti chimeras with a chimerism exceeding 90% were bred with C57BL6/J mates and tested for germline transmission by fur color and transgene PCR analysis (Figure 3F). Mice were viable, fertile, grew normally, and resisted to different forms of tissue damage (T.V., M.E.S., V. Romanello, S.C., V.C., R. Menabò, M. Sandri, F. Di Lisa, and L.S., unpublished data). Immortalized MAFs prepared from the diaphragm of hemizygous *Opa1^{tg}* 7-week-old C57BL6/J male mice displayed an ~1.5 increase in OPA1 levels compared to age- and sex-matched littermate controls MAFs (wild-type [WT]; Figure 5A). Mitochondria were slightly elongated (Figures 5B and 5C) and cristae tighter (Figures 5D and 5E), without any difference in mtDNA levels (Figure 5F) and translation (Figures 5G and 5H). Importantly, in *Opa1^{tg}* MAFs, RCS assembly (Figures 5I and 5J) and glutamate-supported RCR (Figure 5K) were increased. In vivo, an ~50% increase in liver mitochondria OPA1 levels (Figure S5A) was similarly associated to tighter cristae (Figure S5B) and increased RCS levels (Figure S5C). Taken together, these results indicate that RCS assembly is facilitated by increased OPA1 levels and tighter cristae.

Mitochondria-Supported Cell Growth Is Controlled by Cristae Shape

We next wished to address if cristae shape affects mitochondrial-dependent cell growth. We therefore measured the growth of DKO cells (resistant to BID-induced outer membrane permeabilization, caspase-dependent mitochondrial damage, and apoptosis) in galactose media, where most of cellular ATP comes from the respiratory chain (Acín-Pérez et al., 2004). WT and G94E tBID impaired growth in galactose, whereas cells transduced with tBID^{KKAA} that does not cause cristae remodeling did not display any defect (Figure 6A).

We next turned to genetic models of cristae shape changes. Growth in galactose-containing media was impaired upon acute ablation of *Opa1* in MAFs, whereas it was normal for fusion-deficient *Mfn1^{-/-}*, *Mfn2^{-/-}* MEFs (Figures 6B and 6C), where mitochondrial fusion is also inhibited. In *Mfn1^{-/-}*, *Mfn2^{-/-}* MEFs, mtDNA copy number was reduced (Figure S6A), but cristae shape (Figures S6B and S6C), mtDNA translation (Figure S6D), RCS stability (Figure S6E), and assembly (Figure S6F) were not affected. Thus, the galactose growth defect is not the consequence of impaired fusion but correlates with altered cristae shape and RCS. Finally, *Opa1^{tg}* MAFs grew faster than their WT counterparts in galactose media (Figure 6D), further confirming the link between cristae shape, RCS levels, and mitochondria-dependent cellular growth. In conclusion, cristae shape correlates with the efficiency of mitochondria-dependent cell growth.

DISCUSSION

Respiratory chain supercomplexes have been considered BNGE artifacts until direct respirometric experiments on purified RCS

identified them as the functional mitochondrial respiratory units (Acín-Pérez et al., 2008). Since then, RCS have been directly visualized in intact cristae by electron tomography (Davies et al., 2011), complex IV assembly factors that favor RCS formation have been identified (Chen et al., 2012; Vukotic et al., 2012; Strogolova et al., 2012; Lapuente-Brun et al., 2013), and the role of RCS in mitochondrial utilization of reducing equivalents has been demonstrated (Lapuente-Brun et al., 2013). However, the relationship between cristae shape and RCS, as well as between RCS and mitochondrial function, remained obscure. Our results demonstrate that cristae shape regulates respiratory chain supercomplexes stability and assembly, impacting on respiratory efficiency and respiratory cell growth.

To dissect the role of cristae shape in RCS structure and function, we genetically ablated the master cristae shape regulator OPA1. Individual respiratory chain units associate with OPA1 (Zanna et al., 2008), and mitochondrial metabolism is deranged in dominant optic atrophy caused by *OPA1* mutations (Lodi et al., 2004). However, the defect in ATP production in *OPA1* haploinsufficient cells was unexplained: OPA1 is not essential for assembly of respiratory chain complexes and mtDNA levels as well as activities of individual respiratory chain complexes are normal in dominant optic atrophy (Zanna et al., 2008). Conversely, the reduction in mtDNA copy number has been invoked to explain the mitochondrial dysfunction of fusion-deficient cells from *Mfn1*, *Mfn2*-deficient mice (Chen et al., 2010). Our results challenge this hypothesis: upon acute *Opa1* ablation, mtDNA levels are normal, whereas cristae shape, RCS, complex-I-dependent respiration, and respiratory growth are impaired. Conversely, in *Mfn1^{-/-}*, *Mfn2^{-/-}* cells, mtDNA copy number is reduced, but cristae shape, RCS, and respiratory growth are normal. Thus, RCS disorganization shall be regarded as a key mechanism of mitochondrial dysfunction accompanying altered organelle morphology.

The role of OPA1 and cristae shape in RCS organization is further supported by mouse models of *Opa1* conditional ablation and mild overexpression. The first tool allowed us to dissociate cristae biogenesis from mtDNA maintenance: whereas chronic *Opa1* depletion reduces mtDNA copy number and translation, upon acute *Opa1* ablation, mtDNA levels are normal, but cristae are disorganized, impacting on RCS assembly and respiratory function and growth. Thus, mtDNA reduction appears to be a consequence of chronic fusion inhibition in *Opa1^{-/-}* (and double *Mfn^{-/-}*) cells. We can therefore predict that the *Opa1^{fix/fix}* cells will be useful to elucidate how prolonged inhibition of mitochondrial fusion results in mtDNA levels reduction. *Opa1* mild overexpression lends further support to the model linking RCS organization to cristae shape: RCS assembly and respiratory function and growth are increased in *Opa1^{tg}* cells without any measurable change in mtDNA levels and translation. The *Opa1^{tg}* mouse will be instrumental to investigate the role of *Opa1* and cristae shape in vivo.

Apoptotic cristae remodeling further supports the relationship between cristae shape and RCS. The role and mechanisms of cristae remodeling in apoptosis are controversial (Scorrano et al., 2002; Germain et al., 2005; Frezza et al., 2006; Yamaguchi et al., 2008; Merkwirth et al., 2008; Costa et al., 2010). Despite that OPA1-mediated stabilization of cristae shape inhibits

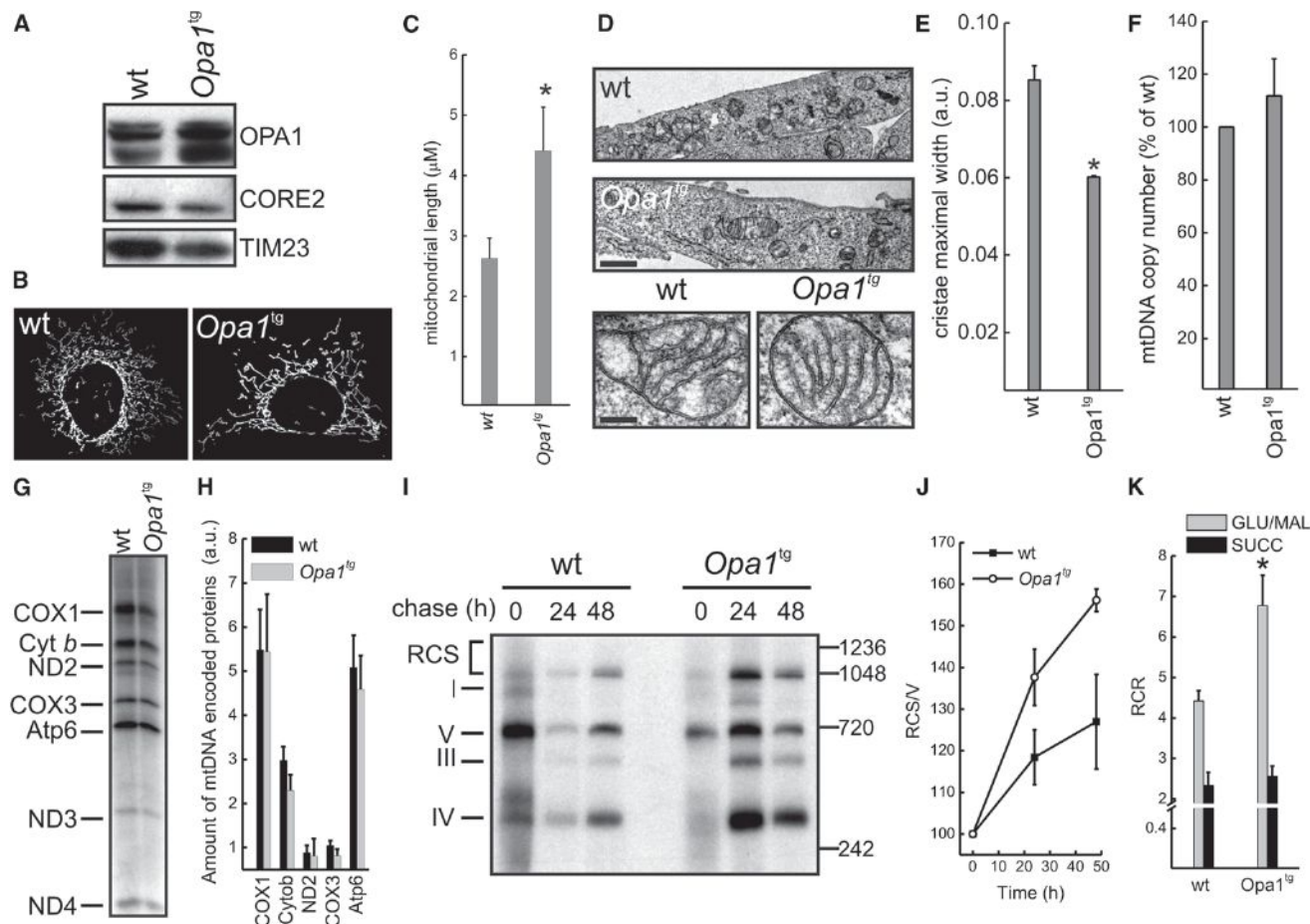


Figure 5. Transgenic Overexpression of OPA1 Increases RCS Assembly

(A) Equal amounts of proteins (20 μ g) from MAFs of the indicated genotypes were separated by SDS-PAGE and immunoblotted with the indicated antibodies. (B) Representative confocal micrographs of mitochondrial morphology in WT and *Opa1^{tg}* MAFs. Mitochondria were visualized by anti-TOM20 immunostaining. The scale bar represents 20 μ m.

(C) Average mitochondrial major axis length. Experiments were as in (B). Data represent average \pm SEM of four independent experiments (five mitochondria per cell, at least 50 cells/experiment). The asterisk denotes $p < 0.05$ in a paired sample Student's *t* test versus WT.

(D) Electron micrographs of MAFs of the indicated genotype. The scale bars represent 2 μ m (top) and 200 nm (bottom).

(E) Morphometric analysis of cristae width in 40 randomly selected mitochondria of MAFs of the indicated genotype. Data represent average \pm SEM of three independent experiments. The asterisk denotes $p < 0.05$ in a paired sample Student's *t* test versus WT.

(F) Mitochondrial DNA copy number quantification. mtDNA was amplified by RT-PCR from total DNA of MAFs of the indicated genotype. Data are normalized to WT MAFs and represent the average \pm SEM of four independent experiments.

(G) mtDNA translation assay. MAFs of the indicated genotype were metabolic labeled in presence of emetine and lysed after 30 min. Protein samples (40 μ g) were separated by SDS-PAGE, and the radioactivity was detected in the fixed and dried gels for 3 days. The mtDNA-encoded proteins are indicated.

(H) Densitometric analysis of the mtDNA-encoded proteins. Experiments are as in (G). Data represent average \pm SEM of four independent experiments.

(I) RCS assembly assay. MAFs of the indicated genotype were metabolically labeled for 2 hr and then chased for the indicated times. Equal amounts of protein (100 μ g) were separated by BN PAGE, and radioactivity was detected in the fixed and dried gels for 1 week. Individual complexes and supercomplexes of the respiratory chain are indicated.

(J) Densitometric analysis of the incorporation rate of radioactivity into RCS. Values are normalized for the autoradiographic signal of complex V. Data represent average \pm SEM of three independent experiments performed as in (H).

(K) RCR of mitochondria isolated from livers of mice of the indicated genotype energized with 5 mM/2.5 mM GLU/MAL or 10 mM SUCC. Data represent mean \pm SEM of four independent experiments. The asterisk denotes $p < 0.05$ in a paired sample Student's *t* test versus WT.

See also Figure S5.

intrinsic apoptosis (Frezza et al., 2006; Yamaguchi et al., 2008; Costa et al., 2010), cristae remodeling has been reckoned as a mere feedback mechanism in situ, occurring after caspase activation (Sun et al., 2007). Our results suggest that, in addition to

its role in cytochrome *c* release, cristae remodeling also impairs mitochondrial function to precipitate apoptosis. The BID α 6 mutant generated here, which does not induce cristae changes and cytochrome *c* mobilization but permeabilizes the outer

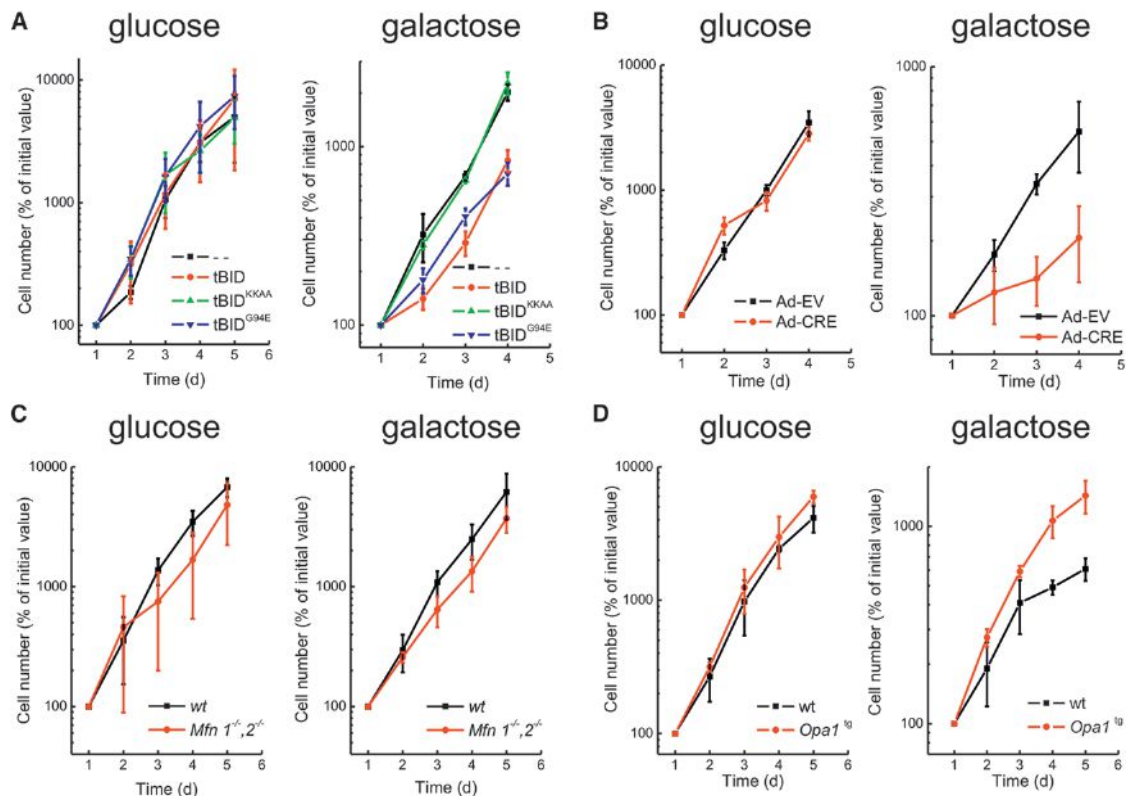


Figure 6. Mitochondria-Dependent Cellular Growth Requires Assembled RCS

(A) Growth curves of DKO MEFs transduced with the indicated retroviruses and grown in DMEM supplemented with the indicated monosaccharides. Data represent mean \pm SEM of five independent experiments.

(B–D) Growth curves of the indicated cell lines cultured in DMEM supplemented with the indicated monosaccharides. Data represent mean \pm SEM of five independent experiments.

See also Figure S6.

membrane, can be a useful tool to dissect in vivo the involvement of cristae remodeling in developmental and homeostatic apoptosis. We think that cristae remodeling influences RCS by targeting OPA1 (Frezza et al., 2006), not by altering membrane potential that is normal during cristae remodeling (Scorrano et al., 2002) or by inhibiting mtDNA translation and insertion of mtDNA-encoded subunits that similarly appear normal in DKO cell-expressing BID (data not shown).

Our work unravels a role for cristae shape in RCS assembly and stability, mitochondrial respiratory efficiency, and respiratory growth, suggesting that shape of biological membranes can influence membrane protein complexes. Moreover, our data highlight the importance of RCS in respiration by complex I-feeding substrates. Finally, we unveil how OPA1 regulates mitochondrial respiratory efficiency. The pathogenesis of dominant optic atrophy where OPA1 is mutated (Alexander et al., 2000) or of other mitochondrial diseases where OPA1 is degraded (Duvezin-Caubet et al., 2006) could also depend on this unexpected OPA1 function. In these latter settings, stabilization of OPA1 could correct RCS and therefore mitochondrial dysfunction, opening novel therapeutic perspectives for currently intractable diseases.

EXPERIMENTAL PROCEDURES

Generation of *Opa1^{flx/flx}* and *Opa1^{tg}* Mice

To generate *Opa1^{flx/flx}* mice, a mouse Bac clone containing the *Opa1* gene was isolated from the C57BL/6J ES BAC clone library. An 11 kb HpaI DNA restriction fragment containing the 5 kb upstream-exon3 was subcloned in a pUC-8 vector. The OPA1 fragment was excised with EcoRV and XmaI to generate blunt ends and inserted into a pKO4.4a-LoxP cut with XhoI and Sall. A LoXP site was introduced between intron1 and exon2 of *Opa1* and a phosphoglycerate kinase (PGK) promoter-driven neomycin resistance gene, flanked by two FRT sequences and with one LoXP sequence downstream, was inserted in intron3. The targeting vector was linearized and electroporated into C57BL6 embryonic stem cells (ESCs). Neomycin-resistant ESC clones were tested for homologous recombination. Three mutated ESC lines were microinjected into C57BL6 blastocysts and implanted in host mice to obtain chimeric mice, which were then bred with C57BL6 mates and their offspring tested by PCR for germline transmission. Colonies were established in a C57BL6 background.

To generate *Opa1^{tg}* mice, the human β -actin promoter was extracted from pDRIVE-h β -ACTIN (InvivoGen) using SspI and NcoI and cloned in pENTRY. The complementary DNA of mouse isoform 1 *Opa1* and polyA extracted from pcDNA3.1-OPA1 (Cipolat et al., 2004) using NheI and EcoI was ligated into pENTRY using Quick Ligase (Ozyme). The transgene was then inserted by homologous recombination in a pDEST vector containing part of the human hypoxanthine phosphoribosyltransferase locus. The resulting vector was

linearized using PvuI and electroporated into C57BL6 BPES cells by Nucleis (France). Homologous recombinants were selected on stringent hypoxanthine aminopterin-thymidine-supplemented medium. Three positive ESC recombinant clones were microinjected into C57BL6 blastocysts and implanted into host pseudopregnant female C57BL6 to obtain chimeric mice. Six chimeras (identified by fur agouti color) were bred with C57BL6 mates, and germline transmission was verified by fur color and PCR. Colonies were established in a C57BL6 and in a Sv129 background by crossbreeding. Details on mouse genotyping and handling can be found in the Extended Experimental Procedures.

BNGE, 2D BN/BNGE, and 2D BN/SDS PAGE

Mitochondria (10 mg/ml) were suspended in buffer D (1 M 6-aminohexanoic acid, 1.25% V/V digitonin, 50 mM Bis-Tris-HCl, pH 7) and centrifuged. The supernatant was collected, and 5% Serva Blue G dye in 1 M 6-aminohexanoic acid was added to 1/3 of the final sample volume. Equal amounts (100 μ g) of mitochondrial proteins were separated by 3%–13% gradient BNGE (Schägger, 1995). For RCS detection, the concentration of digitonin in buffer D was 4% (V/V).

For two-dimensional (2D) Blue Native (BN)/BNGE, the lane cut from the first-dimension BNGE was casted on top of a native 3%–14% gradient gel in 1% (V/V) dodecyl maltoside. For 2D BN/SDS PAGE, the lane cut from the first-dimension BNGE was incubated for 1 hr at 25°C in 1% SDS and 1% β -mercaptoethanol and then casted on top of an 8% or a 16.5% denaturing gel. After electrophoresis, the complexes were electroblotted on a polyvinylidene fluoride (PVDF) membrane and probed with the indicated antibodies.

To detect RCS from radiolabelled cells, samples were treated as described above, and after electrophoresis, the gels were dried and the signal was detected following exposure for 3–6 days.

Pulse-Chase Experiments

Labeling of mtDNA-encoded proteins was performed with [³⁵S]-methionine and cysteine (EXPRE³⁵S³⁵S Protein Labeling Mix, Perkin Elmer Life Sciences). Cells were preincubated for 12 hr in the presence of 40 μ g/ml chloramphenicol in uridine-supplemented medium and then exposed for 2 hr to the [³⁵S] protein labeling mix (pulse) in the presence of 50 μ g/ml cycloheximide. Cells were washed for four times with PBS and cold Dulbecco's modified Eagle's medium (DMEM) and then cultured for the indicated time (chase) prior to lysis and protein separation by BNGE.

To assay basal mtDNA translation, equal protein amounts (40 μ g) from cells metabolically labeled as described above treated for 30 min with 50 μ g/ml emetine were separated by SDS-PAGE.

Mitochondrial Assays

Mitochondria from liver of mice and from the indicated cell lines were isolated as in Frezza et al. (2007). Cytochrome c release, ascorbate/TMPD-driven respiration and cytochrome b₅-dependent NADH oxidation were determined as described (Scorrano et al., 2002). Details can be found in the Extended Experimental Procedures.

Biochemistry

For protein crosslinking, mitochondria treated as indicated were incubated with 1 mM 1-ethyl-3-[3-dimethylaminopropyl]carbodiimide hydrochloride (EDC) or 1 mM bismaleimidohexane (BMH), as previously described (Frezza et al., 2006). Carbonate extraction was performed as previously described (Dimmer et al., 2008). Details and procedures for SDS-PAGE and immunoblotting can be found in the Extended Experimental Procedures.

Molecular Biology

The retroviral vector pMIG-tBid was described previously (Cheng et al., 2001). KKAA, G94E, and G94EKAA mutants were generated by site-direct mutagenesis using KOD polymerase (Biolabs). Details can be found in the Extended Experimental Procedures.

To measure mtDNA copy number, total cellular DNA was amplified using specific oligodeoxynucleotides for *mt-Co2* and *Sdha* by real-time PCR. Details can be found in the Extended Experimental Procedures.

Cell Biology

MEFs and human embryonic kidney 293 cells (HEK293) cells were cultured as described (Gomes et al., 2011). When indicated, in DMEM, glucose was substituted with 0.9 mg/ml galactose. Ecotropic viruses were generated as described (Cheng et al., 2001). WT, *Opa1^{flx/flx}*, *Opa1^{tg}*, and MAFs SV40 transduced cell lines were generated from the diaphragm of the respective 7-week-old mouse killed by cervical dislocation. Details on the procedure can be found in the Extended Experimental Procedures. Acute *Opa1* ablation in *Opa1^{flx/flx}* MAFs was obtained by infection with adenoviruses expressing cytomegalovirus (CMV)-Cre-GFP (ad-CRE; 300 pfu/cell; Vector Biolabs). CMV-GFP (ad-EV)-expressing adenoviruses were used as control.

Cell growth was determined by counting viable cells for the indicated time. *Opa1^{flx/flx}* MAFs were infected and DKO MEFs were transduced 24 or 16 hr before the growth was assessed.

Apoptosis was measured by flow cytometric detection (FACSCalibur) of the Annexin-V-PE positive events in the GFP-positive population. Details can be found in the Extended Experimental Procedures.

Imaging and Transmission Electron Microscopy

For mitochondrial imaging, cells stained with a rabbit polyclonal anti-TOM20 (Santa Cruz; 1:200), as previously described (Frezza et al., 2006), were analyzed by confocal microscopy. Adenovirus-infected cells were identified by GFP expression. Electron microscopy (EM) was performed as described (Scorrano et al., 2002). Details can be found in the Extended Experimental Procedures.

SUPPLEMENTAL INFORMATION

Supplemental Information includes Extended Experimental Procedures and six figures and can be found with this article online at <http://dx.doi.org/10.1016/j.cell.2013.08.032>.

ACKNOWLEDGMENTS

We thank A. Gross (Weizmann Institute) for anti-BID antibody, A. Latorre-Pellicer (CNIC) for mtDNA RT-PCR, and M. Albiero (VIMM) for tail vein injections. L.S. is a senior scientist of the Dulbecco-Telethon Institute. This work is supported by Telethon Italy (GGP12162, GPP10005B, and TCR02016), AIRC Italy, MOH Italy (GR 09.021), and Swiss National Foundation (31-118171). J.A.E. is supported by MINECO (SAF2012-32776 and CSD2007-00020), DGA (B55, PIPAMER O905), and CAM (S2011/BMD-2402). S.C. was supported by a Journal of Cell Science Travelling Fellowship. C.F. was supported by an AIRC Biennial Fellowship. The CNIC is funded by the Instituto de Salud Carlos III-MICIINN and the Pro-CNIC Foundation.

Received: December 28, 2012

Revised: July 25, 2013

Accepted: August 19, 2013

Published: September 19, 2013

REFERENCES

- Acín-Pérez, R., Bayona-Bafaluy, M.P., Fernández-Silva, P., Moreno-Loshuertos, R., Pérez-Martos, A., Bruno, C., Moraes, C.T., and Enriquez, J.A. (2004). Respiratory complex III is required to maintain complex I in mammalian mitochondria. *Mol. Cell* 13, 805–815.
- Acín-Pérez, R., Fernández-Silva, P., Peleato, M.L., Pérez-Martos, A., and Enriquez, J.A. (2008). Respiratory active mitochondrial supercomplexes. *Mol. Cell* 32, 529–539.
- Alexander, C., Votruba, M., Pesch, U.E., Thiselton, D.L., Mayer, S., Moore, A., Rodriguez, M., Kellner, U., Leo-Kottler, B., Auburger, G., et al. (2000). OPA1, encoding a dynamin-related GTPase, is mutated in autosomal dominant optic atrophy linked to chromosome 3q28. *Nat. Genet.* 26, 211–215.
- Campanella, M., Casswell, E., Chong, S., Farah, Z., Wieckowski, M.R., Abramov, A.Y., Tinker, A., and Duchon, M.R. (2008). Regulation of mitochondrial

- structure and function by the F1Fo-ATPase inhibitor protein, IF1. *Cell Metab.* **8**, 13–25.
- Cereghetti, G.M., Stangherlin, A., Martins de Brito, O., Chang, C.R., Blackstone, C., Bernardi, P., and Scorrano, L. (2008). Dephosphorylation by calcineurin regulates translocation of Drp1 to mitochondria. *Proc. Natl. Acad. Sci. USA* **105**, 15803–15808.
- Chen, H., Detmer, S.A., Ewald, A.J., Griffin, E.E., Fraser, S.E., and Chan, D.C. (2003). Mitofusins Mfn1 and Mfn2 coordinately regulate mitochondrial fusion and are essential for embryonic development. *J. Cell Biol.* **160**, 189–200.
- Chen, H., Vermulst, M., Wang, Y.E., Chomyn, A., Prolla, T.A., McCaffery, J.M., and Chan, D.C. (2010). Mitochondrial fusion is required for mtDNA stability in skeletal muscle and tolerance of mtDNA mutations. *Cell* **141**, 280–289.
- Chen, Y.C., Taylor, E.B., Dephoure, N., Heo, J.M., Tonhato, A., Papandreou, I., Nath, N., Denko, N.C., Gygi, S.P., and Rutter, J. (2012). Identification of a protein mediating respiratory supercomplex stability. *Cell Metab.* **15**, 348–360.
- Cheng, E.H., Wei, M.C., Weiler, S., Flavell, R.A., Mak, T.W., Lindsten, T., and Korsmeyer, S.J. (2001). BCL-2, BCL-X(L) sequester BH3 domain-only molecules preventing BAX- and BAK-mediated mitochondrial apoptosis. *Mol. Cell* **8**, 705–711.
- Cipolat, S., Martins de Brito, O., Dal Zilio, B., and Scorrano, L. (2004). OPA1 requires mitofusin 1 to promote mitochondrial fusion. *Proc. Natl. Acad. Sci. USA* **101**, 15927–15932.
- Cipolat, S., Rudka, T., Hartmann, D., Costa, V., Serneels, L., Craessaerts, K., Metzger, K., Frezza, C., Annaert, W., D'Adamo, L., et al. (2006). Mitochondrial rhomboid PARL regulates cytochrome c release during apoptosis via OPA1-dependent cristae remodeling. *Cell* **126**, 163–175.
- Costa, V., Giacomello, M., Hudec, R., Lopreiato, R., Ermak, G., Lim, D., Malorni, W., Davies, K.J., Carafoli, E., and Scorrano, L. (2010). Mitochondrial fission and cristae disruption increase the response of cell models of Huntington's disease to apoptotic stimuli. *EMBO Mol Med* **2**, 490–503.
- Danial, N.N., and Korsmeyer, S.J. (2004). Cell death: critical control points. *Cell* **116**, 205–219.
- Davies, K.M., Strauss, M., Daum, B., Kief, J.H., Osiewacz, H.D., Rycovska, A., Zickermann, V., and Kühlbrandt, W. (2011). Macromolecular organization of ATP synthase and complex I in whole mitochondria. *Proc. Natl. Acad. Sci. USA* **108**, 14121–14126.
- de Brito, O.M., and Scorrano, L. (2008). Mitofusin 2 tethers endoplasmic reticulum to mitochondria. *Nature* **456**, 605–610.
- Dimmer, K.S., and Scorrano, L. (2006). (De)constructing mitochondria: what for? *Physiology (Bethesda)* **21**, 233–241.
- Duvezin-Caubet, S., Jagasia, R., Wagoner, J., Hofmann, S., Trifunovic, A., Hansson, A., Chomyn, A., Bauer, M.F., Attardi, G., Larsson, N.G., et al. (2006). Proteolytic processing of OPA1 links mitochondrial dysfunction to alterations in mitochondrial morphology. *J. Biol. Chem.* **281**, 37972–37979.
- Frey, T.G., and Mannella, C.A. (2000). The internal structure of mitochondria. *Trends Biochem. Sci.* **25**, 319–324.
- Frezza, C., Cipolat, S., Martins de Brito, O., Micaroni, M., Beznoussenko, G.V., Rudka, T., Bartoli, D., Polishuck, R.S., Danial, N.N., De Strooper, B., and Scorrano, L. (2006). OPA1 controls apoptotic cristae remodeling independently from mitochondrial fusion. *Cell* **126**, 177–189.
- Germain, M., Mathai, J.P., McBride, H.M., and Shore, G.C. (2005). Endoplasmic reticulum BIK initiates DRP1-regulated remodeling of mitochondrial cristae during apoptosis. *EMBO J.* **24**, 1546–1556.
- Gomes, L.C., Di Benedetto, G., and Scorrano, L. (2011). During autophagy mitochondria elongate, are spared from degradation and sustain cell viability. *Nat. Cell Biol.* **13**, 589–598.
- Green, D.R., and Kroemer, G. (2004). The pathophysiology of mitochondrial cell death. *Science* **305**, 626–629.
- Griparic, L., and van der Bliek, A.M. (2001). The many shapes of mitochondrial membranes. *Traffic* **2**, 235–244.
- Hackenbrock, C.R. (1966). Ultrastructural bases for metabolically linked mechanical activity in mitochondria. I. Reversible ultrastructural changes with change in metabolic steady state in isolated liver mitochondria. *J. Cell Biol.* **30**, 269–297.
- Landes, T., Emorine, L.J., Courilleau, D., Rojo, M., Belenguer, P., and Arnauné-Pelloquin, L. (2010). The BH3-only Bnip3 binds to the dynamin Opa1 to promote mitochondrial fragmentation and apoptosis by distinct mechanisms. *EMBO Rep.* **11**, 459–465.
- Lapuente-Brun, E., Moreno-Loshuertos, R., Acín-Pérez, R., Latorre-Pellicer, A., Colás, C., Balsa, E., Perales-Clemente, E., Quirós, P.M., Calvo, E., Rodríguez-Hernández, M.A., et al. (2013). Supercomplex assembly determines electron flux in the mitochondrial electron transport chain. *Science* **340**, 1567–1570.
- Legros, F., Lombès, A., Frachon, P., and Rojo, M. (2002). Mitochondrial fusion in human cells is efficient, requires the inner membrane potential, and is mediated by mitofusins. *Mol. Biol. Cell* **13**, 4343–4354.
- Lodi, R., Tonon, C., Valentino, M.L., Iotti, S., Clementi, V., Malucelli, E., Barboni, P., Longanesi, L., Schimpf, S., Wissinger, B., et al. (2004). Deficit of in vivo mitochondrial ATP production in OPA1-related dominant optic atrophy. *Ann. Neurol.* **56**, 719–723.
- Merkwirth, C., Dargazanli, S., Tatsuta, T., Geimer, S., Löwer, B., Wunderlich, F.T., von Kleist-Retzow, J.C., Waisman, A., Westermann, B., and Langer, T. (2008). Prohibitins control cell proliferation and apoptosis by regulating OPA1-dependent cristae morphogenesis in mitochondria. *Genes Dev.* **22**, 476–488.
- Minauro-Sanmiguel, F., Wilkens, S., and García, J.J. (2005). Structure of dimeric mitochondrial ATP synthase: novel F0 bridging features and the structural basis of mitochondrial cristae biogenesis. *Proc. Natl. Acad. Sci. USA* **102**, 12356–12358.
- Paumard, P., Vaillier, J., Couly, B., Schaeffer, J., Soubannier, V., Mueller, D.M., Brèthes, D., di Rago, J.P., and Velours, J. (2002). The ATP synthase is involved in generating mitochondrial cristae morphology. *EMBO J.* **21**, 221–230.
- Pfeiffer, D.R., Guduz, T.I., Novgorodov, S.A., and Erdahl, W.L. (1995). The peptide mastoparan is a potent facilitator of the mitochondrial permeability transition. *J. Biol. Chem.* **270**, 4923–4932.
- Santel, A., and Fuller, M.T. (2001). Control of mitochondrial morphology by a human mitofusin. *J. Cell Sci.* **114**, 867–874.
- Santel, A., Frank, S., Gaume, B., Herrler, M., Youle, R.J., and Fuller, M.T. (2003). Mitofusin-1 protein is a generally expressed mediator of mitochondrial fusion in mammalian cells. *J. Cell Sci.* **116**, 2763–2774.
- Schägger, H. (1995). Native electrophoresis for isolation of mitochondrial oxidative phosphorylation protein complexes. *Methods Enzymol.* **260**, 190–202.
- Scorrano, L., Ashiya, M., Buttle, K., Weiler, S., Oakes, S.A., Mannella, C.A., and Korsmeyer, S.J. (2002). A distinct pathway remodels mitochondrial cristae and mobilizes cytochrome c during apoptosis. *Dev. Cell* **2**, 55–67.
- Smirnova, E., Griparic, L., Shurland, D.L., and van der Bliek, A.M. (2001). Dynamin-related protein Drp1 is required for mitochondrial division in mammalian cells. *Mol. Biol. Cell* **12**, 2245–2256.
- Strauss, M., Hofhaus, G., Schröder, R.R., and Kühlbrandt, W. (2008). Dimeric ribbons of ATP synthase shape the inner mitochondrial membrane. *EMBO J.* **27**, 1154–1160.
- Strogolova, V., Furness, A., Robb-McGrath, M., Garlich, J., and Stuart, R.A. (2012). Rcf1 and Rcf2, members of the hypoxia-induced gene 1 protein family, are critical components of the mitochondrial cytochrome bc1-cytochrome c oxidase supercomplex. *Mol. Cell Biol.* **32**, 1363–1373.
- Sun, M.G., Williams, J., Munoz-Pinedo, C., Perkins, G.A., Brown, J.M., Ellisman, M.H., Green, D.R., and Frey, T.G. (2007). Correlated three-dimensional light and electron microscopy reveals transformation of mitochondria during apoptosis. *Nat. Cell Biol.* **9**, 1057–1065.
- Vogel, F., Bornhövd, C., Neupert, W., and Reichert, A.S. (2006). Dynamic subcompartmentalization of the mitochondrial inner membrane. *J. Cell Biol.* **175**, 237–247.

- Vukotic, M., Oeljeklaus, S., Wiese, S., Vögtle, F.N., Meisinger, C., Meyer, H.E., Zieseniss, A., Katschinski, D.M., Jans, D.C., Jakobs, S., et al. (2012). Rcf1 mediates cytochrome oxidase assembly and respirasome formation, revealing heterogeneity of the enzyme complex. *Cell Metab.* *15*, 336–347.
- Wei, M.C., Lindsten, T., Mootha, V.K., Weiler, S., Gross, A., Ashiya, M., Thompson, C.B., and Korsmeyer, S.J. (2000). tBID, a membrane-targeted death ligand, oligomerizes BAK to release cytochrome c. *Genes Dev.* *14*, 2060–2071.
- Wei, M.C., Zong, W.X., Cheng, E.H., Lindsten, T., Panoutsakopoulou, V., Ross, A.J., Roth, K.A., MacGregor, G.R., Thompson, C.B., and Korsmeyer, S.J. (2001). Proapoptotic BAX and BAK: a requisite gateway to mitochondrial dysfunction and death. *Science* *292*, 727–730.
- Yamaguchi, R., Lartigue, L., Perkins, G., Scott, R.T., Dixit, A., Kushnareva, Y., Kuwana, T., Ellisman, M.H., and Newmeyer, D.D. (2008). Opa1-mediated cristae opening is Bax/Bak and BH3 dependent, required for apoptosis, and independent of Bak oligomerization. *Mol. Cell* *31*, 557–569.
- Yoon, Y., Pitts, K.R., and McNiven, M.A. (2001). Mammalian dynamin-like protein DLP1 tubulates membranes. *Mol. Biol. Cell* *12*, 2894–2905.
- Zanna, C., Ghelli, A., Porcelli, A.M., Karbowski, M., Youle, R.J., Schimpf, S., Wissinger, B., Pinti, M., Cossarizza, A., Vidoni, S., et al. (2008). OPA1 mutations associated with dominant optic atrophy impair oxidative phosphorylation and mitochondrial fusion. *Brain* *131*, 352–367.

The Mitochondrial Chaperone TRAP1 Promotes Neoplastic Growth by Inhibiting Succinate Dehydrogenase

Marco Sciacovelli,^{1,8} Giulia Guzzo,^{1,8} Virginia Morello,³ Christian Frezza,⁴ Liang Zheng,^{4,5} Nazarena Nannini,² Fiorella Calabrese,² Gabriella Laudiero,⁶ Franca Esposito,⁶ Matteo Landriscina,⁷ Paola Defilippi,³ Paolo Bernardi,^{1,*} and Andrea Rasola^{1,*}

¹CNR Institute of Neuroscience, Department of Biomedical Sciences and Venetian Institute of Molecular Medicine

²Department of Cardiac, Thoracic and Vascular Sciences
University of Padova, 35121 Padova, Italy

³Molecular Biotechnology Centre, Department of Genetics, Biology and Biochemistry, University of Torino, 10125 Torino, Italy

⁴Cancer Research United Kingdom, The Beatson Institute for Cancer Research, Glasgow G61 1BD, UK

⁵Strathclyde Institute of Pharmacy and Biomedical Sciences, University of Strathclyde, Glasgow G61 1BD, UK

⁶Department of Molecular Medicine and Medical Biotechnologies, University of Napoli Federico II, 80131 Napoli, Italy

⁷Department of Medical and Surgical Sciences, University of Foggia, 71100 Foggia, Italy

⁸These authors contributed equally to this work

*Correspondence: bernardi@bio.unipd.it (P.B.), rasola@bio.unipd.it (A.R.)

<http://dx.doi.org/10.1016/j.cmet.2013.04.019>

SUMMARY

We report that the mitochondrial chaperone TRAP1, which is induced in most tumor types, is required for neoplastic growth and confers transforming potential to noncancerous cells. TRAP1 binds to and inhibits succinate dehydrogenase (SDH), the complex II of the respiratory chain. The respiratory downregulation elicited by TRAP1 interaction with SDH promotes tumorigenesis by priming the succinate-dependent stabilization of the proneoplastic transcription factor HIF1 α independently of hypoxic conditions. These findings provide a mechanistic clue to explain the switch to aerobic glycolysis of tumors and identify TRAP1 as a promising antineoplastic target.

INTRODUCTION

Tumors undergo sustained growth in a dynamic environment where oxygen and nutrients are often scarce (Denko, 2008; Hanahan and Weinberg, 2011). To cope with the energetic requirements of rapid proliferation in these challenging conditions (Fritz and Fajas, 2010), tumor cells profoundly reorganize their core metabolism (Cairns et al., 2011; Levine and Puzio-Kuter, 2010). Glucose utilization, which provides ATP, essential anabolic intermediates, and antioxidative defenses (Hsu and Sabatini, 2008; Vander Heiden et al., 2009), is boosted and dissociated from oxygen availability (the Warburg effect; Warburg, 1956; Warburg et al., 1927). Key to the Warburg effect is the decrease of mitochondrial respiration (Frezza and Gottlieb, 2009), which allows cancer cells to grow in the hypoxic conditions found in the interior of the tumor mass (Hsu and Sabatini, 2008).

The molecular mechanisms that inhibit oxidative phosphorylation (OXPHOS) in tumors are understood only partially. The tran-

scription factor HIF1 (hypoxia-inducible factor 1) decreases the flux of pyruvate into the Krebs cycle and, hence, the flow of reducing equivalents needed to power the electron transport chain (ETC) and stimulates glycolysis by inducing glucose transporters and glycolytic enzymes (Denko, 2008; Semenza, 2010b). HIF is activated by hypoxia as well as by the accumulation of the Krebs cycle metabolites succinate and fumarate that inhibit the prolyl hydroxylases (PHDs) responsible for proteasomal degradation of the HIF1 α subunit (Selak et al., 2005). Succinate accumulation can originate from loss-of-function mutations in any of the genes encoding for succinate dehydrogenase (SDH) subunits (or their assembly factor SDHAF2), which cause hereditary paraganglioma-pheochromocytoma syndrome and are associated to a number of other neoplasms (Bardella et al., 2011).

Within this conceptual framework, we have analyzed the activity of TRAP1, an evolutionarily conserved chaperone of the Hsp90 family mainly located in the mitochondrial matrix and overexpressed in a variety of tumor cell types, where it exerts antiapoptotic functions through mechanisms that are only partially understood (Altieri et al., 2012; Kang et al., 2007). Our results indicate that TRAP1 supports tumor progression by downmodulating mitochondrial respiration through a decrease in the activity of SDH, which leads to HIF1 α stabilization even in the absence of hypoxic conditions, by increasing succinate levels.

RESULTS

Mitochondrial TRAP1 Promotes Neoplastic Transformation

We found that TRAP1 is localized in mitochondria of cancer cell models (Figures S1A and S1B available online), as expected (Altieri et al., 2012), and that downregulation of TRAP1 expression by RNAi abrogated any transforming potential. In fact, knockdown of TRAP1 expression made SAOS-2 osteosarcoma cells, HCT116 colon carcinoma cells, and HeLa cervix carcinoma cells (dubbed shTRAP1 cells; Figures S1C–S1E) unable

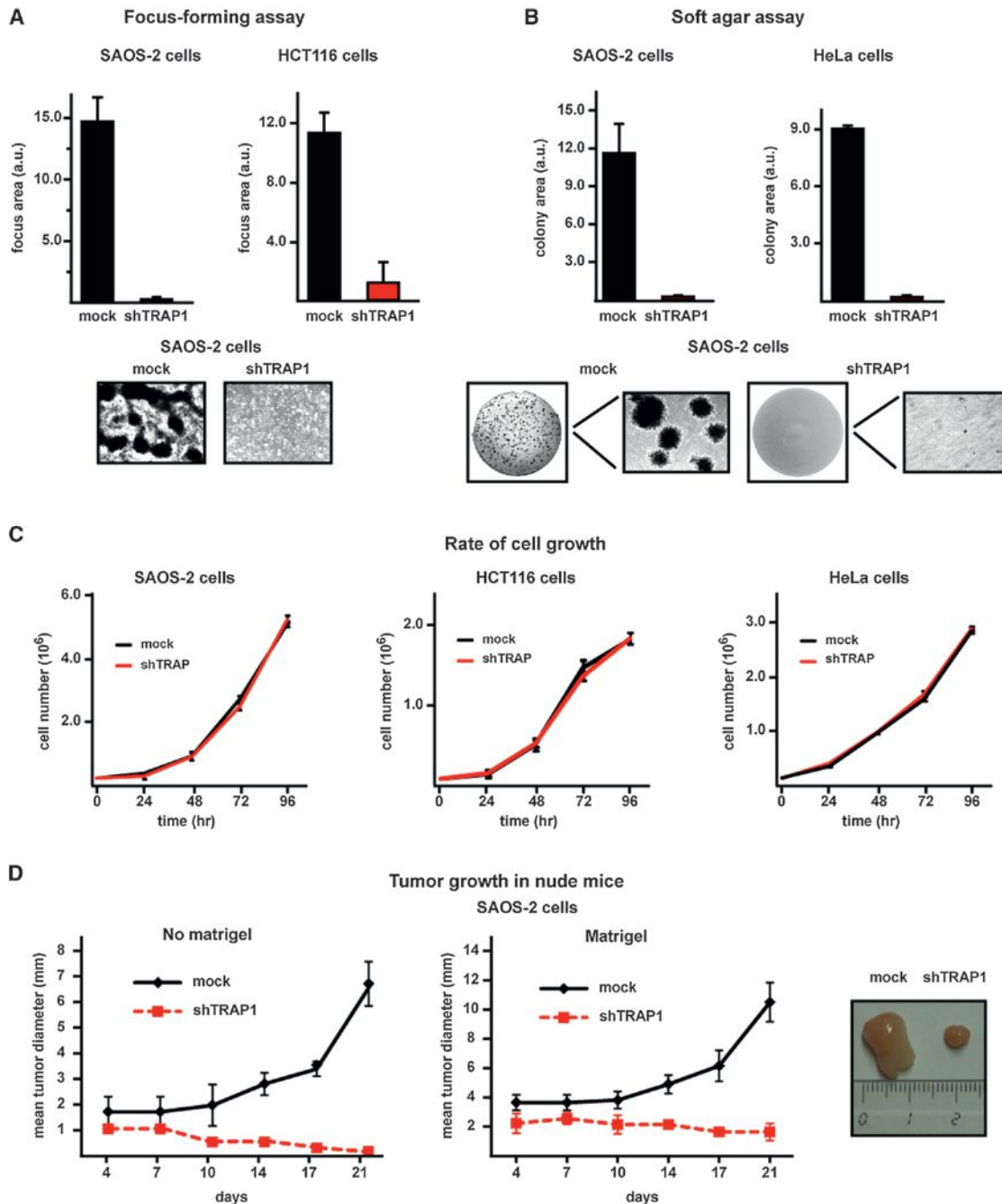


Figure 1. TRAP1 Knockdown Inhibits In Vitro and In Vivo Neoplastic Transformation

(A and B) Human osteosarcoma SAOS-2 cells, human colorectal carcinoma HCT116 cells, and human cervix carcinoma HeLa cells lose the capability to form foci (A) or colonies in soft agar (B) after knocking down TRAP1 expression. Cells stably transfected with a scrambled shRNA or with TRAP1 shRNAs are dubbed mock and shTRAP1, respectively. Data indicate the total focus or colony area at the 25th experimental day. Representative areas showing focus or colony growth are reported.

(C) Rate of growth of mock and shTRAP1 SAOS-2, HCT116, and HeLa cells.

(D) Kinetics of tumor growth in nude mice after injection of SAOS-2 cells without or with a Matrigel bolus (left and right, respectively); representative tumors grown with Matrigel are shown on the right. Data are reported as mean \pm SD values ($n \geq 3$).

to both form foci (Figure 1A) and grow in soft agar (Figure 1B) without affecting the rate of cell growth (Figure 1C). Notably, shTRAP1 tumor cells lost the ability to develop tumor masses when injected into nude mice (Figure 1D).

Conversely, when the TRAP1 complementary DNA (cDNA) was expressed in either RWPE-1 prostate epithelial cells or fibroblasts, these nontransformed cells acquired the capacity to form colonies in soft agar (Figures 2A and 2D), and downregulation of

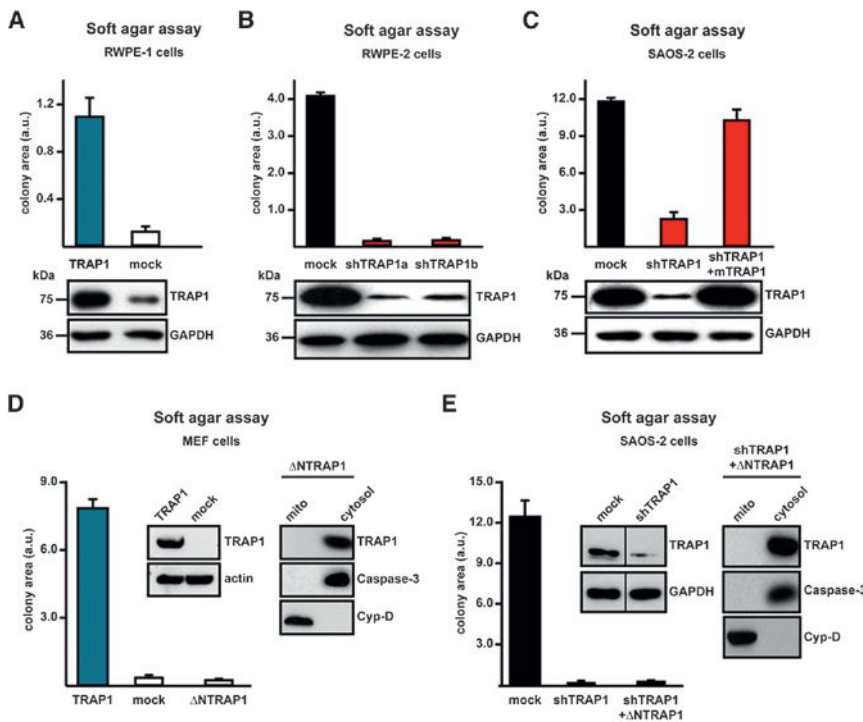


Figure 2. Mitochondrial TRAP1 Confers Transforming Potential to Cells

(A and B) Soft agar tumorigenesis assays were performed both in nontransformed cells (i.e., human epithelial prostate RWPE-1 cells (A) and MEFs (D)), stably transfected with either a TRAP1 cDNA or with a scrambled shRNA (mock); and in transformed cells, i.e., human epithelial prostate RWPE-2 cells obtained by *v*-Ki-Ras expression in RWPE-1 cells (B); cells dubbed shTRAP1a and shTRAP1b were transfected with different TRAP1 shRNAs.

(C) Expression of a mouse TRAP1 cDNA (mTRAP1) insensitive to human-directed shTRAP1 constructs reinstated the capability to form foci in human osteosarcoma SAOS-2 cells stably transfected with TRAP1 shRNAs (shTRAP1).

(D and E) Growth of colonies in soft agar was also assessed in MEF cells (D) or in SAOS-2 shTRAP1 cells (E) stably transfected with a TRAP1 construct lacking the mitochondrial import sequence (Δ NTRAP1). Western immunoblots show TRAP1 expression levels in the different cell types; GAPDH or actin are shown as loading controls. In (D) and (E), the cytosolic localization of Δ NTRAP1 was assessed by subcellular fractionation; caspase-3 and cyclophilin D (Cyp-D) are used to verify purity of cytosolic and mitochondrial fractions, respectively. Data are reported as mean \pm SD values ($n \geq 3$).

TRAP1 expression in RWPE-2 prostate cells, which are transformed by expression of *v*-Ki-Ras in RWPE-1 cells (Rasola et al., 2010a), abolished their tumorigenic features (Figure 2B). Moreover, stable transfection of a murine TRAP1 cDNA, which is insensitive to human-directed small hairpin RNA (shRNA) constructs, reinstated the tumorigenic capability of shTRAP1 cells (Figure 2C). Mitochondrial localization of TRAP1 was essential for its proneoplastic activity, as expression of a TRAP1 cDNA devoid of its mitochondrial targeting sequence was not tumorigenic in either cancer or nontransformed cells (Figures 2D and 2E).

TRAP1 Binds SDH and Inhibits its Succinate:Coenzyme Q Reductase Enzymatic Activity

We then asked whether TRAP1 promotes transformation by acting on mitochondrial metabolism, thus contributing to the Warburg phenotype. This could occur through an inhibitory effect on respiration. We used a blue native (BN)-PAGE approach (Figure 3A), which allows the separation and characterization of protein complexes under nondenaturing conditions (Wittig and Schägger, 2008), to investigate a possible interaction between TRAP1 and ETC complexes. By cutting BN-PAGE bands and running them on an SDS-PAGE, we could observe the association between TRAP1 and both complex IV (cytochrome oxidase, COX) and complex II (succinate dehydrogenase, SDH) (Figure 3A). Moreover, by performing an immunoblot directly on the BN-PAGE, we found TRAP1 to be in correspondence with both complex IV and complex II bands; notably, these bands were diffused, and TRAP1 colocalized with their upper portion, suggesting that TRAP1 contributes to form a multimeric complex of higher molecular weight than the ETC complex per se (Figure 3B). We confirmed the interaction between

TRAP1 and complex II/SDH through further approaches, including (1) immunoprecipitation, finding coimmunoprecipitation (coIP) of TRAP1 with SDH and vice versa (Figure 3C), and (2) mitochondrial protein crosslinking with dimethyl 3,3'-dithiobis-propionimidate (DTBP), a homobifunctional compound that reacts with the primary amines of two interacting proteins at an average distance of about 8 Å (Giorgio et al., 2009), followed by TRAP1 immunoprecipitation in order to determine whether TRAP1 and SDH are closely associated. We found that two TRAP1/SDH complexes are formed in mitochondria (Figure 3D).

We then measured whether TRAP1 affects complex II enzymatic activity. Complex II couples the Krebs cycle to OXPHOS by oxidizing succinate to fumarate and then transferring electrons to coenzyme Q; hence, the enzyme is called either SDH or succinate:coenzyme Q reductase (SQR; Cecchini, 2003; Lemarie and Grimm, 2011). SQR activity can be assessed spectrophotometrically in permeabilized mitochondria after inhibition of the other ETC complexes by recording the reduction of 2,6-dichlorophenolindophenol (DCPIP) in the presence of succinate as an electron donor and coenzyme Q1 as an intermediate electron acceptor. The slope of the absorbance decline of DCPIP is directly proportional to SQR activity (see Figure S2A). We found that SQR enzymatic activity was increased in mitochondria from shTRAP1 cells relative to those derived from control cells (Figures 4A, S2A, and S2B). TRAP1 did not affect either the cytochrome oxidase enzymatic activity of complex IV (Figure S2C) or complex II protein levels (Figure S2D) or mitochondrial mass (Figure S2E). Specificity of TRAP1 inhibition on SDH was assessed by (1) expression of the mouse TRAP1 (in shTRAP1 cells) that is insensitive to human-directed shTRAP1 constructs, which resulted in inhibition of SQR activity to values similar to those of mock cells (Figure 4A), and (2) using an inhibitor of

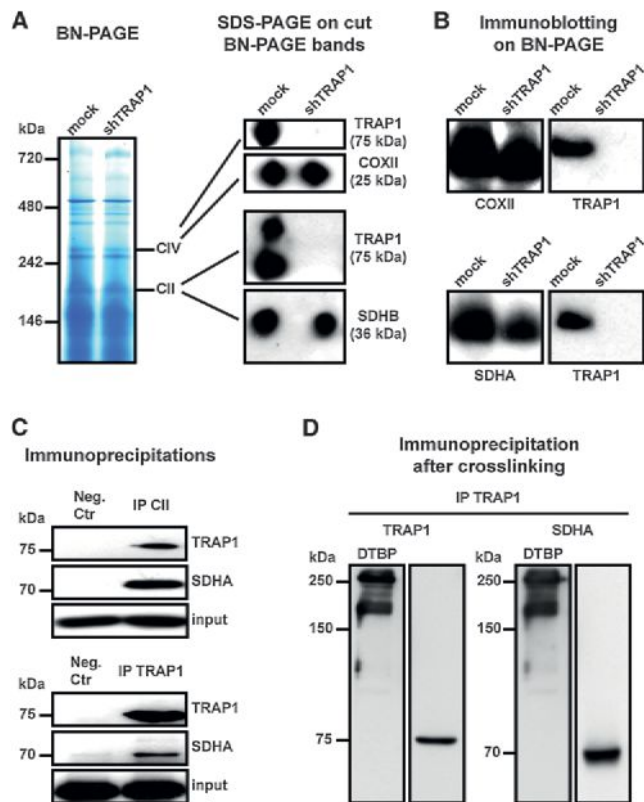


Figure 3. TRAP1 Binds to ETC Complexes IV and II

(A) Blue native gel electrophoresis. Bands corresponding to complex IV (cytochrome oxidase, COX) and complex II (succinate dehydrogenase, SDH) were cut, run on a SDS-PAGE, and probed with anti-TRAP1, anti-COX subunit II (COXII), and anti-SDH subunit B (SDHB) antibodies.

(B) Western immunoblotting was performed directly on a BN-PAGE. Probing was carried out with an anti-TRAP1 antibody and, in parallel lanes, with either an anti-COXII or an anti-SDH subunit A (SDHA) antibody. Note the smeared signal of both COXII and SDHA, suggesting that a population of complexes II and IV is present in the BN-PAGE; TRAP-1 is in the upper part of each complex band.

(C) Complex II and TRAP1 immunoprecipitations (IPs) on lysates of SAOS-2 mock cells. The interaction between TRAP1 and SDHA is shown by coIP. Immunoglobulin G (IgG) is used in negative isotype controls.

(D) Crosslinking experiments on mitochondria from mock SAOS-2 cells. TRAP1 was immunoprecipitated after mitochondrial treatment with the crosslinker DTBP, loaded in parallel on separate lanes of an SDS-PAGE, and probed with either an anti-TRAP1 or an anti-SDHA antibody.

TRAP1/Hsp90 ATPase activity (Felts et al., 2000), 17-allylamino-17-demethoxygeldanamycin (17-AAG), whose availability to mitochondria was recently shown in situ (Xie et al., 2011); 17-AAG specifically increased SQR activity in control mitochondria, whereas shTRAP1 mitochondria were insensitive to the drug (Figures 4A, 4B, and S2B). Notably, the effect of 17-AAG was unrelated to Hsp90, as Hsp90 protein levels were the same in mock and shTRAP1 cells (Figure S2F). The SQR activity of ETC complex II was further inhibited in mitochondria from control cells that progressed through the focus-forming assay compared to mitochondria from the same cells kept in standard culture conditions, whereas no change in SQR activity could be appreciated in mitochondria from shTRAP1 cells during the

focus-forming experiments (Figure 4B). 17-AAG could still reactivate the SDH enzyme in mitochondria of TRAP1-expressing cells undergoing the focus-forming process (Figure 4B), indicating that even the enhanced inhibition of SQR activity occurring during the in vitro transformation progression is mediated by TRAP1 and remains reversible. In further accord with an inhibitory function of TRAP1 on ETC complex II, mitochondria from MEF cells stably expressing TRAP1 showed a diminished SQR activity compared to controls, and this inhibition was increased during the focus-forming assay; 17-AAG reactivated SDH selectively in mitochondria from TRAP1-expressing MEFs (Figure 4C).

TRAP1 Induction Inhibits Complex II Enzymatic Activity in Human Colorectal Cancers

TRAP1 expression was shown to be increased in a variety of tumor types (Kang et al., 2007 and <http://www.proteinatlas.org/>). We analyzed the SQR activity of ETC complex II in a set of human colorectal cancer samples and compared it with that measured in the surrounding nontransformed mucosa for each patient. In all colorectal cancer samples at stage IV, characterized by metastases to lymph nodes and to distant sites, and in the majority of samples of stage I–III, characterized by the absence of distant metastases, TRAP1 was upregulated relative to normal mucosa (Costantino et al., 2009). When we measured SQR activity in extracts from these samples, we found that TRAP1 upregulation was always paralleled by a decrease in SQR activity, and that this decrease could be partially rescued by adding 17-AAG before starting recordings (Figure 4D). In a small subset of stage I–III colorectal cancers, TRAP1 expression was not induced relative to surrounding nontumor tissues. In these samples, we could not detect any difference in SQR activity between samples from tumor and normal mucosa (Figure 4E), strengthening the link between TRAP1 and the regulation of complex II activity.

TRAP1 Inhibits Cell Oxygen Consumption Rate and ATP Production by OXPHOS

The SQR assays described so far measure the maximal enzymatic activity of complex II, as the complex is made accessible in permeabilized mitochondria and exposed to an excess of substrates. We next analyzed whether TRAP1 also affects the oxygen consumption rate (OCR) of living cells. Downregulation of TRAP1 markedly increased mitochondrial-dependent respiration in all cancer cell models we tested (Figures 5A, S3A, and S3B); in full accord with the effect of the drug on SQR activity (see Figure 4A), the TRAP1 inhibitor 17-AAG increased OCR only in TRAP1-expressing cells (Figure S4A). In shTRAP1 cells, the extra OCR was used to make ATP, as it was inhibited by the ATP synthase blocker oligomycin; moreover, addition of the uncoupler FCCP increased respiration well above the basal level, indicating an increased respiratory capacity that remained fully sensitive to ETC inhibition by rotenone (Figure 5A). The comparison with control cells is striking because, unlike shTRAP1 cells, they already utilize their maximal respiratory capacity under basal conditions, as shown by the lack of OCR increase with FCCP (Figure 5A), an arrangement implying that any additional ATP requirement must be provided by glycolysis. Consistently, we found that OXPHOS marginally contributes to ATP synthesis in mock cells, whereas a high proportion of the

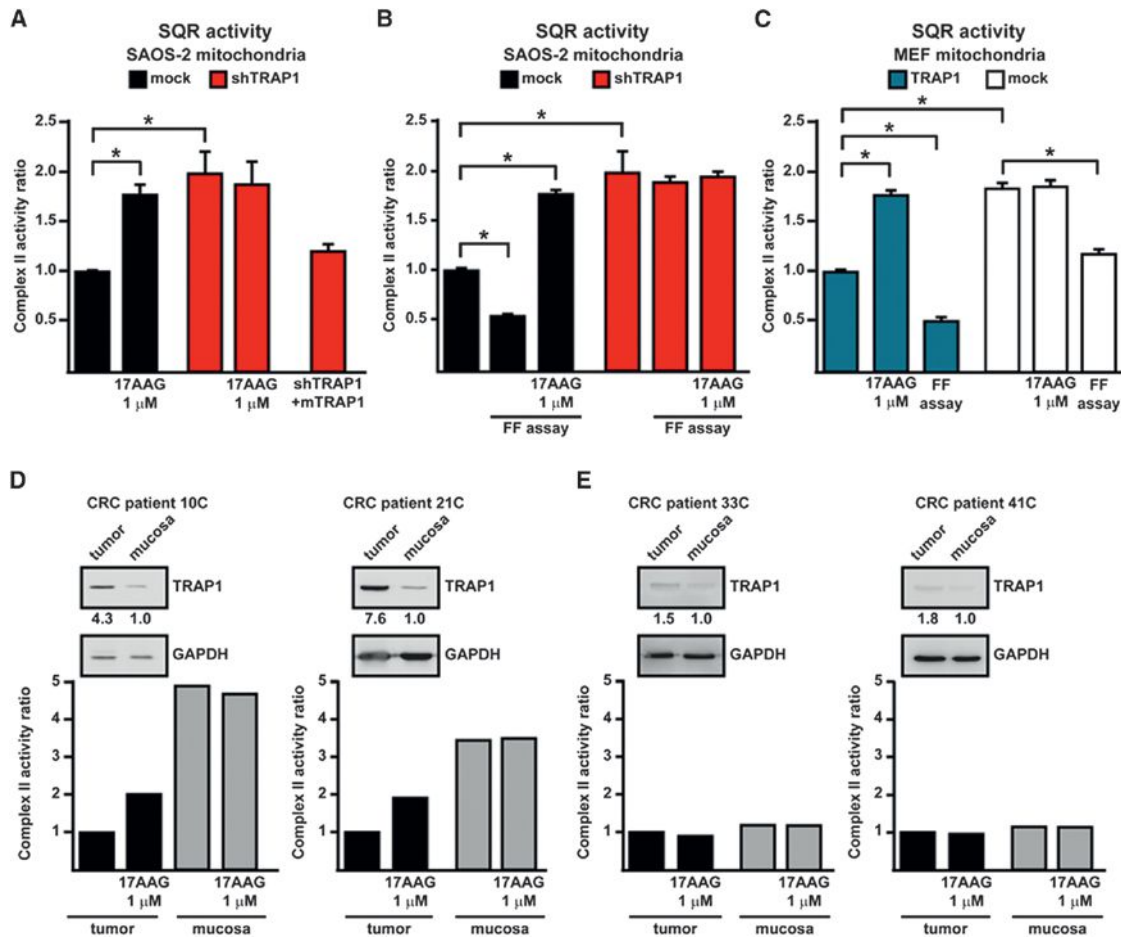


Figure 4. TRAP1 Downregulates the Enzymatic Activity of RC Complex II

(A and B) Analysis of the SQR enzymatic activity of complex II in mitochondria from SAOS-2 cells. In (A), analysis is performed on mitochondria from cultured cells; in (B), complex II activity values of mitochondria from cultured cells are compared with mitochondrial extracts from focus-forming assays obtained at the 15th experimental day (i.e., 1–2 days before cells that did not form foci massively underwent death). Mock indicates SAOS-2 cells stably transfected with a scrambled shRNA; shTRAP1 indicates SAOS-2 cells stably transfected with a TRAP1 shRNA; shTRAP1 + mTRAP1 indicates SAOS-2 shTRAP1 cells transfected with a mouse TRAP1 cDNA insensitive to human-directed shTRAP1 constructs (see Figure 2C). Enzyme activity values are compared to those of SAOS-2 mock cells in culture.

(C) SQR activity is measured on mitochondria from MEFs kept in culture or undergoing a focus-forming assay (15th day). TRAP1 indicates cells stably transfected with the TRAP1-containing vector; cells stably transfected with a control vector are dubbed mock. Enzyme activity values are compared to those of mitochondria from TRAP1-expressing MEFs in culture. TRAP1 inhibitor 17-AAG was added 5 min before starting recordings. Bar graphs report mean ± SD values (n ≥ 3); *p < 0.01 with a Student's t test analysis.

(D and E) Representative analyses of SQR activity on human colorectal cancer (CRC) samples are compared to surrounding noncancerous mucosae of the same patient. As shown in the insets, TRAP1 expression was compared between each CRC and noncancerous mucosa by western immunoblot followed by densitometric analysis normalized to GAPDH, which was used as a loading control. TRAP1 was considered induced when the ratio of the protein level between tumor sample and surrounding noncancerous mucosa was ≥ 3. Samples reported in (D) were obtained from metastatic CRC tumors and display an increase of TRAP1 expression in tumors with respect to mucosae; samples reported in (E) were obtained from nonmetastatic CRC tumors and do not show any relevant increase of TRAP1 expression.

intracellular ATP content is provided by glycolysis, with a marked increase of glycolytic ATP during the *in vitro* tumorigenic process; instead, in shTRAP1 cells, most of the ATP comes from OXPHOS (Figure 5B). Moreover, expression of the TRAP1 cDNA in nontransfected fibroblasts markedly inhibited basal OCR and abolished any respiratory reserve (Figure 5C), mimicking the respiratory pattern of TRAP1-expressing tumor cells. Expression in shTRAP1 cells of the murine TRAP1 insensitive to human-directed shTRAP1 constructs determined an OCR pattern indistinguishable from that of mock cells (Figure 5D).

SDH Inhibitors Selectively Affect Respiration, Survival, and Soft Agar Growth in shTRAP1 Cells

A low concentration of the ETC complex II inhibitors 3-nitropropionic acid (3-NP), which inactivates SDH after covalent binding with an Arg residue in the catalytic core of SDHA (Huang et al., 2006), or thenoyltrifluoroacetone (TTFA), which blocks electron transfer from succinate to coenzyme Q at the quinone-binding site in subunits B and D (Huang et al., 2006), inhibited OCR in shTRAP1 cells but were inactive in the presence of TRAP1 (Figures S4B and S4C), paralleling the downmodulation of the SQR

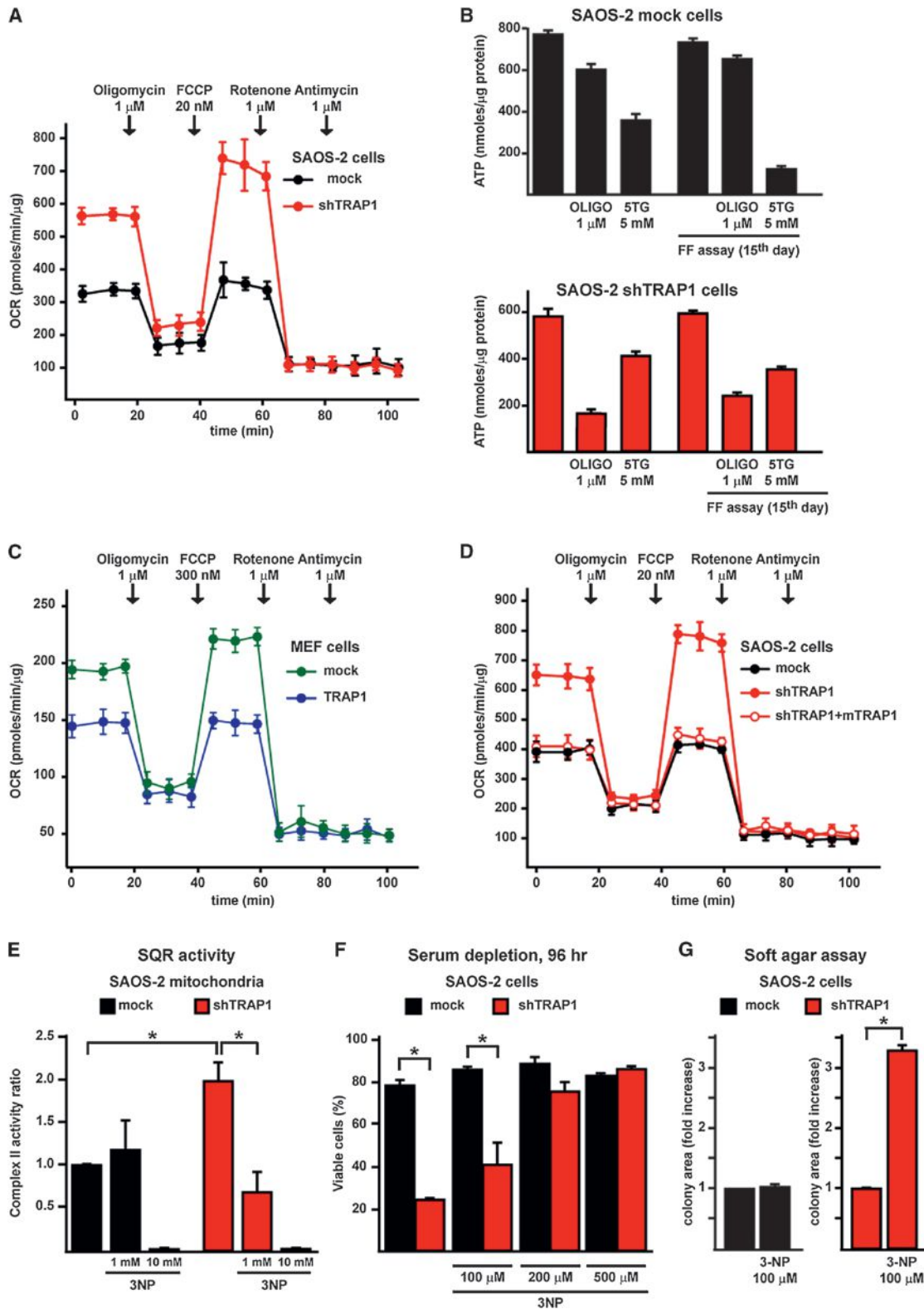


Figure 5. TRAP1-Induced Downmodulation of SDH Activity Decreases Cell Oxygen Consumption Rate and OXPHOS-Dependent Synthesis of ATP and Prompts Resistance to Stress Stimuli

(A) Representative traces of OCR experiments performed on monolayers of living SAOS-2 cells. Subsequent additions of the ATP synthase inhibitor oligomycin, the uncoupler FCCP, the ETC complex I inhibitor rotenone, and the ETC complex III inhibitor antimycin A were carried out.

(legend continued on next page)

activity induced by 3-NP only in TRAP1-expressing mitochondria (Figure 5E). These data indicate that TRAP1 limits maximal respiration by acting at ETC complex II. We also found that 3-NP inhibits death in a dose-dependent fashion in shTRAP1, but not in mock SAOS-2 cells placed in conditions of long-term starvation that mimic the paucity of nutrients found in the inner tumor mass during the phases of its rapid accrual (Figure 5F). Moreover, treatment with 3-NP partially restored the ability of shTRAP1 cells to form colonies in soft agar, whereas it was ineffective on the colonies formed by control cells (Figure 5G).

TRAP1 Induces Succinate Accumulation and HIF1 α Stabilization, which Is Required for Tumor Cell Growth

It was shown that succinate induces HIF1 by inhibiting PHDs, the enzymes that hydroxylate HIF1 α , allowing its subsequent ubiquitin-dependent degradation (Selak et al., 2005). We observed that during the focus-forming assay, the intracellular level of succinate increased only in TRAP1-expressing cells (Figure 6A), matching the downmodulation of their SDH enzymatic activity (Figure 4B). In keeping with these results, HIF1 α was detectable exclusively in TRAP1-expressing cells during the focus-forming process (Figure 6B), whereas it was hydroxylated on Pro residues (i.e., primed for proteasomal degradation) both in culture conditions, independently of the presence of TRAP1, and in shTRAP1 cells exposed to focus-forming conditions (Figure 6C). HIF2 α , which shares some redundant functions with HIF1 α and whose expression is increased in a broad spectrum of cancer cell types (Keith et al., 2012), was not stabilized in our experimental conditions (Figure 6D). We then used pimonidazole, a compound that is reductively activated under hypoxic conditions and forms protein adducts by reacting with Cys residues (Arteel et al., 1998), to understand whether HIF1 α stabilization could at least partially depend on hypoxic conditions occurring during the formation of foci. Remarkably, we could not detect any induction of pimonidazole-protein adducts in TRAP1-expressing cells during the process of *in vitro* tumorigenesis, even when HIF1 α had already been stabilized (Figure 6E), which demonstrates that pseudohypoxic conditions elicited by the presence of TRAP1 are sufficient to promote HIF1 α stabilization. Tumor samples obtained from nude mice xenografted with TRAP1-expressing SAOS-2 cells (see Figure 1D) were characterized by densely packed cells, amidst which fibrotic and necrotic areas could be observed (Figure 6F, marked as F and N, respectively);

HIF1 α was clearly detected in the majority of cells, the signal being particularly strong in the nuclei of cells where proliferation markers were also evident (compare the MIB/Ki67 and the HIF1 α staining in Figure 6F). In these samples, cells displayed a punctate TRAP1 signal that fits well with its mitochondrial localization (see the high-magnification TRAP1 staining in Figure 6F). The addition of dimethyl succinate, a membrane-permeable succinate analog, to the focus-forming culture medium both stabilized HIF1 α (Figure 7A) and rescued the capability to form colonies (Figure 7B) in shTRAP1 cells, while it did not further increase the tumorigenicity of TRAP1-expressing cells (Figure 7B). Moreover, HIF1 α inhibition either with a cell-permeable esterified form of α -ketoglutarate (1-trifluoromethylbenzyl- α -ketoglutarate, TakG), which reverses HIF1 α stabilization by restoring PHD enzymatic activity (MacKenzie et al., 2007; Tennant et al., 2009), or with RNAi on HIF1 α or HIF1 β , the latter being the stable subunit of the heterodimeric HIF transcription factors (Keith et al., 2012), fully abolished formation of foci in TRAP1-expressing tumor cells and in MEFs transfected with a TRAP1 cDNA (Figures 7C–7F). Taken together, these data indicate that TRAP1 prompts neoplastic growth by inducing a succinate-dependent stabilization of HIF1 α .

DISCUSSION

Tumor cells tend to increase their glycolytic activity without a matching increase of oxidative phosphorylation (Warburg, 1956; Warburg et al., 1927). Inhibition of the tumor suppressor p53 or activation of the transcription factor HIF1 curtails OXPHOS by inducing the autophagic degradation of respiratory complexes and by abrogating the synthesis of some of their subunits (such as SDHB) or assembly factors (Denko, 2008; Semenza, 2010a; Vousden and Ryan, 2009). Conversely, OXPHOS inhibition can play a causal role in tumorigenesis. Inactivating mutations in mitochondrial DNA (mtDNA) genes encoding for subunits of ETC complexes I and III were found associated with renal oncocytomas (Gasparre et al., 2008) as well as thyroid and prostate cancers (Abu-Amero et al., 2005; Petros et al., 2005). However, these mutations are confined to a small set of neoplasms, and the lack of clear-cut molecular mechanisms hampers the definition of whether OXPHOS inhibition as such can play a general tumorigenic role. Key findings of the present work demonstrate that the mitochondrial chaperone TRAP1, which is widely expressed in most tumors, but

(B) ATP levels were measured in mock or shTRAP1 SAOS-2 cells kept in standard culture conditions (bars on the left) or in a focus-forming assay for 15 days (i.e., 1–2 days before cells that did not form foci massively underwent death (bars on the right). Where indicated, cells were treated for 2 hr with the ATP synthase inhibitor oligomycin or the hexokinase inhibitor 5-thiogluconate (5TG) in a no-glucose medium to discriminate between ATP produced by OXPHOS and by glycolysis.

(C and D) Representative traces of OCR experiments performed on monolayers of living MEF cells (C) or SAOS-2 cells (D). Experiments were carried out as in (A).

(E) Analysis of the effect of the SDH inhibitor 3-NP on the SQR enzymatic activity of complex II in mitochondria from SAOS-2 cells. 3-NP was added 5 min before starting recordings; 10 mM 3-NP was used to fully inhibit the SDH enzyme.

(F) Cytofluorimetric cell death analysis of SAOS-2 cells starved in a medium without serum for 96 hr with or without the reported concentrations of 3-NP. Viable cells are identified as double negative for propidium iodide and Annexin V-FITC.

(G) Soft agar assay on SAOS-2 cells. Data are reported as fold increase of colony area of mock cells grown with 3-NP compared with mock cells kept without the drug (left) and, separately, as fold increase of colony area of shTRAP1 cells grown with 3-NP compared with shTRAP1 cells kept without the drug (right). In SAOS-2 experiments, mock indicates cells stably transfected with a scrambled shRNA; shTRAP1 indicates cells stably transfected with a TRAP1 shRNA; shTRAP1 + mTRAP1 indicates cells stably transfected with a TRAP1 shRNA and expressing a mouse TRAP1 cDNA. In the experiment with MEFs, cells were stably transfected with either a TRAP1 cDNA or a scrambled shRNA (mock). All bar graphs report mean \pm SD values ($n \geq 3$); * $p < 0.01$ with a Student's *t* test analysis.

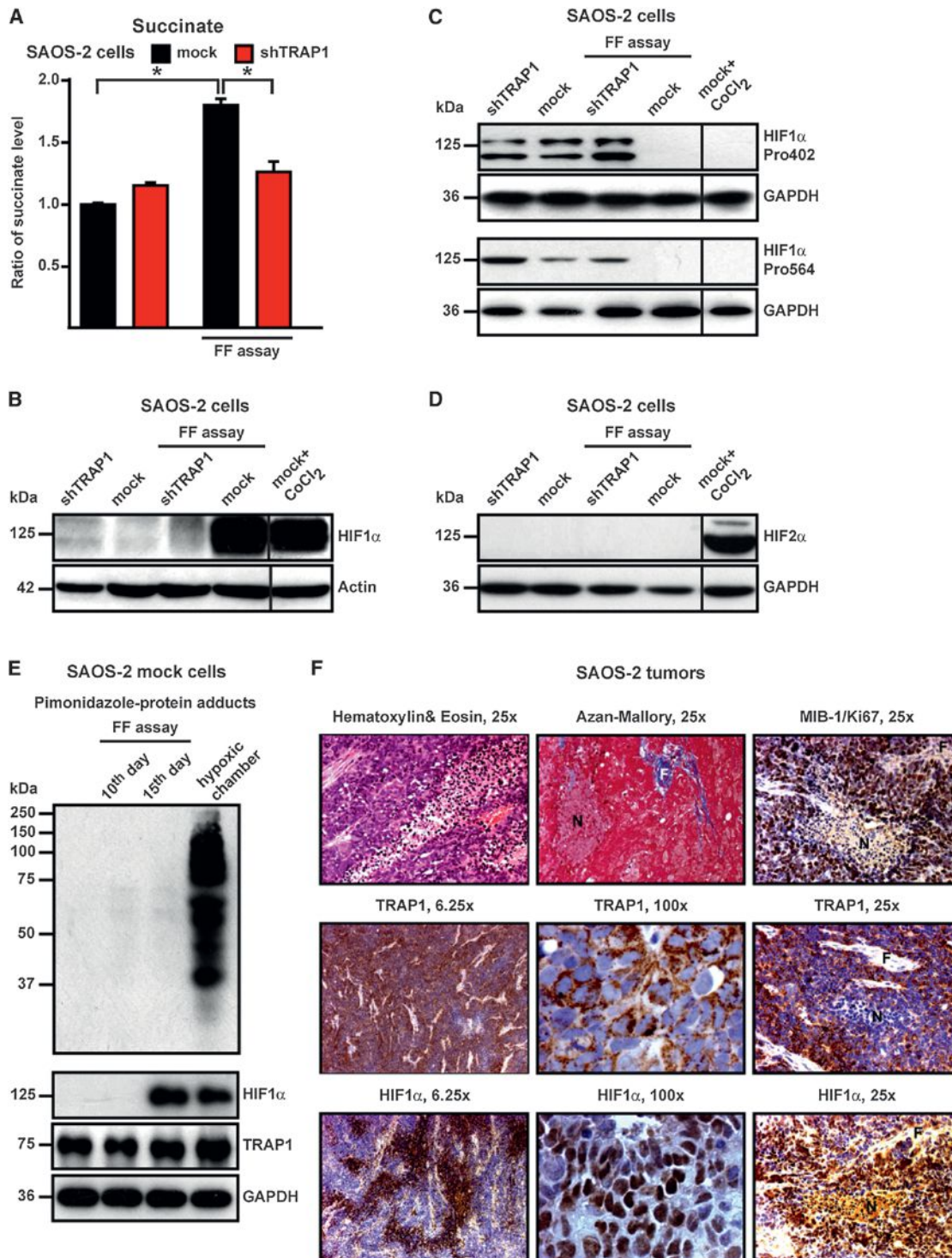


Figure 6. TRAP1 Increases Intracellular Succinate Concentration and Stabilizes HIF1 α in a Hypoxia-Independent Way

(A) Bar graphs showing liquid chromatography-mass spectrometry (LC-MS) measurements of intracellular succinate level. Values are compared with cultured mock SAOS-2 cells.

(B–D) Western immunoblots showing HIF1 α expression (B), HIF1 α hydroxylation of the Pro402 and Pro564 residues (C), and HIF2 α expression in cultured cells and on extracts from focus-forming assays obtained at the 15th experimental day (i.e., 1–2 days before cells that did not form foci massively underwent death). CoCl₂ is used as a positive control for HIF1 α and HIF2 α stabilization. Blots were probed with an anti-actin (B) or an anti-GAPDH (C and D) antibody to check for protein load.

(E) Detection of pimonidazole-protein adducts in SAOS-2 mock cells kept in either normal culture or focus-forming conditions for 10 or 15 days. Pimonidazole (200 μ M) was added on the focus-forming plate 2 hr before lysis. As a positive control, cells were kept for 24 hr in a hypoxic chamber (0.5% O₂). On
(legend continued on next page)

not in highly proliferating, nontransformed cells (<http://www.proteinatlas.org/>), is a component of the molecular machinery that decreases mitochondrial respiration and that this event is crucial for neoplastic progression. Indeed, we find that TRAP1 behaves as an oncogene since (i) without TRAP1, tumorigenesis is blunted both *in vitro* and *in vivo*, and (ii) TRAP1 expression confers tumorigenic potential to nontransformed cells. We observe that TRAP1-mediated inhibition of SDH limits the maximal rate of respiration and leads to succinate accumulation followed by HIF1 α , but not HIF2 α , stabilization. Remarkably, the membrane-permeable succinate analog dimethyl succinate could both elicit HIF1 α stabilization and rescue the tumorigenic phenotype of shTRAP1 cells, highlighting the mechanistic connection between TRAP1-dependent succinate accumulation and HIF1 α -dependent tumor formation.

The role played by the transcription factor HIF1 in tumorigenesis is complex. Once activated by inhibition of the proteasomal degradation of its α subunit (either HIF1 α or HIF2 α), and by the ensuing association with the stable β subunit (HIF1 β), HIF1 can boost evolution of neoplasms by promoting angiogenesis, epithelial-mesenchymal transition, and the glycolytic switch (Brahimi-Horn et al., 2011; Semenza, 2010a). In multiple tumor models, both HIF1 α and HIF2 α promote neoplastic progression by regulating sets of genes that are only partially shared, and independent roles for HIF1 α and HIF2 α can depend on the cancer type or on its growth and progression stages (Keith et al., 2012). However, both α subunits can play a tumor suppressor function in specific tumor types, such as renal cell carcinoma (HIF1 α) or lung adenocarcinoma (HIF2 α), through poorly defined mechanisms. In our model, HIF1 α stabilization, and the ensuing HIF activation, have a crucial proneoplastic role, as promoting HIF1 α degradation or knocking down either HIF1 α or HIF1 β abolishes the neoplastic potential of TRAP1-expressing cells. Instead, we could not observe any HIF2 α stabilization, ruling out its role in the TRAP1-dependent tumorigenic process. It is interesting that HIF2 α accumulates at higher O₂ concentrations than HIF1 α (Keith et al., 2012), and the possibility exists that, at variance with what we observe for HIF1 α , pseudohypoxic conditions are insufficient or unable to stabilize HIF2 α .

HIF1 α stabilization emerges after several days of *in vitro* transformation. This is not at all surprising because excess succinate can be utilized in multiple pathways, including increased heme synthesis (Frezza et al., 2011), and because SDH becomes more strongly inhibited by TRAP1 during the focus-forming assay. The latter observation also suggests that a threshold SDH inhibition must be reached to allow for succinate accumulation. Despite a partial respiratory inhibition, TRAP1-expressing cells fully utilize their residual respiratory capacity to produce ATP, as shown by OCR experiments, but reorient their metabolism toward glycolysis to meet any energy demand that

exceeds respiratory capacity, in complete accord with Warburg's observations.

TRAP1 is likely to begin a feedforward loop, as it inhibits SDH and respiration (hence OXPHOS) and induces HIF1, which in turn further inhibits OXPHOS (Denko, 2008; Semenza, 2010b) and directly downregulates SDH by induction of miR-210 (Puisségur et al., 2011). Notably, we have determined that TRAP1-dependent stabilization of HIF1 α occurs in a pseudohypoxic way (i.e., in the absence of any hypoxic stress). This observation has potential implications for the kinetics of tumor development, as TRAP1 could induce HIF1 transcriptional activity even before the dysregulated accrual of the tumor mass creates hypoxic areas in its inner core.

At variance with the complete block of the SDH enzyme, which is an extreme case caused by loss-of-function mutations only seen in specific subsets of tumors (Bardella et al., 2011), the partial and reversible SDH inhibition caused by TRAP1 and its increased expression levels would mediate a more general proneoplastic function, which fits with TRAP1 identification as a bona fide inducible target of the proto-oncogene c-Myc (Coller et al., 2000).

Tumor cells could be endowed with a multichaperone mitochondrial complex, as TRAP1 interacts with cyclophilin D, Hsp90, and Hsp60 (Ghosh et al., 2010; Kang and Altieri, 2009). Given the multiplicity of chaperone client proteins, we cannot exclude further interactions of TRAP1 with other mitochondrial components. For instance, TRAP1 is involved in the inhibition of the mitochondrial permeability transition pore (Kang et al., 2007), whose opening irreversibly commits cells to death (Rasola and Bernardi, 2007; Rasola et al., 2010b), and we have observed that keeping the pore locked can be used by tumor cells to evade apoptosis (Rasola et al., 2010a). Thus, TRAP1 could take part in several mitochondrial changes that crucially contribute to the neoplastic phenotype. Targeting its chaperone activity and molecular interactors could dismantle the metabolic and survival adaptations of neoplastic cells, paving the way to the development of highly selective, mitochondriotropic antineoplastic drugs.

EXPERIMENTAL PROCEDURES

Detailed methods can be found in the Supplemental Experimental Procedures.

Cell Cultures and Tissue Samples

Experiments were performed on different cell models: human SAOS-2 osteosarcoma cells, human HCT116 colorectal carcinoma cells, RWPE1/RWPE2 prostate epithelial cells, HeLa cervix carcinoma cells, and MEFs. TRAP1, HIF1 α , and HIF1 β expression was knocked down by stable transfections with shRNAs. Cells transfected with scrambled shRNA were always used as controls. TRAP1 re-expression in interfered human cells was obtained by using a mouse cDNA. Stable transfection of a TRAP1 cDNA was performed in MEF cells that show negligible levels of the endogenous protein. Tissue

the same samples, both HIF1 α stabilization and the expression level of TRAP1 were evaluated; blots were probed with an anti-GAPDH to check for protein load.

(F) Immunohistochemical inspections of tumors formed by SAOS-2 control cells after injection in nude mice (see Figure 1F). Hematoxylin and eosin (H&E) and Azan-Mallory staining reveal tumors rich in densely packed cells, with few fibrotic areas (F) and a large number of necrotic regions (N). TRAP1 is visible in most cells (see the 6.25 \times magnification) as a punctate signal (100 \times magnification), which is compatible with its mitochondrial localization. HIF1 α expression is evident all along the samples (see the 6.25 \times magnification), mainly in the nuclear compartment of cells (100 \times magnification), and the signal is particularly strong in the perinecrotic areas, where the proliferation marker MIB-1/Ki67 is also found (25 \times magnification).

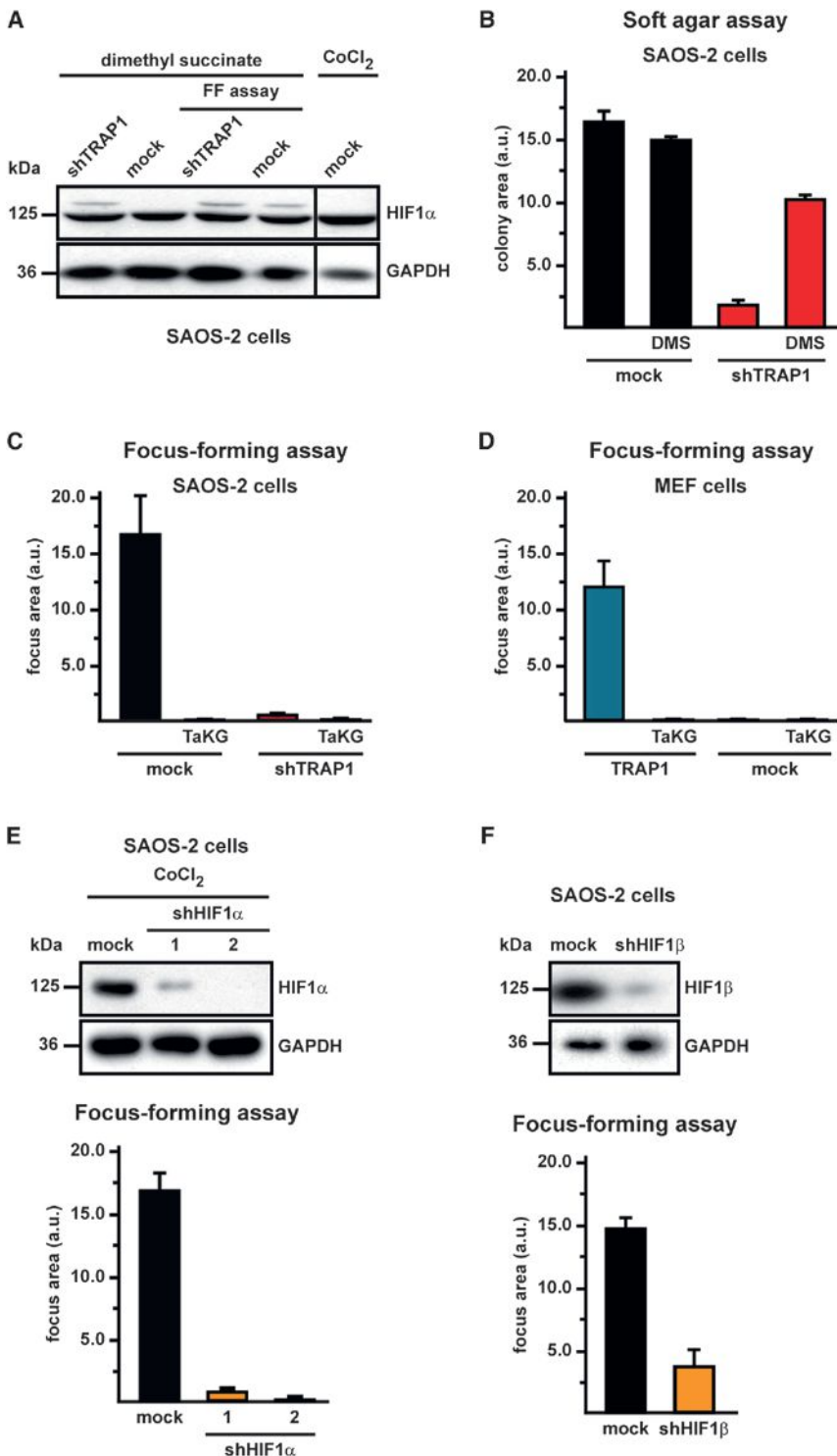


Figure 7. TRAP1 Favors Tumor Growth through Succinate-Dependent Stabilization of HIF1 α

(A) Western immunoblot showing HIF1 α stabilization in SAOS-2 cells kept either in culture or in focus-forming conditions in the presence of the cell-permeable succinate analog dimethyl succinate (20 mM, 48 hr). Extracts from focus-forming assays were obtained at the 15th experimental day (i.e., 1–2 days before cells that did not form foci massively underwent death). Blots were probed with an anti-GAPDH to check for protein load. Cells are dubbed as in previous figures with respect to TRAP1 expression.

(B) Soft agar experiments performed on SAOS-2 cells treated with dimethyl succinate (5 mM). Data indicate the total colony area at the 25th experimental day.

(C–F) Focus-forming assays on SAOS-2 cells (C) or MEFs (D) grown with or without TaKG and on SAOS-2 cells in which HIF1 α (E) or HIF1 β (F) expression had been knocked down by RNAi. Data are reported as in Figure 1A. In (E), CoCl₂ treatment is used to maximize HIF1 α expression. In (F), knocking down of HIF1 β is obtained with a mixture of three different shRNAs. Bar graphs report mean \pm SD values (n \geq 3); *p < 0.01 with a Student's t test analysis. Cells are dubbed as in previous figures.

(2) soft agar assays, in which cells are embedded in an agar matrix; only transformed cells, which escape anoikis death signals, can grow to form colonies; (3) cell injection in nude mice, in order to follow the growth of primary tumors. Samples obtained from these assays were also exploited for investigating changes in complex II enzymatic activity in succinate levels and in HIF1 α stabilization and distribution.

Cytofluorimetric Analyses

Cytofluorimetric analyses were utilized to analyze cell death induction with the use of Annexin V-FITC and propidium iodide probes as well as mitochondrial mass with the use of N-acridine orange.

Mitochondria Purification

Mitochondria were isolated through sequential centrifugations after mechanical cell disruption. In order to establish submitochondrial protein localization, isolated mitochondria were partially digested with different concentrations of trypsin.

Western Immunoblots and Immunoprecipitations, BN-PAGE, and Crosslinkings

Western immunoblot and immunoprecipitation experiments were performed following standard techniques.

BN-PAGE experiments were carried out on isolated mitochondria in order to identify ETC complexes. After a first electrophoresis in nondenaturing conditions, bands were visualized with Coomassie blue staining, cut, and run on SDS-PAGE for the identification of protein components by western immunoblot. Crosslinking assays were performed on isolated mitochondria incubated with the membrane-permeable, homobifunctional reagent DTBP prior to TRAP1 immunoprecipitation.

samples from both tumor and normal, noninfiltrated peritumoral mucosa were obtained from patients with colorectal carcinoma during surgical cancer removal after express written informed consent was obtained from all patients.

Tumorigenesis Assays

Three different tumorigenesis assays were performed: (1) focus-forming assays, in which cells were grown to confluence and kept in culture for the subsequent 25 days; tumor cells lose contact inhibition and overgrow to form foci;

ETC Complex II Activity Assays and Oxygen Consumption Rate Experiments

Complex II enzymatic activity was investigated, measuring the SQR activity with classical spectrophotometric approaches on cell or tumor lysates. Complex IV enzymatic activity was investigated, measuring the oxidation of reduced cytochrome *c*. Each measurement of the respiratory chain (RC) complex activity was normalized for protein amount and for citrate synthase activity. In vivo respiration was followed in a kinetic mode by measuring the oxygen consumption rate (OCR) of cell monolayers with an extracellular flux analyzer.

Immunohistochemical and Immunoelectron Microscopy Analyses

Immunohistochemical inspections were performed on serial sections of paraffin-embedded tumor samples obtained from xenografted nude mice following standard procedures. Immunoelectron microscopy (immuno-EM) inspections were performed on antibody-labeled fixed cells using the gold-enhanced protocol.

Determination of Intracellular Succinate Level

Intracellular succinate level was analyzed on lysates obtained by scraping cells placed in a cold methanol/acetonitrile solution. After spinning down the insoluble material, the supernatant was collected, and metabolites were separated using a liquid chromatography system coupled online to an LTQ Orbitrap mass spectrometer equipped with an electrospray ionization source.

Intracellular ATP Determination

Intracellular ATP was quantified by the luciferin/luciferase method. Cells were kept for 2 hr in the different experimental conditions.

Statistical Analysis

Student's *t* test was used to compare pairs of data groups. In all figures, bar graphs report mean \pm SD values ($n \geq 3$); **p* < 0.05.

SUPPLEMENTAL INFORMATION

Supplemental Information includes Supplemental Experimental Procedures and four figures and can be found with this article online at <http://dx.doi.org/10.1016/j.cmet.2013.04.019>.

ACKNOWLEDGMENTS

We thank Eyal Gottlieb, Stefano Indraccolo, and Valentina Giorgio for insightful discussions; Matteo Curtarello and Luca Persano for help with hypoxic chamber experiments; Roman S. Polishchuk for electron microscopy analyses; Elena Trevisan for technical assistance; and our system operators Otello Piovani and Marco Ardina for inexhaustible help. This work was supported by grants from Progetto Strategico di Ateneo dell'Università di Padova ("Models of Mitochondrial Diseases"), Associazione Italiana Ricerca sul Cancro (grant number 8722), Ministero Istruzione Università Ricerca (Fondo per gli Investimenti della Ricerca di Base (grant number RBAP11S8C3), and Telethon (grant numbers GGP 11082 and GPP100005A). The work performed by C.F. and L.Z. was supported by Cancer Research UK.

Received: September 24, 2012

Revised: February 14, 2013

Accepted: April 5, 2013

Published: June 4, 2013

REFERENCES

Abu-Amero, K.K., Alzahrani, A.S., Zou, M., and Shi, Y. (2005). High frequency of somatic mitochondrial DNA mutations in human thyroid carcinomas and complex I respiratory defect in thyroid cancer cell lines. *Oncogene* 24, 1455–1460.

Altieri, D.C., Stein, G.S., Lian, J.B., and Languino, L.R. (2012). TRAP-1, the mitochondrial Hsp90. *Biochim. Biophys. Acta* 1823, 767–773.

Arteel, G.E., Thurman, R.G., and Raleigh, J.A. (1998). Reductive metabolism of the hypoxia marker pimonidazole is regulated by oxygen tension independent of the pyridine nucleotide redox state. *Eur. J. Biochem.* 253, 743–750.

Bardella, C., Pollard, P.J., and Tomlinson, I. (2011). SDH mutations in cancer. *Biochim. Biophys. Acta* 1807, 1432–1443.

Brahimi-Horn, M.C., Bellot, G., and Pouyssegur, J. (2011). Hypoxia and energetic tumour metabolism. *Curr. Opin. Genet. Dev.* 21, 67–72.

Cairns, R.A., Harris, I.S., and Mak, T.W. (2011). Regulation of cancer cell metabolism. *Nat. Rev. Cancer* 11, 85–95.

Cecchini, G. (2003). Function and structure of complex II of the respiratory chain. *Annu. Rev. Biochem.* 72, 77–109.

Coller, H.A., Grandori, C., Tamayo, P., Colbert, T., Lander, E.S., Eisenman, R.N., and Golub, T.R. (2000). Expression analysis with oligonucleotide microarrays reveals that MYC regulates genes involved in growth, cell cycle, signaling, and adhesion. *Proc. Natl. Acad. Sci. USA* 97, 3260–3265.

Costantino, E., Maddalena, F., Calise, S., Piscazzi, A., Tirino, V., Fersini, A., Ambrosi, A., Neri, V., Esposito, F., and Landriscina, M. (2009). TRAP1, a novel mitochondrial chaperone responsible for multi-drug resistance and protection from apoptosis in human colorectal carcinoma cells. *Cancer Lett.* 279, 39–46.

Denko, N.C. (2008). Hypoxia, HIF1 and glucose metabolism in the solid tumour. *Nat. Rev. Cancer* 8, 705–713.

Felts, S.J., Owen, B.A., Nguyen, P., Trepel, J., Donner, D.B., and Toft, D.O. (2000). The hsp90-related protein TRAP1 is a mitochondrial protein with distinct functional properties. *J. Biol. Chem.* 275, 3305–3312.

Frezza, C., and Gottlieb, E. (2009). Mitochondria in cancer: not just innocent bystanders. *Semin. Cancer Biol.* 19, 4–11.

Frezza, C., Zheng, L., Folger, O., Rajagopalan, K.N., MacKenzie, E.D., Jerby, L., Micaroni, M., Chaneton, B., Adam, J., Hedley, A., et al. (2011). Haem oxygenase is synthetically lethal with the tumour suppressor fumarate hydratase. *Nature* 477, 225–228.

Fritz, V., and Fajas, L. (2010). Metabolism and proliferation share common regulatory pathways in cancer cells. *Oncogene* 29, 4369–4377.

Gasparre, G., Hervouet, E., de Laplanche, E., Demont, J., Pennisi, L.F., Colombel, M., Mège-Lechevallier, F., Scoazec, J.Y., Bonora, E., Smeets, R., et al. (2008). Clonal expansion of mutated mitochondrial DNA is associated with tumor formation and complex I deficiency in the benign renal oncocytoma. *Hum. Mol. Genet.* 17, 986–995.

Ghosh, J.C., Siegelin, M.D., Dohi, T., and Altieri, D.C. (2010). Heat shock protein 60 regulation of the mitochondrial permeability transition pore in tumor cells. *Cancer Res.* 70, 8988–8993.

Giorgio, V., Bisetto, E., Soriano, M.E., Dabbeni-Sala, F., Basso, E., Petronilli, V., Forte, M.A., Bernardi, P., and Lippe, G. (2009). Cyclophilin D modulates mitochondrial F0F1-ATP synthase by interacting with the lateral stalk of the complex. *J. Biol. Chem.* 284, 33982–33988.

Hanahan, D., and Weinberg, R.A. (2011). Hallmarks of cancer: the next generation. *Cell* 144, 646–674.

Hsu, P.P., and Sabatini, D.M. (2008). Cancer cell metabolism: Warburg and beyond. *Cell* 134, 703–707.

Huang, L.S., Sun, G., Cobessi, D., Wang, A.C., Shen, J.T., Tung, E.Y., Anderson, V.E., and Berry, E.A. (2006). 3-nitropropionic acid is a suicide inhibitor of mitochondrial respiration that, upon oxidation by complex II, forms a covalent adduct with a catalytic base arginine in the active site of the enzyme. *J. Biol. Chem.* 281, 5965–5972.

Kang, B.H., and Altieri, D.C. (2009). Compartmentalized cancer drug discovery targeting mitochondrial Hsp90 chaperones. *Oncogene* 28, 3681–3688.

Kang, B.H., Plescia, J., Dohi, T., Rosa, J., Doxsey, S.J., and Altieri, D.C. (2007). Regulation of tumor cell mitochondrial homeostasis by an organelle-specific Hsp90 chaperone network. *Cell* 131, 257–270.

Keith, B., Johnson, R.S., and Simon, M.C. (2012). HIF1 α and HIF2 α : sibling rivalry in hypoxic tumour growth and progression. *Nat. Rev. Cancer* 12, 9–22.

Lemarie, A., and Grimm, S. (2011). Mitochondrial respiratory chain complexes: apoptosis sensors mutated in cancer? *Oncogene* 30, 3985–4003.

- Levine, A.J., and Puzio-Kuter, A.M. (2010). The control of the metabolic switch in cancers by oncogenes and tumor suppressor genes. *Science* 330, 1340–1344.
- MacKenzie, E.D., Selak, M.A., Tennant, D.A., Payne, L.J., Crosby, S., Frederiksen, C.M., Watson, D.G., and Gottlieb, E. (2007). Cell-permeating alpha-ketoglutarate derivatives alleviate pseudohypoxia in succinate dehydrogenase-deficient cells. *Mol. Cell. Biol.* 27, 3282–3289.
- Petros, J.A., Baumann, A.K., Ruiz-Pesini, E., Amin, M.B., Sun, C.Q., Hall, J., Lim, S., Issa, M.M., Flanders, W.D., Hosseini, S.H., et al. (2005). mtDNA mutations increase tumorigenicity in prostate cancer. *Proc. Natl. Acad. Sci. USA* 102, 719–724.
- Puisségur, M.P., Mazure, N.M., Bertero, T., Pradelli, L., Grosso, S., Robbe-Sermesant, K., Maurin, T., Lebrigand, K., Cardinaud, B., Hofman, V., et al. (2011). miR-210 is overexpressed in late stages of lung cancer and mediates mitochondrial alterations associated with modulation of HIF-1 activity. *Cell Death Differ.* 18, 465–478.
- Rasola, A., and Bernardi, P. (2007). The mitochondrial permeability transition pore and its involvement in cell death and in disease pathogenesis. *Apoptosis* 12, 815–833.
- Rasola, A., Sciacovelli, M., Chiara, F., Pantic, B., Brusilow, W.S., and Bernardi, P. (2010a). Activation of mitochondrial ERK protects cancer cells from death through inhibition of the permeability transition. *Proc. Natl. Acad. Sci. USA* 107, 726–731.
- Rasola, A., Sciacovelli, M., Pantic, B., and Bernardi, P. (2010b). Signal transduction to the permeability transition pore. *FEBS Lett.* 584, 1989–1996.
- Selak, M.A., Armour, S.M., MacKenzie, E.D., Boulahbel, H., Watson, D.G., Mansfield, K.D., Pan, Y., Simon, M.C., Thompson, C.B., and Gottlieb, E. (2005). Succinate links TCA cycle dysfunction to oncogenesis by inhibiting HIF- α prolyl hydroxylase. *Cancer Cell* 7, 77–85.
- Semenza, G.L. (2010a). Defining the role of hypoxia-inducible factor 1 in cancer biology and therapeutics. *Oncogene* 29, 625–634.
- Semenza, G.L. (2010b). HIF-1: upstream and downstream of cancer metabolism. *Curr. Opin. Genet. Dev.* 20, 51–56.
- Tennant, D.A., Frezza, C., MacKenzie, E.D., Nguyen, Q.D., Zheng, L., Selak, M.A., Roberts, D.L., Dive, C., Watson, D.G., Aboagye, E.O., and Gottlieb, E. (2009). Reactivating HIF prolyl hydroxylases under hypoxia results in metabolic catastrophe and cell death. *Oncogene* 28, 4009–4021.
- Vander Heiden, M.G., Cantley, L.C., and Thompson, C.B. (2009). Understanding the Warburg effect: the metabolic requirements of cell proliferation. *Science* 324, 1029–1033.
- Vousden, K.H., and Ryan, K.M. (2009). p53 and metabolism. *Nat. Rev. Cancer* 9, 691–700.
- Warburg, O. (1956). On the origin of cancer cells. *Science* 123, 309–314.
- Warburg, O., Wind, F., and Negelein, E. (1927). The Metabolism of Tumors in the Body. *J. Gen. Physiol.* 8, 519–530.
- Wittig, I., and Schägger, H. (2008). Features and applications of blue-native and clear-native electrophoresis. *Proteomics* 8, 3974–3990.
- Xie, Q., Wondergem, R., Shen, Y., Cavey, G., Ke, J., Thompson, R., Bradley, R., Daugherty-Holtrop, J., Xu, Y., Chen, E., et al. (2011). Benzoquinone ansamycin 17AAG binds to mitochondrial voltage-dependent anion channel and inhibits cell invasion. *Proc. Natl. Acad. Sci. USA* 108, 4105–4110.

Subscribe to Active Zone

The Cell Press Neuroscience Newsletter



Featuring:

- Cutting-edge neuroscience from Cell Press and beyond
- Interviews with leading neuroscientists
- Special features: Podcasts, Webinars and Review Issues
- Neural Currents - cultural events, exhibits and new books
- *And much more*

Read now at
bit.ly/activezone



Cell
PRESS

The Intrinsic Apoptosis Pathway Mediates the Pro-Longevity Response to Mitochondrial ROS in *C. elegans*

Callista Yee,¹ Wen Yang,¹ and Siegfried Hekimi^{1,*}

¹Department of Biology, McGill University, Montreal, QC H3A 1B1, Canada

*Correspondence: siegfried.hekimi@mcgill.ca

<http://dx.doi.org/10.1016/j.cell.2014.02.055>

SUMMARY

The increased longevity of the *C. elegans* electron transport chain mutants *isp-1* and *nuo-6* is mediated by mitochondrial ROS (mtROS) signaling. Here we show that the mtROS signal is relayed by the conserved, mitochondria-associated, intrinsic apoptosis signaling pathway (CED-9/Bcl2, CED-4/Apaf1, and CED-3/Casp9) triggered by CED-13, an alternative BH3-only protein. Activation of the pathway by an elevation of mtROS does not affect apoptosis but protects from the consequences of mitochondrial dysfunction by triggering a unique pattern of gene expression that modulates stress sensitivity and promotes survival. In vertebrates, mtROS induce apoptosis through the intrinsic pathway to protect from severely damaged cells. Our observations in nematodes demonstrate that sensing of mtROS by the apoptotic pathway can, independently of apoptosis, elicit protective mechanisms that keep the organism alive under stressful conditions. This results in extended longevity when mtROS generation is inappropriately elevated. These findings clarify the relationships between mitochondria, ROS, apoptosis, and aging.

INTRODUCTION

The observed association of the aging process with the biology of reactive oxygen species (ROS), in particular ROS originating from mitochondria (mtROS), has led to the formulation of the oxidative stress theory of aging. Recently, however, more nuanced interpretations have been proposed to explain the basic observations that led to the formulation of the theory (Lapointe and Hekimi, 2010; Sena and Chandel, 2012). One possibility is that ROS damage is not causally involved in the aging process but that ROS levels are correlated with the aged phenotype because they modulate signal transduction pathways that respond to cellular stresses brought about by aging (Hekimi et al., 2011). In other words, ROS generation may be enhanced by the aging process because, in their role as signaling mole-

cules, ROS help to alleviate the cellular stresses caused by aging. This hypothesis is supported by findings in a variety of organisms, in particular in *C. elegans* where changes in ROS generation or detoxification can be uncoupled from any effect on lifespan (Doonan et al., 2008; Van Raamsdonk and Hekimi, 2009, 2010; Yang et al., 2007). Most strikingly, moderate mitochondrial dysfunction (Felkai et al., 1999; Feng et al., 2001; Yang and Hekimi, 2010b), severe loss of mtROS detoxification (Van Raamsdonk and Hekimi, 2009), and elevated mtROS generation (Yang and Hekimi, 2010a), as well as treatments with pro-oxidants (Heidler et al., 2010; Lee et al., 2010; Van Raamsdonk and Hekimi, 2012; Yang and Hekimi, 2010a), can all lengthen rather than shorten lifespan. In addition, the pro-longevity effects of both dietary restriction (Schulz et al., 2007), and reduced insulin signaling in *C. elegans* (Zarse et al., 2012), appear to involve an increase in ROS levels. Such observations are not limited to *C. elegans*. For example, mtROS signaling can act to extend chronological lifespan of the yeast *S. cerevisiae* (Pan et al., 2011).

The longevity phenotype of *isp-1(qm150)* (Feng et al., 2001) and *nuo-6(qm200)* (Yang and Hekimi, 2010b) mutants is most unequivocally connected to mtROS generation (Yang and Hekimi, 2010a). *isp-1* encodes the “Rieske” iron sulfur protein, one of the major catalytic subunits of mitochondrial complex III, and *nuo-6* encodes the mitochondrial complex I subunit NDUF4. The *qm150* and *qm200* mutations are missense mutations that do not lead to a full loss of protein function. Mitochondria isolated from both mutants show elevated superoxide generation, as measured by fluorescence sorting of purified mitochondria incubated with the dye MitoSox (Yang and Hekimi, 2010a). This is a very specific phenotype that is not accompanied by an increase in overall mitochondrial oxidative stress, nor by a measurable increase in overall oxidative damage. The long-lived phenotype can also be phenocopied by treatment of the wild-type with a very low level (0.1 mM) of the superoxide generator paraquat (PQ). In contrast, treatment of the mitochondrial mutants with PQ has no effect, suggesting that treatment with PQ extends lifespan by the same mechanisms as the mitochondrial mutations (Yang and Hekimi, 2010a).

Increased longevity can also result from induction of the mitochondrial unfolded protein stress response (mtUPR), which can be triggered by RNA interference knockdown of mitochondrial components (Dillin et al., 2002; Durieux et al., 2011; Lee et al., 2003). This response is however distinct from the response to

elevated mtROS as the lifespan increases produced by the elevated mtROS in the mutants and by the activated mtUPR are fully additive (Yang and Hekimi, 2010b).

How might elevated mtROS promote longevity? ROS are well known to act as modulators in signal transduction pathways, and it is as such that they might be enhancing longevity. One candidate signaling pathway that could include potential mtROS sensors as well as a mechanism of downstream signaling is the intrinsic apoptosis pathway. Apoptosis is a highly controlled process that in mammals is sensitive to mitochondrial function, including mtROS, via the intrinsic apoptosis signaling pathway (Wang and Youle, 2009). In *C. elegans* the intrinsic apoptotic machinery consists of the BH3-only protein EGL-1, CED-9 (Bcl2-like), CED-4 (Apaf1-like), and CED-3 (Casp9-like). CED-9 is tethered to the outer mitochondrial membrane and binds CED-4. However, in contrast to vertebrates, there is no evidence for any role for mtROS in regulating apoptosis in *C. elegans*.

Interestingly, the individual proteins or pairs of interacting proteins of the apoptotic signaling machinery appear to be able to carry out apoptosis-independent functions. For example, EGL-1 and CED-9 affect mitochondrial dynamics (Lu et al., 2011), CED-4 and CED-3 promote neuronal regeneration (Pinan-Lucarre et al., 2012), CED-4 appears to be involved in hypoxic preconditioning (Dasgupta et al., 2007) and S-phase checkpoint regulation (Zermati et al., 2007). These and similar findings in other organisms (Galluzzi et al., 2008) suggest that the proteins of the intrinsic apoptotic pathway have bona fide signal transduction activities in other processes. However, in no case to date has the full pathway, from a BH3-only protein to a caspase, been found to be involved in a process distinct from apoptosis.

Here, we show that the *isp-1* and *nuo-6* mutations and 0.1 mM PQ treatment induce a unique pattern of changes in gene expression. Strikingly, we found that mutations in the conserved intrinsic apoptosis signaling pathway (*ced-9*, *ced-4*, and *ced-3*) suppress the longevity of *isp-1* and *nuo-6* mutants, independently of inhibition of apoptosis. Moreover, unlike apoptosis, which requires the BH3-only protein EGL-1, the suppression of *isp-1* and *nuo-6* requires the BH3-only protein CED-13, which is not required for apoptosis. Treatment with PQ can bypass the need for CED-13, suggesting that mitochondrial ROS acts directly on activation of the pathway, possibly by acting on CED-9 and CED-4, which are associated with mitochondria. Loss of apoptotic signaling also suppresses most of the other phenotypes of *isp-1* and *nuo-6*, such as slow development, slow behaviors, altered gene expression, and sensitivity to heat, but not the primary defects of low oxygen consumption and low ATP levels. The finding that the hypometabolic and hypersensitive phenotypes can be suppressed at the same time as longevity, without suppression of the low oxygen consumption and ATP concentration, indicates that these phenotypes are actively induced by mtROS to protect from mitochondrial dysfunction.

RESULTS

Pro-Longevity mtROS Signaling Induces a Unique Pattern of Gene Expression

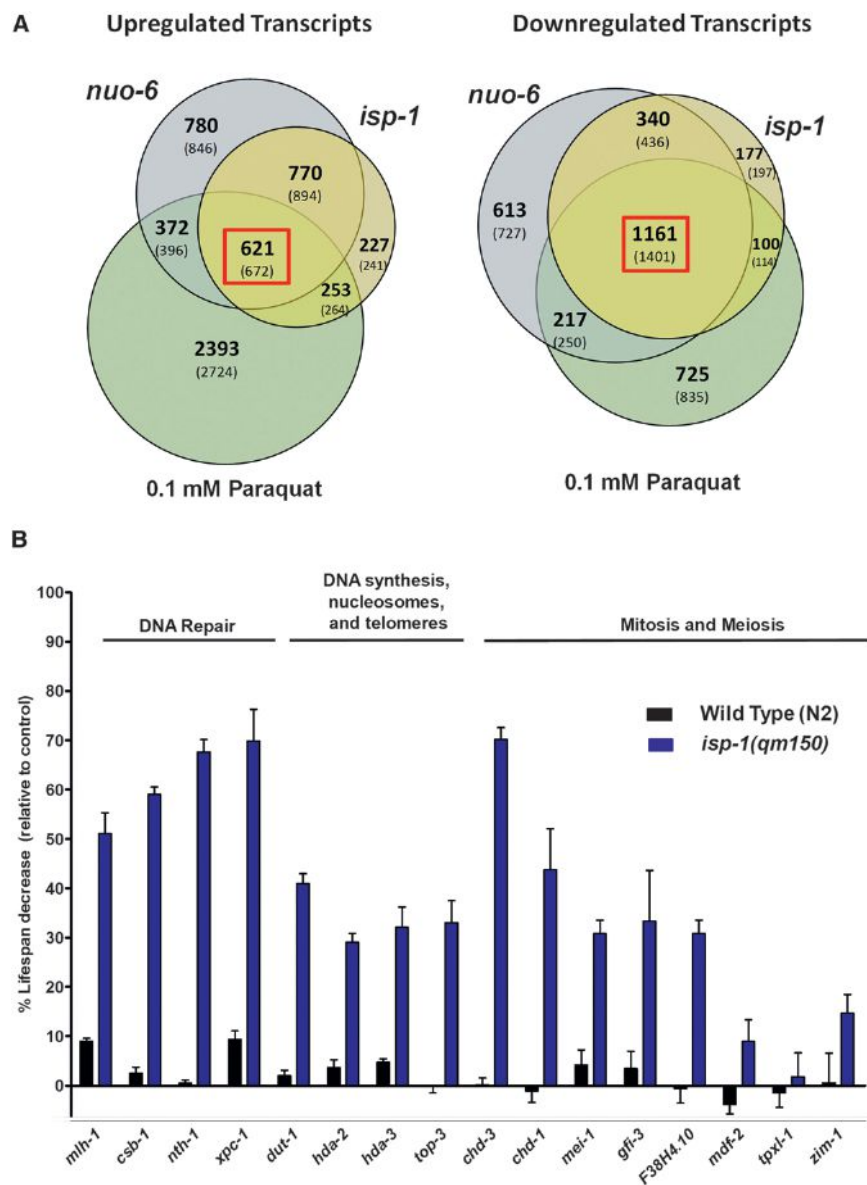
The effects of *isp-1(qm150)* and *nuo-6(qm200)* mutations on longevity are not additive, and a low dose of PQ (0.1 mM)

increases the lifespan of the wild-type, but not of either of the mutants, (Yang and Hekimi, 2010a, b). These observations suggest that a common mechanism underlies the increased longevity in all three conditions. To test this further, we used Affymetrix *C. elegans* microarrays to characterize patterns of gene expression in the two mutants and in wild-type PQ-treated worms. The lists of genes with significantly altered expression overlap considerably (Table S1 available online); 621 genes were upregulated and 1,161 were downregulated in all three conditions (Figure 1A). This confirms that PQ treatment and the two mutations induce common changes in worm physiology. However, the only feature revealed by Gene Ontology (GO)-term analysis was a downregulation of large families of kinases and phosphatases whose expression is linked to the production of sperm (Reinke et al., 2000). GO-term analysis did not reveal any obvious pattern pointing to a specific biological process that could be responsible for the slow aging phenotype (Table S2). In particular, the list of genes upregulated in all three conditions is not significantly enriched in ROS-detoxifying activities or ROS-damage repair activities (Table S3). This strongly suggests that the longevity increase under the three conditions is not the result of an over-compensatory increase in oxidative defenses in response to increased levels of mtROS.

We compared the lists of gene with similar lists obtained by genome-wide expression studies of other mutants and treatments related to the aging process (Table S4). The overlaps were from 1% to 20% for upregulated genes and from 0% to 33% for downregulated genes. The highest overlap was with the short-lived *gas-1(fc21)* mutant. Although *gas-1* is short-lived, it encodes a subunit of a mitochondrial complex I, which is likely the source of the similarities. However, the comparison did not identify a particular process by GO-term analysis (Table S2). Finally, in contrast to a recent study in yeast where mitochondrial ROS signaling ultimately resulted in the specific silencing at subtelomeric loci (Schroeder et al., 2013), we found a uniform distribution of the downregulated loci across all chromosomes (Figure S1). Taken together our findings suggest that the pattern of gene expression induced by elevated mtROS is unique, which is consistent with the observation that PQ treatment is fully or partially additive to the pro-longevity effects of mutations in *daf-2*, *eat-2*, and *clk-1*, and is not fully suppressed by mutations in *daf-16*, *aak-2*, *wwp-1*, *hif-1*, *skn-1*, or *hsf-1* (Yang and Hekimi, 2010a).

The Changes in Gene Expression Are Necessary for the Pro-Longevity Effect of mtROS

To provide a proof-of-principle demonstration of the relevance for lifespan of the observed changes in gene expression, we focused on a small group of genes. The possibility that genome instability is important in determining lifespan remains a strong hypothesis in biogerontology. Furthermore, there are strong links between DNA damage and general stress responses (Ermolaeva et al., 2013). We tested 16 upregulated genes belonging to this group (Figures 1B, S2 and S3). All numerical values and statistics for survival data presented in the paper are provided in Table S5. The knockdown of 3 of the genes in *isp-1* mutants only had a very small effect on lifespan. The knockdown of the 13 other genes



had a much larger effect on the mutant than on the wild-type and the knockdown of 7 of these had virtually no effect on the wild-type but strongly suppressed the longevity of the mutants (Figures 1B, S2 and S3). The fact that the knockdown of at least some of the upregulated genes limits the longevity of *isp-1* without affecting the wild-type strongly suggest that at least some and probably many of the changes in gene expression we observed are necessary for the longevity resulting from mtROS signaling.

The Longevity Response of *isp-1* and *nuo-6*, but Not that of Other Longevity Mutants, Requires the Conserved Intrinsic Apoptotic Signaling Pathway

The intrinsic pathway of apoptosis, which uses conserved signaling proteins, is physically associated with mitochondria,

Figure 1. Whole-Genome Expression Profiling of *isp-1* and *nuo-6* Mutants, and the Wild-Type Treated with 0.1 mM Paraquat

(A) Venn diagrams illustrating the number of significantly upregulated or downregulated transcripts found in each condition tested when compared to untreated wild-type. Bolded numbers represent the actual number of probes whose expression was significantly changed relative to wild-type expression, while numbers in brackets represent the maximum number of different transcripts that could be detected as a result of high homology.

(B) Lifespan changes resulting from treatment of wild-type and *isp-1* mutants with RNAi against genes that are upregulated in all three conditions and whose activities are expected to be involved in genome stability. The majority of genes had large effects on the mutant but no, or very little, effect on the wild-type.

Bars represent the degree of lifespan shortening relative to control and error bars represent SEM. See also Figures S1, S2, and S3; Tables S1, S2, S3, S4, and S6. Numerical values and statistical analyses for all lifespan experiments are presented in Table S5.

and in vertebrates is sensitive to mitochondrial oxidative stress. We therefore tested whether this pathway was involved in the pro-longevity signal in worms by scoring the lifespan of double mutants of *isp-1* and *nuo-6* with *ced-9gf*, *ced-4*, and *ced-3* mutations (Figures 2A–2B, S4A–S4D). The mutations in all three *ced* genes significantly suppressed the longevity of both *isp-1* and *nuo-6*, without having any significant effects on lifespan by themselves. The suppression by *ced-4(n1162)* was consistently the most robust. The suppression by *ced-9(n1950)* was somewhat less effective, possibly because it is a gain-of-function allele and might therefore not be fully equivalent to a loss of *ced-4(n1162)*. The somewhat lesser suppression by *ced-3(n717)* suggests that CED-4 recruits other effectors as well.

We tested possible effects of *ced-4* on other lifespan mutants that had previously been shown to be genetically distinct from *isp-1/nuo-6*, including *eat-2*, *clk-1*, *daf-2*, and *glp-1*. For this, we tested lifespan in double-mutant combination with *ced-4*, but no effects on the lifespan of these mutants were detected (Figures S4E–S4H). In addition, previous findings had suggested that RNAi against subunits of the ETC prolong lifespan by a mechanism that is distinct from that of the genomic mutants *isp-1* and *nuo-6* (Yang and Hekimi, 2010b). We therefore tested RNAi against *isp-1* and *nuo-6* on *ced-4* mutants and, as predicted, *ced-4* did not suppress the longevity induced by the RNAi treatments (Figures S4I and S4J). We conclude that

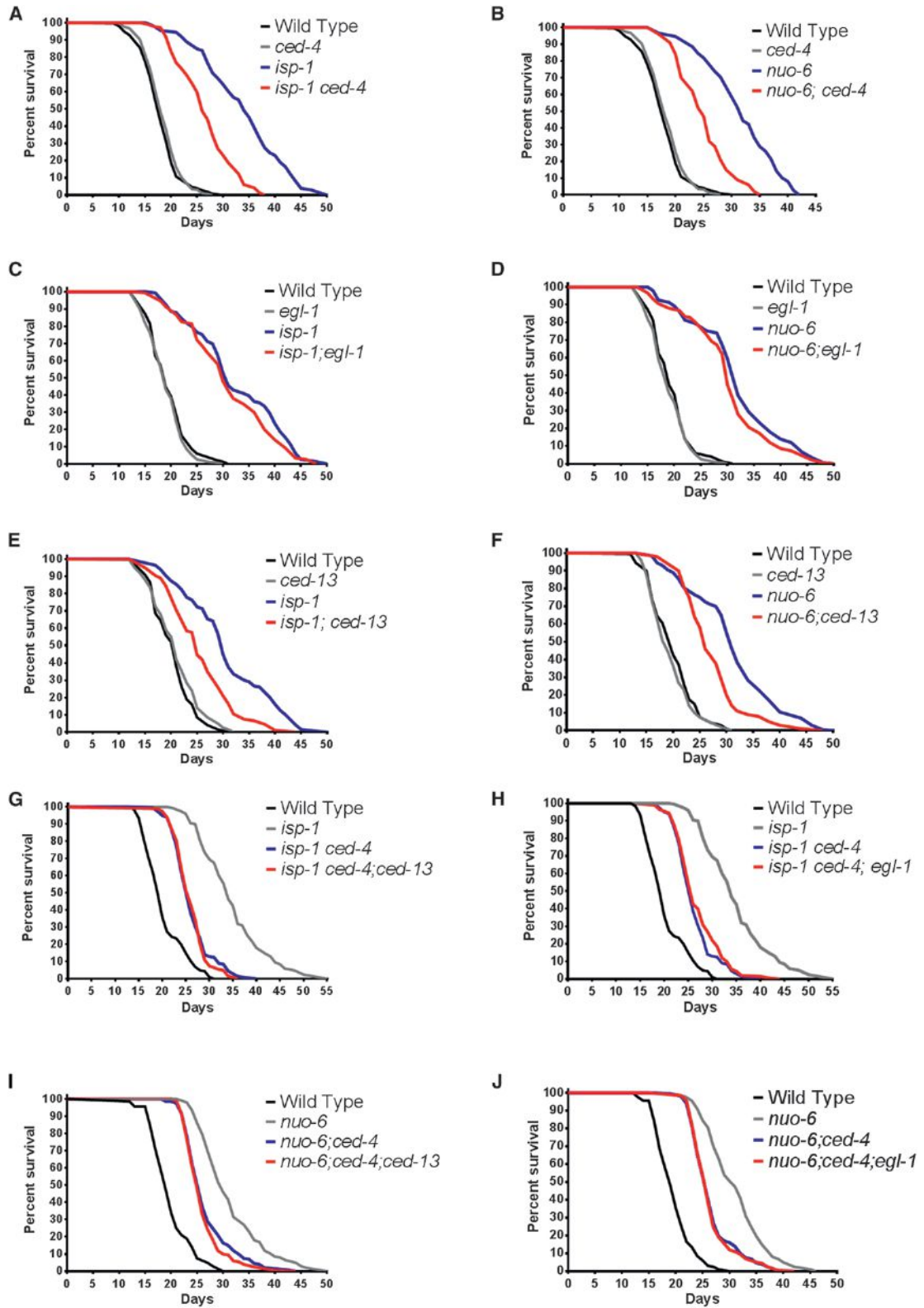


Figure 2. Genetic Interactions between Longevity and Cell Death Genes

(A and B) Effect of *ced-4*(n1162) on the survival of *isp-1*(qm150) and *nuo-6*(qm200).
 (C and D) Effect of *egl-1*(n1084n3082) on the survival of *isp-1* and *nuo-6*.

(legend continued on next page)

the intrinsic apoptotic signaling machinery uniquely mediates the longevity of *isp-1* and *nuo-6*.

The Longevity Response Is Independent of Apoptosis Per Se

As *ced-9gf*, *ced-4*, and *ced-3* affect apoptosis, we scored embryonic and pharyngeal apoptosis in *isp-1* and *nuo-6* mutants as well as in *ced-4*, *isp-1 ced-4*, and *nuo-6;ced-4* double mutants (Table S6). The pattern of apoptosis in the mitochondrial mutants was indistinguishable from the wild-type, and the pattern of apoptosis in the double mutants with *ced-4* was indistinguishable from that produced by the *ced-4* mutation alone, that is, most cell deaths were eliminated. These findings indicated that *isp-1* and *nuo-6* do not affect normal or mutant apoptosis, but they cannot establish whether the normal pattern of apoptosis is necessary for the mutants' increased longevity. For this we turned to the BH3-only protein EGL-1, which is required for all apoptosis in *C. elegans*. We scored both apoptosis and lifespan in *egl-1* mutants as well as in *egl-1;isp-1* and *egl-1;nuo-6* double mutants. As expected, the *egl-1* mutation, like the *ced-4* mutation, abolished apoptosis in all three genotypes (Table S6). However, in contrast to *ced-4*, *ced-9*, and *ced-3*, *egl-1* had no effect at all on lifespan (Figures 2C and 2D). Thus it is not the absence of apoptosis in the intrinsic pathway mutants that suppresses the lifespan of the mitochondrial mutants.

The Activity of the Intrinsic Apoptotic Signaling Pathway on Longevity Requires CED-13, an Alternative BH3-Only Protein

For canonical apoptotic signaling, the intrinsic pathway requires stimulation by a BH3-only protein. CED-13 is the only other protein in *C. elegans* to possess a BH3 domain (Schumacher et al., 2005). CED-13 has been shown to be able to have some effect on somatic apoptosis when overexpressed and is also able to interact with CED-9 in vitro in a way that is similar to that of EGL-1 (Fairlie et al., 2006). However, loss of CED-13 has very limited effects and only on DNA damage-induced germline apoptosis. We found however that the *ced-13(sv32)* mutation suppressed the longevity of *isp-1* and *nuo-6* mutants as efficiently as the mutations in the genes of the core pathway (Figures 2E and 2F). We verified whether CED-13 acted indeed in the same pathway as the other CED proteins by testing whether the effects of *ced-13(sv32)* were additive to those of *ced-4(n1162)* for suppression of the lifespan of *isp-1*. We found that the lifespan of the triple mutants *isp-1 ced-4;ced-13* and *nuo-6;ced-4;ced-13* were indistinguishable from those of the double mutants *isp-1 ced-4* and *nuo-6;ced-4*, respectively (Figures 2G and 2I), indicating that *ced-13* acts in the same pathway as *ced-4*. As expected, *egl-1* had no effect either in triple combinations (Figures 2H and 2J). Thus, rather than EGL-1, CED-13 is the

BH3-only protein that is required for pro-longevity signaling through the intrinsic pathway.

mtROS Act Downstream of CED-13 for Longevity

We first determined if treatment with 0.1 mM PQ (which does lengthen wild-type lifespan) or with 0.5 mM PQ (which is too toxic to lengthen wild-type lifespan) had any effect on apoptosis (Table S6). No effect was found at either concentration, which is consistent with mtROS being capable of regulating the CED-13-dependent activation of the pathway and not apoptosis. We then treated mutants of all four genes (*ced-13*, *ced-9gf*, *ced-4*, and *ced-3*) with 0.1 mM PQ. The effect of PQ on lifespan was almost completely suppressed by *ced-4* and *ced-9*, partially by *ced-3* but not at all by *ced-13* and *egl-1* (Figure 3). This suggested that PQ (and thus mtROS) act downstream of CED-13. As the *ced-13* mutation is capable of suppressing the lifespan of *isp-1* and *nuo-6* mutants, its inability to suppress the longevity induced by PQ suggests that the level of mtROS is insufficient in the *isp-1* and *nuo-6* mutants to trigger the pathway in the absence of stimulation by CED-13 but that the level of mtROS induced by PQ treatment is sufficient to directly activate the mitochondria-associated CED-9 and/or CED-4. Although *ced-4* does not suppress the longevity induced by RNAi against ETC subunits the position of CED-13 upstream of CED-4 and of mtROS could in principle allow it to regulate RNAi-dependent longevity through a parallel pathway. However, no suppression of *isp-1(RNAi)* by *ced-13* or *egl-1* was observed (Figure S5). All further analyses of the pathway described below were conducted with *ced-4* for part of the pathway downstream of ROS activity, with *ced-13* for the part of the pathway upstream of ROS activity, and with *egl-1* as control for apoptosis per se.

Loss of the Intrinsic Pathway Signaling Does Not Suppress Low Oxygen Consumption and ATP Levels

isp-1 and *nuo-6* encode subunits of mitochondrial respiratory complexes and the mutations lead to reduced oxygen consumption (Figure S6A and Table S5). This is likely a primary phenotype directly resulting from altered function of the electron transport chain. Lower electron transport chain function is expected to lead to ATP depletion. We found that ATP levels were low in both mutants and particularly severely in *isp-1* mutants (Figure S6B and Table S5). Neither oxygen consumption nor ATP levels were affected in *ced-4*, *ced-13*, or *egl-1*. To test whether suppression by the *ced* mutations was achieved by restoration of electron transport or ATP levels, we measured oxygen consumption and ATP levels in suppressed double mutants (Figures S6C and S6D and Table S5). No effect on oxygen consumption or ATP levels was observed, indicating that this is not the mechanism by which phenotypic suppression is achieved.

(E and F) Effect of *ced-13(sv32)* on the survival of *isp-1* and *nuo-6*.

(G) Effects of *ced-4* and *ced-13* on *isp-1* survival in the triple mutant combination.

(H) Effects of *ced-4* and *egl-1* on *isp-1* survival in the triple mutant combination.

(I) Effects of *ced-4* and *ced-13* on *nuo-6* survival in the triple mutant combination.

(J) Effects of *egl-1* and *ced-4* on *nuo-6* survival in the triple mutant combination.

See also Table S7; Figures S4 and S5. Numerical values and statistical analyses for all lifespan experiments are presented in Table S5.

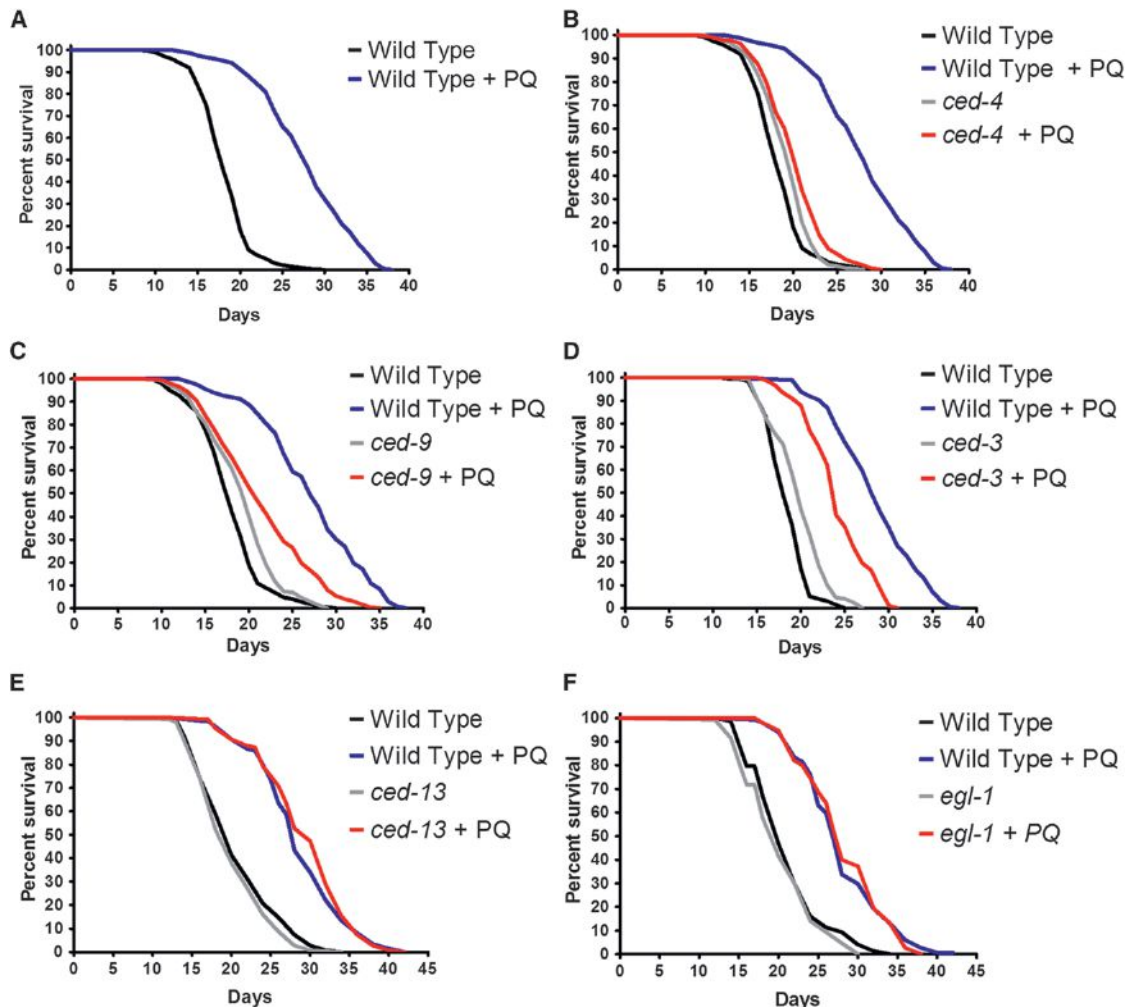


Figure 3. Lifespan Extension by 0.1 mM PQ Requires the Intrinsic Apoptosis Pathway

(A) Effect of 0.1 mM PQ treatment on the wild-type.

(B–F) Effects of 0.1 mM PQ treatment on: (B) *ced-4*(n1162), (C) *ced-9*(n1950 *gf*), (D) *ced-3*(n717), (E) *ced-13*(sv32), and (F) *egl-1*(n1084n3082). See also Table S5. Numerical values and statistical analyses for all lifespan experiments are presented in Table S5.

Loss of the Intrinsic Pathway Suppresses the Hypometabolic and Gene Expression Phenotypes of *isp-1* and *nuo-6* Mutants

The *isp-1* and *nuo-6* mutations induce other phenotypes in addition to an increase in lifespan, including slow embryonic and postembryonic development, as well as slow behaviors such as pumping, defecation, and thrashing. Mutations in *ced-13* and *ced-4*, but not *egl-1*, partially suppressed all these phenotypes of both *isp-1* and *nuo-6*, (Figure 4 and Table S5). The fact that the *egl-1* mutation, which abolishes cell death but has no effect on lifespan, had no effect on any of the phenotypes implies, as for longevity, that these phenotypes do not depend on changes in apoptosis. One phenotype that is not rescued and is in fact worsened by *ced-4* is brood size (Figure 4D). This suggests that the germline phenotype due to mitochondrial dysfunction does not involve the longevity pathway we have uncovered. Recent findings suggest that

apoptosis in the germline is necessary for oocyte quality (An-dux and Ellis, 2008), which might be the cause of the reduction in brood size.

As described above, the *isp-1* and *nuo-6* mutations result in many changes in gene expression relative to wild-type. We determined whether *ced-4*(n1162), which suppresses the increased lifespan of the mutants as well as most other phenotypes also suppressed the gene expression changes. Using Affymetrix *C. elegans* microarrays as before, we compared the changes in gene expression in *isp-1 ced-4* and *nuo-6; ced-4* double mutants relative to wild-type to those in the single mutants relative to wild-type (Table S1). The *ced-4* mutation partially suppressed both upregulated and downregulated changes in both *isp-1* and *nuo-6*. 57% of the genes upregulated in *nuo-6* were back to wild-type levels in *nuo-6; ced-4*, and 36% of the genes upregulated in *isp-1* were back to wild-type level in *isp-1 ced-4*. Similarly *ced-4* suppressed the

downregulation of 62% of the genes in the case of *nuo-6* but only 18% in the case of *isp-1*. GO-term analysis of the list of genes affected by *ced-4* in both mutants showed a meaningful enrichment only in the kinases and phosphatases linked to sperm production that were downregulated in the mutants (Table S2). However, as the low brood size of the mutants was not suppressed by *ced-4* the significance of this observation is unclear.

Constitutive Activation of the CED Pathway Leads to Heat-Stress Hypersensitivity

To further investigate the hypothesis that the CED pathway is a stress pathway that responds to mitochondrial dysfunction, we examined the effects of a severe heat stress. To establish the level of stress on mitochondrial function produced by this treatment we measured ATP levels after the animals had experienced 37°C for 1.5 hr. The stress led to a severe ATP depletion in all genotypes (Figure 5A and Table S5). However, the depletion was substantially more severe for the two mitochondrial mutants. While the wild-type, *ced-13*, *ced-4*, and *egl-1* experienced an ~30% drop, *isp-1* and *nuo-6* lost >50% of their already low ATP levels. Surprisingly, but consistent with our other findings, *ced-13* and *ced-4*, but not *egl-1*, suppressed the severity of this effect (Figure 5B and 5C, and Table S5). To explore this further, we treated young adult for 4 hr at 37°C and scored survival (Treinin et al., 2003). Treatment of all genotypes with this longer heat stress decreased survival, but much more severely in the mitochondrial mutants. Treatment of the wild-type, *ced-13*, *ced-4*, and *egl-1* resulted in ~80% survival but the treatment killed virtually all *isp-1* or *nuo-6* mutants (Figure 5D and Table S5). Again, *ced-13* or *ced-4*, but not *egl-1*, suppressed the mitochondrial mutants such that the double mutants had much higher survival rates (40%–50%). Taken together these observations suggest that resources required for acute survival are not available in animals in which the CED pathway is strongly and constitutively activated by mitochondrial dysfunction because they have been diverted to processes involved in long-term survival.

CED-13 Acts Upstream of mtROS for All Phenotypes

We focused on *isp-1* to explore further the epistatic relationships in the *ced-13*-dependent pathway. Previous observations indicated that the longevity effect of PQ is not additive to *isp-1* (Yang and Hekimi, 2010a), which we have confirmed (Table S5). On the other hand, the observation that *ced-13* does not suppress the longevity induced by PQ treatment (Figure 3), places its action upstream of that of mtROS. This suggests that PQ should suppress the suppressed longevity of *isp-1;ced-13* double mutants, which is what we observed (Figure 6A). Similarly, the slow defecation, pumping, and thrashing of *isp-1* mutants are partially suppressed by *ced-13* and by *ced-4* (Figures 4A–4C). If mtROS act downstream of *ced-13* but upstream of *ced-4*, PQ treatment should suppress the suppressive effect of *ced-13* but not that of *ced-4*, which is what we observed (Figures 6B–6D). Finally, *ced-13* and *ced-4* partially suppress the lethality induced by heat treatment (Figure 5D). Thus treatment with PQ should partially suppress the lethality suppression of *ced-13* but not that of *ced-4*, which is what we observed (Figure 6E).

SOD-3 Is Involved in Generating the Pro-Longevity mtROS Signal

Treatment with PQ and altered ETC function in the mitochondrial mutants are believed to generate superoxide (Yang and Hekimi, 2010a). However, only peroxide is believed to cross membranes readily, which might be necessary to affect the CED pathway proteins, which are associated with the outer mitochondrial membrane. The main mitochondrial superoxide dismutase SOD-2 is not required to generate the pro-longevity ROS signal, as PQ treatment can further lengthen the already long lifespan of *sod-2* mutants (Van Raamsdonk and Hekimi, 2009), which we have confirmed (Table S5). *sod-3*, which encodes a minor, inducible, mitochondrial superoxide dismutase very similar to SOD-2 in structure, was the only ROS handling enzyme whose expression was found to be increased by microarray analysis (Table S3). Interestingly, we found that *sod-3* was absolutely required for the pro-longevity signal induced by PQ treatment as this treatment was without effect on longevity in the *sod-3(tm760)* knockout background. (Figure 6F). This suggests that peroxide is the necessary intermediate for pro-longevity signaling. The specificity of the action of SOD-3 could be achieved by specific submitochondrial localization in relation to the outer membrane localization of CED-4/CED-9 complexes. Interestingly, both SODs have recently been found to be closely associated with the ETC (Suthammarak et al., 2013).

DISCUSSION

A Model for Lifespan Determination by Mitochondrial Dysfunction and mtROS Signaling

Previous studies have suggested that the mechanism of lifespan extension operating in the long-lived *isp-1* and *nuo-6* mutants is based on increased mtROS generation due to mitochondrial dysfunction. Here, we provide further evidence for this by showing that PQ treatment and the mutations induce a common pattern of changes in gene expression which is at least in part required for longevity. Most importantly, we show that the mtROS signal requires the activity of the intrinsic apoptosis signaling pathway (including CED-9, CED-4, and CED-3), activated by a dedicated BH3-only protein, CED-13 (Figure 7). However, the recruitment of this pathway by mtROS and the consequences on longevity are fully independent of apoptosis per se. The known association of CED-9 and CED-4 with mitochondria; their involvement in sensing mtROS in vertebrates; and our findings from epistasis analysis that PQ, and therefore ROS, acts immediately downstream of CED-13 suggest that this pathway is the most immediately affected by mtROS and likely functions upstream of other pathways that might also be engaged (Lee et al., 2010; Walter et al., 2011). We found that loss of CED-3 suppresses less efficiently than loss of CED-4, suggesting that CED-4 could have other effectors in addition to CED-3, which is consistent with the existence of CED-3-independent activities of CED-4. ROS-independent activation by CED-13 provides the opportunity for input from upstream signals to modulate the sensitivity of the pathway to mtROS. For example, *ced-13* expression appears to be regulated by *cep-1*, the *C. elegans* homolog of p53 (Schumacher et al., 2005). Furthermore, *cep-1* appears to affect lifespan modulation by

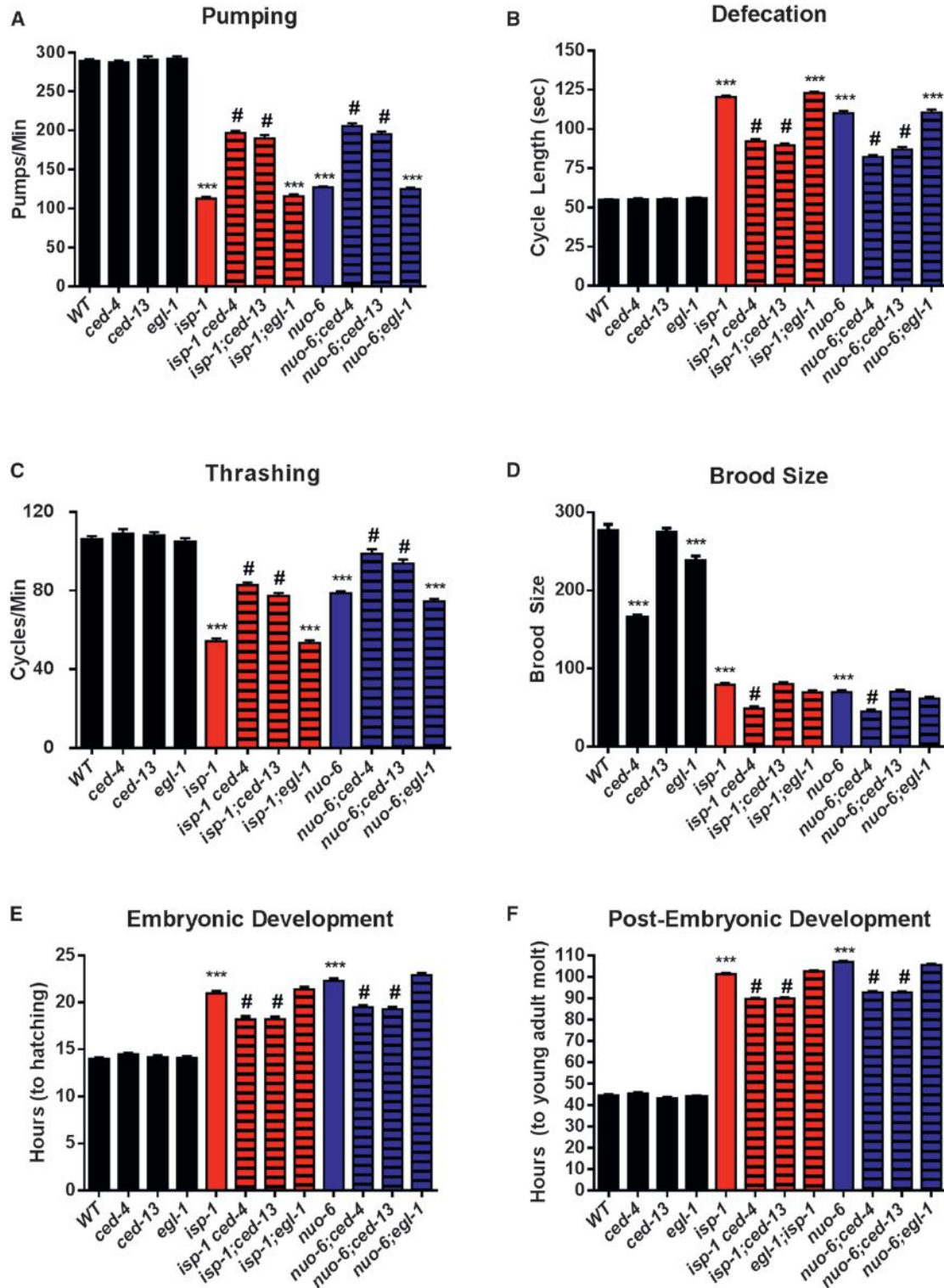


Figure 4. The Behavioral and Growth Defects of *isp-1(qm150)* and *nuo-6(qm200)* Mutants Are Partially Suppressed by *ced-4(n1162)* and *ced-13(sv32)* but Not *egl-1(n1084n3082)*

(A) Pharyngeal pumping rate. *isp-1* and *nuo-6* pump at a significantly slower rate than the wild-type. Loss of *ced-4* or *ced-13* but not *egl-1* partially rescues the slow pumping rates of *isp-1* and *nuo-6*. None of the cell death genes affects the pumping rate of the wild-type.

(B) Defecation cycle length. *isp-1* and *nuo-6* mutants have a significantly lengthened defecation cycle length. Loss of *ced-4* or *ced-13* but not *egl-1* partially rescues the slow defecation phenotype of *isp-1* and *nuo-6*. None of the cell death genes affect the defecation cycle length of the wild-type.

(legend continued on next page)

mitochondrial dysfunction in a complex manner (Baruah et al., 2014; Ventura et al., 2009). Thus the action of CED-13 might have affinities with that of BH3-only proteins such as PUMA and NOXA, which are regulated by p53 (Nakano and Vousden, 2001; Oda et al., 2000).

Loss of the CED pathway cannot rescue the low oxygen consumption and the low ATP levels. This is expected as *isp-1* and *nuo-6* mutations are point mutations in subunits of the mitochondrial respiratory chain and the ATP and oxygen phenotypes are likely primary defects that cannot be fixed. However, the loss of the CED pathway abolishes a large part of the increased longevity and several other phenotypes of the mutants, such as slow growth and behavior, a large subset of the changes in gene expression, and the hypersensitivity to heat stress. Taken together this suggests that mtROS acts in the mutants through the CED pathway to trigger phenotypic changes that alleviate the consequences of the primary defects, including protective changes that ultimately result in increased lifespan. Interestingly, the slow growth and behavioral phenotypes are the type of effects expected from mitochondrial dysfunction and the resulting low ATP production. Even slow aging can be postulated to result from low energy production, based on the observation that cold temperature and low metabolic rates are associated with longer lifespans. Thus it appears that the mtROS/CED pathway amplifies phenotypes that would be produced to a lesser extent by the immediate effects of mitochondrial dysfunction on energy metabolism alone. This could be a protective mechanism that, in the wild-type, allows the mitochondria to recover their function when the dysfunction is only transient, sparing ATP and rerouting its use to protective mechanisms (Figure 7). In this model, longevity in the mutants is the result of both a slowing down of ATP-dependent processes that limit lifespan and by an abnormally intense activation of the protective pathway induced by elevated mtROS acting through the CED cascade. This model is consistent with the finding that, in contrast to the mutants that are only partially suppressed by *ced-4* and *ced-9gf*, the longevity induced by PQ, which does not affect oxygen consumption nor ATP levels (Yang and Hekimi, 2010a), can be almost completely suppressed by *ced-4* and *ced-9gf* (Figure 3).

Activation of the Apoptotic Pathway by mtROS

In vertebrates mtROS are involved in the regulation of apoptosis by the intrinsic mitochondrial pathway. However, no clear role

for mtROS in *C. elegans* apoptosis has yet been discovered. We confirmed this by showing that neither mtROS-generating mitochondrial mutations nor PQ treatment affect the extent of somatic apoptosis (Table S5). Two biological roles for apoptosis have been proposed: a role in shaping the development of multicellular organisms by eliminating cells that are not needed, and a protective role by eliminating cells that are damaged. In the somatic lineage of worms, apoptosis appears to have a developmental role but in the germline it might have a protective role for fertility by eliminating damaged gamete precursors (Gartner et al., 2008) and reallocating resources to produce high-quality gametes (Andux and Ellis, 2008). In vertebrates, the mtROS-sensitive intrinsic pathway is part of a protective program and participates in the elimination of defective cells, including cells with defective mitochondria. Our findings suggest that in *C. elegans*, the intrinsic apoptotic machinery, including CED-9, CED-4, and CED-3, is also sensitive to mtROS when stimulated by the BH3-only protein CED-13. Stimulation by CED-13 leads to the activation of a protective program but not to apoptosis. How stimulation of the same pathway by CED-13 and EGL-1 results in different outcomes is unknown at the present time but likely involves cell type-specific differences. A program of protective apoptosis similar to that in vertebrates is probably not possible in *C. elegans* because of its very small number of postmitotic cells. Losing damaged cells is not an option without losing important functions and bodily integrity. However, stimulating protective and repair mechanisms in the face of injury remains useful. Thus it appears that what is conserved from nematode to vertebrates is the use of the proteins of the intrinsic pathway to transduce a mtROS signal that stimulates a protective response to mitochondrial dysfunction. It is interesting to speculate whether a nonapoptotic protective function of the intrinsic pathway is also acting in vertebrate postmitotic cells such as neurons and could have a role in protecting from neurodegeneration.

EXPERIMENTAL PROCEDURES

Strains and Genetics

All strains were maintained by standard methods, at 20°C, on solid agar (NGM plates), fed *E. coli* OP50, and grown continuously. The following genotypes were used: Bristol N2 (wild-type); LGI: *nuo-6(qm200)*, *sod-2(ok1030)*; LGII: *eat-2(ad1116)*; LGIII: *daf-2(e1370)*, *clk-1(qm30)*, *ced-4(n1162)*, *ced-9(n1950)*; *glp-1 (e2141ts)*; LGIV: *isp-1(qm150)*, *ced-3(n1717)*; LGV: *egl-1(n1084n3082)*; LGX: *ced-13(sv32)*, *sod-3(tm783)*.

(C) Thrashing rate. *isp-1* and *nuo-6* mutants have a significantly decreased rate of thrashing. Loss of *ced-4* or *ced-13* but not *egl-1* partially rescues the slow thrashing phenotype of *isp-1* and *nuo-6*. None of the cell death genes affect the thrashing rate of the wild-type.

(D) Brood size (the number of progeny produce by self-fertilization of a single hermaphrodite). Both *isp-1* and *nuo-6* have significantly reduced brood sizes. The reduction in brood size was enhanced by loss of *ced-4* but not *ced-13* or *egl-1*. Loss of *ced-4*, and to a lesser degree *egl-1*, also significantly reduced brood size the wild-type background.

(E) Length of embryonic development. The time taken for a 2-cell stage embryo to reach hatching is significantly increased in *isp-1* and *nuo-6* mutants. Loss of *ced-4* and *ced-13* but not *egl-1* partially rescues this phenotype of *isp-1* and *nuo-6*. None of the cell death genes affect the rate of embryonic development of the wild-type.

(F) Length of postembryonic development. The time taken for freshly hatched L1-stage larva to reach the young adult stage is significantly increased in *isp-1* and *nuo-6* mutants. Loss of *ced-4* and *ced-13* but not *egl-1* partially rescues this phenotype of *isp-1* and *nuo-6*. None of the cell death genes affect the rate of postembryonic development of the wild-type. Bars represent the mean value of 25 animals. Error bars represent standard error of the mean. Significance was determined using a Student's t test (***) denotes $p < 0.0001$ as compared to the wild-type; # denotes $p < 0.0001$ as compared to either *isp-1* or *nuo-6* single mutants).

Complete numerical values and statistics are provided in Table S5.

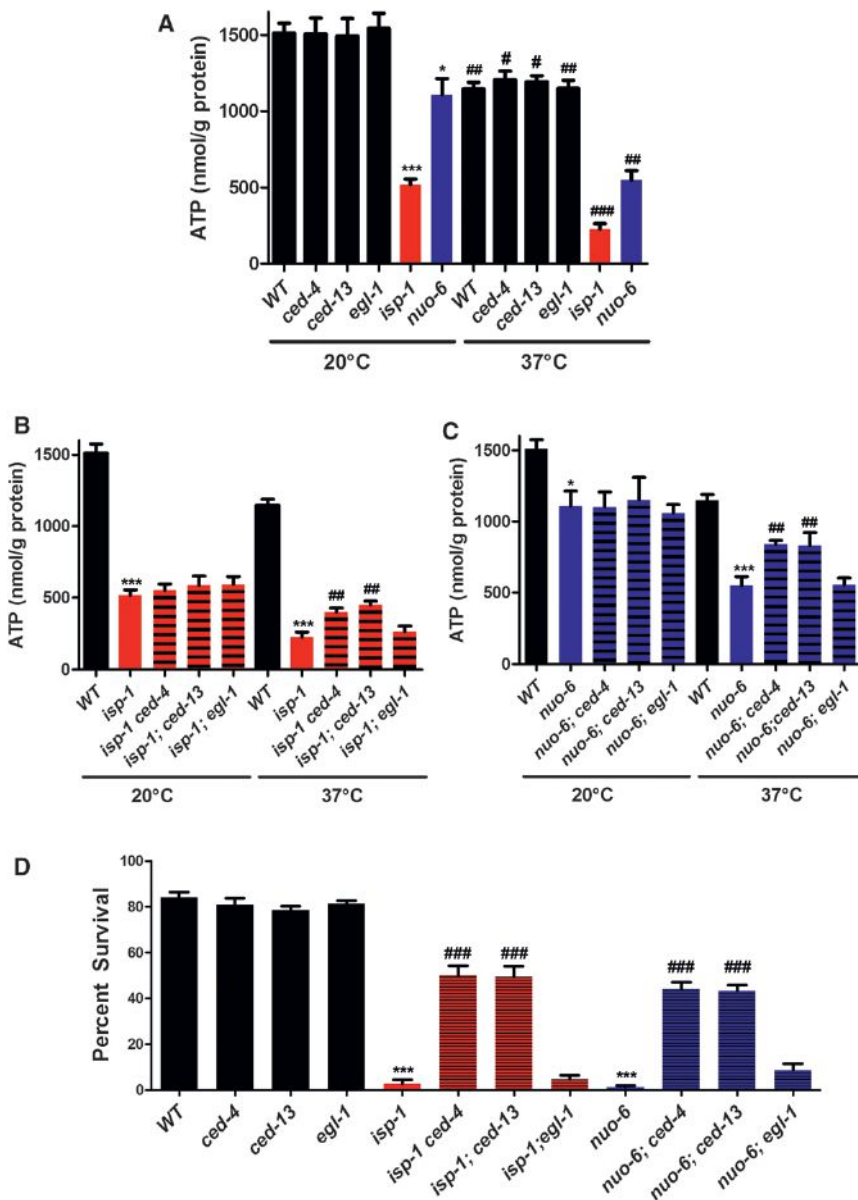


Figure 5. Effects of *isp-1*, *nuo-6* and Cell Death Genes on ATP Levels and Survival under Heat Stress

(A) *isp-1* and *nuo-6* mutants, but not *ced-4*, *ced-13* or *egl-1* mutants exhibit reduced ATP levels when grown under standard conditions (20°C). Acute exposure (1.5 hr) to heat (37°C) reduces the ATP levels of all genotypes.

(B) Loss of *ced-4*, *ced-13* or *egl-1* does not affect ATP levels in *isp-1* mutants at 20°C. However, the reduction in ATP levels after heat stress is significantly reduced in *ced-4; isp-1* and *isp-1; ced-13*, but not *egl-1; isp-1* double mutants compared to *isp-1(qm150)*.

(C) Mutations in *ced-4*, *ced-13* and *egl-1* do not affect ATP levels in *nuo-6* mutants at 20°C. However, the reduction in ATP levels after heat stress is significantly less in *ced-4; nuo-6* and *nuo-6; ced-13*, but not *egl-1; isp-1* double mutants compared to *isp-1(qm200)*.

(D) Exposure to heat stress for 4 hr significantly decreases the survival of all genotypes, but much more severely for *isp-1(qm150)* and *nuo-6(qm200)* mutants. However, loss of *ced-4* or *ced-13* but not *egl-1* strongly rescues the survival of *isp-1* and *nuo-6* mutants.

Significance was determined using a Student's t test (A) * denotes $p < 0.05$, *** denotes $p < 0.0001$ as compared to the wild-type. # denotes $p < 0.05$ compared to the control at 20°C, ## denotes $p < 0.05$ compared to the wild-type at 37°C. ### denotes $p < 0.005$ compared to the wild-type at 37°C. (B) *** denotes $p < 0.0005$ relative to the wild-type control, ## denotes $p < 0.05$ relative to *isp-1(qm150)* at 37°C. (C) * denotes $p < 0.05$ as compared to the wild-type control at 20°C, *** denotes $p < 0.001$ as compared to the wild-type control at 37°C, ## denotes $p < 0.005$ as compared to the *nuo-6(qm200)* at 37°C. Error bars represent standard error of the mean. Complete numerical values and statistics are provided in Table S5.

Lifespan Analysis

All lifespan measurements were performed at 20°C and set up using a 4 hr limited lay. An experimental pool of 50 animals was used for each genotype in any given experiment, and lost or animals that died prematurely were replaced from a backup pool. Statistical analysis was performed using GraphPad Prism (v5.0) and Student's t tests in Microsoft Excel.

Paraquat Treatment

Paraquat (Sigma-Aldrich, St. Louis, USA) was added to NGM plates at a final concentration of 0.1 mM, 0.15 mM or 0.5 mM. OP50 grown on regular NGM plates was transferred onto NGM-PQ plates using a platinum pick instead of seeding directly onto the NGM-PQ plates. Control NGM plates containing no PQ were treated in a similar fashion.

Gene Expression Studies

A total of 2,000 synchronized young adults grown at 20°C on NGM plates were collected, frozen in liquid nitrogen, and total RNA was extracted using a

QIAGEN RNeasy Tissue Microarray Mini kit. Total RNA samples were analyzed for concentration and dissolution spectrophotometrically using a Nanodrop ND-100 Spectrophotometer. RNA samples were processed by Génome Québec (Montreal) and hybridized onto Affymetrix C. elegans GeneChips. Raw expression data were analyzed using FlexArray v1.6.1 (Génome Québec) and normalized using the GC-RMA method. Comparisons of each genotype were compared to the wild-type using the Empirical Base (Wright & Simon) algorithm and fold changes were represented on a log₂ scale. A threshold of $p < 0.05$ and a fold change of 1.3 (log₂) was set to determine differentially expressed targets.

Comparisons of Gene Expression Patterns

Comparisons made to other published data sets were done using raw Affymetrix data sets wherever possible (obtained from NCBI Gene Expression Omnibus [GEO] (<http://www.ncbi.nlm.nih.gov/geo/>)). Raw data were imported to FlexArray and handled identically to the data that was generated in this study. For studies that did not deposit their data to GEO or used technologies other than Affymetrix, comparisons of gene lists (upregulated and downregulated transcripts) were conducted using Microsoft Excel.

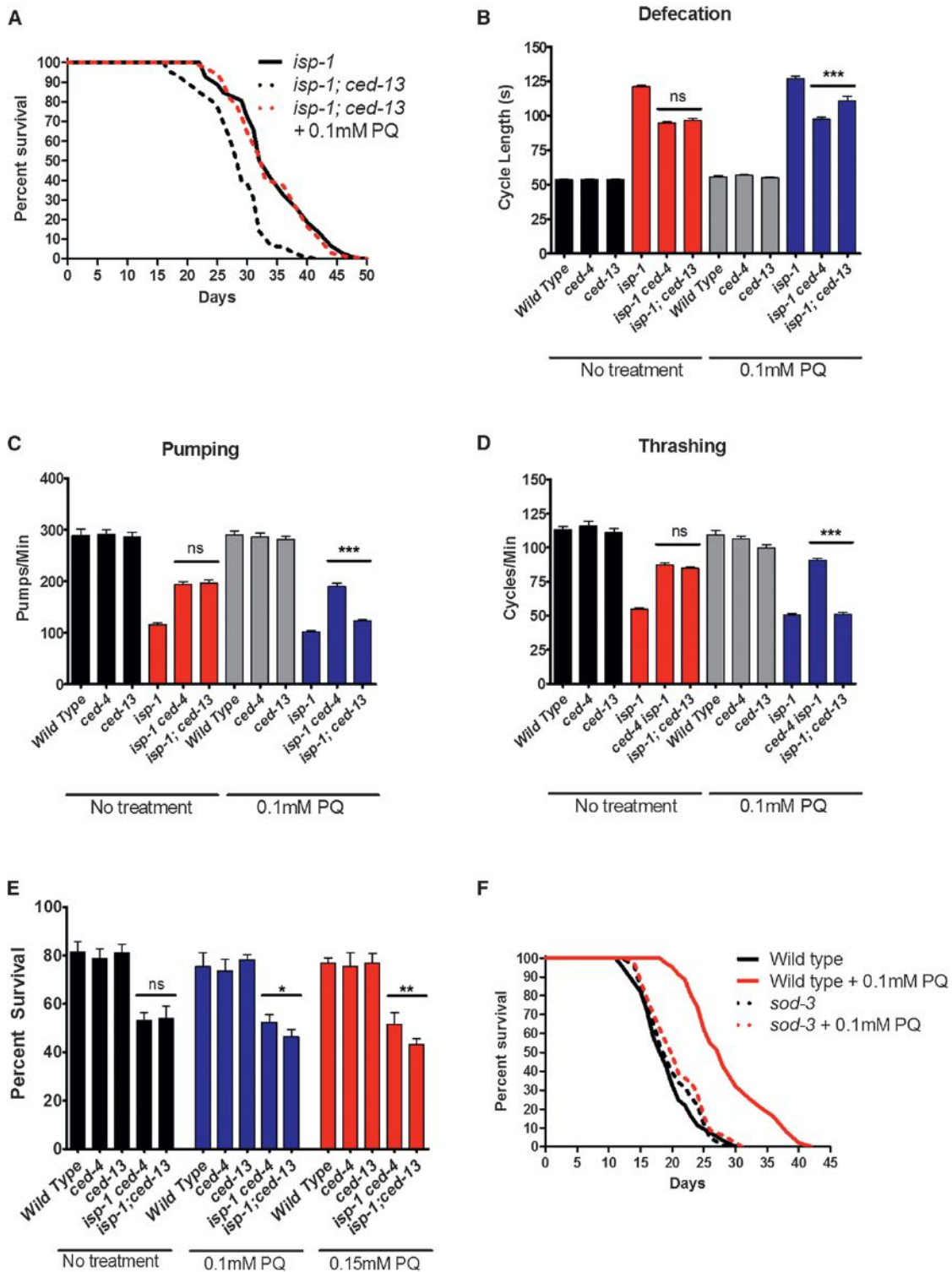


Figure 6. Epistatic Relationships between Genotypes and Treatments

(A) Treatment of *isp-1;ced-13* with 0.1 mM PQ rescues lifespan to the *isp-1* level ($n > 50$, $p < 0.0001$ for the difference between treated and untreated double mutant).

(B) Treatment with 0.1 mM PQ does not affect the defecation of *isp-1; ced-4* but partially restores the defecation of *isp-1;ced-13* toward the *isp-1* level ($n = 25$).

(C) Treatment with 0.1 mM PQ does not affect the pumping rate of *isp-1; ced-4* but partially restores *isp-1;ced-13* pumping toward the *isp-1* level ($n = 10$).

(D) Treatment with 0.1 mM PQ does not affect the thrashing rate of *isp-1; ced-4* but partially restores *isp-1;ced-13* thrashing toward the *isp-1* level ($n = 15$).

(legend continued on next page)

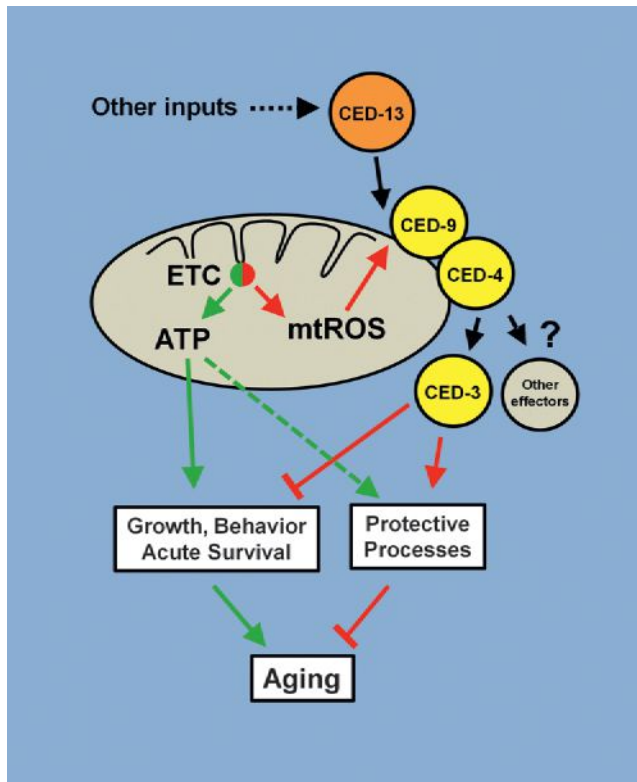


Figure 7. A Model for the Regulation of Lifespan by mtROS Signaling through the Intrinsic Apoptosis Pathway

The intrinsic apoptosis pathway (composed of CED-9, CED-4, and CED-3) is sensitive to mtROS from the ETC when it is activated by the alternative BH3-only protein CED-13. Mitochondrial dysfunction leads to an increase in mtROS which activates the CED signaling pathway to reduce ATP usage and redistribute it to protective rather than active functions. We propose that the mitochondrial dysfunction in *isp-1(qm150)* and *nuc-6(qm200)* mutants induces the mutant phenotypes, including longevity, both by directly lowering ATP generation and by stimulating mtROS signaling to alter ATP usage. In the wild-type this mechanism could provide a protective role in case of transient mitochondrial dysfunction or nutrient shortage. In the mutants its continuous action leads to the mutant phenotypes, including longevity.

Gene Ontology Term Analysis

GO-term analysis was performed using Cytoscape (v2.8.3) and the BiNGO plugin (v2.44). A hypergeometric test using the Benjamini & Hochberg false discovery rate (FDR) correction was implemented at a significance level of 0.05.

Measurement of Apoptosis

Quantification of corpses or cells was performed as previously described (Lu et al., 2009; Schwartz, 2007).

Whole-Worm Phenotypes

All phenotypes were measured as before (Yang and Hekimi, 2010b).

Oxygen Consumption

Mixed populations of worms were collected and washed 3x in M9 to a final volume of 50 μ L of packed worms. A total of 25 μ L of worms were then resus-

ended to a final volume of 50 μ L using M9 buffer and loaded into a chamber of an Oroboros Oxygraph-2K. The remaining 25 μ L of worms were freeze-thawed 3x in liquid nitrogen and resuspended in lysis buffer for immediate determination of protein concentration by a BCA Protein Assay kit (Thermo Scientific, Rockford, USA).

ATP Measurements

Young adult populations were collected using a 4 hr limited lay. Worms were picked and washed three times in M9. Worm pellets were subjected to 3 cycles of freeze-thaw using liquid nitrogen and subsequently spun down for 15 min at top speed. The resulting supernatant was assayed using an ATP Determination kit (Life Technologies, Carlsbad, USA). Protein concentrations were determined as described above.

Heat Stress Assays

Young adults were picked onto NGM plates that were preheated to 37°C and incubated for 4 hr at 37°C. Animals were allowed to recover for 30 min and scored for viability. For ATP measurements after heat stress, mixed populations were transferred onto preheated NGM plates and incubated for 1.5 hr at 37°C. Animals were then collected and washed three times with M9 and flash frozen and stored in liquid nitrogen. ATP measurements were performed as described above. For experiments performed using paraquat, paraquat plates were made as described and worms were grown on paraquat for one generation. Young animals that were grown on paraquat were subsequently assayed on preheated paraquat plates.

ACCESSION NUMBERS

The GEO accession number for all gene array data in this paper is GSE54024.

SUPPLEMENTAL INFORMATION

Supplemental Information includes six figures and seven tables and can be found with this article online at <http://dx.doi.org/10.1016/j.cell.2014.02.055>.

ACKNOWLEDGMENTS

We thank Robyn Branicky for thoughtfully commenting on the manuscript, Eve Bigras for technical assistance, and Steve Hodgkinson for technical advice. Some strains were provided by the CGC, which is funded by NIH Office of Research Infrastructure Programs (P40 OD010440). The work was funded by grants from the Canadian Institutes of Health Research to S.H.: MOP-114891, MOP-123295, MOP-97869 and INE-117889 (through the CoEN initiative (www.coen.org), as well as by McGill University. S.H. is Strathcona Chair of Zoology and Campbell Chair of Developmental Biology.

Received: October 7, 2013

Revised: January 14, 2014

Accepted: February 19, 2014

Published: May 8, 2014

REFERENCES

- Andux, S., and Ellis, R.E. (2008). Apoptosis maintains oocyte quality in aging *Caenorhabditis elegans* females. *PLoS Genet.* *4*, e1000295.
- Baruah, A., Chang, H., Hall, M., Yuan, J., Gordon, S., Johnson, E., Shtessel, L.L., Yee, C., Hekimi, S., Derry, W.B., and Lee, S.S. (2014). CEP-1, the *Caenorhabditis elegans* p53 homolog, mediates opposing longevity outcomes in mitochondrial electron transport chain mutants. *PLoS Genet.* *10*, e1004097.

(E) Treatment with 0.1 mM and 0.15 mM PQ decreases the acute survival of *isp-1;ced-13* worms but not of *isp-1 ced-4* at 37°C (for 4 hr). Significance for all experiments was determined using the Student's t test (* denotes $p < 0.05$, ** denotes $p < 0.01$, *** denotes $p < 0.001$).

(F) Treatment with 0.1 mM PQ increases wild-type lifespan but not *sod-3(tm783)* lifespan ($n = 150$, $p < 0.0001$ for the difference between the wild-type and *sod-3* treated with PQ). Error bars represent mean + SEM. See also Figure S6. Complete numerical values and statistics are provided in Table S5.

- Dasgupta, N., Patel, A.M., Scott, B.A., and Crowder, C.M. (2007). Hypoxic preconditioning requires the apoptosis protein CED-4 in *C. elegans*. *Curr. Biol.* *17*, 1954–1959.
- Dillin, A., Hsu, A.L., Arantes-Oliveira, N., Lehrer-Graiwer, J., Hsin, H., Fraser, A.G., Kamath, R.S., Ahringer, J., and Kenyon, C. (2002). Rates of behavior and aging specified by mitochondrial function during development. *Science* *298*, 2398–2401.
- Doonan, R., McElwee, J.J., Matthijssens, F., Walker, G.A., Houthoofd, K., Back, P., Matscheski, A., Vanfleteren, J.R., and Gems, D. (2008). Against the oxidative damage theory of aging: superoxide dismutases protect against oxidative stress but have little or no effect on life span in *Caenorhabditis elegans*. *Genes Dev.* *22*, 3236–3241.
- Durieux, J., Wolff, S., and Dillin, A. (2011). The cell-non-autonomous nature of electron transport chain-mediated longevity. *Cell* *144*, 79–91.
- Ermolaeva, M.A., Segref, A., Dakhovnik, A., Ou, H.L., Schneider, J.I., Utermöhlen, O., Hoppe, T., and Schumacher, B. (2013). DNA damage in germ cells induces an innate immune response that triggers systemic stress resistance. *Nature* *501*, 416–420.
- Fairlie, W.D., Perugini, M.A., Kvangsakul, M., Chen, L., Huang, D.C., and Colman, P.M. (2006). CED-4 forms a 2 : 2 heterotetrameric complex with CED-9 until specifically displaced by EGL-1 or CED-13. *Cell Death Differ.* *13*, 426–434.
- Felkai, S., Ewbank, J.J., Lemieux, J., Labbé, J.C., Brown, G.G., and Hekimi, S. (1999). CLK-1 controls respiration, behavior and aging in the nematode *Caenorhabditis elegans*. *EMBO J.* *18*, 1783–1792.
- Feng, J., Bussi re, F., and Hekimi, S. (2001). Mitochondrial electron transport is a key determinant of life span in *Caenorhabditis elegans*. *Dev. Cell* *1*, 633–644.
- Galluzzi, L., Joza, N., Tasdemir, E., Maiuri, M.C., Hengartner, M., Abrams, J.M., Tavernarakis, N., Penninger, J., Madeo, F., and Kroemer, G. (2008). No death without life: vital functions of apoptotic effectors. *Cell Death Differ.* *15*, 1113–1123.
- Gartner, A., Boag, P.R., and Blackwell, T.K. (2008). Germline survival and apoptosis. *WormBook*, 1–20, ed. The *C. elegans* Research Community, *WormBook*, <http://dx.doi.org/10.1895/wormbook.1.145.1>, <http://www.wormbook.org>.
- Heidler, T., Hartwig, K., Daniel, H., and Wenzel, U. (2010). *Caenorhabditis elegans* lifespan extension caused by treatment with an orally active ROS-generator is dependent on DAF-16 and SIR-2.1. *Biogerontology* *11*, 183–195.
- Hekimi, S., Lapointe, J., and Wen, Y. (2011). Taking a “good” look at free radicals in the aging process. *Trends Cell Biol.* *21*, 569–576.
- Lapointe, J., and Hekimi, S. (2010). When a theory of aging ages badly. *Cell. Mol. Life Sci.* *67*, 1–8.
- Lee, S.S., Lee, R.Y., Fraser, A.G., Kamath, R.S., Ahringer, J., and Ruvkun, G. (2003). A systematic RNAi screen identifies a critical role for mitochondria in *C. elegans* longevity. *Nat. Genet.* *33*, 40–48.
- Lee, S.J., Hwang, A.B., and Kenyon, C. (2010). Inhibition of respiration extends *C. elegans* life span via reactive oxygen species that increase HIF-1 activity. *Curr. Biol.* *20*, 2131–2136.
- Lu, N., Yu, X., He, X., and Zhou, Z. (2009). Detecting apoptotic cells and monitoring their clearance in the nematode *Caenorhabditis elegans*. *Methods Mol. Biol.* *559*, 357–370.
- Lu, Y., Rolland, S.G., and Conradt, B. (2011). A molecular switch that governs mitochondrial fusion and fission mediated by the BCL2-like protein CED-9 of *Caenorhabditis elegans*. *Proc. Natl. Acad. Sci. USA* *108*, E813–E822.
- Nakano, K., and Vousden, K.H. (2001). PUMA, a novel proapoptotic gene, is induced by p53. *Mol. Cell* *7*, 683–694.
- Oda, E., Ohki, R., Murasawa, H., Nemoto, J., Shibue, T., Yamashita, T., Tokino, T., Taniguchi, T., and Tanaka, N. (2000). Noxa, a BH3-only member of the Bcl-2 family and candidate mediator of p53-induced apoptosis. *Science* *288*, 1053–1058.
- Pan, Y., Schroeder, E.A., Ocampo, A., Barrientos, A., and Shadel, G.S. (2011). Regulation of yeast chronological life span by TORC1 via adaptive mitochondrial ROS signaling. *Cell Metab.* *13*, 668–678.
- Pinan-Lucarre, B., Gabel, C.V., Reina, C.P., Hulme, S.E., Shevkopyas, S.S., Slone, R.D., Xue, J., Qiao, Y., Weisberg, S., Roodhouse, K., et al. (2012). The core apoptotic executioner proteins CED-3 and CED-4 promote initiation of neuronal regeneration in *Caenorhabditis elegans*. *PLoS Biol.* *10*, e1001331.
- Reinke, V., Smith, H.E., Nance, J., Wang, J., Van Doren, C., Begley, R., Jones, S.J., Davis, E.B., Scherer, S., Ward, S., and Kim, S.K. (2000). A global profile of germline gene expression in *C. elegans*. *Mol. Cell* *6*, 605–616.
- Schroeder, E.A., Raimundo, N., and Shadel, G.S. (2013). Epigenetic silencing mediates mitochondria stress-induced longevity. *Cell Metab.* *17*, 954–964.
- Schulz, T.J., Zarse, K., Voigt, A., Urban, N., Birringer, M., and Ristow, M. (2007). Glucose restriction extends *Caenorhabditis elegans* life span by inducing mitochondrial respiration and increasing oxidative stress. *Cell Metab.* *6*, 280–293.
- Schumacher, B., Schertel, C., Wittenburg, N., Tuck, S., Mitani, S., Gartner, A., Conradt, B., and Shaham, S. (2005). *C. elegans* ced-13 can promote apoptosis and is induced in response to DNA damage. *Cell Death Differ.* *12*, 153–161.
- Schwartz, H.T. (2007). A protocol describing pharynx counts and a review of other assays of apoptotic cell death in the nematode worm *Caenorhabditis elegans*. *Nat. Protoc.* *2*, 705–714.
- Sena, L.A., and Chandel, N.S. (2012). Physiological roles of mitochondrial reactive oxygen species. *Mol. Cell* *48*, 158–167.
- Suthammarak, W., Somerlot, B.H., Opheim, E., Sedensky, M., and Morgan, P.G. (2013). Novel interactions between mitochondrial superoxide dismutases and the electron transport chain. *Aging Cell* *12*, 1132–1140.
- Treinin, M., Shliar, J., Jiang, H., Powell-Coffman, J.A., Bromberg, Z., and Horowitz, M. (2003). HIF-1 is required for heat acclimation in the nematode *Caenorhabditis elegans*. *Physiol. Genomics* *14*, 17–24.
- Van Raamsdonk, J.M., and Hekimi, S. (2009). Deletion of the mitochondrial superoxide dismutase *sod-2* extends lifespan in *Caenorhabditis elegans*. *PLoS Genet.* *5*, e1000361.
- Van Raamsdonk, J.M., and Hekimi, S. (2010). Reactive Oxygen Species and Aging in *Caenorhabditis elegans*: Causal or Casual Relationship? *Antioxid. Redox Signal.* *13*, 1911–1953.
- Van Raamsdonk, J.M., and Hekimi, S. (2012). Superoxide dismutase is dispensable for normal animal lifespan. *Proc. Natl. Acad. Sci. USA* *109*, 5785–5790.
- Ventura, N., Rea, S.L., Schiavi, A., Torgovnick, A., Testi, R., and Johnson, T.E. (2009). p53/CEP-1 increases or decreases lifespan, depending on level of mitochondrial bioenergetic stress. *Aging Cell* *8*, 380–393.
- Walter, L., Baruah, A., Chang, H.W., Pace, H.M., and Lee, S.S. (2011). The homeobox protein CEH-23 mediates prolonged longevity in response to impaired mitochondrial electron transport chain in *C. elegans*. *PLoS Biol.* *9*, e1001084.
- Wang, C., and Youle, R.J. (2009). The role of mitochondria in apoptosis*. *Annu. Rev. Genet.* *43*, 95–118.
- Yang, W., and Hekimi, S. (2010a). A mitochondrial superoxide signal triggers increased longevity in *Caenorhabditis elegans*. *PLoS Biol.* *8*, e1000556.
- Yang, W., and Hekimi, S. (2010b). Two modes of mitochondrial dysfunction lead independently to lifespan extension in *Caenorhabditis elegans*. *Aging Cell* *9*, 433–447.
- Yang, W., Li, J., and Hekimi, S. (2007). A Measurable increase in oxidative damage due to reduction in superoxide detoxification fails to shorten the life span of long-lived mitochondrial mutants of *Caenorhabditis elegans*. *Genetics* *177*, 2063–2074.
- Zarse, K., Schmeisser, S., Groth, M., Priebe, S., Beuster, G., Kuhlow, D., Guthke, R., Platzer, M., Kahn, C.R., and Ristow, M. (2012). Impaired insulin/IGF1 signaling extends life span by promoting mitochondrial L-proline catabolism to induce a transient ROS signal. *Cell Metab.* *15*, 451–465.
- Zermati, Y., Mouhamad, S., Stergiou, L., Besse, B., Galluzzi, L., Boehler, S., Pauleau, A.L., Rosselli, F., D’Amelio, M., Amendola, R., et al. (2007). Nonapoptotic role for Apaf-1 in the DNA damage checkpoint. *Mol. Cell* *28*, 624–637.

ROS-Triggered Phosphorylation of Complex II by Fgr Kinase Regulates Cellular Adaptation to Fuel Use

Rebeca Acín-Pérez,¹ Isabel Carrascoso,¹ Francesc Baixauli,¹ Marta Roche-Molina,¹ Ana Latorre-Pellicer,¹ Patricio Fernández-Silva,² María Mittelbrunn,¹ Francisco Sanchez-Madrid,¹ Acisclo Pérez-Martos,² Clifford A. Lowell,³ Giovanni Manfredi,⁴ and José Antonio Enriquez^{1,2,*}

¹Centro Nacional de Investigaciones Cardiovasculares Carlos III (CNIC), Melchor Fernández Almagro, 3, 28029 Madrid, Spain

²Departamento de Bioquímica y Biología Molecular y Celular, Facultad de Ciencias, Universidad de Zaragoza, 50009 Zaragoza, Spain

³Department of Laboratory Medicine, University of California, San Francisco, San Francisco, CA 94143, USA

⁴Brain and Mind Research Institute, Weill Medical College of Cornell University, New York, NY 10065, USA

*Correspondence: jaenriquez@cnic.es

<http://dx.doi.org/10.1016/j.cmet.2014.04.015>

SUMMARY

Electron flux in the mitochondrial electron transport chain is determined by the superassembly of mitochondrial respiratory complexes. Different superassemblies are dedicated to receive electrons derived from NADH or FADH₂, allowing cells to adapt to the particular NADH/FADH₂ ratio generated from available fuel sources. When several fuels are available, cells adapt to the fuel best suited to their type or functional status (e.g., quiescent versus proliferative). We show that an appropriate proportion of superassemblies can be achieved by increasing CII activity through phosphorylation of the complex II catalytic subunit FpSDH. This phosphorylation is mediated by the tyrosine-kinase Fgr, which is activated by hydrogen peroxide. Ablation of Fgr or mutation of the FpSDH target tyrosine abolishes the capacity of mitochondria to adjust metabolism upon nutrient restriction, hypoxia/reoxygenation, and T cell activation, demonstrating the physiological relevance of this adaptive response.

INTRODUCTION

To utilize fuels efficiently, cells must exquisitely integrate the activities of membrane receptors and transporters, the intracellular compartmentalization of molecules, the enzymatic balance of each metabolic step, and the elimination of byproducts (Stanley et al., 2013). Appropriate orchestration of all these changes is critical for the cell's ability to adapt to changing functional requirements, such as quiescence, proliferation, and differentiation, and to environmental changes, including survival in response to diverse insults. Factors known to influence this adaptation include the cellular response to oxygen availability (hypoxia-inducible factors HIF1 α and HIF1 β); regulators of energy availability such as mammalian target of rapamycin (mTOR), AMP-activated protein kinase, sirtuin, and forkhead box (FOXO); and mediators of the response to reactive oxygen

species (ROS), such as peroxisome proliferator-activated receptor gamma coactivator-1 alpha (PGC-1 α). The involvement of these factors illustrates the interconnection between the use of alternate carbon substrates (carbohydrates, amino acids, fatty acids and ketone bodies) and the cellular response to stress, particularly oxidative stress.

At the core of this process are mitochondria. In response to changes in fuel source, mitochondria must modify their location, structure, and metabolite fluxes in order to balance their contribution to anabolism (lipogenesis and antioxidant defenses from citrate, gluconeogenesis, serine and glycine biosynthesis from pyruvate, nucleotide biosynthesis) and catabolism (TCA cycle, β -oxidation, oxidative phosphorylation). Mitochondria are central to ATP synthesis, redox balance, and ROS production, parameters directly dependent on fuel use. All catabolic processes converge on the mitochondrial electron transport chain (mETC) by supplying electrons in the form of NADH⁺H⁺ or FADH₂. The relative proportion of electrons supplied via NADH and FADH₂ varies with the fuel used; for example, oxidative metabolism of glucose generates a NADH/FADH₂ electron ratio of 5, whereas for a typical fatty acid (FA) such as palmitate the ratio is \approx 2 (Speijer, 2011).

Our recent work on the dynamic architecture of the mETC reveals that supercomplex formation defines specific pools of CIII, CIV, CoQ, and cyt c for the receipt of electrons derived from NADH or FAD (Lapuente-Brun et al., 2013). Since CIII preferentially interacts with CI, the amount of CI determines the relative availability of CIII for FADH₂- or NADH-derived electrons. The regulation of CI stability is thus central to cellular adaptation to fuel availability. A substrate shift from glucose to FA requires greater flux from FAD, and this is achieved by a reorganization of the mETC superstructure in which CI is degraded, releasing CIII to receive FAD-derived electrons (Lapuente-Brun et al., 2013; Stanley et al., 2013). Failure of this adaptation results in the harmful generation of reactive oxygen species (ROS) (Speijer, 2011). The proportion of supercomplexes dedicated to receiving NADH electrons is further dependent on the structure and dynamics of mitochondrial cristae (Cogliati et al., 2013; Lapuente-Brun et al., 2013), so that reducing the number of cristae favors flux from FAD. In agreement with this, ablation of the mitochondrial protease OMA1, which prevents optic atrophy 1 (OPA1)-specific proteolysis and cristae remodeling,

impairs FA degradation in mice, resulting in obesity and impaired temperature control (Quirós et al., 2012).

Cells are normally exposed to a mixed supply of fuels, but despite this, cells are often predisposed to preferentially use one source over another, according to their physiological role or status (Stanley et al., 2013). T cells, for example, switch from oxidative to glycolytic metabolism upon activation, coinciding with entry into a proliferative state, and later increase FA oxidation when they differentiate into regulatory T cells. These changes require remodeling of the mETC NADH/FADH₂ flux capacity, but how cells regulate this choice of carbon source is not understood.

Here, we show that fuel choice is regulated via tyrosine phosphorylation of complex II (CII) subunit FpSDH, mediated by ROS-activation of the tyrosine kinase Fgr. This activation is required to adjust the level of complex I (CI) to optimize NADH/FADH₂ electron use. Our data show this mechanism operating in three physiological situations: upon T lymphocyte activation, in the adaptation of liver and cultured cells to starvation, and in the adaptation of cells to hypoxia/reoxygenation.

RESULTS

Above-Normal CII Activity in Cells Expressing Mutant CI

Our laboratory has isolated mouse cell lines carrying different proportions of a null ND6 mutation (Acín-Pérez et al., 2003): EB2615 (30% mutant mtDNA), E23 (66%), E12 (80%), FG12-1 (95%), and FG23-1 (98%). Mitochondria from ND6 mutants showed reductions in CI proportional to the mutation load (Figure 1A). Interestingly, the lines with the highest mutation loads showed elevated activity of CII (Figure 1B). Similar observations have been reported in human cells derived from patients with CI deficiencies (Cardol et al., 2002; Fan et al., 2008; Majander et al., 1991; Pitkanen and Robinson, 1996) and in CI-deficient mice (Kruse et al., 2008). Increased CII activity was proposed to compensate for impaired activity of CI, but the underlying mechanism is unknown. This compensatory phenomenon is specific for CI-deficient cells, since cells lacking CIII or CIV showed no changes in CII activity (Figure S1A).

As reported (Acín-Pérez et al., 2003; Bai and Attardi, 1998), the amount of CI was reduced in cells with a high ND6 mutant load (FG12-1, FG23-1; Figure 1C, upper panel), whereas CII content was unchanged, despite above-normal activity determined spectrophotometrically (Figure 1B) and by in-gel assay (data not shown). G3PDH activity did not differ between WT and ND6 mutants (Figure 1D), indicating that increased CII activity does not reflect a generalized response of enzymes that donate electrons to CIII and is a specific response to CI deficiency.

As a further control, we treated WT FBalb/cJ cells with the specific inhibitor rotenone (200 nM), which blocks CI activity without affecting CI assembly. Rotenone-mediated inhibition of CI was accompanied by a parallel increase in CII activity, after short and long rotenone treatment, indicating that loss of CI function, not its physical absence, is responsible for the high CII activity (Figure 1E).

CII Activity Is Regulated by Phosphorylation

Several groups have proposed that CII subunit A (FpSDH) is a kinase target (Bykova et al., 2003; Salvi et al., 2007; Schulen-

berg et al., 2003). To investigate FpSDH phosphorylation, we separated mitochondrial proteins by 2D IEF/SDS-PAGE (isoelectric focusing followed by SDS polyacrylamide gel electrophoresis) and detected FpSDH protein by immunoblot (Figure 1F). The CI subunit NDUFS3 was used as a reference since the stability and migration of this protein are unaffected by the failure of CI assembly (Figure S1B). FpSDH in FG23-1 samples migrated as multiple spots, running at more acidic positions than samples from WT FBalb/cJ cells. This is compatible with increased phosphorylation of the protein in mutant cells. Treatment of permeabilized FG23-1 mitochondria with calf-intestine phosphatase (CIP) to remove phosphoryl residues restored the WT migration pattern, confirming that the altered pattern is due to phosphorylation (Figure 1F, lower panels). Moreover, blockade of CI activity in FBalb/cJ cells reproduced the FpSDH mobility pattern seen in FG23-1 cells (not shown). These observations indicate that FpSDH is phosphorylated when CI activity is impaired. Consistent with these findings, most FpSDH from FG23-1 mitochondrial samples eluted in the phosphorylated fraction after separation on phosphoprotein-enrichment columns, and this effect was blocked by pre-treatment of permeabilized mitochondria with CIP (Figure S1C). In contrast, FpSDH from FBalb/cJ mitochondria was more concentrated in nonphosphorylated fractions (Figure S1C). The activity of CII in mitochondria from FBalb/cJ and FG23-1 cells was sensitive to CIP-mediated dephosphorylation, but this reduction was proportionally more severe in FG23-1 mitochondria, suggesting that phosphorylation increases CII activity (Figure 1G).

Phosphorylation of FpSDH Is Triggered by ROS

Cells lacking CI contain high levels of ROS (Robinson, 1998), and ND6-deficient cells produce abundant hydrogen peroxide (Moreno-Loshuertos et al., 2006) (Figure 2A), an effect mimicked by treatment with the CI inhibitor rotenone (Dlasková et al., 2008; Radad et al., 2006). Short and long rotenone treatment of WT cells showed an increase in CII activity (Figure 1E) that was accompanied by a parallel increase in ROS production (Figure S2A). ROS modulate several signaling pathways (Dröge, 2002; Hamanaka and Chandel, 2010), prompting us to evaluate the involvement of ROS in CII activation. Culturing cells for 1 week with N-acetyl cysteine (NAC, 5 mM) lowered basal H₂O₂ levels and decreased CII activity in control and mutant cells (Figures 2A and 2B), but the reduction was proportionally stronger in FG23-1 cells (Figure 2B). Since NAC is not a direct ROS scavenger but rather a precursor of glutathione, which changes the redox status of the cell, we investigated H₂O₂-dependent CII activity stimulation in isolated mitochondria. Addition of H₂O₂ to WT mouse liver mitochondria increased CII activity (Figure 2C) and the phosphorylation of FpSDH (Figure 2D). CII activation was blunted by the presence of catalase, which catalyzes H₂O₂ decomposition (Figure 2C). As a further control, we analyzed the response to moderate ROS production of fibroblasts lacking supercomplex assembly factor I (SCAFI), which is required for association between CIII and CIV (Lapuente-Brun et al., 2013). The response of WT and SCAFI-deficient fibroblasts to ROS (generated by incubation in the presence of xanthine and xanthine oxidase) was indistinguishable, indicating that ROS-induced upregulation of CII is a

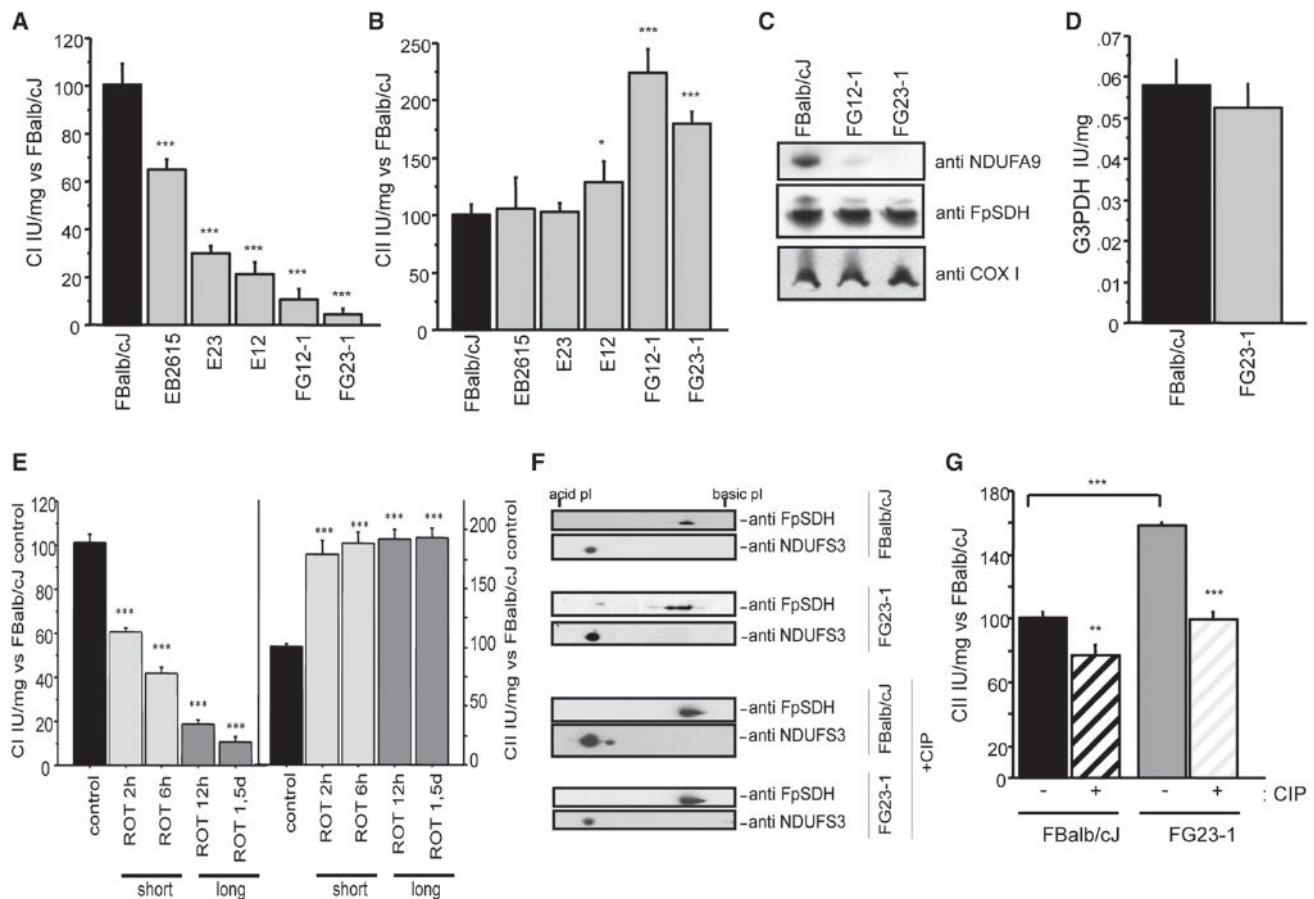


Figure 1. Phosphorylation of FpSDH Increases CII Activity in CI-Deficient Cells

(A) Fibroblast lines with mutations in ND6 show decreased CI activity in proportion to the mutation load. Activity is expressed as the percentage of activity in FBalb/cJ cells (WT, no mutation; n = 12): EB2615 (70%; n = 6); E23 (34%; n = 6); E12 (20%; n = 9); FG12-1 (5%; n = 9); and FG23-1 (2%; n = 9).

(B) CII activity (CoQ reduction) in cell lines with high loads of the iC13887 ND6 mutation, expressed as the percentage of activity in FBalb/cJ cells (n = 18): EB2615 (n = 9); E23 (9 n = 9); E12 (n = 12); FG12-1 (n = 9); and FG23-1 (n = 20).

(C) Western blot after BNGE, detecting subunits of CI (NDUFA9), CII (FpSDH), and CIV (COX I).

(D) G3PDH activity in FG23-1 and FBalb/cJ (n = 6).

(E) Activities of CI (left) and CII (right) in a time course rotenone treatment of FBalb/cJ (200 nM) as a percentage of activity in untreated cells (n ≥ 6). Short: 2 and 6 hr treatment; long: 12 hr and 1.5 day treatment.

(F) FpSDH immunoblot after 2D IEF/SDS-PAGE (IEF strip pH 3–10) of control and calf intestine phosphatase (CIP)-treated mitochondrial protein (100 μg) from FBalb/cJ and FG23-1 cells. The acidic shift of FpSDH spots in FG23-1 cells is blocked by CIP. The CI subunit NDUFS3 was used to align and compare the blots.

(G) CII activity in CIP-treated mitochondria from FBalb/cJ and FG23-1 cells (n = 6). Data are presented as the percentage of activity in untreated FBalb/cJ.

p < 0.001; *p < 0.0001. Enzyme activities were determined spectrophotometrically.

All data are presented as mean ± SD. See also Figure S1.

general response independent of the assembly of supercomplexes containing CIV (Lapiente-Brun et al., 2013) (Figure 2E). To determine whether CII is activated by superoxide or hydrogen peroxide produced in the mitochondrial matrix, we generated FBalb/cJ- and FG23-1-derived lines expressing mitochondria-targeted catalase (mt-cat) or MnSOD (Figure S2B). ROS production as well as catalase and MnSOD activities measured before and after overexpression confirmed that the cells were expressing functional enzymes (Figures S2C–S2F). Control and CI mutant cells also exhibited basal differences in catalase and MnSOD activities, as previously shown (Moreno-Loshuertos et al., 2006). The expected elevation in H₂O₂ production and CII activity in FG23-1 cells and rote-

none-treated FBalb/cJ cells was decreased by expression of mt-cat, but not MnSOD (Figures 2F and 2G), suggesting that the key activator of the pathway is H₂O₂ and not superoxide.

CII Is Activated by Phosphorylation on FpSDH Mediated by a Src-Type Tyrosine Kinase

We next analyzed immunoprecipitated FpSDH by western blot with anti-phospho-Tyr, anti-phospho-Ser, and anti-phospho-Thr antibodies. Only Tyr phosphorylation of FpSDH was detected in FBalb/cJ and FG23-1 cells, but the signal was stronger in FG23-1 cells (Figure 3A). Incubation of isolated mouse liver mitochondria with protein kinase inhibitors revealed that CII activity and FpSDH phosphorylation were reduced by PP2, an

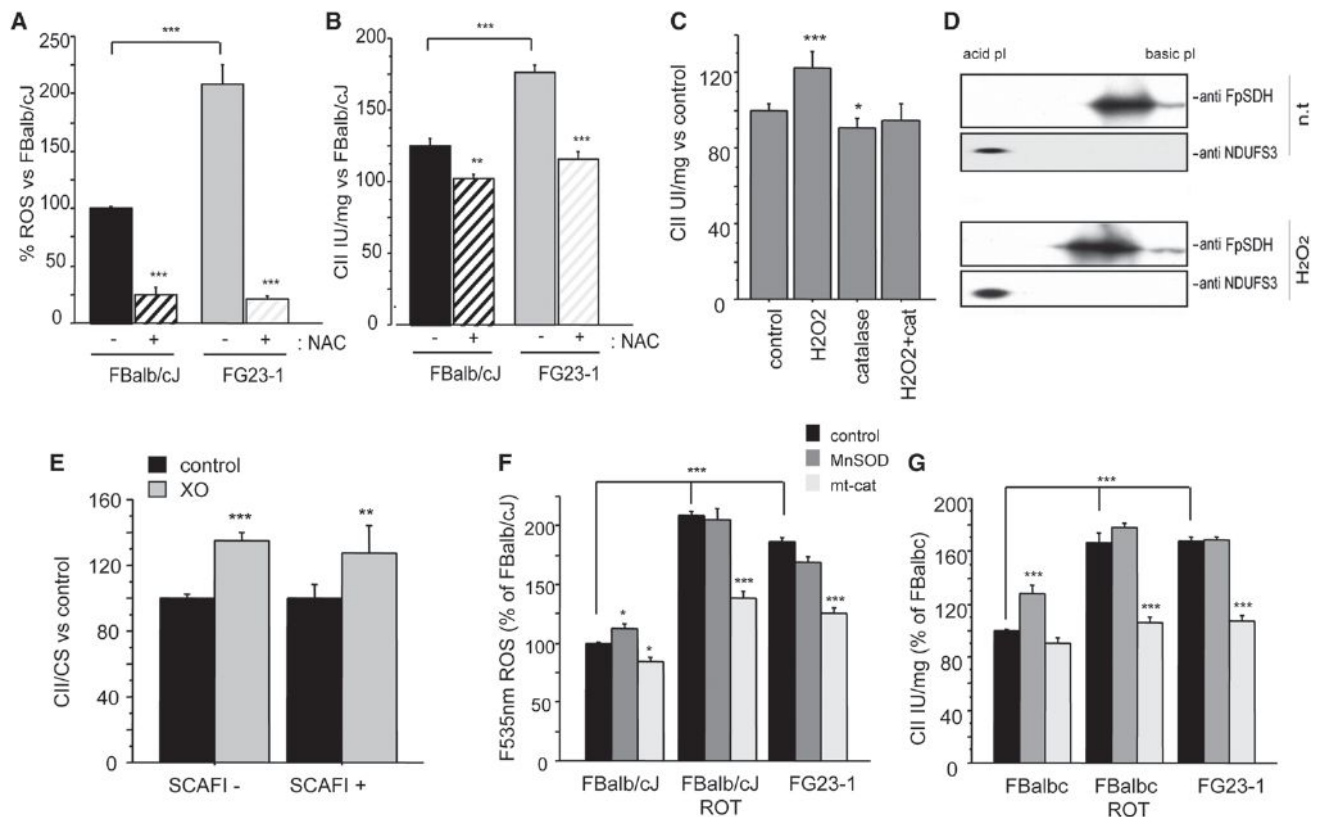


Figure 2. FpSDH Phosphorylation and CII Activity Are ROS Dependent

(A) ROS (H₂O₂) levels measured in nontreated (n.t.) FG23-1 and FBalb/cJ cells and in cells treated with NAC (5 mM, 7 days) (control, n = 35; NAC, n = 12). (B) Effect of NAC treatment on CII activity in FBalb/cJ and in FG23-1 cells (untreated, n = 15; NAC, n = 4). Data in (A) and (B) are presented as the percentage of nontreated FBalb/cJ cells. (C) CII activity in isolated mouse liver mitochondria treated for 10 min with H₂O₂ (50 μM), catalase (25 U/ml), or both (n ≥ 4). (D) 2D IEF/SDS-PAGE (IEF strips pH 4–7) Western analysis of FpSDH from H₂O₂-treated mouse liver mitochondria. (E) CII activity in mitochondria isolated from SCAFI- (left) and SCAFI+ (right) fibroblasts treated with the ROS generator xanthine oxidase (XO) (n = 4). Data are presented as the percentage of activity in nontreated fibroblasts. (F) H₂O₂ production in FG23-1 and rotenone-treated FBalb/cJ fibroblasts is prevented by expression of mitochondrially targeted catalase (mt-cat, n = 5). (G) Elevated CII activity in FG23-1 and rotenone-treated FBalb/cJ cells is prevented by expression of mt-cat but not MnSOD (n = 3). *p < 0.01; **p < 0.001; ***p < 0.0001.

All data are presented as mean ± SD. See also Figure S2.

inhibitor of Src-family kinases (SFK), whereas no effect was observed with the cAMP/cGMP-dependent protein kinase inhibitor H89 or the PKA agonist 8Br-cAMP (Figures 3B and 3C). These results thus suggest that FpSDH is phosphorylated *in vivo* by a Src-type tyrosine kinase.

H₂O₂ can promote phosphorylation on Tyr residues by activating Tyr kinases (Balamurugan et al., 2002; Chiarugi, 2008; Minetti et al., 2002) or by inhibiting Tyr phosphatases (Chiarugi, 2008). We incubated isolated mouse liver mitochondria with H₂O₂ in the presence of either PP2, to inhibit SFKs, or orthovanadate (Ov), a general inhibitor of Tyr-phosphatases. PP2 reduced the activity of CII and prevented the activation induced by H₂O₂, whereas Ov had no effect. If we assume that Ov is able to inhibit the phosphatase involved, these results are compatible with a model in which H₂O₂ promotes FpSDH phosphorylation by activating a PP2-sensitive kinase (Figure 3D). Full demonstration of this mechanism would require the identification of the phosphatase involved.

The Src-Type Tyrosine Kinase Fgr Interacts with CII *In Vivo*

The SFKs Lyn, Fyn, Fgr, and Csk have been reported to localize in mitochondria (Augereau et al., 2005; Salvi et al., 2005; Tibaldi et al., 2008). Immunoblot analysis of mitochondrial preparations pretreated with proteinase K detected several tyrosine protein kinases (Src, Lyn, and Fgr), the regulator of Src-type tyrosine kinases Csk (itself a Tyr kinase), and the Ser/Thr kinase PKA (Figure 3E). To establish whether any of these interact with CII, we performed coimmunoprecipitation experiments targeting FpSDH. Mitochondrial membranes were solubilized either with the nonionic detergent dodecyl-maltoside (DDM), to isolate individual respiratory complexes, or with the milder detergent digitonin (DIG), to isolate supercomplexes. In the DDM lysates, none of the probed protein-kinases was coimmunoprecipitated with CII (Figure 3F), whereas in DIG lysates anti-FpSDH specifically coimmunoprecipitated the Src-family kinase Fgr, suggesting physical interaction between Fgr and

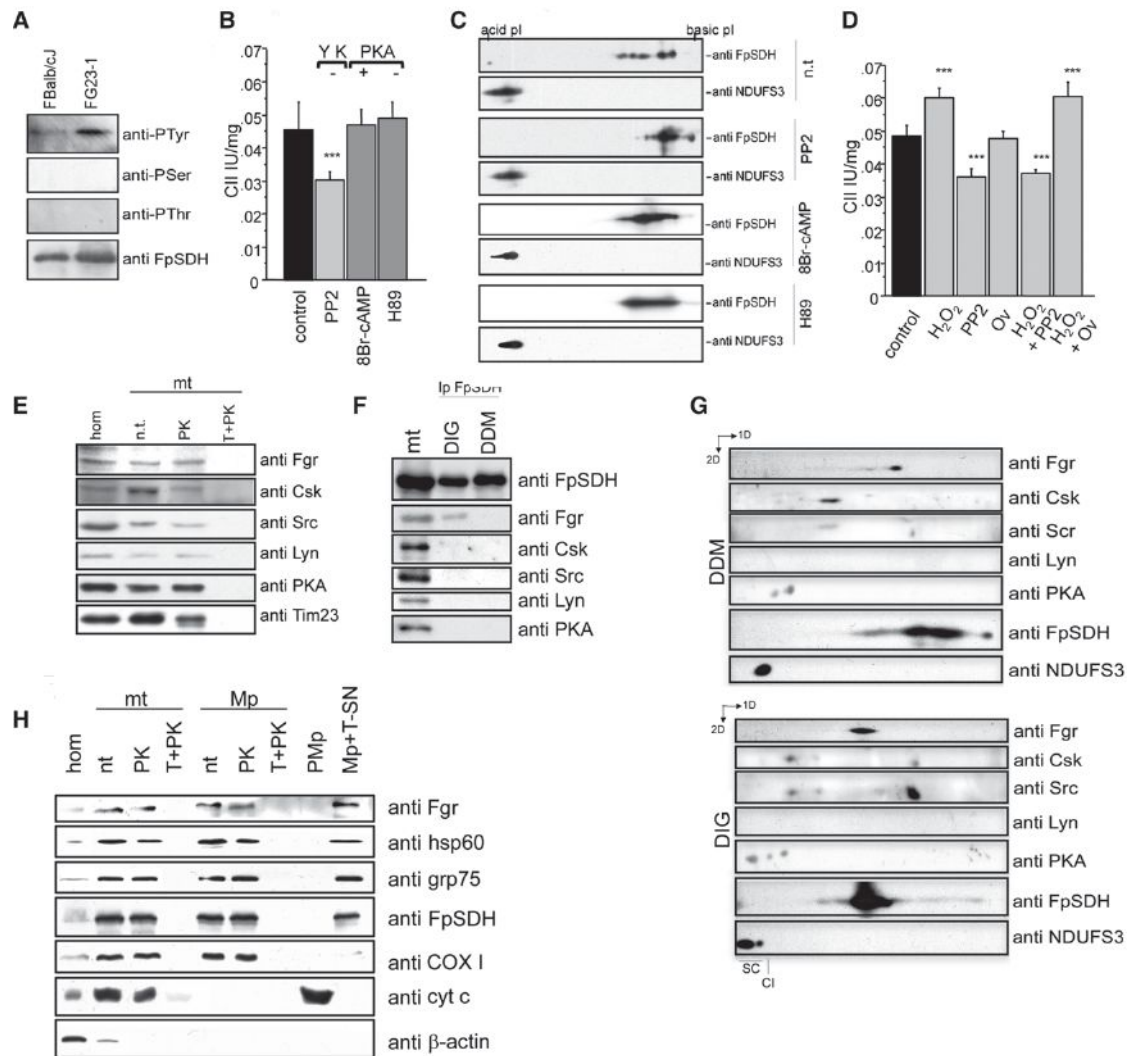


Figure 3. The Src-Type Kinase Fgr Phosphorylates CII

(A) Immunoblot phosphoprotein analysis in FpSDH immunoprecipitates from FBalb/cJ and FG23-1 cells.

(B) Complex II activity in mouse liver mitochondria incubated with the Tyr kinase inhibitor PP2, the PKA agonist 8Br-cAMP, or the PKA antagonist H89 (n = 5).

(C) 2D IEF/SDS-PAGE (3–10 IEF strips) Western analysis of mouse mitochondria treated with PP2, 8Br-cAMP, or H89. PP2 induces a basic shift in FpSDH compared with nontreated mitochondria (n.t.). Modulation of PKA activity had no effect on FpSDH phosphorylation. NDUFS3 (Cl) was detected to align and compare blots.

(D) H₂O₂-induced activation of complex II is blocked by the Tyr kinase inhibitor PP2, but not by the Tyr phosphatase inhibitor orthovanadate (Ov) (n = 6).

(E) Intact mouse mitochondria (mt) protect a portion of Fgr, Csk, Src, Lyn, and PKA kinases from digestion by proteinase K: hom, cell homogenate; n.t., non-treated; PK, proteinase K; T+PK, proteinase K treatment of mitochondria solubilized with Triton X-100. Tim23 was used as a marker of intact mitochondria.

(F) Anti-FpSDH specifically coimmunoprecipitates Fgr kinase from mitochondria solubilized with digitonin (DIG), which preserves intact supercomplexes, but not dodecyl maltoside (DDM), which resolves individual respiratory complexes. mt, fully solubilized mitochondria.

(G) 2D BNGE/SDS-PAGE of DDM- and DIG-solubilized mitochondria, showing comigration of Fgr and FpSDH in DIG-treated mitochondria. Note comigration of Csk and Src in both preparations.

(H) Mitochondrial Fgr is located in the matrix. Fractionation experiment showing protection of Fgr from PK digestion in intact mitochondria (mt) and mitoplasts (Mp) but not in either fraction solubilized with Triton X-100 (T+PK). Fgr was present in the supernatant fraction of Triton X-100-solubilized mitoplasts (Mp+T-SN). P-Mp, post-mitoplast fraction. Markers used: hsp60 and Grp75, mitochondrial matrix; FpSDH, association with inner membrane; COX I, inner membrane; cyt c, intermembrane space; β-actin, cytoplasm.

All data are presented as mean ± SD.

CII in the mitochondrial inner membrane. To confirm this, we separated DIG and DDM lysates by BNGE followed by denaturing SDS-PAGE (Figure 3G). Fgr kinase was detectable in both preparations but only comigrated with CII in the DIG-lysed

samples. None of the other kinases analyzed comigrated with FpSDH, but Src/Csk and PKA both appeared to be associated with high molecular weight complexes (Figure 3G). Interestingly, Src comigrated with its regulator Csk in both

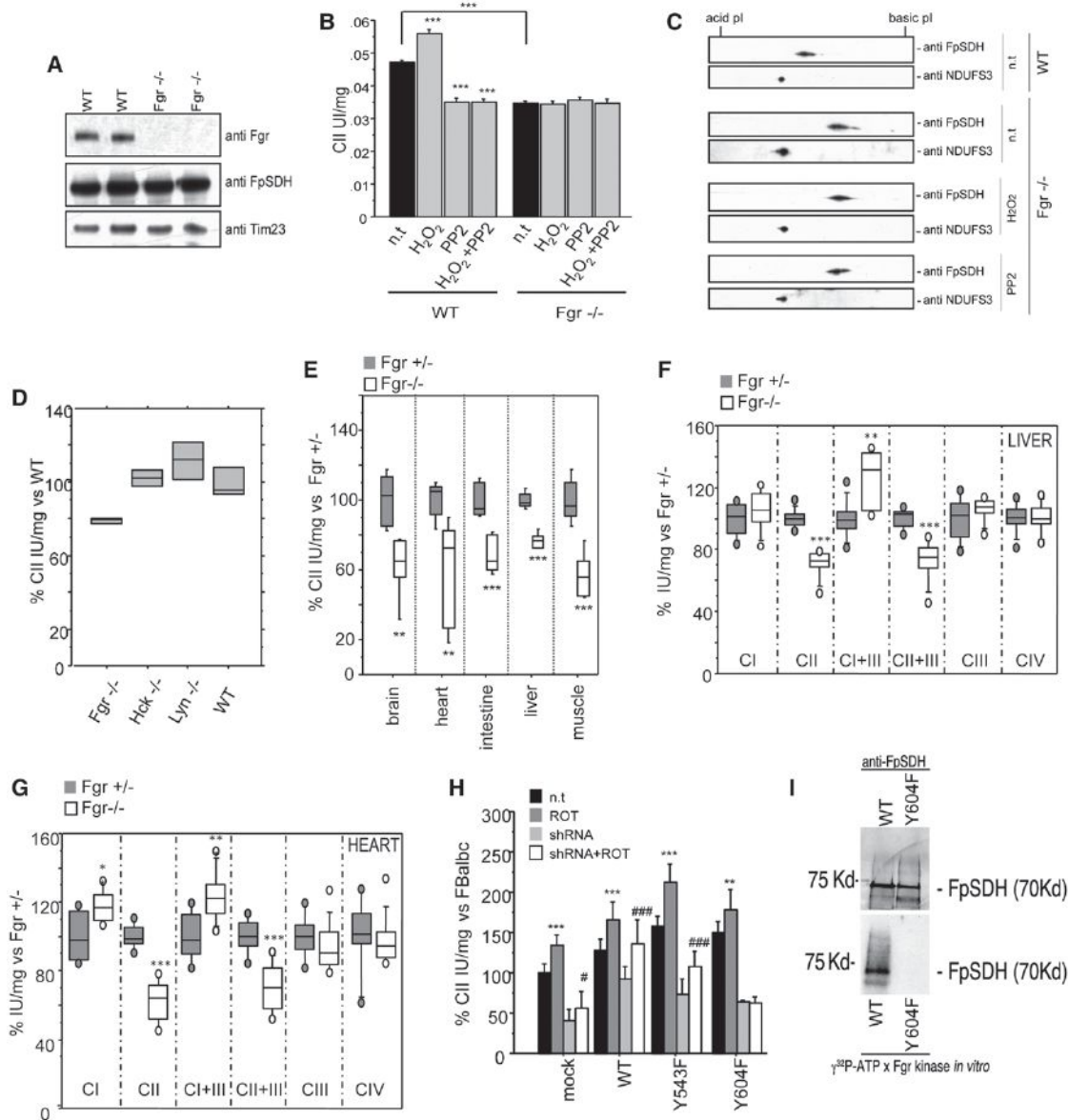


Figure 4. CII Is Regulated by Fgr Phosphorylation at Tyr604

(A) SDS-PAGE western analysis of Fgr tyrosine kinase in liver mitochondrial protein preparations from control or *Fgr*^{-/-} mice. (B) CII activity in isolated liver mitochondria from WT or *Fgr*^{-/-} mice in the presence of H₂O₂, PP2, or both. Data are presented as mean ± SD. (C) 2D IEF/SDS-PAGE (IEF strips pH 4–7) Western analysis of FpSDH from WT liver mitochondria and from nontreated or H₂O₂- or PP2-treated *Fgr*^{-/-} liver mitochondria. NDUFS3 (CI) is used to align and compare blots. (D) Complex II activity in liver mitochondria from different Tyr kinase null mice. (E) Complex II activity in tissue homogenates from *Fgr*^{+/-} and *Fgr*^{-/-} null mice (n = 4). (F and G) Individual and combined mitochondrial complex activities in isolated mitochondria from liver (F) and heart (G) (n ≥ 4). In (D)–(G), lines extending from the boxes indicate the variability outside the upper and lower quartiles. (H) CII activity in Fbalb/cJ cells silenced for endogenous FpSDH and re-expressing WT and mutant FpSDH variants (n = 4). ROT, rotenone (200 nM); shRNA, silencing of endogenous FpSDH. Data are presented as the percentage of activity in nontreated, mock-infected Fbalb/cJ (mean ± SD). Statistical significance versus nontreated: **p < 0.001; ***p < 0.0001. Statistical significance versus shRNA: #, p < 0.01; ###, p < 0.0001. (I) Fgr in vitro phosphorylation (bottom) and FpSDH immunodetection (top) of immunocaptured complex II from Fbalb/cJ cells expressing WT FpSDH (left line) or the Y604F mutant (right line). See also Figure S3.

preparations, suggesting strong interaction between these kinases. The mitochondrial matrix localization of Fgr kinase was confirmed by subfractionation of pure mouse liver mitochondria (Figure 3H).

Ablation of Fgr Abolishes the Activation of CII

To demonstrate the role of Fgr in the regulation of CII we examined liver mitochondria from *fgr*^{-/-} mice (Lowell et al., 1994), in which Fgr is undetectable but CII content is normal (Figure 4A).

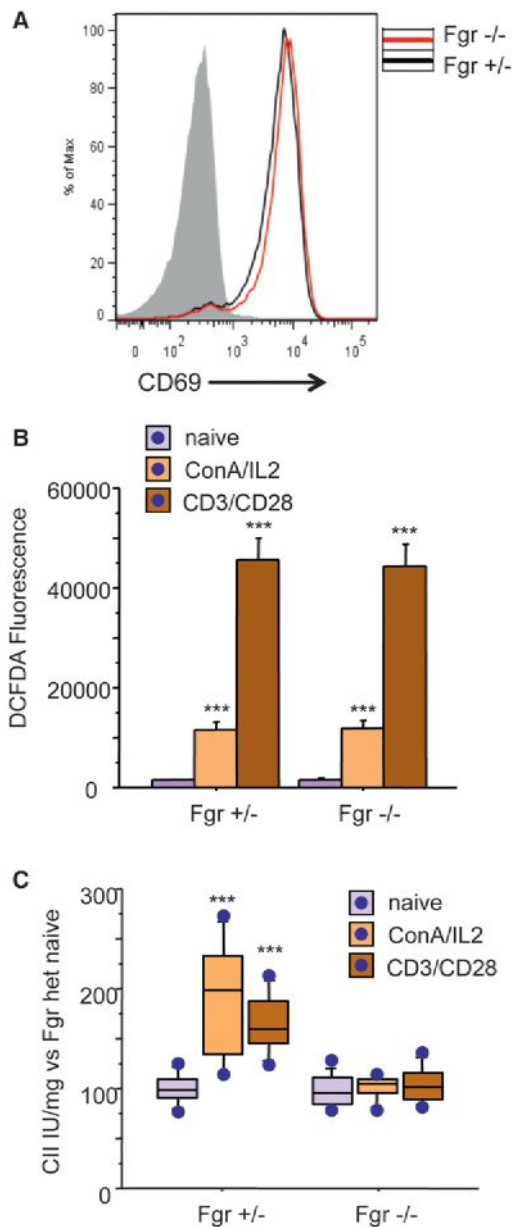


Figure 5. T Cell Activation and CII Activity Response

(A) Flow cytometry analysis of T cell activation. Naive T cells from $Fgr^{+/-}$ and $Fgr^{-/-}$ mice were activated with anti-CD3/CD28, and activation was assessed by detection of CD69. Gray line: negative control. The chart shows data from one representative experiment of four.

(B) Flow cytometry analysis of ROS production (2,7-DCFH₂-DA) in resting T cells and upon CD3/CD28 or ConA activation (n = 3). Data are presented as mean \pm SD.

(C) CII activity measured in resting and activated T cells (n = 4). Data are presented as the percentage of activity compared to resting T cells. Lines extending from the boxes indicate the variability outside the upper and lower quartiles.

Basal CII activity in these mitochondria was below normal and insensitive to H₂O₂ or PP2 (Figure 4B), and FpSDH phosphorylation was prevented (Figure 4C). CII activity was normal in mitochondria from Lyn and Hck Tyr kinase knockout mice (Figure 4D).

The absence of Fgr affected CII activity in all analyzed tissues (Figure 4E), whereas activities of the other mitochondrial respiratory complexes remained unchanged or, in the case of CI or combined CI+III, increased (Figures 4F and 4G). We can thus conclude that Fgr is the tyrosine kinase responsible for FpSDH phosphorylation, that it interacts with its substrate, and that FpSDH phosphorylation activates CII.

Fgr Activates CII through FpSDH Phosphorylation on Y604

Analysis of mouse FpSDH identified six candidate tyrosines for phosphorylation (Figure S3A), three of them in Fgr target motifs predicted by Scansite and Prediction of PK phosphorylation site (PPSP). One residue, Y604, which is conserved among mammals (Figure S3B), was previously identified as an Fgr target in in vitro phosphorylation assays (Salvi et al., 2007). The same report showed phosphorylation of Y543, but in silico predictions indicate this residue is not an Fgr target.

To identify the residue involved in CII regulation, we measured CII activity in FBalb/cJ cells transfected with WT FpSDH or one of the mutant FpSDH variants Y543F and Y604F. To ascertain the effect of the specific residues, we also silenced endogenous FpSDH expression (Figure S3C) and analyzed the response to treatment with rotenone (Figure 4H). In cells silenced for endogenous FpSDH, re-expressed WT and Y543F FpSDH restored rotenone-activated CII activity, but this effect was not seen in cells re-expressing the single mutant Y604F (Figure 4H). We next immunocaptured CII from cells expressing WT or Y604F FpSDH and performed Fgr in vitro phosphorylation assays. As proposed for rat (Salvi et al., 2007), mouse FpSDH was phosphorylated by Fgr. In contrast, Fgr was unable to phosphorylate the Y604F FpSDH variant (Figure 4I). No other CII proteins were labeled by this approach. These results confirm the in silico prediction that FpSDH Y604 is the unique Fgr target in CII.

ROS/Fgr/CII Regulatory Pathway in T Lymphocyte Activation

Activation of resting T cells with anti-CD3/CD28 antibodies (Abs), concanavalin A/IL2 (ConA/IL2), or phorbol-12-myristate-13-acetate (PMA) plus ionomycin triggers ROS production (Kamiński et al., 2010; Nagy et al., 2003). In response to anti-CD3/CD28 Abs or ConA/IL2, T cells isolated from $Fgr^{+/-}$ and $Fgr^{-/-}$ produced similar levels of ROS (Figures 5A and 5B). However, whereas CII activity was increased in $Fgr^{+/-}$ T cells, it remained unaffected in $Fgr^{-/-}$ cells (Figure 5C). Consistent with this result, restimulation of T lymphoblasts with PMA/ionomycin increased CII activity in $Fgr^{+/-}$ but not $Fgr^{-/-}$ cells (not shown).

ROS/Fgr/CII Pathway in Starvation and Serum Deprivation

One of the better-characterized ways in which liver cells adapt to starvation is through phosphorylation-mediated inhibition of pyruvate dehydrogenase (Huang et al., 2003), which reduces mitochondrial utilization of pyruvate and has been proposed to increase ROS production (Ten and Starkov, 2012). We recently reported that electrons derived from NADH and FADH₂ follow separate routes along the mETC, and that this is important for metabolic adaptation to starvation, with an increase in the rate of FADH₂ oxidization occurring at the expense of the NADH route

(Lapiente-Brun et al., 2013). Since Fgr-kinase activates CII (and hence use of FADH₂ electrons), we conducted a more detailed evaluation of the consequences of the lack of Fgr-kinase for liver mitochondria function. The significantly lower maximum CII activity in mitochondrial preparations from Fgr null liver was accompanied by lower-succinate-driven respiration and ATP synthesis (Figure 6A). Maximum CI activity was similar for both genotypes (Figure 6B). Surprisingly, pyruvate-plus-malate- and glutamate-plus-malate-driven respiration rates were below normal in well-fed Fgr null mice, and in the case of pyruvate-plus-malate this was accompanied by significantly lower ATP synthesis (Figure 6B). Lack of Fgr kinase thus appears to have a broader than anticipated effect on liver energy metabolism. No significant differences in citrate synthase activity were detected that could explain this decline in CI dependent respiration (Figure 6A). But although both the CI (NADH route) and the CII (FADH₂ route) are altered in Fgr^{-/-} liver mitochondria, the balance of electron supply potential to the mETC from NADH and FADH₂ is shifted, increasing the CI/CII activity ratio (Figure 6C). Starving Fgr^{-/-} mice overnight increased CI activity in liver mitochondria and reduced CII activity (Figures 6A, 6B, and S4), sharply increasing the CI/CII activity ratio, whereas the ratio in mitochondria from starved control mice decreased (Figure 6C). Feeding mitochondria with pyruvate or glutamate should generate intramitochondrial NADH, for delivery of electrons to CI. As expected, starvation-induced downregulation of pyruvate dehydrogenase activity reduced pyruvate-plus-malate-driven respiration and ATP synthesis in Fgr^{+/-} and Fgr null mice (Figure 6B). In contrast, starvation only decreased respiration and ATP synthesis driven by glutamate-plus-malate in Fgr^{-/-} mice, despite the higher maximal CI respiration (Figure 6B). These observations unexpectedly show that lack of Fgr kinase affects liver glutamate utilization.

To avoid the complex pleiotropic effects of Fgr-kinase ablation in liver, we mimicked starvation in cultured embryonic fibroblasts (derived from Fgr^{+/-} and Fgr^{-/-} littermates) by overnight serum deprivation. Serum-deprived Fgr^{+/-} fibroblasts showed the typical mitochondrial hyperfusion phenotype required to maintain ATP production upon nutrient deprivation (Gomes et al., 2011), whereas Fgr^{-/-} mitochondria were fragmented (Figure 6D). Consistently, mitochondria from serum-deprived Fgr^{-/-} cells showed higher processing of OPA1 (Figure 6E). Serum deprivation increased CII activity in Fgr^{+/-} but not Fgr^{-/-} cells (Figure 6F), recapitulating the lack of CII activation in Fgr^{-/-} liver mitochondria from overnight-starved mice. To assess whether starvation responses were due only to Fgr-dependent CII phosphorylation, we analyzed the effects of serum deprivation in fibroblasts silenced for endogenous FpSDH and exogenously re-expressing WT or Y604F FpSDH. Serum deprivation triggered OPA-1 processing in Y604F cells (Figure 6E), mimicking the result in Fgr null fibroblasts, and only cells re-expressing WT FpSDH upregulated CII activity after serum deprivation (Figure 6G). The blunted CII activation in Y604F cells compromised cell survival after serum deprivation, revealed by a higher proportion of apoptotic annexin V positive Y604F cells (Figures 6H and S5C).

ROS/Fgr/CII Pathway in Reoxygenation-Induced Metabolic Reprogramming

A drop in O₂ availability triggers several adaptive mechanisms, including reduction in the activities and protein levels of

OXPHOS components and in ROS production (Ali et al., 2012; Heather et al., 2012; Papandreou et al., 2006), and a notable accumulation of succinate (Casarano et al., 1976). However, sudden reoxygenation, as occurs in reperfusion after ischemia, is accompanied by a sharp increase in ROS production as the electron transport chain readapts to oxygen availability. To evaluate the role of ROS-mediated phosphorylation of FpSDH in this adaptation, we cultured Fgr^{+/-} and Fgr^{-/-} fibroblasts for 48 hr at 21% O₂ (normoxia), 1% O₂ (hypoxia), or 1% O₂ followed by reoxygenation at 21% O₂ for an additional 48 hr. Immunostaining and western blot analysis indicated that ROS-mediated mitochondrial biogenesis upon reoxygenation was impaired in Fgr^{-/-} cells, with only Fgr^{+/-} cells recovering normoxic mitochondrial numbers and shape (Figures 7A and 7B). In both genotypes, hypoxia reduced the amount of the mitochondrial proteins Tom20 and FpSDH (Figure 7B), consistent with the reported loss of mitochondria upon hypoxia (Kim et al., 2011). In the FpSDH re-expression model, hypoxia reduced mitochondrial content (measured as the FpSDH:actin and Tom20:actin ratios) in FpSDH-silenced fibroblasts re-expressing WT or Y604F FpSDH. As predicted, reoxygenation restored or increased mitochondrial protein content in cells re-expressing WT FpSDH, and this recovery was impaired in Y604F cells; however, Y604F cells did show partial mitochondrial recovery, differing from the more severe phenotype in Fgr^{-/-} fibroblasts (Figure 7B). The reason for this difference is likely that germline lack of Fgr affects targets other than CII required for full recovery.

To test the metabolic effect of reoxygenation, we measured CII activity in Fgr^{+/-} and Fgr^{-/-} fibroblasts cultured with 25 mM glucose or the more physiological 10 mM. Hypoxia did not alter CII activity under any conditions, and reoxygenation increased CII activity only in Fgr^{+/-} cells (Figures 7C and S5A). Likewise, in re-expression assays only WT FpSDH fibroblasts upregulated CII activity upon posthypoxia reoxygenation (Figures 7C and S5B). CII has been proposed to trigger apoptosis, depending on its attachment to the inner mitochondrial membrane (reviewed in Grimm, 2013). When detached, CII is not assembled as a holocomplex, and its succinate ubiquinol reductase (SQR or CII) activity, which involves coenzyme Q reduction, is decreased. However, succinate dehydrogenase (SDH) activity is unaltered, resulting in superoxide leakage that leads to apoptosis (Albayrak et al., 2003; Lemarie et al., 2011). SDH activity was slightly higher in Y604F-expressing cells in normoxia, but the proportion of apoptotic cells (annexin V positive) was unaffected. Upon reoxygenation, the balance between CII and SDH activity in cells re-expressing WT FpSDH shifted toward CII, whereas in cells re-expressing Y604F it shifted more toward SDH (Figure 7D). This was reflected in significantly more severe apoptosis after hypoxia/reoxygenation in Y604F-re-expressing cells, in which CII activation is blunted, but not in cells re-expressing WT FpSDH (Figures 7D and S5C).

BNGE revealed a hypoxia-induced generalized decrease in the content of assembled OXPHOS complexes and Tom20 (consistent with loss of mitochondrial proteins evident in Figure 7B), with no alteration in the proportion of CIII dedicated to each coenzyme Q pool (Figure 7E). Posthypoxia reoxygenation of WT re-expressing cells restored OXPHOS complexes and supercomplex assembly while maintaining these proportions.

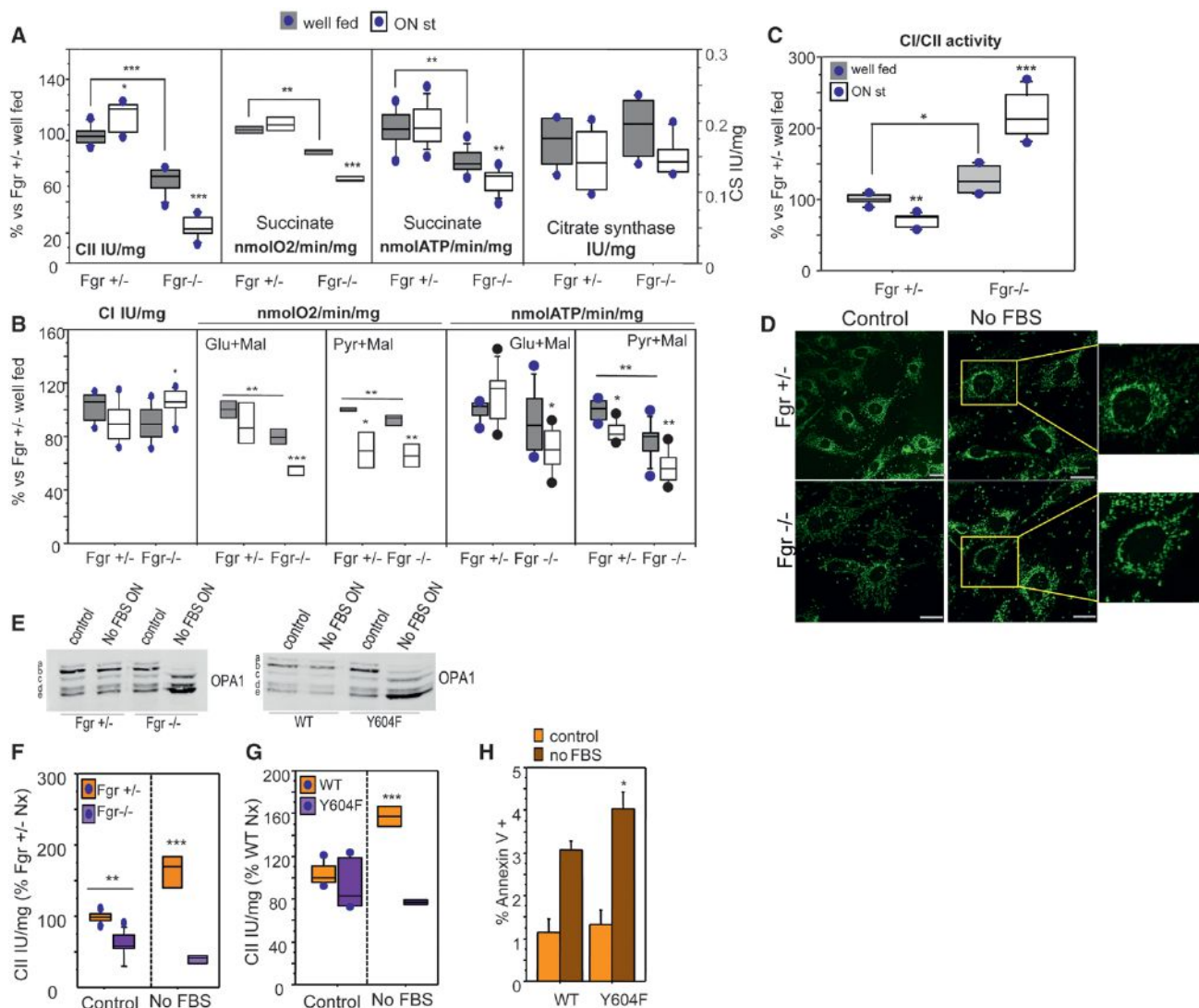


Figure 6. Mitochondria Lacking Fgr or Expressing Y604F FpSDH Respond Abnormally to Starvation and Serum Deprivation

(A) Succinate-driven OXPHOS function in mouse liver mitochondria from *Fgr*^{+/-} and *Fgr*^{-/-} mice fed a normal diet (well fed) or starved overnight (ON st, n ≥ 4). CII activity (left), succinate-driven respiration (center left), succinate-driven ATP synthesis (center right), and citrate synthase activity (CS, right).

(B) NADH-driven OXPHOS function in mouse liver mitochondria from *Fgr*^{+/-} and *Fgr*^{-/-} mice fed a normal diet or starved overnight (n ≥ 4). CI activity (left), glutamate-driven respiration (center left), pyruvate-driven respiration (center), glutamate-driven ATP synthesis (center right), and pyruvate-driven ATP synthesis (right) are shown.

(C) Rate of use of NADH/FADH reducing equivalents in mouse liver mitochondria from *Fgr*^{+/-} and *Fgr*^{-/-} mice (n ≥ 4). Data in (A)–(C) are presented as the percentage of values obtained in well-fed *Fgr*^{+/-} mice. Lines extending from the boxes indicate the variability outside the upper and lower quartiles.

(D) Immunostaining of mitochondria (Tom20, green) in *Fgr*^{+/-} and *Fgr*^{-/-} fibroblasts cultured with serum or without serum overnight (No FBS ON).

(E) Immunoblot showing the migration of OPA1 in lysates from control and serum-deprived *Fgr*^{+/-} and *Fgr*^{-/-} cells (left) or control and serum-deprived FpSDH-silenced fibroblasts re-expressing WT or Y604F FpSDH (right).

(F) CII activity in *Fgr*^{+/-} and *Fgr*^{-/-} fibroblasts grown in 10 mM glucose in the indicated conditions (n ≥ 5). Data are presented as the percentage activity in *Fgr*^{+/-} cells grown in normoxia; lines extending from the boxes indicate the variability outside the upper and lower quartiles.

(G) CII activity in FpSDH-silenced fibroblasts re-expressing WT or Y604F FpSDH, cultured at 5 mM glucose under the indicated oxygenation conditions (n ≥ 5). Data are presented as the percentage of activity in WT-expressing cells grown in normoxia; lines extending from the boxes indicate the variability outside the upper and lower quartiles.

(H) Apoptotic events in FpSDH-silenced fibroblasts re-expressing WT or Y604F FpSDH and grown with or without serum. Apoptosis was determined by flow cytometry as the percentage of cells positive for annexin V and propidium iodide (n = 3). Data are presented as mean ± SD. *p < 0.01; **p < 0.001; ***p < 0.0001. See also Figures S4 and S5.

In contrast, reoxygenated Y604F-expressing cells restored the normoxic level of CII dedicated to NADH but not the amount dedicated to FADH₂ (CIII+IV and free CII) (Figure 7E), indicating

a higher-than-normal dedication to processing electrons from the NADH-CoQ pool than from the FADH₂-CoQ pool (La-puente-Brun et al., 2013).

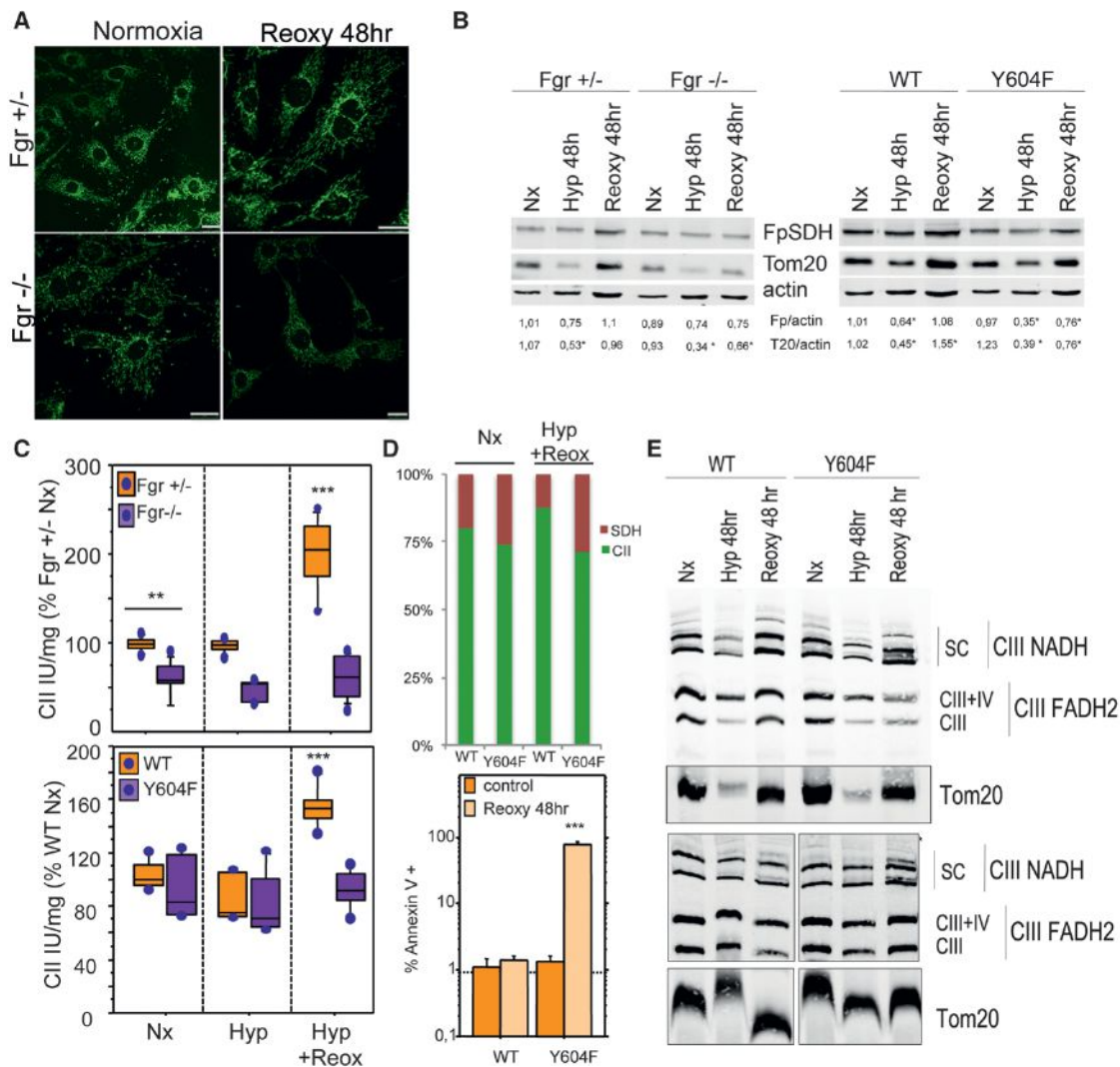


Figure 7. Mitochondria Lacking Fgr or Expressing Y604F FpSDH Respond Abnormally to Hypoxia-Reoxygenation

(A) Immunostaining of mitochondria (Tom20, green) in $Fgr^{+/-}$ and $Fgr^{-/-}$ fibroblasts cultured in normoxia (21% O_2) or hypoxia (1% O_2) for 48 hr followed by 48 hr normoxia (Reoxy 48 hr).

(B) Left: Immunoblot analysis of $Fgr^{+/-}$ and $Fgr^{-/-}$ cells cultured under normoxia (Nx), hypoxia for 48 hr (Hyp 48 hr), or hypoxia followed by normoxia (Reoxy 48 hr). Right: Immunoblot analysis of FpSDH-silenced fibroblasts re-expressing WT or Y604F FpSDH and cultured under the indicated oxygenation conditions. Numbers beneath blots show FpSDH (Fp):actin and Tom20 (T20):actin ratios ($n = 4$).

(C) Top: CII activity in $Fgr^{+/-}$ and $Fgr^{-/-}$ fibroblasts grown in 10 mM glucose under the indicated conditions ($n \geq 5$). Bottom: FpSDH-silenced fibroblasts re-expressing WT or Y604F FpSDH, cultured with 5 mM glucose under the indicated oxygenation conditions ($n \geq 5$). Data are presented as the percentage activity in $Fgr^{+/-}$ cells or WT-FpSDH-re-expressing cells grown in normoxia; lines extending from the boxes indicate the variability outside the upper and lower quartiles.

(D) Top: Relative activities of CII (CoQ reduction) and SDH in WT- and Y604F-re-expressing FpSDH-silenced cells grown in normoxia or through a hypoxia/reoxygenation cycle. For each cell line and condition, 100% = the sum of CII and SDH activities; absolute SDH activity did not differ between cell lines and conditions. Bottom: Apoptotic events in FpSDH-silenced fibroblasts re-expressing WT or Y604F FpSDH and grown in normoxia or through a hypoxia/reoxygenation cycle. Apoptosis was determined by flow cytometry as the percentage of annexin V- and PI-positive cells ($n = 3$). Data are presented as mean \pm SD.

(E) BNGE of FpSDH-silenced fibroblasts re-expressing WT or Y604F FpSDH cultured at 5 mM glucose under the indicated oxygenation conditions; the blot reveals the distribution of CIII (anti-core 1 immunodetection) among the different forms of free complex and supercomplexes. The outer membrane protein Tom20 is used as a mitochondrial protein loading control. Upper and lower panels are taken from two independent experiments. Note that upon reoxygenation the amount of CIII super assembled with CI is abnormally elevated in the Y604F mutant. See also Figure S5.

DISCUSSION

The data presented here demonstrate that Tyr phosphorylation of FpSDH increases CII activity in vivo, and that this mechanism triggers remodeling of the mETC to reset its capacity for pro-

cessing NADH- versus $FADH_2$ -derived electrons. This Tyr phosphorylation is H_2O_2 mediated, is catalyzed by the Src-family kinase Fgr, and specifically targets Y604 in FpSDH. The finding that the catalytic subunit of CII can be phosphorylated is consistent with earlier observations (Bykova et al., 2003; Schulenberg

et al., 2003). Moreover, our proposal that Fgr is the tyrosine kinase responsible for this phosphorylation concurs with a previous report demonstrating that Fgr, but not Lyn, is able to promote the *in vitro* phosphorylation of Y535 and Y596 of rat FpSDH, which correspond to Y543 and Y604 in mouse (Salvi et al., 2007).

H₂O₂-triggered activation of CII provides a mechanism for the association of increased CII activity and defective CI, observed in human patients and in a range of organisms from *Chlamydomonas reinhardtii* (Cardol et al., 2002) and *Rhodobacter capsulatus* (Dupuis et al., 1998) to mouse and humans (Esteite et al., 2005; Fan et al., 2008; Majander et al., 1991). Another feature of ROS-driven activation of CII is that since hydrogen peroxide can permeate through cell membranes, any extramitochondrial source of H₂O₂ can potentially activate CII, suggesting a mechanism to promote metabolic adaptation in response to signals that increase H₂O₂. Our results thus show that activation of CII by Fgr kinase in response to a primary wave of extramitochondrial ROS can trigger a secondary wave of ROS production as a consequence of CII activation. This pathway provides a mechanism for amplifying ROS signals within the cell. The increase in CII activity triggered by H₂O₂ is a quick response mechanism, independent of gene expression and therefore not involving any increase in mitochondrial biogenesis or regulation through PGC-1 α , a common feature of mitochondrial disease (Moreno-Loshuertos et al., 2006; Acín-Perez et al., 2009; Srivastava et al., 2009; Wenz et al., 2008).

FpSDH activity is regulated by acetylation on several lysine residues, and deacetylation mediated by sirtuin 3 (Cimen et al., 2010; Finley et al., 2011) increases CII activity independently of ROS. The regulation of CII acetylation is incompletely understood, but fuel availability is likely to play a part, probably in a complex tissue-specific pattern (Boyle et al., 2013; Finley et al., 2011). The convergence of multiple posttranslational modifications on the catalytic subunit of CII highlights the importance of fine-tuning CII activity to ensure correct cell metabolism. This role has remained unappreciated despite the considerable knowledge accumulated on the function of the tricarboxylic acid (TCA) cycle. Two other TCA cycle enzymes, aconitase and KGDH, are known to be reversibly downregulated by physiological increases in ROS levels (Bulteau et al., 2003; Moreno-Loshuertos et al., 2006). Our current results show that CII should be included among the TCA cycle enzymes regulated by ROS.

Our results also show that Src-family kinase signaling operates within mitochondria, regulating the fundamental metabolic processes of the TCA cycle and oxidative phosphorylation. SFKs are implicated in a wide variety of signaling pathways, regulating cell growth, differentiation, cell shape, migration, and survival (Ingley, 2008; Parsons and Parsons, 2004). Moreover, the physiological role of SFK activation by H₂O₂ has also been shown in another model system: the role of Lyn kinase as a redox sensor activated by H₂O₂ in leukocyte wound attraction (Yoo et al., 2011). The role of reversible protein phosphorylation in mitochondria is an emerging field (Pagliarini and Dixon, 2006; Pagliarini et al., 2005), and several mitochondrial proteins have been proposed as Tyr phosphorylation targets (Augereau et al., 2005; Salvi et al., 2005, 2007; Tibaldi et al., 2008). Moreover, a number of SFKs have been proposed to localize in mito-

chondria (Pagliarini and Dixon, 2006; Tibaldi et al., 2008). One previous report has described the function of a mitochondrial SFK, demonstrating that c-Src enhances the activity of subunit II of cytochrome c oxidase, the terminal mETC enzyme (Miyazaki et al., 2003). Thus the TCA cycle and the mETC are both positively regulated by the action of SFKs: Fgr for the TCA cycle and c-Src for the mETC. By bringing the regulation of mitochondrial energetic metabolism within the remit of cellular signaling pathways regulated by SFKs, these findings have broad implications for the integration of cell adaptation and energy regulation. The results presented here highlight the importance of this regulation in the adaptation to loss of CI, regulation of CII activity during the metabolic switch upon activation of naive T cells, and metabolic adaptation of mitochondria to starvation and hypoxia/reoxygenation. CII has also been proposed to act as universal oxygen sensor (Baysal, 2006), suggesting that this pathway is also critically important in situations where cells need to respond rapidly to changes in fuel availability or O₂ concentration.

EXPERIMENTAL PROCEDURES

Further details of methods are provided in Supplemental Experimental Procedures.

Cell Culture

Cell lines were grown in Dulbecco's modified Eagle's medium (DMEM; GIBCOBRL) supplemented with 5% fetal bovine serum (FBS; GIBCOBRL). Fibroblasts from Fgr^{+/-} and Fgr null mice were isolated from mouse ear and immortalized by transfection with pLOX-Ttag-iresTK (Addgene) and grown in DMEM with 10% FBS. FBalb/cJ and FG23-1 cells expressing MnSOD or HA-tagged mt-catalase and FBalb/cJ cells overexpressing different forms of FpSDH and silenced for the endogenous FpSDH were generated by viral infection using polybrene (8 μ g/ml).

Isolation of Mitochondria and Mitochondrial Fractions from Mouse Liver and Cell Lines

Mitochondria were isolated from cell lines as described (Schägger and von Jagow, 1991) with some modifications, and from mouse liver as described (Fernández-Vizarra et al., 2002).

OXPHOS Function and Enzyme Activities

O₂ consumption was measured in mouse liver mitochondria (100 μ g as described (Hofhaus et al., 1996). ATP synthesis in isolated mitochondria (15–25 μ g mitochondrial protein) was measured using a kinetic luminescence assay (Vives-Bauza et al., 2007). Mitochondrial fractions were prepared and the activities of individual complexes measured spectrophotometrically (Birch-Machin and Turnbull, 2001). Catalase activity was measured in total cell lysates (300 μ g) (Moreno-Loshuertos et al., 2006). Total SOD and MnSOD (KCN insensitive) activities were assessed in total cell lysates (50 μ g) using the SOD Assay Kit (Sigma-Aldrich).

Blue-Native Gel Electrophoresis

Cell-culture-derived mitochondria (50–75 μ g) were separated on 5%–13% gradient blue native gels (Schägger and von Jagow, 1991).

Isoelectric Focusing and 2D SDS-PAGE

Mitochondrial preparations (100 μ g) were processed with by Ready Prep 2D Cleanup (BioRad) and applied to pH 3–10 or pH 4–7 IPG strips (BioRad) and incubated overnight at room temperature. Isoelectric focusing and second dimension SDS-PAGE were run under standard conditions.

Phosphoprotein Enrichment

Phosphoprotein-enriched mitochondrial fractions were isolated on phosphoprotein enrichment columns (QIAGEN).

Immunocapture

Complex II and FpSDH were immunocaptured from mitochondria isolated from either cells or mouse liver. For details see Supplemental Experimental Procedures.

In Vitro Fgr Phosphorylation

Recombinant Fgr kinase (Abnova) was used to phosphorylate complex II immunocaptured from cells expressing WT and Y604F FpSDH (Salvi et al., 2007).

Immunological Analysis

Antibodies used in this study are listed in Supplemental Experimental Procedures.

H₂O₂ Production

H₂O₂ production was measured in cultured cells grown in the absence or presence of 5 mM NAC for 7 days (Moreno-Loshuertos et al., 2006).

Isolation and Stimulation of Naive CD4⁺ and CD8⁺ T Cells

CD4⁺ and CD8⁺ T cells were purified from splenic cell suspensions obtained from 8- to 10-week-old Fgr^{+/-} and Fgr^{-/-} male mice. To obtain differentiated T lymphoblasts, naive T cells were cultured with concanavalin A (Sigma) and human recombinant IL-2 (50 U/ml, Glaxo).

Flow Cytometry ROS Production Determination

ROS production in naive or activated T lymphocytes and in cells before and after overexpression of detoxifying enzymes was assessed by flow cytometry of 2,7-DCFH₂-DA or MitoSOX staining (Kamiński et al., 2012).

Determination of Apoptosis in Cultured Cells

Apoptosis was monitored by flow cytometry detection of annexin V and propidium iodide (PI) staining in 10⁶ cells resuspended in 10 mM HEPES/NaOH (pH 7.4), 140 mM NaCl, 2.5 mM CaCl₂.

Mouse Strains

Animal studies were approved by the local ethics committee. Analyses were performed in 8- to 11-week-old male mice.

In Silico Analysis

See Supplemental Experimental Procedures.

Statistical Analysis

Comparisons between groups were made by one-way ANOVA. Pairwise comparisons were made by Fisher's PLSD post hoc test. Differences were considered statistically significant at $p < 0.05$. Data were analyzed with StatView (Adept Scientific, UK).

SUPPLEMENTAL INFORMATION

Supplemental Information includes five figures and Supplemental Experimental Procedures and can be found with this article online at <http://dx.doi.org/10.1016/j.cmet.2014.04.015>.

ACKNOWLEDGMENTS

We thank Dr. Concepción Jimenez and Andrés Gonzalez-Guerra for technical assistance, Anatoly A. Starkov for a valuable discussion, and Dr. Simon Bartlett (CNIC) for English editing. This study was supported by grants from the Ministerio de Economía y Competitividad (SAF2012-1207 and CSD2007-00020), the Comunidad de Madrid (CAM/API1009), and the EU (UE0/MCA1108 and UE0/MCA1201). R.A.-P. is recipient of a Ramon y Cajal contract. The CNIC is supported by the Ministerio de Economía y Competitividad and the Pro-CNIC Foundation.

Received: November 26, 2013

Revised: February 13, 2014

Accepted: April 3, 2014

Published: May 22, 2014

REFERENCES

- Acín-Pérez, R., Bayona-Bafaluy, M.P., Bueno, M., Machicado, C., Fernández-Silva, P., Pérez-Martos, A., Montoya, J., López-Pérez, M.J., Sancho, J., and Enríquez, J.A. (2003). An intragenic suppressor in the cytochrome c oxidase I gene of mouse mitochondrial DNA. *Hum. Mol. Genet.* *12*, 329–339.
- Acín-Pérez, R., Salazar, E., Brosel, S., Yang, H., Schon, E.A., and Manfredi, G. (2009). Modulation of mitochondrial protein phosphorylation by soluble adenyl cyclase ameliorates cytochrome oxidase defects. *EMBO Mol Med* *1*, 392–406.
- Albayrak, T., Scherhammer, V., Schoenfeld, N., Braziulis, E., Mund, T., Bauer, M.K.A., Scheffler, I.E., and Grimm, S. (2003). The tumor suppressor cybL, a component of the respiratory chain, mediates apoptosis induction. *Mol. Biol. Cell* *14*, 3082–3096.
- Ali, S.S., Hsiao, M., Zhao, H.W., Dugan, L.L., Haddad, G.G., and Zhou, D. (2012). Hypoxia-adaptation involves mitochondrial metabolic depression and decreased ROS leakage. *PLoS ONE* *7*, e36801.
- Augereau, O., Claverol, S., Boudes, N., Basurko, M.-J., Bonneu, M., Rossignol, R., Mazat, J.-P., Letellier, T., and Dachary-Prigent, J. (2005). Identification of tyrosine-phosphorylated proteins of the mitochondrial oxidative phosphorylation machinery. *Cell. Mol. Life Sci.* *62*, 1478–1488.
- Bai, Y., and Attardi, G. (1998). The mtDNA-encoded ND6 subunit of mitochondrial NADH dehydrogenase is essential for the assembly of the membrane arm and the respiratory function of the enzyme. *EMBO J.* *17*, 4848–4858.
- Balamurugan, K., Rajaram, R., Ramasami, T., and Narayanan, S. (2002). Chromium(III)-induced apoptosis of lymphocytes: death decision by ROS and Src-family tyrosine kinases. *Free Radic. Biol. Med.* *33*, 1622–1640.
- Baysal, B.E. (2006). A phenotypic perspective on Mammalian oxygen sensor candidates. *Ann. N Y Acad. Sci.* *1073*, 221–233.
- Birch-Machin, M.A., and Turnbull, D.M. (2001). Assaying mitochondrial respiratory complex activity in mitochondria isolated from human cells and tissues. *Methods Cell Biol.* *65*, 97–117.
- Boyle, K.E., Newsom, S.A., Janssen, R.C., Lappas, M., and Friedman, J.E. (2013). Skeletal muscle MnSOD, mitochondrial complex II, and SIRT3 enzyme activities are decreased in maternal obesity during human pregnancy and gestational diabetes mellitus. *J. Clin. Endocrinol. Metab.* *98*, E1601–E1609.
- Bulteau, A.-L., Ikeda-Saito, M., and Szwedda, L.I. (2003). Redox-dependent modulation of aconitase activity in intact mitochondria. *Biochemistry* *42*, 14846–14855.
- Bykova, N.V., Egsgaard, H., and Møller, I.M. (2003). Identification of 14 new phosphoproteins involved in important plant mitochondrial processes. *FEBS Lett.* *540*, 141–146.
- Cardol, P., Matagne, R.F., and Remacle, C. (2002). Impact of mutations affecting ND mitochondria-encoded subunits on the activity and assembly of complex I in *Chlamydomonas*. Implication for the structural organization of the enzyme. *J. Mol. Biol.* *319*, 1211–1221.
- Cascarano, J., Ades, I.Z., and O'Conner, J.D. (1976). Hypoxia: a succinate-fumarate electron shuttle between peripheral cells and lung. *J. Exp. Zool.* *198*, 149–153.
- Chiarugi, P. (2008). Src redox regulation: there is more than meets the eye. *Mol. Cells* *26*, 329–337.
- Cimen, H., Han, M.-J., Yang, Y., Tong, Q., Koc, H., and Koc, E.C. (2010). Regulation of succinate dehydrogenase activity by SIRT3 in mammalian mitochondria. *Biochemistry* *49*, 304–311.
- Cogliati, S., Frezza, C., Soriano, M.E., Varanita, T., Quintana-Cabrera, R., Corrado, M., Cipolat, S., Costa, V., Casarin, A., Gomes, L.C., et al. (2013). Mitochondrial cristae shape determines respiratory chain supercomplexes assembly and respiratory efficiency. *Cell* *155*, 160–171.
- Dlasková, A., Hlavatá, L., and Ježek, P. (2008). Oxidative stress caused by blocking of mitochondrial complex I H(+) pumping as a link in aging/disease vicious cycle. *Int. J. Biochem. Cell Biol.* *40*, 1792–1805.
- Dröge, W. (2002). Free radicals in the physiological control of cell function. *Physiol. Rev.* *82*, 47–95.

- Dupuis, A., Chevillet, M., Darrouzet, E., Duborjal, H., Lunardi, J., and Issartel, J.P. (1998). The complex I from *Rhodobacter capsulatus*. *Biochim. Biophys. Acta* 1364, 147–165.
- Esteite, N., Hinttala, R., Wibom, R., Nilsson, H., Hance, N., Naess, K., Teär-Fahnehjelm, K., von Döbeln, U., Majamaa, K., and Larsson, N.-G. (2005). Secondary metabolic effects in complex I deficiency. *Ann. Neurol.* 58, 544–552.
- Fan, W., Waymire, K.G., Narula, N., Li, P., Rocher, C., Coskun, P.E., Vannan, M.A., Narula, J., Macgregor, G.R., and Wallace, D.C. (2008). A mouse model of mitochondrial disease reveals germline selection against severe mtDNA mutations. *Science* 319, 958–962.
- Fernández-Vizarrá, E., López-Pérez, M.J., and Enriquez, J.A. (2002). Isolation of biogenetically competent mitochondria from mammalian tissues and cultured cells. *Methods* 26, 292–297.
- Finley, L.W.S., Haas, W., Desquiret-Dumas, V., Wallace, D.C., Procaccio, V., Gygi, S.P., and Haigis, M.C. (2011). Succinate dehydrogenase is a direct target of sirtuin 3 deacetylase activity. *PLoS ONE* 6, e23295.
- Gomes, L.C., Di Benedetto, G., and Scorrano, L. (2011). During autophagy mitochondria elongate, are spared from degradation and sustain cell viability. *Nat. Cell Biol.* 13, 589–598.
- Grimm, S. (2013). Respiratory chain complex II as general sensor for apoptosis. *Biochim. Biophys. Acta* 1827, 565–572.
- Hamanaka, R.B., and Chandel, N.S. (2010). Mitochondrial reactive oxygen species regulate cellular signaling and dictate biological outcomes. *Trends Biochem. Sci.* 35, 505–513.
- Heather, L.C., Cole, M.A., Tan, J.-J., Ambrose, L.J.A., Pope, S., Abd-Jamil, A.H., Carter, E.E., Dodd, M.S., Yeoh, K.K., Schofield, C.J., and Clarke, K. (2012). Metabolic adaptation to chronic hypoxia in cardiac mitochondria. *Basic Res. Cardiol.* 107, 268.
- Hofhaus, G., Shakeley, R.M., and Attardi, G. (1996). Use of polarography to detect respiration defects in cell cultures. *Methods Enzymol.* 264, 476–483.
- Huang, B., Wu, P., Popov, K.M., and Harris, R.A. (2003). Starvation and diabetes reduce the amount of pyruvate dehydrogenase phosphatase in rat heart and kidney. *Diabetes* 52, 1371–1376.
- Ingle, E. (2008). Src family kinases: regulation of their activities, levels and identification of new pathways. *Biochim. Biophys. Acta* 1784, 56–65.
- Kamiński, M.M., Sauer, S.W., Klemke, C.-D., Süß, D., Okun, J.G., Krammer, P.H., and Gülow, K. (2010). Mitochondrial reactive oxygen species control T cell activation by regulating IL-2 and IL-4 expression: mechanism of ciprofloxacin-mediated immunosuppression. *J. Immunol.* 184, 4827–4841.
- Kamiński, M.M., Sauer, S.W., Kamiński, M., Opp, S., Ruppert, T., Grigaravičius, P., Grudnik, P., Gröne, H.-J., Krammer, P.H., and Gülow, K. (2012). T cell activation is driven by an ADP-dependent glucokinase linking enhanced glycolysis with mitochondrial reactive oxygen species generation. *Cell Rep* 2, 1300–1315.
- Kim, H., Scimia, M.C., Wilkinson, D., Trelles, R.D., Wood, M.R., Bowtell, D., Dillin, A., Mercola, M., and Ronai, Z.A. (2011). Fine-tuning of Drp1/Fis1 availability by AKAP121/Siah2 regulates mitochondrial adaptation to hypoxia. *Mol. Cell* 44, 532–544.
- Kruse, S.E., Watt, W.C., Marcinek, D.J., Kapur, R.P., Schenkman, K.A., and Palmiter, R.D. (2008). Mice with mitochondrial complex I deficiency develop a fatal encephalomyopathy. *Cell Metab.* 7, 312–320.
- Lapiente-Brun, E., Moreno-Loshuertos, R., Acín-Pérez, R., Latorre-Pellicer, A., Colás, C., Balsa, E., Perales-Clemente, E., Quirós, P.M., Calvo, E., Rodríguez-Hernández, M.A., et al. (2013). Supercomplex assembly determines electron flux in the mitochondrial electron transport chain. *Science* 340, 1567–1570.
- Lemarie, A., Huc, L., Pazarentzos, E., Mahul-Mellier, A.-L., and Grimm, S. (2011). Specific disintegration of complex II succinate:ubiquinone oxidoreductase links pH changes to oxidative stress for apoptosis induction. *Cell Death Differ.* 18, 338–349.
- Lowell, C.A., Soriano, P., and Varmus, H.E. (1994). Functional overlap in the src gene family: inactivation of hck and fgr impairs natural immunity. *Genes Dev.* 8, 387–398.
- Majander, A., Huoponen, K., Savontaus, M.L., Nikoskelainen, E., and Wikström, M. (1991). Electron transfer properties of NADH:ubiquinone reductase in the ND1/3460 and the ND4/11778 mutations of the Leber hereditary optic neuroretinopathy (LHON). *FEBS Lett.* 292, 289–292.
- Minetti, M., Mallozzi, C., and Di Stasi, A.M.M. (2002). Peroxynitrite activates kinases of the src family and upregulates tyrosine phosphorylation signaling. *Free Radic. Biol. Med.* 33, 744–754.
- Miyazaki, T., Neff, L., Tanaka, S., Horne, W.C., and Baron, R. (2003). Regulation of cytochrome c oxidase activity by c-Src in osteoclasts. *J. Cell Biol.* 160, 709–718.
- Moreno-Loshuertos, R., Acín-Pérez, R., Fernández-Silva, P., Movilla, N., Pérez-Martos, A., Rodríguez de Córdoba, S.R., Gallardo, M.E., and Enriquez, J.A. (2006). Differences in reactive oxygen species production explain the phenotypes associated with common mouse mitochondrial DNA variants. *Nat. Genet.* 38, 1261–1268.
- Nagy, G., Koncz, A., and Perl, A. (2003). T cell activation-induced mitochondrial hyperpolarization is mediated by Ca²⁺- and redox-dependent production of nitric oxide. *J. Immunol.* 171, 5188–5197.
- Pagliarini, D.J., and Dixon, J.E. (2006). Mitochondrial modulation: reversible phosphorylation takes center stage? *Trends Biochem. Sci.* 31, 26–34.
- Pagliarini, D.J., Wiley, S.E., Kimple, M.E., Dixon, J.R., Kelly, P., Worby, C.A., Casey, P.J., and Dixon, J.E. (2005). Involvement of a mitochondrial phosphatase in the regulation of ATP production and insulin secretion in pancreatic beta cells. *Mol. Cell* 19, 197–207.
- Papandreou, I., Cairns, R.A., Fontana, L., Lim, A.L., and Denko, N.C. (2006). HIF-1 mediates adaptation to hypoxia by actively downregulating mitochondrial oxygen consumption. *Cell Metab.* 3, 187–197.
- Parsons, S.J., and Parsons, J.T. (2004). Src family kinases, key regulators of signal transduction. *Oncogene* 23, 7906–7909.
- Pitkanen, S., and Robinson, B.H. (1996). Mitochondrial complex I deficiency leads to increased production of superoxide radicals and induction of superoxide dismutase. *J. Clin. Invest.* 98, 345–351.
- Quirós, P.M., Ramsay, A.J., Sala, D., Fernández-Vizarrá, E., Rodríguez, F., Peinado, J.R., Fernández-García, M.S., Vega, J.A., Enriquez, J.A., Zorzano, A., and López-Otin, C. (2012). Loss of mitochondrial protease OMA1 alters processing of the GTPase OPA1 and causes obesity and defective thermogenesis in mice. *EMBO J.* 31, 2117–2133.
- Radad, K., Rausch, W.-D., and Gille, G. (2006). Rotenone induces cell death in primary dopaminergic culture by increasing ROS production and inhibiting mitochondrial respiration. *Neurochem. Int.* 49, 379–386.
- Robinson, B.H. (1998). Human complex I deficiency: clinical spectrum and involvement of oxygen free radicals in the pathogenicity of the defect. *Biochim. Biophys. Acta* 1364, 271–286.
- Salvi, M., Brunati, A.M., and Toninello, A. (2005). Tyrosine phosphorylation in mitochondria: a new frontier in mitochondrial signaling. *Free Radic. Biol. Med.* 38, 1267–1277.
- Salvi, M., Morrice, N.A., Brunati, A.M., and Toninello, A. (2007). Identification of the flavoprotein of succinate dehydrogenase and aconitase as in vitro mitochondrial substrates of Fgr tyrosine kinase. *FEBS Lett.* 581, 5579–5585.
- Schägger, H., and von Jagow, G. (1991). Blue native electrophoresis for isolation of membrane protein complexes in enzymatically active form. *Anal. Biochem.* 199, 223–231.
- Schulenberg, B., Aggeler, R., Beechem, J.M., Capaldi, R.A., and Patton, W.F. (2003). Analysis of steady-state protein phosphorylation in mitochondria using a novel fluorescent phosphosensor dye. *J. Biol. Chem.* 278, 27251–27255.
- Speijer, D. (2011). Oxygen radicals shaping evolution: why fatty acid catabolism leads to peroxisomes while neurons do without it: FADH₂/NADH flux ratios determining mitochondrial radical formation were crucial for the eukaryotic invention of peroxisomes and catabolic tissue differentiation. *Bioessays* 33, 88–94.
- Srivastava, S., Diaz, F., Iommarini, L., Aure, K., Lombes, A., and Moraes, C.T. (2009). PGC-1α/β induced expression partially compensates for

respiratory chain defects in cells from patients with mitochondrial disorders. *Hum. Mol. Genet.* 18, 1805–1812.

Stanley, I.A., Ribeiro, S.M., Giménez-Cassina, A., Norberg, E., and Danial, N.N. (2013). Changing appetites: the adaptive advantages of fuel choice. *Trends Cell Biol.* 24, 118–127.

Ten, V.S., and Starkov, A. (2012). Hypoxic-ischemic injury in the developing brain: the role of reactive oxygen species originating in mitochondria. *Neurol. Res. Int.* 2012, 542976.

Tibaldi, E., Brunati, A.M., Massimino, M.L., Stringaro, A., Colone, M., Agostinelli, E., Arancia, G., and Toninello, A. (2008). Src-Tyrosine kinases are

major agents in mitochondrial tyrosine phosphorylation. *J. Cell. Biochem.* 104, 840–849.

Vives-Bauza, C., Yang, L., and Manfredi, G. (2007). Assay of mitochondrial ATP synthesis in animal cells and tissues. *Methods Cell Biol.* 80, 155–171.

Wenz, T., Diaz, F., Spiegelman, B.M., and Moraes, C.T. (2008). Activation of the PPAR/PGC-1 α pathway prevents a bioenergetic deficit and effectively improves a mitochondrial myopathy phenotype. *Cell Metab.* 8, 249–256.

Yoo, S.K., Starnes, T.W., Deng, Q., and Huttenlocher, A. (2011). Lyn is a redox sensor that mediates leukocyte wound attraction in vivo. *Nature* 480, 109–112.

Cell Career Network just got better!



- Additional reach via extended network
- Post a job within 5 minutes via self service
- More intuitive feel and easier navigation
- New vacancy packages and pricing

Your recruitment process just became even easier.
Get started today!

careers.cell.com/recruiters



Cell
PRESS

Introducing the China Gateway

The home for Chinese scientists



The new Cell Press China Gateway is the ultimate destination for Chinese scientists. Now highlights of the latest research, regional events, and featured content from Cell Press are accessible online, on a single webpage.

The Cell Press China Gateway was designed with you in mind. We hope you'll make yourself at home.

Visit us at www.cell.com/china

Cell Systems

A new journal from Cell Press launching July 2015 offering breadth and visibility for quantitative integrative research.



Launching July 2015, Cell Systems is the home for outstanding research toward systems-level understanding and applications in the life sciences and related areas, offering a venue to reach colleagues across science, engineering, and biomedical disciplines.

- High-quality, cutting-edge basic and applied research
- Broad scope
- Peer review and publication tailored to multidisciplinary data-intensive research
- Flexible open access options

Learn more at www.cell.com/cell-systems

CellPress
Your work is our life

MEMBRANE POTENTIAL ASSAYS

Tested and Validated with
Plate Reader, Flow Cytometry,
or Microscopy Based Systems

JC-1 and TMRE
Assays Available

Adaptable
to HTS



BIOCHEMICALS • ASSAY KITS • ANTIBODIES
PROTEINS • RESEARCH SERVICES

Visit www.CaymanChem.com/Bioenergetics for
more information on Cayman's Mitochondrial Assays

Call us at 800-364-9897 or Email us at sales@caymanchem.com

OXYGEN CONSUMPTION ASSAYS

MitoXpress®-Xtra
Novel Phosphorescent Probe

Plate Reader-Based

Adaptable to HTS

Measure O₂
Consumption



BIOCHEMICALS • ASSAY KITS • ANTIBODIES
PROTEINS • RESEARCH SERVICES

Visit www.CaymanChem.com/Bioenergetics for
more information on Cayman's Mitochondrial Assays

Call us at 800-364-9897 or Email us at sales@caymanchem.com